Contract No. A032-096
Final Report
March 1995

Environmental Chamber Studies of Atmospheric Reactivities of Volatile Organic Compounds. Effects of Varying ROG Surrogate and NOx

California Environmental Protection Agency
Air Resources Board
Research Division

Environmental Chamber Studies of Atmospheric Reactivities of Volatile Organic Compounds. Effects of Varying ROG Surrogate and NOx

Final Report

Contract No. A032-096

Prepared for:

California Air Resources Board
Research Division
2020 L Street
Sacramento, California 95814

Prepared by:

William P.L. Carter
Dongmin Luo
Irina Malkina
and
John A. Pierce

Statewide Air Pollution Research Center
and
College of Engineering
Center for Environmental Research and Technology
University of California
Riverside, California 92521

March 1995

PREFACE

This report describes work carried out at the University of California under funding from the California Air Resources Board (CARB) through contract number A032-096, the Coordinating Research Council, Inc. (CRC) through project number ME-9, the National Renewable Energy Laboratory (NREL) through contract ZF-2-12252, and the California South Coast Air Quality Management District (SCAQMD) through contract no. C91323. CARB, CRC and NREL funded most of the experimental work, and the SCAQMD funded the building where the experiments were conducted.

The opinions and conclusions in this document are entirely those of the authors. Mention of trade names and commercial products does not constitute endorsement or recommendation for use.

ABSTRACT

A series of indoor environmental chamber experiments were conducted to measure incremental reactivities of representative volatile organic compounds (VOCs) in irradiations of various reactive organic gas (ROG) surrogate - NO_x - air mixtures designed to represent or approximate conditions of urban photochemical smog. Incremental reactivities are defined as the change in to ozone formation or OH radical levels caused by adding the VOC to a "base case" experiment, divided by the amount added. The base case included irradiations, at both relatively high and low NO_x levels, of a surrogate mixture of 8 VOCs which model calculations predicted would yield the same results as use of a full ambient ROG mixture, and high NO_x experiments where ethylene alone represented the ambient ROGs. The test VOCs included carbon monoxide, n-butane, n-hexane, n-octane, ethylene, propene, trans-2-butene, benzene, toluene, m-xylene, formaldehyde, and acetaldehyde. The data obtained show that VOC have a greater range of incremental reactivities when simplified base case ROG surrogates are used than with the more realistic 8-component surrogate. Reducing NO_x reduced incremental reactivities by differing amounts for different VOCs, with ozone reactivities of propene, trans-2-butene, acetaldehyde, and the aromatics becoming negative in the low NO_x experiments. These results are consistent with model predictions. The model simulated reactivities in experiments with the more complex surrogate reasonably well, though it was more variable in the simulations of the simpler systems, which are more sensitive to differences among the VOCs. Model calculations indicated that experimentally measured incremental reactivities may correlate well with those in the atmosphere under high NO_x conditions, but not when NO_x is low. Thus the best use for data from incremental reactivity experiments is evaluating the models used to predict reactivities in the atmosphere.

ACKNOWLEDGEMENTS

The authors wish to acknowledge and thank Mr Bart Croes of the CARB, Mr. Tim Belian of the CRC, Dr. Alan Lloyd of the SCAQMD, Mr. Brent Bailey of NREL, and the members of the CRC/APRAC reactivity committee for their support of this project and their patience with the delays in completing this report. We also gratefully acknowledge Dr. Joseph Norbeck, Director of the University of California, Riverside's College of Engineering Center for Environmental Research and Technology (CE-CERT) for providing significant salary support and equipment used in this project.

Valuable assistance in constructing the chamber facility and conducting the experiments for this program was provided by Mr William D. Long. Mr. Robert Walters assisted in improvements to the pure air and temperature control system used in this project. Assistance in conducting the experiments was provided by Ms. Kathalena M. Smihula and Mr. Armando D. Avallone. Mr. Dennis Fitz assisted in the preparation of this report. Dr. Harvey Jeffries of the University of North Carolina provided the ambient VOC data and assignments used in the analysis discussed in Section II.

EXECUTIVE SUMMARY

Introduction

The formation of ground-level ozone is caused by the gas-phase interactions of emitted volatile organic compounds (VOCs) and oxides of nitrogen (NO_x) in the presence of sunlight. Although traditional VOC control strategies to reduce ozone have focused on reducing the total mass of VOC emissions, not all VOCs are equal in the amount of ozone formation they cause. Control strategies which take into account these differences in "reactivities" of VOCs might provide a means for additional ozone reduction which could supplement mass-based controls. Examples include conversion of motor vehicles to alternative fuels and solvent substitutions. However, before reactivity-based strategies can be implemented, there must be a means to quantify VOC reactivity which is sufficiently reliable that it can be used in regulatory applications.

The most direct quantitative measure of the degree to which a VOC contributes to ozone formation in a photochemical air pollution episode is its "incremental reactivity". This is defined as the amount of additional ozone formation resulting from the addition of a small amount of the compound to the emissions in the episode, divided by the amount of compound added. This depends both on the VOC and on the conditions of the environment where it emitted, such as NO_x levels and the nature and level of other reactive organic gases (ROGs) which are present. Incremental reactivities in the atmosphere can be calculated using computer airshed models, given a model for airshed conditions and a mechanism for the VOCs' atmospheric chemical reactions. This approach was used in the development of the "Maximum Incremental Reactivity" (MIR) scale (Carter, 1993, 1994), which has been adopted by the California Air Resources Board (ARB) for the derivation of reactivity adjustment factors for use in vehicle emissions standards (CARB 1991).

However, model calculations of reactivity can be no more reliable than the chemical mechanisms upon which they are based. Therefore, mechanisms must be evaluated under controlled conditions by comparing their predictions against results of environmental chamber experiments. The Statewide Air Pollution Research Center (SAPRC), in conjunction with the College of Engineering, Center for Environmental Research and Technology (CE-CERT), has been conducting a multi-year environmental chamber program to address these data needs. This program is being carried out in several phases, as discussed below.

In the first phase of this program, we measured the incremental reactivities of 36 representative VOCs under relatively high NO_x, conditions using a simplified "surrogate" mixture to represent ROGs in the atmosphere and a blacklight light source (Carter et al., 1993a). These data were important in providing experimental reactivity data for a large variety of VOCs under conditions where O_3 formation is most sensitive to VOC emissions. However, they

provided no information concerning the effect on VOC reactivity on variations of environmental conditions, such as varying NO_x levels or the nature of the other ROGs present. In addition, the 3-component mixture used to represent the other reactive organics in the atmosphere (referred to as the "base ROG surrogate") greatly oversimplified actual atmospheric systems.

The second phase of this program had two major components. The first consisted of measuring incremental reactivities of representative VOCs using different base ROG surrogate mixtures and under lower NO_x conditions. The second consisted of obtaining experimental data to assess the effect of varying the light source on the ability of models to simulate the results of environmental chamber experiments. The second component is discussed in a separate report "Environmental Chamber Studies of Atmospheric Reactivities of Volatile Organic Compounds. Effects of Varying Chamber and Light Source" (Carter et al., 1995a). This report describes our study of the effects of varying base ROG surrogate and NO_x conditions on experimentally measured incremental reactivities.

Modeling Effects of Base ROG Surrogates on Incremental Reactivity Experiments

Incremental reactivity experiments consist of measuring the effect of adding a test VOC to a "base case" experiment designed to simulate an already polluted atmosphere. The base case experiment consists of a one-day irradiation of NO_x and a "base ROG surrogate" designed to represent the mixture of reactive organic pollutants in the atmosphere. Use of highly simplified mixtures as the base ROG surrogate, such as the 3-component mixture employed in our Phase I study, has the important advantages of experimental simplicity and more straightforward use of the results for mechanism evaluation. However, if the chemical conditions of the experiments are too unrealistic, the data may not provide an appropriate test to the parts of the mechanism which are important in affecting predictions of atmospheric reactivity. To determine the most appropriate surrogates to use for such a study, we conducted a modeling study of the effects of varying ROG surrogates on experimental measurements of incremental reactivity, and how experimental incremental reactivities correlate with those in the atmosphere.

The results of this modeling study indicated that an 8-component surrogate designed to represent a similar level of chemical detail as used in current airshed models provides an excellent representation of the ambient ROG mixture for reactivity experiments, and that use of more complex mixtures would not yield experimentally distinguishable results. The effect of ignoring unreactive carbon in the ROG surrogate was calculated to be negligible. However, the calculations also showed that even if the exact same ROG mixture is used in the experiments as occurs in the atmosphere, reactivities in environmental chamber experiments would not necessarily be the same or even correlate with those in the atmosphere. The best correlations are obtained with reactivities under maximum reactivity conditions and with IntOH reactivities under various conditions. No correlation

is obtained with ozone reactivities under maximum ozone or NO_x-limited conditions.

The 3-component "mini-surrogate" used in the Phase I study was calculated to yield measurable differences in reactivities for many species, and significantly higher reactivities for formaldehyde and acetone. However, the calculations also indicated that experiments using the simpler 3-component mini-surrogates are more sensitive to effects of differences among VOCs, and thus potentially more useful for mechanism evaluation. Since such mechanism evaluations are complicated by uncertainties in the m-xylene mechanism, calculations were conducted to determine whether use of an even simpler surrogate consisting of ethylene alone might provide equivalent information while minimizing problems due to ROG surrogate mechanism uncertainties. It was found that the ethylene surrogate gives almost equivalent maximum reactivity results as the "mini-surrogate", but tends to be more sensitive to NO_x-sink species under NO_x-limited conditions. The latter may be an advantage from the point of view of evaluating this aspect of VOC mechanisms.

Based on these results, it was determined that incremental reactivity experiments using both the lumped surrogate, and ethylene alone as the surrogate, would, in conjunction with the mini-surrogate experiments already conducted, provide useful and complementary information concerning the effect of ROG surrogate on incremental reactivity. These experiments are discussed in the following sections.

Environmental Chamber Experiments

Incremental reactivity experiments were carried out using two different ROG surrogates and two different NO_x levels. The "ethene surrogate" experiments used ethene as the base ROG surrogate and were carried out at the relatively high NO_x levels where VOCs have their highest incremental reactivities. The "full surrogate" experiments used the 8-component mixture derived as a result of the modeling study discussed above, and were carried out at both the relatively high "maximum incremental reactivity" NO_x levels and at ~4 times lower NO_x levels where O_3 formation is NO_x-limited. The compounds studied under all three conditions were carbon monoxide, n-butane, n-octane, propene, trans-2-butene, m-xylene, and formaldehyde. Experiments with ethane, ethene, benzene, toluene, and acetaldehyde were carried out under a subset of these conditions.

The results were analyzed to derive the following measures of reactivity: (1) the effect of the VOC on the total amount of O_3 formed and NO oxidized, which is referred to as its "total" reactivity; (2) the effect of the VOC on integrated radical levels, or its "IntOH" reactivity; and (3) the "direct" reactivity of the VOC, which is an estimate of the amount of O_3 formation and NO oxidation caused directly by radicals formed in the reactions of the test VOC or its direct reaction products. The latter can be estimated under high NO_x conditions based on the assumption that the total effect of the VOC on O_3 formation and NO

oxidation is the direct reactivity plus the effect of the VOC on the amount of reaction of the components of the base ROG surrogate, which in turn can be estimated from the IntOH reactivities and the correspondence between O_3 formation, NO oxidation, and IntOH levels in the "base case" experiments where the test VOC is not present. Derivation of these separate components of reactivity are useful for understanding the mechanistic basis behind the observed reactivities, and for evaluating whether the current mechanisms appropriate represent these components.

The results of these experiments are expressed in terms of "mechanistic reactivities", which are analogous to incremental reactivities except they are relative to the amount of test VOC reacted up to the time of the observation, rather than the amount added. Mechanistic reactivities are useful because, to a first approximation, they are independent on how rapidly the VOC reacts, and thus allow comparisons of reactivity characteristics of VOCs which react at different rates. It is the most uncertain component of incremental reactivity because atmospheric reaction rate constants are reasonably well characterized for most VOCs.

Table EX-1 gives a summary of selected total and direct mechanistic reactivity results obtained using the different ROG surrogates and NO_x levels from this work. Comparable results from our Phase I study are also shown for comparison. It can be seen that decreasing the NO_x levels causes the total mechanistic reactivities to decrease, but the extent of decrease varies depending on the type of compound. In addition, the nature of the base ROG surrogate

Table EX-1. Summary of experimentally measured total and direct mechanistic reactivities for selected VOCs[a].

Compound	--- Total Mechanistic Reactivity ---				Direct Mechanistic React'y		
	High NO_x			Low NO_x	High NO_x		
	Ethene	Mini Srg	Full Srg	Full Srg	Ethene	Mini Srg	Full Srg
CO	1.1±0.2	0.7±0.2	0.5	0.3±0.1	1.2±0.3	0.8±0.1	0.7
n-Butane	1.2±0.4	0.8±0.3	1.2±0.1	0.6±0.1	1.7±0.6	2.2±0.4	1.9±0.1
n-Octane	-0.8±0.2	-4.4±1.2	0.8±0.2	0.3±0.2	1.8±0.4	2.3±1.0	2.3±0.3
Propene	2.3±0.3	2.7±0.7	1.0±0.1	0.0±0.1		[b]	0.2±0.1
t-2-Butene	6.0±1.1	5.4±1.0	1.0±0.1	-0.1±0.2			0.2±0.1
Toluene		7.0±1.0	2.8±0.5	-0.5±0.1			1.0±0.4
m-Xylene	7.6±0.7	7.6±2.5	4.9±0.8	-0.7±0.3			
Acetald.		0.4±0.2	0.6±0.2	-0.2±0.1		1.4±0.2	1.7±0.4

[a] Units are moles of O_3 per mole VOC reacted. Most values are weighted averages of results of several experiments. "Ethene", "Mini Srg" and "Full Srg" refer to the base ROG surrogate, where "Full Srg" refers to the 8-component mixture derived in this work, and "Mini Srg" refers to experiments from the Phase I study using the 3-component mixture. The "Ethene" and "Full Srg" data are from this study.

[b] Blank means that direct mechanistic reactivities could not be determined with sufficient precision to be meaningful.

significantly affects total mechanistic reactivities for some compounds, particularly n-octane, whose total reactivity is positive with the full surrogate but negative with the simplified ones, with the data using the mini-surrogate being more similar to those using the ethene surrogate than those using the 8-component mixture. On the other hand, the nature of the base ROG surrogate does not appear to have a significant effect on direct mechanistic reactivities, at least for those compounds where this could be determined. These observations are generally consistent with results of model simulations using an updated version of the SAPRC detailed chemical mechanism.

Discussion and Conclusions

The experimental data and model simulations have shown that the presence of other VOC pollutants can significantly affect the incremental reactivities of added VOCs. For example, the model predicted, and the experimental data confirmed, that the incremental reactivity of n-octane could change sign, and the absolute reactivities of species such as alkenes, aromatics, and formaldehyde could change significantly, depending on the mixture used to represent the base ROG. VOCs were found to have much smaller differences in ozone effects when reacting in the presence of a more complex mixture designed to represent ambient ROG pollutants than when reacting in the presence of more simplified mixtures such as the 3-component "mini-surrogate" used in our Phase I study. This is attributed to species in the more complex mixture, such as formaldehyde and (perhaps to a lesser extent) internal alkenes, which provide radical sources early in the irradiations, and tend to make the system less sensitive to the radical input or termination processes caused by the test VOC.

On the other hand, model simulations showed that it is probably not necessary to use a highly complex mixture to adequately represent the effects of other ROG pollutants in experimental studies of incremental reactivity. Use of a simple 8-component mixture, containing approximately the level of chemical detail as incorporated in condensed "lumped molecule" mechanisms in airshed models, was calculated to provide indistinguishable reactivity results in chamber experiments as use of a ambient ROG mixture containing the full set of compounds measured in the atmosphere. But simplifying this 8-component mixture further was found to have non-negligible effects on reactivity.

Using a realistic ROG surrogate is obviously necessary if experimental reactivity data are to correspond to reactivities in the atmosphere. However, it is not sufficient. Model calculations showed that even if the ambient mixture itself is used as the ROG surrogate, the extent to which chamber reactivities correlate with those in the atmosphere depended significantly on NO_x conditions. Under high NO_x conditions, experimental incremental reactivities correlate moderately well with atmospheric reactivities in the MIR scale, though the correlation was poor for acetaldehyde, and the correlation with the chamber data could only predict the atmosphere reactivities for the other VOCs to within ±50%. Under low NO_x conditions, there was *no correlation at all* between atmospheric

reactivity and reactivity in the chamber experiments. This was true whether using real chamber data or chamber data simulated by the model. Reactivities under low NO_x conditions are influenced by differing and often opposing factors, and apparently balances among these factors are quite different in the chamber experiments than in the atmosphere.

It may be possible someday to design an experimental system which gives better correlations between experimental and atmospheric reactivities, but we suspect it would be extremely difficult and expensive, and may yield data with large experimental uncertainties. In the meantime, we must rely on model simulations to predict reactivities in the atmosphere. The role of the chamber data is thus not to directly measure atmospheric reactivity, but rather to evaluate and if necessary calibrate the models which must be used for this purpose.

Experiments with both realistic and simplified ROG surrogates are necessary for an adequate evaluation of the ability of models to predict reactivity. Use of realistic surrogates are obviously necessary to test the ability of the mechanism to simulate reactivities in chemically realistic conditions. However, experiments with simpler surrogates are more sensitive to differences among VOCs, particularly in terms of their effects on radical levels. This means that model simulations of those experiments would be more sensitive to errors in the mechanisms of the VOCs. This is consistent with the results of this study, where in general the mechanism performed better in simulating reactivity in the experiments using the more complex surrogate than it did in the experiments using the mini-surrogate or ethylene alone.

The experimental data in this study confirmed the model predictions concerning the importance of NO_x in affecting a VOC's incremental reactivity. As expected, the incremental and mechanistic reactivities of all VOCs were reduced under low NO_x conditions. As also expected, this reduction was the greatest for VOCs, such as aromatics, acetaldehyde, and the higher alkenes, which are believed to have significant NO_x sinks in their mechanisms. All these NO_x sink species were found to have negative reactivities in our low NO_x experiments. This includes species, such as alkenes and acetaldehyde, which are calculated to have positive reactivities under low NO_x conditions in the atmosphere (Carter, 1993, 1994). Thus, low NO_x chamber reactivity experiments appear to be highly sensitive to effects of NO_x sinks in VOC's mechanisms – much more so than is apparently the case in the atmosphere. This high sensitivity may be the cause of the poor correlation between low NO_x chamber data and atmospheric reactivities. However, this also means that the chamber data should provide a highly sensitive test to this aspect of the mechanism.

The current detailed chemical mechanism was found to perform remarkably well in simulating the reactivities of the VOCs with the realistic 8-component surrogate, both under high and low NO_x conditions. An exception was that the

model did not correctly predict the effects of aromatics on radical levels under low NO_x conditions. In addition, the model did not give totally satisfactory performance in simulating the incremental reactivity of formaldehyde and performed poorly in simulating the incremental reactivity of n-octane using the ethene surrogate. In general, the model performance was more variable in simulating the experiments with the highly simplified (ethylene only) surrogate, though the observed reactivity trends were correctly predicted. The greater variability is attributable in part to the greater sensitivity of the simpler systems to mechanism differences, as indicated above. However, it can also be attributable to the greater sensitivity of simulations of the ethene reactivity experiments to uncertainties in reaction conditions and the ethene mechanism. With more base ROG components present, errors in the mechanisms and amounts of each individual component becomes relatively less important in affecting the result.

While problems and uncertainties with the mechanisms remain, the results of this study generally give a fairly optimistic picture of the ability of the model to simulate reactivities under atmospheric conditions. This optimism is in part due to the fact that systems with realistic mixtures tend to be less sensitive to errors in the mechanisms than systems that are perhaps most useful for mechanism evaluation. However, one would clearly have more confidence in the fundamental validity of reactivity predictions if the model could satisfactorily predict reactivities in simple as well as complex chemical systems. The data obtained thus far indicate that if the model can simulate reactivity with simple ROG surrogates, it should be able to do so in the more realistic chemical system.

Although this study, in conjunction with our Phase I work, has provided a large experimental data base on VOC reactivity, it is not comprehensive. For example, only a relatively small number of VOCs have been studied using the more realistic 8-component surrogate. The mini-surrogate provide a more comprehensive data set, but the data quality for some important VOCs was not as good as can be obtained using the present facility, and many important VOCs, such as branched alkane isomers, have been inadequately studied. No information has been obtained concerning the effect of temperature on reactivity, and there is only limited information concerning the effects of varying the light sources. Experiments which address some of these issues are discussed in a separate report (Carter et al., 1995a), or are now underway as part of our ongoing studies.

TABLE OF CONTENTS

LIST OF TABLES

LIST OF FIGURES

I. INTRODUCTION

The formation of ground-level ozone is caused by the gas-phase interactions of emitted volatile organic compounds (VOCs) and oxides of nitrogen (NO_x) in the presence of sunlight. Traditional VOC control strategies to reduce ozone have focused on reducing the total mass of VOC emissions, but not all VOCs are equal in the amount of ozone formation they cause. Control strategies which take into account these differences in "reactivities" of VOCs might provide a means for additional ozone reduction which could supplement mass-based controls. Examples of such control strategies include conversion of motor vehicles to alternative fuels and solvent substitutions. However, before reactivity-based VOC strategies can be implemented, there must be a means to quantify VOC reactivity which is sufficiently reliable that it can be used in regulatory applications.

The most direct quantitative measure of the degree to which a VOC contributes to ozone formation in a photochemical air pollution episode is its "incremental reactivity" (Carter and Atkinson, 1987; 1989; Chang and Rudy, 1990; Russell, 1990; Carter, 1991, 1993, 1994). This is defined as the amount of additional ozone formation resulting from the addition of a small amount of the compound to the emissions in the episode, divided by the amount of compound added. This depends not only on the VOC and its atmospheric reactions, but also on the conditions of the environment in which the VOC is emitted, such as NO_x levels and the nature and level of other reactive organic gases (ROGs) which are present. Incremental reactivities of VOCs in the atmosphere cannot be measured experimentally because it is not feasible to duplicate in the laboratory all the environmental factors which affect reactivity. They can, however, be calculated using computer airshed models, given a model for airshed conditions and a mechanism for the VOCs' atmospheric chemical reactions. For example, a set of models for airshed conditions throughout the U.S. and a detailed chemical mechanism were used to calculate a "Maximum Incremental Reactivity" (MIR) scale (Carter, 1993, 1994). Reactivities in this scale were calculated based on effects of VOCs on ozone formation under relatively high NO_x conditions where changes in VOC emissions have the greatest effect on ozone formation (Carter, 1991, 1994). This scale has been adopted by the California Air Resources Board (ARB) for the derivation of reactivity adjustment factors for use in vehicle emissions standards (CARB 1991).

However, such calculations can be no more reliable than the chemical mechanisms upon which they are based. To be minimally suitable for this purpose, such mechanisms need to be evaluated under controlled conditions by comparing their predictions against results of environmental chamber experiments in which the VOCs react in the presence of NO_x to form ozone. Although the MIR scale gives reactivity factors for over 100 compounds (Carter, 1993, 1994), at the time the chemical mechanism used to calculate it was developed, less than a dozen compounds had been tested against results of environmental chamber experiments.

Furthermore, only a few of those experiments provided direct tests of the mechanisms' ability to predict incremental reactivities.

The Statewide Air Pollution Research Center (SAPRC), in conjunction with the College of Engineering, Center for Environmental Research and Technology (CE-CERT), has been conducting a multi-year environmental chamber program to address these data needs. In the first phase of this program, we measured the incremental reactivities of 36 representative VOCs under maximum incremental reactivity conditions using a simplified "surrogate" mixture to represent ROGs in the atmosphere and a blacklight light source. The results have been described previously (Carter et al., 1993a). As expected, it was found that incremental reactivities of VOCs varied widely, even after differences in their atmospheric reaction rates were taken into account. A large part of these differences could be attributed to differences among VOCs in their effects on radical levels, and in addition VOCs were found to differ in the amounts of O_3 formation and NO oxidation estimated to be caused by their direct reactions. The current chemical mechanism was found to be able to simulate the experimental reactivity data to within the experimental uncertainty for approximately half the VOCs studied, and qualitatively predicted the observed reactivity trends. However, the results indicated that refinements are needed to the mechanisms for a number of compounds, including branched alkanes, alkenes, aromatics, acetone, and possibly even formaldehyde. The possibility that some of the discrepancies were due to uncertainties in the model for the base case experiment could not be ruled out, and the data for some of the compounds provided an imprecise test of the mechanism because of run-to-run variability of conditions.

These Phase I data were important in providing experimental reactivity data for a large variety of VOCs under conditions where O_3 formation is most sensitive to VOC emissions. However, they provided no information concerning the effect on VOC reactivity on variations of environmental conditions, such as relative NO_x levels or the nature of the other ROGs which are present. All the Phase I experiments employed "maximum reactivity" conditions where NO_x was in excess, an 3-component ROG surrogate mixture which oversimplifies the complex mixture of ROGs in actual atmospheres, and employed a blacklight light source which does not give a good representation of sunlight in some wavelength regions. In addition, there appeared to be an inconsistency between the results of this study and past environmental chamber data concerning the mechanism for m-xylene which provided the best fits to the results of the base case experiments.

Phase II of this project had two major components. The first consisted of measuring incremental reactivities of representative VOCs using different ROG surrogate mixtures and under lower NO_x conditions. The second consisted of obtaining experimental data to assess the consistency and utility of the entire environmental chamber data base used to evaluate the chemical mechanisms. The major effort in this regard was to determine the effect of varying the light source on the ability of models to simulate the results of environmental chamber

experiments. The work on the second component is discussed in the document entitled "Environmental Chamber Studies of Atmospheric Reactivities of Volatile Organic Compounds. Effects of Varying Chamber and Light Source" (Carter et al., 1995a). In this document, we describe the work on the effects of varying ROG surrogate and NO_x conditions on experimentally measured incremental reactivities.

As indicated above, the ROG surrogate used in the Phase I study is a highly simplified approximation of the ROGs actually emitted into the atmosphere. Although the main purpose of the Phase I study was not to simulate atmospheric conditions exactly, but instead to provide data for mechanism evaluation, if the chemical conditions of the experiments are too unrealistic, the data may not provide an appropriate test to the parts of the mechanism which are important in affecting predictions of atmospheric reactivity. On the other hand, it can be argued that use of even simpler ROG surrogates may be preferable for mechanism evaluation, since if mechanisms for important components of the base ROG are uncertain, one is unsure if poor fits of calculated to experimental reactivities may be due in errors of the base ROGs' mechanisms rather than that of the test VOC, or (worse) whether good fits may be due to compensating errors. The best way to evaluate this would be to measure incremental reactivities using differing ROG surrogates, both to determine the effect of changing the ROG surrogate on incremental reactivity, and how use of different types of ROG surrogates affect the model's ability to predict reactivity.

To determine the most appropriate surrogates to use for such a study, we first conducted a modeling study of the effects of varying ROG surrogates on experimental measurements of incremental reactivity, and how experimental incremental reactivities correlate with those in the atmosphere. The results of the initial modeling study, the subsequent experimental measurements, and the evaluation of the current detailed mechanism using the experiments, are discussed in this report.

Another limitation of the Phase I study was that it measured incremental reactivities only under relatively high NO_x, "maximum reactivity" conditions. Previous modeling work (e.g., Carter and Atkinson, 1989; Carter, 1991, 1994) indicate that VOC reactivities can be quite different under lower NO_x conditions, because they are affected by different aspects of a VOC's reaction mechanism. In particular, reactivities under low NO_x conditions are highly sensitive to NO_x sinks in the VOCs' oxidation mechanisms, but this aspect of the mechanism has no effect on high NO_x or maximum reactivities. Therefore, as part of this phase of the program, we measured incremental reactivities of representative VOCs under low NO_x conditions, using the most realistic of the ROG surrogates employed. The results of these experiments, and the performance of the current mechanisms, are also presented in this report.

II. MODELING ANALYSIS OF ROG SURROGATES

Incremental reactivity determinations involve measuring (or calculating) the effect of adding a particular VOC to a mixture containing NO_x and other reactive organic gases. Previous modeling analyses have shown that the other reactive organic species which are present might affect the incremental reactivity of the added VOC (e.g., Carter, 1991). Because of this, when using environmental chamber experiments to measure incremental reactivity, it is important that the ROG mixture employed in the experiment to represent VOCs in the atmosphere (the "ROG surrogate") be good representation of atmospheric VOCs in terms of their effect on reactivity results. It is also important that the effect that differences between the experimental ROG surrogate and atmospheric mixtures be understood. One approach in conducting such experiments is to use a highly complex mixture designed simulate closely as possible those measured in the atmosphere. However, this has experimental difficulties, and the complexity of the system reduces the utility of the data for detailed mechanism evaluation. Another approach is to use highly simplified mixtures which is experimentally more tractable and provides a better test for mechanism evaluation, and allow the mechanism to take into account the effects of the different VOCs present in the atmosphere. This is essentially the approach employed in our Phase I study (Carter et al., 1993a). However, to have confidence in this approach, reactivity data using different ROG surrogates must be obtained so the ability of the mechanism to account for these effects to be evaluated. This necessarily includes experiments with more realistic ROG surrogates, for comparison with results with simpler mixture.

Before conducting experiments with varying ROG surrogates, a modeling analyses was carried out to evaluate alternative ROG surrogates for use in environmental chamber experiments to measure incremental reactivities of VOCs. One objective was to find a ROG surrogate mixture which is as simple as possible, yet would yield results which are equivalent to use of realistic ambient ROG mixtures. A second objective was to evaluate how closely reactivities measured using the 3-component mini-surrogate employed in the previous studies would correspond to reactivities measured using more realistic surrogates. A third objective was to evaluate the use of an even simpler surrogates than this mini-surrogate, which might reduce some of the uncertainties and potential for compensating errors when using reactivity data for evaluating mechanisms. This study and its findings are described in this section.

A. Derivation of Ambient ROG Mixture

The composition of the ambient ROG mixture used as the basis for deriving the ROG surrogate for chamber experiments is given on Table 1. The derivation of this mixture is summarized below.

Table 1. Detailed composition of the ambient air ROG mixture.

SAPRC Species	Description	ppb/ppmC	Carbon %
ETHANE	Ethane	19.1	3.83
PROPANE	Propane	15.6	4.69
N-C4	n-Butane	19.5	7.80
N-C5	n-Pentane	6.0	3.01
N-C6	n-Hexane	2.1	1.28
N-C7	n-Heptane	1.0	0.71
N-C8	n-Octane	0.7	0.54
N-C9	n-Nonane	0.8	0.73
N-C10	n-Decane	2.2	2.25
N-C11	n-Undecane	0.4	0.39
2-ME-C3	Isobutane	8.1	3.26
2-ME-C4	Iso-Pentane	15.4	7.68
22-DM-C4	2,2-Dimethyl Butane	0.4	0.25
23-DM-C4	2,3-Dimethyl Butane	1.0	0.58
24-DM-C5	2,4-Dimethyl Pentane	0.6	0.41
23-DM-C5	2,3-Dimethyl Pentane	1.1	0.76
CYCC5	Cyclopentane	0.8	0.39
ME-CYCC5	Methylcyclopentane	1.6	0.98
CYCC6	Cyclohexane	0.8	0.46
ME-CYCC6	Methylcyclohexane	0.7	0.52
ET-CYCC6	Ethylcyclohexane	0.2	0.14
BR-C6	Branched C6 Alkanes	6.2	3.72
BR-C7	Branched C7 Alkanes	3.6	2.49
BR-C8	Branched C8 Alkanes	4.3	3.47
BR-C9	Branched C9 Alkanes	1.8	1.65
BR-C10	Branched C10 Alkanes	2.1	2.08
BR-C12	Branched C12 Alkanes	0.2	0.24
BR-C13	Branched C13 Alkanes	0.1	0.08
CYC-C7	C7 Cycloalkanes	0.1	0.09
	Total Alkanes	173.1	54.48
ETHENE	Ethene	13.4	2.68
PROPENE	Propene	3.0	0.90
1-BUTENE	1-Butene	2.5	0.98
3M-1-BUT	3-Methyl-1-Butene	0.3	0.14
1-PENTEN	1-Pentene	0.8	0.39
1-HEXENE	1-Hexene	0.6	0.34
2M-1-BUT	2-Methyl-1-Butene	0.8	0.41
T-2-BUTE	trans-2-Butene	1.0	0.41
C-2-BUTE	cis-2-Butene	0.8	0.34
13-BUTDE	1,3-Butadiene	0.5	0.21
ISOPRENE	Isoprene	0.5	0.24
CYC-HEXE	Cyclohexene	0.2	0.12
A-PINENE	a-Pinene	0.5	0.54
3-CARENE	3-Carene	0.2	0.16
C5-OLE1	C5 Terminal Alkanes	0.3	0.17
C6-OLE1	C6 Terminal Alkanes	0.4	0.26
C7-OLE1	C7 Terminal Alkanes	1.5	1.06
C8-OLE1	C8 Terminal Alkanes	0.3	0.21
C9-OLE1	C9 Terminal Alkanes	0.6	0.50
C11-OLE1	C11 Terminal Alkanes	0.1	0.11
C5-OLE2	C5 Internal Alkenes	2.9	1.43
C6-OLE2	C6 Internal Alkenes	1.2	0.72
C7-OLE2	C7 Internal Alkenes	0.4	0.27
C8-OLE2	C8 Internal Alkenes	0.2	0.17
C9-OLE2	C9 Internal Alkenes	0.2	0.20
C10-OLE2	C10 Internal Alkenes	0.1	0.11
C11-OLE2	C11 Internal Alkenes	0.1	0.11
	Total Alkenes	33.5	13.29
BENZENE	Benzene	3.3	1.98
TOLUENE	Toluene	9.0	6.27
C2-BENZ	Ethyl Benzene	1.2	0.98
N-C3-BEN	n-Propyl Benzene	0.4	0.33
I-C3-BEN	Isopropyl Benzene	0.3	0.24
C9-BEN1	C9 Monosub. Benzenes	0.2	0.19
S-C4-BEN	s-Butyl Benzene	0.3	0.30
C10-BEN1	C10 Monosub. Benzenes	0.2	0.19
C11-BEN1	C11 Monosub. Benzenes	0.6	0.63
C12-BEN1	C12 Monosub. Benzenes	0.0	0.06
O-XYLENE	o-Xylene	1.8	1.45
M-XYLENE	m-Xylene	4.2	3.37
C9-BEN2	C9 Disub. Benzenes	2.6	2.37
C10-BEN2	C10 Disub. Benzenes	2.0	2.03
C11-BEN2	C11 Disub. Benzenes	0.1	0.10
C12-BEN2	C12 Disub. Benzenes	0.0	0.04
135-TMB	1,3,5-Trimethyl Benzene	0.7	0.67
123-TMB	1,2,3-Trimethyl Benzene	0.6	0.55
124-TMB	1,2,4-Trimethyl Benzene	2.5	2.28
C9-BEN3	C9 Trisub. Benzenes	0.1	0.06
C10-BEN3	C10 Trisub. Benzenes	1.0	0.98
C11-BEN3	C11 Trisub. Benzenes	0.1	0.10
C12-BEN3	C12 Trisub. Benzenes	0.0	0.04
C10-BEN4	C10 Tetrasub. Benzenes	0.4	0.40
C9-STYR	C9 Styrenes	0.3	0.31
C10-STYR	C10 Styrenes	0.3	0.30
	Total Aromatic HC's	32.3	26.19
FORMALD	Formaldehyde	7.9	0.79
ACETALD	Acetaldehyde	4.8	0.95
PROPALD	C3 Aldehydes	0.7	0.21
C4-RCHO	C4 Aldehydes	0.3	0.12
C5-RCHO	C5 Aldehydes	1.1	0.53
C6-RCHO	C6 Aldehydes	0.7	0.44
	Total Aldehydes	15.5	3.05
ACETONE	Acetone	3.1	0.93
MEK	C4 Ketones	1.1	0.44
	Total Ketones	4.2	1.37
BENZALD	Benzaldehyde	0.2	0.11
ACETYLEN	Acetylene	7.5	1.50

1. Hydrocarbon Portion

After discussions with Bart Croes of the CARB, Jeffries of the University of Carolina (UNC) and others, we concluded that for the hydrocarbon portion of the ROG mixture it is appropriate to use the same data as used by Jeffries and co-workers to derive the "SynUrban" mixture for the current UNC/CRC project (Jeffries et al., 1992). This is based on EPA canister data collected in 66 US cities from 1985-1988. The averaged detailed composition data was provided by Dr. Jeffries and were assigned SAPRC detailed model species with the assistance of Bart Croes. Table 2 presents the averaged hydrocarbon data we received and our model species assignments. There are a number of ambiguities

Table 2. EPA All City Average hydrocarbon data used to derive ambient ROG Mixture, and assignments to SAPRC Model Species. Data from Jeffries et al. (1992).

ID#	ppbC/ ppmC	Description on Spreadsheet	SAPRC Model Species Assignment
		Alkanes	
1	73.6	n-butane	N-C4
2	46.3	propane	PROPANE
3	39.7	ethane	ETHANE
4	31.2	n-pentane	N-C5
5	19.0	n-decane	N-C10
6	13.3	n-hexane,2-ethyl-1-butene	N-C6
7	7.6	n-nonane	N-C9
8	7.4	n-heptane	N-C7
9	7.3	n-butane	N-C4
10	5.6	n-octane	N-C8
11	4.6	unknown	(ignored) [a]
12	4.3	c10	N-C10
13	4.0	c11	N-C11
14	3.4	unknown	(ignored)
15	2.8	c7	BR-C7
16	2.5	c12	BR-C12
17	2.3	c3	PROPANE
18	2.2	c6	BR-C6
19	1.7	c9	BR-C9
20	1.5	c8	BR-C8
21	0.8	paraffin	(ignored)
22	0.8	c4	2-ME-C3
26	79.6	isopentane	2-ME-C4
27	33.0	isobutane	2-ME-C3
28	21.6	4-methylnonane	BR-C10
29	21.1	2-methylpentane	BR-C6
30	15.3	3-methylpentane	BR-C6
31	13.3	2-methylhexane	BR-C7
32	8.3	3-methylhexane	BR-C7
33	5.4	3-methylheptane	BR-C8
34	4.5	2-methylheptane	BR-C8
36	4.0	4-methyloctane	BR-C9
37	3.1	3-methyloctane	BR-C9
38	0.8	c13	BR-C13
39	7.9	2,3-dimethylpentane	23-DM-C5
40	6.0	2,3-dimethylbutane	23-DM-C4
41	4.2	2,4-dimethylpentane	24-DM-C5
42	2.8	2,5-dimethylhexane,3-mecyclohexen	BR-C8
44	2.8	2,4-dimethylhexane	BR-C8
45	2.6	2,2-dimethylbutane	22-DM-C4
46	2.0	2,4-dimethylheptane	BR-C9
47	1.5	2,5-dimethylhexane	BR-C8
48	1.5	2,3-dimethylheptane	BR-C9
49	1.4	3,3-dimethylpentane	BR-C7
51	0.9	2,5-dimethylheptane	BR-C9
58	12.7	2,2,4-trimethylpentane	BR-C8
59	4.8	2,3,4-trimethylpentane	BR-C8
60	3.9	2,2,5-trimethylhexane	BR-C9
63	10.2	methylcyclopentane	ME-CYCC5
64	5.4	methylcyclohexane	ME-CYCC6
65	4.8	cyclohexane	CYCC6
66	4.0	cyclopentane	CYCC5
67	1.5	ethylcyclohexane	ET-CYCC6
68	0.9	cycloheptane	CYC-C7
		Aromatics	
79	20.5	benzene	BENZENE
80	65.0	toluene	TOLUENE

Table 2 (continued)

ID#	ppbC/ ppmC	Description on Spreadsheet	SAPRC Model Species Assignment
81	10.2	ethylbenzene	C2-BENZ
82	4.6	isoamylbenzene	C11-BEN1
83	3.4	n-propylbenzene	N-C3-BEN
84	3.1	sec-butylbenzene	S-C4-BEN
86	2.5	isopropylbenzene	I-C3-BEN
87	1.9	n-amylbenzene	C11-BEN1
88	0.6	n-hexylbenzene	C12-BEN1
89	34.9	m&p-xylene	M-XYLENE
90	15.0	o-xylene	O-XYLENE
91	9.6	m-ethyltoluene	C9-BEN2
92	7.1	1.3-diethylbenzene	C10-BEN2
93	7.1	p-ethyltoluene	C9-BEN2
94	6.5	o-ethyltoluene	C9-BEN2
95	5.6	1-methyl-4-isopropylbenzene	C10-BEN2
97	4.8	1,4-diethylbenzene	C10-BEN2
98	3.2	p,m,o-methylstyrene	C9-STYR
100	2.2	1,2-diethylbenzene	C10-BEN2
101	23.6	1,2,4-trimethylbenzene	124-TMB
102	7.4	1,2-dimethyl-3-ethylbenzene	C10-BEN3
103	6.9	1,3,5-trimethylbenzene	135-TMB
104	5.7	1,2,3-trimethylbenzene	123-TMB
105	4.0	c10	0.5 C10-BEN1 +0.35 C10-BEN2 +0.15 C10-BEN3
106	3.9	c9	0.5 C9-BEN1 +0.35 C9-BEN2 +0.15 C9-BEN3
107	3.1	2,6-dimethylstyrene	C10-STYR
108	2.2	1,2-dimethyl-4-ethylbenzene	C10-BEN3
109	2.0	c11	0.5 C11-BEN2 +0.50 C11-BEN3
110	1.5	1,2,4,5-tetramethylbenzene	C10-BEN4
111	1.4	1,2,3,5-tetramethylbenzene	C10-BEN4
112	1.2	1,2,3,4-tetramethylbenzene	C10-BEN4
113	0.9	c12	0.5 C12-BEN2 +0.50 C12-BEN3
		Alkenes	
118	27.8	ethylene	ETHENE
119	9.3	propene	PROPENE
120	8.8	2-methylpropylene,butene-1	1-BUTENE
124	7.7	2,3,3-trimethyl-1-butene	C7-OLE1
126	4.3	2-methyl-1-butene	2M-1-BUT
127	4.2	c9	0.5 C9-OLE1 +0.5 C9-OLE2
128	4.0	1-pentene	1-PENTEN
129	3.5	c5	0.5 C5-OLE1 +0.5 C5-OLE2
130	3.5	2-methyl-1-pentene,1-hexene	1-HEXENE
132	3.2	c6	0.5 C6-OLE1 +0.5 C6-OLE2
133	3.1	1-nonene	C9-OLE1
135	2.5	c8	0.5 C8-OLE1 +0.5 C8-OLE2
136	2.3	c10	0.5 C10-OLE1 +0.5 C10-OLE2
137	2.3	2,3,3-trimethyl-1-butene	C7-OLE1
138	2.2	c11	0.5 C11-OLE1 +0.5 C11-OLE2
139	1.4	c4	1-BUTENE
140	1.4	3-methyl-1-butene	3M-1-BUT
141	1.1	c7	0.5 C7-OLE1 +0.5 C7-OLE2
142	1.1	4-methyl-1-pentene	C6-OLE1
143	0.9	1-octene	C8-OLE1
144	0.9	olefin	(ignored)
145	0.8	c7	0.5 C7-OLE1 +0.5 C7-OLE2
146	8.5	c-2-pentene	C5-OLE2
147	4.3	t-2-butene	T-2-BUTE
148	4.3	t-2-pentene	C5-OLE2
149	3.5	c-2-butene	C-2-BUTE
150	2.2	2-methyl-2-pentene	C6-OLE2
151	1.9	t-4-methyl-2-pentene	C6-OLE2
152	1.2	c&t-3-methyl-2-pentene	C6-OLE2
154	1.1	t-heptene-2	C7-OLE2

Table 2 (continued)

ID#	ppbC/ ppmC	Description on Spreadsheet	SAPRC Model Species Assignment
155	1.1	c	(ignored)
159	0.8	c-heptene-2	C7-OLE2
163	0.6	c-4-methyl-2-pentene	C6-OLE2
166	0.5	c-2-octene	C8-OLE2
170	0.3	2-methyl-2-butene	C5-OLE2
171	2.5	isoprene	ISOPRENE
172	2.2	1,3-butadiene	13-BUTDE
177	1.2	cyclohexene	CYC-HEXE
179	5.6	a-pinene	A-PINENE
180	1.7	delta-3-carene	3-CARENE
		Acetylenes	
182	15.6	acetylene	ACETYLEN

[a] Unknowns constituted 1% of the mixture. No attempt was made to assign them.

in the component descriptions, some involving unspeciated aromatics and others unspeciated alkenes. The assignments we used for unspeciated aromatics were the same as used by Jeffries et al. (1989). However, Jeffries et al. (1989) assumed that all unspeciated alkenes were terminal, while Croes (private communication) assumed equal amounts of terminal and internal alkenes for the unspeciated alkanes when analyzing the earlier EPA data derive the hydrocarbon composition to use when calculating reactivity scales (Carter, 1993, 1994). The latter assumption was used in these assignments.

Table 3 shows a summary of the classes of species in the hydrocarbon mixture derived using the assignments on Table 2 and compares them with the hydrocarbon composition used in our reactivity modeling studies with the composition the "SynUrban" mixture used by Jeffries et al. (1993). These data are given in terms of moles of lumped molecule condensed model species per mole carbon hydrocarbon, because this is the basis for deriving the ROG surrogate mixture for chamber studies (see below). The percentages next to the composition data give the difference between the mixture derived in this work and the one in the first column. In some cases, the composition was derived assuming the unspeciated alkenes are all terminal, as assumed by Jeffries et al. (1989) ("UNC Olefin Ass't") is shown for comparison. The following additional mixtures are shown for comparison:

- "Old EPA Mixture" is the EPA all city average data from Jeffries et al. (1989), which was used in the reactivity calculations of Carter (1991) EPA report. It was derived assuming that all the unspeciated alkenes are terminal, so it is also compared with the new composition when derived with this same assumption. The new mixture has significantly less ethene and slightly more alkanes and aromatics than the old mixture. Regardless

Table 3. Comparison of Lumped Model Species for various ambient air hydrocarbon mixtures or hydrocarbon surrogates.

Lumped Model Species	Lumped Model Species / ROG Hydrocarbon (ppb/ppmC, Difference)				
	Old EPA Mixture	New Mixture		New Mixture (UNC Olefin ass't)	
Lumped Alkanes #1	73.7	74.1	1%		
Lumped Alkanes #2	21.6	23.4	8%		
Ethylene	20.3	14.0	-31%		
Terminal Alkenes	15.3	10.8	-29%	12.2	-20%
Internal & Dialkenes	8.2	10.9	32%	9.5	15%
Monoalkyl Benzenes	13.5	13.9	3%		
Higher Aromatics	16.1	17.0	6%		
	ARB Mix #1	New Mixture			
Lumped Alkanes #1	71.4	74.1	4%		
Lumped Alkanes #2	22.2	23.4	5%		
Ethylene	14.1	14.0	0%		
Terminal Alkenes	12.5	10.8	-14%		
Internal & Dialkenes	13.4	10.9	-19%		
Monoalkyl Benzenes	14.1	13.9	-1%		
Higher Aromatics	17.2	17.0	-1%		
	UNC SynUrban	New Mixture		New Mixture (UNC Olefin ass't)	
Lumped Alkane #1	73.7	74.1	1%		
Lumped Alkane #1	70.7	74.1	5%		
Lumped Alkane #2	24.8	23.4	-6%		
Ethylene	13.6	14.0	3%		
Terminal Alkenes	11.2	10.8	-3%	12.2	9%
Internal & Dialkenes	9.4	10.9	16%	9.5	1%
Monoalkyl Benzenes	14.8	13.9	-6%		
Higher Aromatics	18.4	17.0	-8%		

of how the unspeciated olefins are assigned, the new mixture has a significantly higher internal to terminal olefin ratio than the older mixture, even if the unspeciated olefins are processed in the same way. Note that the assignments for the unspeciated olefins has a non-negligible effect on the overall olefin composition.

- "ARB Mix #1" is the hydrocarbon composition that was provided by Croes for calculating the 1991 reactivity scale for the ARB (Carter, 1993, 1994, ARB, 1991). It is based on 1987-1988 EPA air quality data. It is similar to the new mixture, except that it has an ~20% lower alkene/alkane ratio. This presumably represents the variability of the EPA data base, and it is not clear which mixture is more realistic.

- "UNC SynUrban" is the hydrocarbons in the current UNC ROG surrogate mixture, which was derived from the same data as our mixture. The agreement is within ±9% when the unspeciated olefins are assigned assuming they are all terminal. It is not clear why the agreement is not better than this, since the two mixtures are derived based on the same data. However, the main difference between the hydrocarbons in the UNC SynUrban mixture and the mixture we derive is the difference in the internal /terminal alkene ratio caused by different assignments for the unspeciated alkenes.

2. Oxygenate Portion

The EPA aldehyde data base was used to derive the UNC SynUrban surrogate composition (Jeffries et al. 1989, 1992). However, that data base includes only measurements for formaldehyde and acetaldehyde, while the SCAQS data base also include data for a number of other higher aldehydes and ketones (Croes et al., 1993). The EPA and SCAQS data bases are consistent in indicating that formaldehyde and acetaldehyde each constitute ~1% of the total ROG carbon, but the SCAQS data indicate that the ketones and higher aldehydes constitute almost 3% of the total ROG. Because it is more complete, we use the SCAQS rather than the EPA data base to derive the oxygenate component of the mixture. The SCAQS aldehyde data we used is the same as that used to derive the ROG mixture for calculating the ARB reactivity scale (ARB, 1991), and was provided by Bart Croes. The total oxygenates constitute 4.75% of the ROG carbon. The constituents are listed in Table 1, and the concentrations of all the hydrocarbons are reduced so the total mixture (hydrocarbon + oxygenates) is normalized to 1 carbon.

B. Derivation of the Lumped Molecule (Lumped) Surrogate

The mixture in Table 1 was used to derive a simplified ROG surrogate which we designate the "lumped molecule", or (for simplicity) the "lumped" surrogate. Although simplified, it is designed to have the same level of chemical detail as incorporated in the current generation of airshed models. It is based on (1) aggregating the mixture into lumped model species in a condensed (lumped molecule) mechanism used in airshed models, and (2) using a single "real" compound to represent each lumped species. The condensed mechanism and lumping approach is the latest version of the SAPRC condensed mechanism, which was recently implemented in the UAM (Lurmann et al., 1991) and the SARMAP models. Since it is documented by Lurmann et al. (1991), it is not discussed in detail here. For each lumped species which does not represent a specific compound, the representative compound chosen was the one which had the most environmental chamber data available to test its mechanism. The various lumped model species, and the compound representing them, are summarized below.

The Lumped Alkanes #1 (ALK1) group consists of alkanes, alcohols, ethers, and other saturated compounds which react with OH radicals with a 300 K constant of less than 10^4 $ppm^{-1} \cdot min^{-1}$. This group is derived using "reactivity weighting"

with IntOH = 110 ppt-min. [See Carter and Lurmann, 1990 and Lurmann et al., 1992 for a discussion of reactivity weighting. The IntOH of 110 ppt-min is appropriate for regional model application (Stockwell, private communication, 1989 as cited by Carter and Lurmann, 1990), but the results are not highly sensitive to this.] n-Butane is used to represent this class, since there is by far the most environmental chamber data for this compound.

The Lumped Alkanes #2 (ALK2) group consists of alkanes, alcohols, ethers, and other saturated compounds which react with OH radicals with a 300 K constant of greater than 10^4 ppm^{-1} min^{-1}. This group represents the individual compounds on mole for mole basis, as is the case for all the other groups except ALK1 and ARO1. It is represented by n-octane, based on availability of chamber data. N-octane-NO_x-air chamber experiments have been carried out in both the SAPRC and UNC chambers, and its incremental reactivity has been measured in our previous reactivity experiments.

Ethylene (ETHE) is represented explicitly.

The group designated Terminal Alkenes (OLE1) represents all alkenes which react with OH radicals with 300 K rate constants of less than 7.5×10^4 ppm^{-1} min^{-1}. (This includes isobutene but not 2-methyl-1-butene.) It is represented by propene because (1) there is by far the most chamber data for it; and (2) the mechanisms for the other terminal alkenes are derived mainly from that for propene.

The Internal + Dialkene (OLE2) group represents all alkenes which react with OH radicals with a 300 K rate constant of greater than 7.5×10^4 ppm^{-1} min^{-1}. This includes most alkenes with more than one substituent around the bond (other than isobutene), and conjugated olefins such as isoprene. It also includes styrenes, since they are lumped as alkenes in the SAPRC mechanism. Although the compound in this group with the most chamber data is probably isoprene, isoprene is usually represented by a separate model species in current models, and it is not a good representative of most of the other alkenes in this group. Trans-2-butene is used to represent this group because a fair amount of chamber data are available for it, including incremental reactivity experiments, and because the general SAPRC internal alkene mechanism is derived based on that estimated for the 2-butenes.

The Monoalkyl Benzene (ARO1) group consists of aromatic hydrocarbons which react with OH radicals with a 300 K rate constant of less than 2×10^4 ppm^{-1} min^{-1}, which include benzene and the monoalkylbenzenes. These are represented using reactivity weighting (see discussion of ALK1, above), except that the group is assigned the OH rate constant of toluene independently of the mixture being represented. (The reactivity weighting factor affects primarily the representation of benzene.) Toluene is used to represent this group, since it is both the dominant species in it, and the one with the most chamber data.

The Higher Aromatic (ARO2) group consists of aromatic hydrocarbons which react with OH radicals with a 300 K rate constant of greater than 2 x 10^4 ppm^{-1} min^{-1}. This includes xylenes, polyalkylbenzenes, and naphthalenes. It is represented by m-xylene, which has the most SAPRC environmental chamber data, whose rate constant is closer to the average for this group than the other xylene isomers.

Formaldehyde (HCHO) is represented explicitly.

Acetaldehyde (CCHO) and higher aldehydes (RCHO) are separate model species in the condensed SAPRC mechanism, though for most other condensed mechanisms they are lumped together. They are also lumped together for the purpose of deriving this surrogate, and are represented by acetaldehyde.

Ketones in the mixture consist of acetone and higher ketones, in amounts of 3 ppb/ppmC and 1 ppb/ppmC, respectively. Because of the relatively low amounts of ketones in this mixture and their low or moderate reactivities, the effect of including them in the surrogate is too small to justify the non-negligible additional experimental effort this would involved. Therefore, the ketones are ignored when developing the ROG surrogate.

The composition of this 9-compound surrogate is summarized on Table 4.The "Inert/Lost Carbon" include the "extra" carbons in the compounds in the ambient mixture which are represented by example compounds with fewer carbons, the fractions of species treated as inert for groups where reactivity weighting was employed, and the ketones. Although this is not strictly speaking a part of the mixture, it must be included as a "virtual reactant" when computing the effective ppmC of the mixture for the purpose of comparing with other mixtures.

It has been argued that the unrepresented "lost carbon" in this mixture may have a non-negligible effect on the system, and they should not be ignored

Table 4. Composition of the "Lumped Molecule" ROG Surrogate

Compound	ppb/ppmC
n-Butane	70.7
n-Octane	22.3
Ethylene	13.4
Propene	10.4
t-2-Butene	10.4
Toluene	13.3
m-Xylene	16.3
Formaldehyde	7.9
Acetaldehyde	7.6
(Inert/Lost Carbon	193.1)

(Jeffries, private communication). This is examined in model calculations discussed in the following section, and it is concluded that their effect is unlikely to be significant.

C. Calculated Effects of Complexity of ROG Surrogate on Mechanistic Reactivities

Although the lumped ROG surrogate given in Table 4 has the same degree of chemical detail as the condensed mechanisms used in current urban and regional airshed models, it is still a major simplification of realistic ambient ROG mixtures. Model simulations, using the SAPRC detailed mechanism (Carter, 1990) were conducted to assess whether use of ROG surrogates with this level of detail, or even simpler surrogates such as the "mini-surrogate" used in the Phase I experiments (Carter et al., 1993a) will significantly affect results of reactivity experiments. Three types of experiments were examined:

- Maximum Reactivity experiments were based on the ROG and NO_x conditions of the Phase I maximum reactivity experiments (Carter et al., 1993a), with the amount of ROG adjusted to yield comparable final ozone levels as the mini-surrogate. The initial ROG (counting "inert/lost" carbon in the surrogate, and the "inert" carbon in the ambient mixture) was 5.5 ppmC, and the initial NO_x was 0.5 ppm.[1]

- Maximum Ozone experiments were derived by reducing the NO_x in the maximum reactivity experiments to approximately the level where the highest ozone levels were achieved in the simulations of the base case runs with the ambient mixture. This turned out to be 0.2 ppm initial NO_x.

- Low NO_x experiments were derived by arbitrarily reducing the initial NO_x in the maximum ozone experiments by another factor of 4, i.e., to 0.05 ppm.

For each type of experiment, the differences between using the following mixtures for the base ROG surrogates were examined:

The Ambient Mix was the ambient mixture used to calculate the 1991 reactivity scale for the ARB (Carter, 1993, 1994; ARB, 1991). (These calculations were conducted prior to the derivation of the new ambient mixture discussed above, but the slight differences of the mixtures should not affect the qualitative results.)

The Ambient Mix with No Lost Carbon employed the same mixture as that discussed above, but was represented by a modified version of the SAPRC mechanism

---

[1] Note that ROG/NO_x of 11 may be maximum ozone or NO_x-limited ratio in an airshed scenario, but it is maximum a reactivity ratio under the conditions of these 6-hour runs.)

was where the effects of the additional carbons on the lumped model species were not ignored. This is to examine the significance of concerns about the "lost carbon" in the ROG surrogate – the standard SAPRC mechanism does not provide a good test in this regard because it also ignores "lost carbon".

The mechanism was modified by having each "lost" carbon in the standard mechanism appear as 1/4 of an MEK molecule whenever the lumped model species reacts.[2] This is more appropriate than simply adding the additional carbon in some form to the initial mixture, since its effect on the initial reaction rate of the lumped model species is already taken into account.[3] The effect of the additional carbon is only "lost" when the lumped model species reacts, and the products are represented by model species with fewer carbons than the actual products which are formed. Since this additional carbon appears in product species, and since MEK is the generic non-aldehyde model species used for products in the SAPRC mechanism, using MEK is an appropriate way to represent the lost carbon in this mechanism. This approach probably over-estimates the effect of this extra carbon, since it uses smaller molecules to represent larger molecules, and larger molecules tend to have lower reactivity per carbon than smaller molecules of similar type. However, erring on the side of overestimating the effect of the lost carbon is useful for the purpose of this test, since if the effect is calculated to be minor, it is probably safe to conclude that it is indeed minor.

The "Full Surrogate" was derived based on the ambient mixture used to calculate the 1991 reactivity scale, using procedures which are exactly the same as the derivation of the "lumped molecule" surrogate in Table 4 from the ambient mixture in Table 1. The relative differences of the various hydrocarbon components are as indicated on Table 3. Note that for calculations where this surrogate was compared with the "ambient mix with no lost carbon", the modified (lost C = 1/4 MEK) mechanism was used for this surrogate as well. The standard mechanism was used for all other calculations.

The "without acetaldehyde" surrogate consisted of the "full surrogate" except that acetaldehyde was removed and formaldehyde was increased to yield the same total moles of aldehydes. (Removing acetaldehyde from the surrogate would simplify the experiments and remove a potential source of irreproducibility, since special procedures are necessary to prepare this compound for injection.)

---

[2] For example, in the standard SAPRC mechanism, the mechanism for the reaction of OH radicals with 1-pentene is represented as: "OH + 1-PENTENE → RO2-R. + RO2. + HCHO + RCHO + -C", where "-C" is an inert counter species representing lost carbon. In the modified mechanism, this reaction is represented as: OH + 1-PENTENE → RO2-R. + RO2. + HCHO + RCHO + 0.25 MEK.

[3] The SAPRC mechanism uses lumped group rate constants derived to represent the mixture of species being represented.

The "without acetaldehyde and n-butane" surrogate consists of the "without acetaldehyde" surrogate, but with the n-butane and n-octane replaced by an equal molar amount of n-hexane. (Simplifying the alkanes will simplify the GC analyses, and make it easier to measure the reactivities of n-butane and n-octane.)

The "without acetaldehyde and toluene" surrogate consisted of the "without acetaldehyde" surrogate but with the toluene removed and the m-xylene increased to yield an equal number of moles of aromatics. (Simplifying the aromatics would simplify the GC analyses, and remove a potential source of variability.)

The "without acetaldehyde, toluene and n-butane" surrogate consisted as the "without acetaldehyde and n-butane" surrogate but with toluene removed and m-xylene increased as with the other "without toluene" surrogate.

The "Mini-Surrogate" was the same three-component (ethene, n-hexane, and m-xylene) surrogate as used in the Phase I reactivity experiments (Carter et al., 1993a). This surrogate is more reactive than the ambient mixture on a per carbon basis. To make this more comparable to the ambient mixture in overall reactivity, 274 ppb/ppmC of "inert carbon" is added to the mixture. This number was chosen to give this mixture the same incremental reactivity in the ambient mixture as the "base case, least squares error" reactivity scale of Carter (1993, 1994).

The "Ethylene Surrogate" employed ethylene alone to represent the simplest possible surrogate which might provide at least an approximate representation of the chemical environment in which VOCs react. For a single compound to be suitable for a base ROG surrogate, it must at a minimum (1) have a reasonably well understood mechanism; (2) provide sufficient internal radical sources so its NO_x-air reactions provide a reactive system, but (3) not have such high radical sources that the it produces an unnaturally radical rich environment; and (4) be easy to deal with experimentally. Ethylene is the most qualified on all these counts. 456 ppb/ppmC of "inert carbon" is added to this "mixture" to yield a surrogate which gives the maximum ozone at the same nominal ROG/NO_x ratio as the mini-surrogate. (I.e., 544 ppbC of ethylene is nominally 1 ppmC ROG surrogate.)

Incremental reactivities of representative VOCs were calculated for each type of experiment and ROG surrogate. The calculations consisted of model simulations of the base case experiment, combined with simulations of the experiment with a test VOC added. The results are given in terms of the effects of the VOC on ozone formed + NO oxidized, $\Delta([O_3]-[NO])$, and also the effect of the VOC on integrated OH radical levels, or IntOH. The former is more generally useful measure of effects of VOC on the chemical factors affecting O_3 than reactivity with respect to $[O_3]$ alone, since it provides a meaningful measure even when excess NO suppresses O_3 formation. The latter is a useful measure of

the effect of the VOC on radical levels, which affects O_3 reactivity by affecting how rapidly all other VOCs present react to form ozone.

The results of these calculations are given in terms of mechanistic reactivities because this normalizes out the large effects of differences of VOCs in how rapidly they react, which (in a relative sense at least) are not affected by changes in the base ROG mixture. [Mechanistic reactivities refer to the effect of adding the VOC (on $\Delta([O_3]-[NO])$ or IntOH) relative by the amount of VOC reacted, while incremental reactivities refer to the effects relative to the amount of VOC added.] For simplicity, these model simulations calculated "true" incremental or mechanistic reactivity, i.e., the effect of adding only small amounts of the VOC to the mixture. Although this is an approximation of what can be experimentally measured, it should be sufficient for determining the magnitude of the effect of changing the ROG surrogate.

Incremental reactivities were calculated for CO, methane, propane, n-butane, n-octane, iso-octane, ethene, propene, trans-2-butene, isobutene, 1-hexene, benzene, toluene, m-xylene 135-trimethylbenzene, formaldehyde, acetaldehyde, acetone, methanol and ethanol. Although this is not a comprehensive list of all compounds of interest, they represent a full variety of types of mechanisms which might respond differently to changes in the ROG surrogate.

The comparisons of the mechanistic reactivities in the simulated experiments using the different ROG surrogate mixtures are shown on Figures 1-7. These give plots of the mechanistic reactivities calculated for runs with the simplified surrogates against those calculated for comparable using the ambient mixture. Each point represents a different VOC; for example, the highest point on the plots for the "maximum reactivity" experiments is formaldehyde, and the lowest point is n-octane. All points lying on the line would mean the mechanistic reactivities are exactly the same in the experiments with the surrogate as in the experiments with the ambient mixture, i.e., that the model predicts that using the surrogate would yield identical measured reactivities as using the ambient mixture.

Figure 1 compares the $d(O_3-NO)$ and IntOH reactivities calculated for the three types of experiments the 9-component "lumped molecule" ROG surrogate and the ambient mixture. The circles show the reactivities calculated with the standard SAPRC mechanism, and the diamonds show the reactivities calculated with the version of the mechanism which represents lost product carbons as MEK. It can be seen that regardless of which mechanism is used, the experiments with the surrogate are calculated to yield essentially identical reactivities as experiments with the ambient mixture. The small differences that are seen would be impossible to detect experimentally. Note that the SAPRC mechanism represents the chemical detail of the complex mixture to the extent possible given the current knowledge at the time the Carter (1990) mechanism was developed, so this

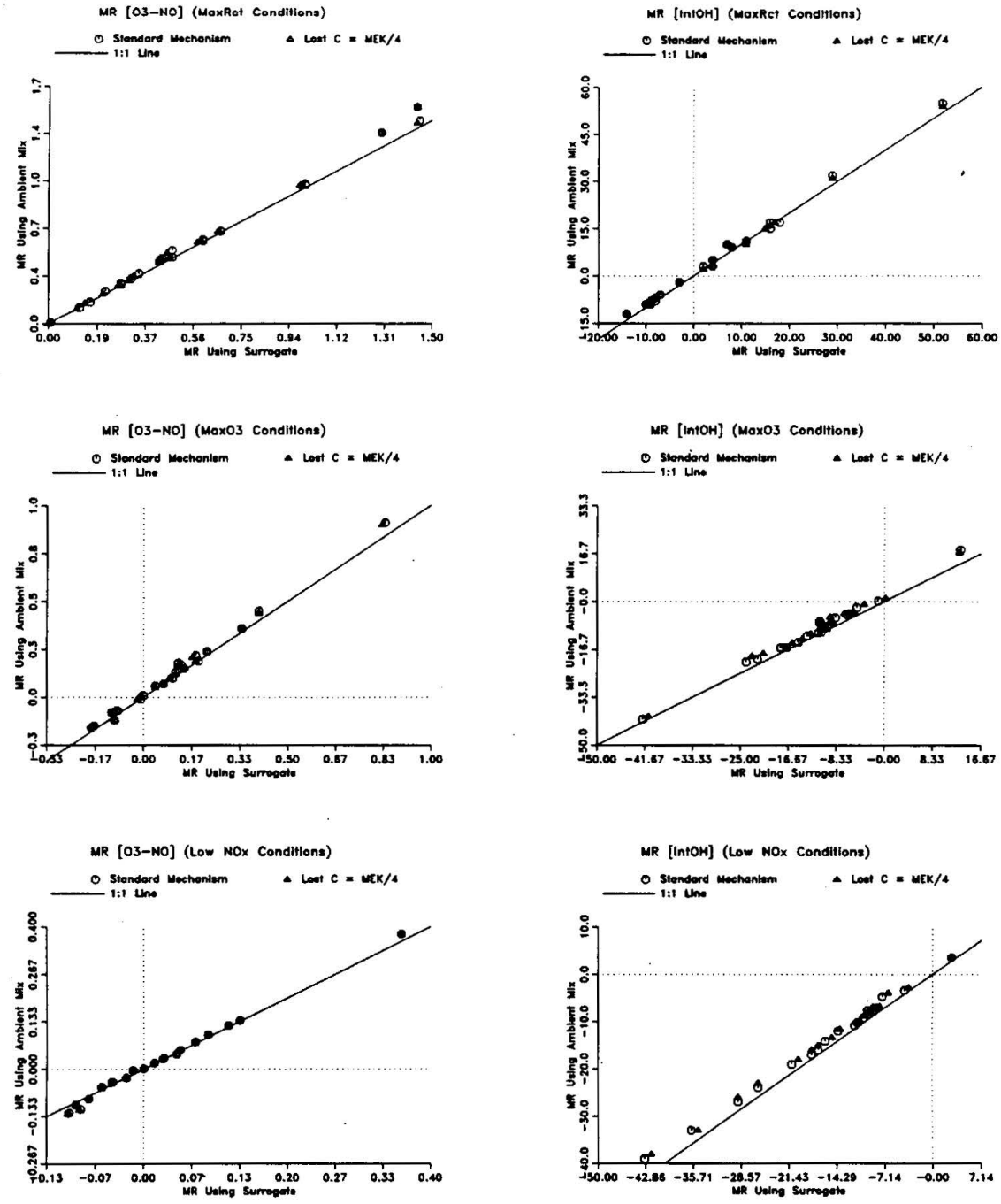

Figure 1. Plots of Calculated Mechanistic Reactivities of Representative Species in Chamber Experiments Using the Lumped ROG Surrogate Against those for Experiments using the Ambient ROG Mixture. The "Lost C = MEK/4" mechanism represents lost carbons by MEK.

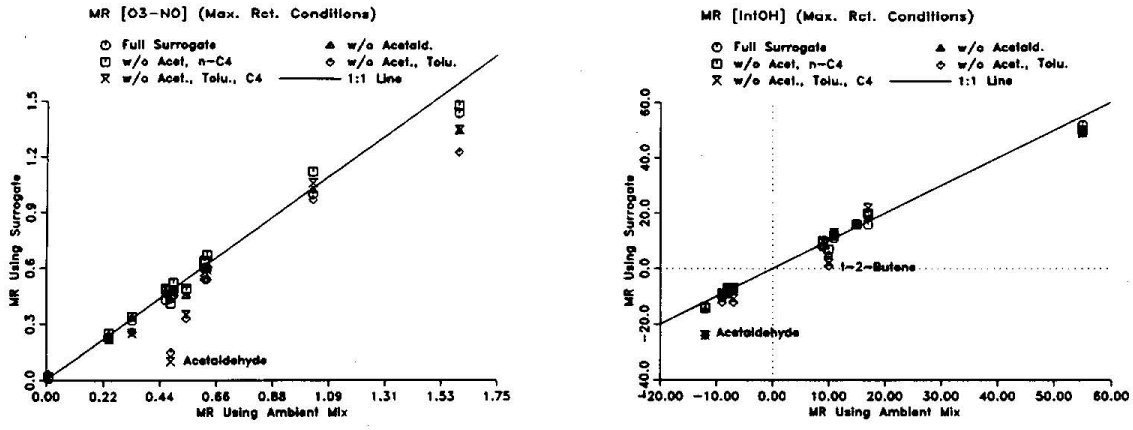

Figure 2. Plots of calculated mechanistic reactivities of selected species in maximum reactivity chamber experiments using various ROG surrogates, against those for similar experiments using the ambient ROG Mixture.

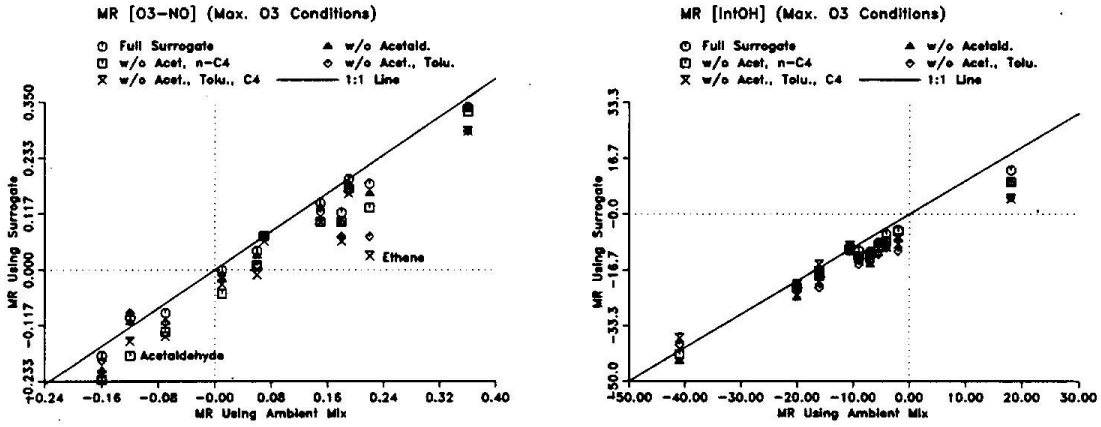

Figure 3. Plots of calculated mechanistic reactivities of selected species in maximum ozone chamber experiments using various ROG surrogates, against those for similar experiments using the ambient ROG mixture.

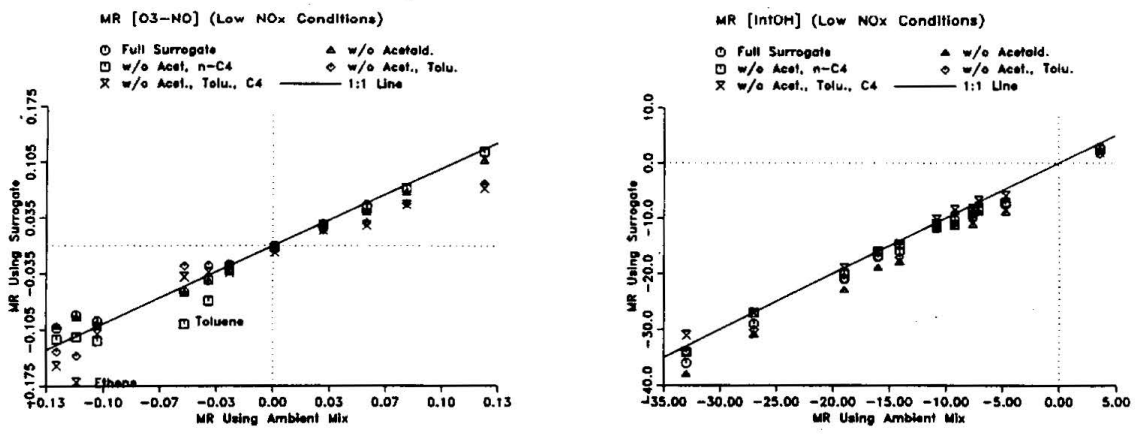

Figure 4. Plots of calculated mechanistic reactivities of selected species in NO_x-limited chamber experiments using various ROG surrogates, against those for similar experiments using the ambient ROG mixture.

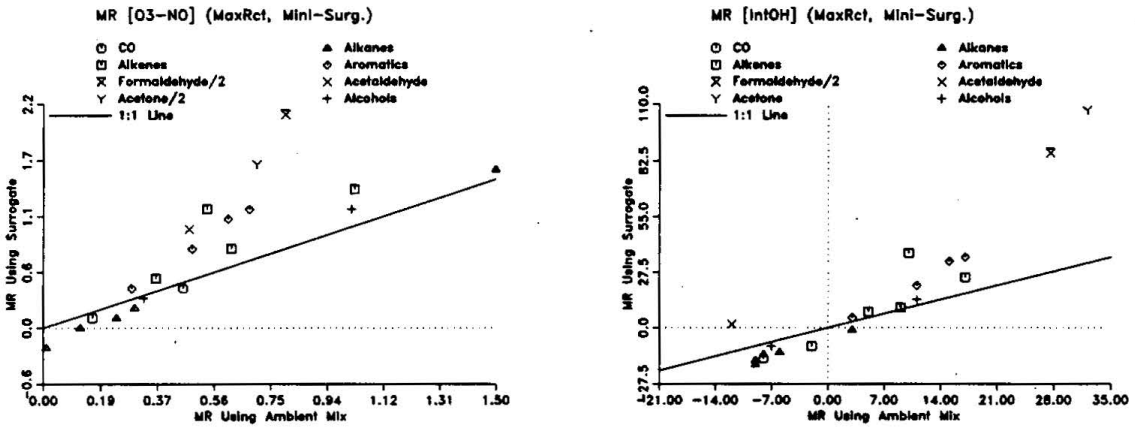

Figure 5. Plots of calculated mechanistic reactivities of selected species in maximum reactivity chamber experiments using the 3-component mini-surrogate, against those for similar experiments using the ambient ROG mixture.

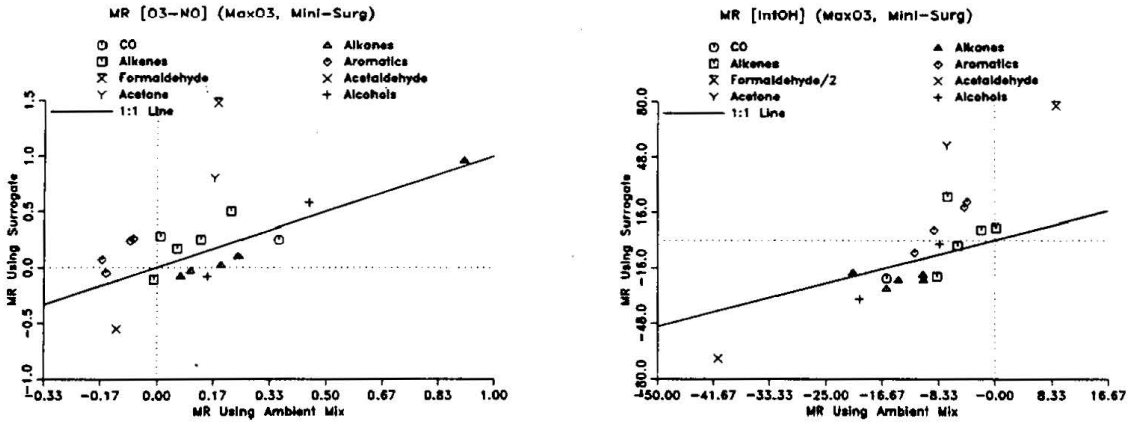

Figure 6. Plots of calculated mechanistic reactivities of selected species in maximum ozone chamber experiments using the 3-component mini-surrogate, against those for similar experiments using the ambient ROG mixture.

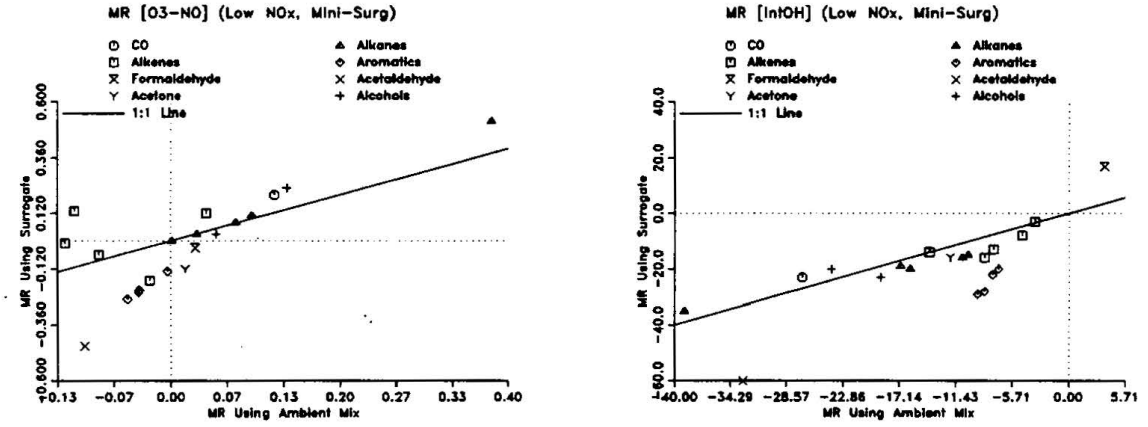

Figure 7. Plots of calculated mechanistic reactivities of representative species in NO_x-limited chamber experiments using the 3-component mini-surrogate, against calculated mechanistic reactivities for similar experiments using the ambient ROG mixture.

result is not due to the same condensed mechanism being used to simulate both mixtures.

Figure 1 also shows that the model with MEK representing the lost carbons gives essentially identical results as the standard mechanism. (The models are also almost identical in predictions for the base case experiment, except obviously for MEK.) This should alleviate concerns about the lack of representation of "lost carbon" in the ROG surrogate, at least for one day experiments. As indicated above, it is probable that MEK overstates the effect of lost carbon, so if the reactivities are insensitive to this model for the lost carbons, they should be even less sensitive to a more realistic one.

Figures 2-4 show the comparisons of the d(O_3-NO) and IntOH mechanistic reactivities for various simplifications of the lumped molecule surrogate. Different symbols are shown for the different ROG surrogates, and individual compounds where the discrepancies are the worst for the simpler surrogates are identified on selected plots. (A slightly smaller number of representative compounds are shown on these plots than on Figure 1 and subsequent figures, for easier readability.) The results show that removing acetaldehyde from the surrogate and replacing it with formaldehyde has a only a small effect compared to experimental uncertainties, suggesting that this simplification, which has significant experimental advantages, may be appropriate. Simplifying the alkanes and/or the aromatics also has only a small effect in most cases, but for some VOCs the effects may be non-negligible. For example, simplifying the alkanes has a non-negligible effect on the predicted d(O_3-NO) reactivities of toluene under low NO_x conditions and of acetaldehyde under maximum ozone conditions. Simplifying the aromatics significantly affects the predicted d(O_3-NO) and IntOH reactivities of acetaldehyde under maximum reactivity conditions, and also affects the d(O_3-NO) reactivity of ethene under maximum ozone conditions. Since the experimental advantages of simplifying alkanes or aromatics are not as great as that of removing acetaldehyde, these latter two simplifications may not be appropriate.

Figures 5-7 show the comparisons of the d(O_3-NO) and IntOH mechanistic for the 3-component mini-surrogate we used in our previous reactivity experiments. In this case, different symbols are used for different classes of compounds, and the formaldehyde and acetone reactivities have been divided by 2 on selected plots to make their magnitudes more comparable with those for the other VOCs. These figures show that the mini-surrogate yields greater differences in reactivities compared to using the ambient mixture or the "lumped molecule" surrogates. The largest effect of using the mini-surrogate is on the reactivities of formaldehyde under maximum reactivity or maximum ozone conditions, but the reactivities of the other VOCs are affected to some extent as well. This is probably due to the lack of formaldehyde in this mini-surrogate, causing a greater sensitivity of the mini-surrogate to radical initiation and radical termination effects. This greater sensitivity, however, makes experiments with

this mixture more useful for testing model predictions concerning this aspect of the mechanism.

Figure 8 shows plots of the maximum ozone in the base case experiments and mechanistic reactivities of selected VOCs against initial NO_x concentrations at a constant nominal base ROG level of 5.5 ppmC. Note that the 0.5 ppm NO_x level is taken as "maximum reactivity" conditions in the previous plots (though slightly lower NO_x may be slightly closer to the "true" MIR point for some VOCS), 0.2 ppm NO_x is used for "maximum ozone" conditions, and 0.05 ppm is used for "Low NO_x" conditions for all the surrogates. The maximum ozone and reactivities calculated for the ethylene surrogate are also shown. It can be seen that the 9-component surrogate tracks the NO_x-dependence of the maximum ozone and VOC reactivities of the ambient mixture very closely. The mini-surrogate does not track the ambient mixture as closely, particularly for formaldehyde and n-octane under maximum reactivity conditions. The discrepancies are apparently due to the greater sensitivity of the mini-surrogate experiments to radical initiation/termination effects under maximum reactivity conditions.

Figure 8 also shows that the reactivities using the simple ethylene surrogate track the reactivities using the mini-surrogate remarkably well, particularly under maximum ozone to maximum reactivity conditions. This suggests that use of ethylene as the ROG surrogate may give essentially equivalent results in reactivity experiments to use of the mini-surrogate. (It also suggests that the high NO_x reactivities measured in the previous program using the mini-surrogate may not be highly sensitive to the m-xylene mechanism, since almost the same reactivity results are calculated to occur if m-xylene were absent.) The correspondences between these two surrogates is shown for a larger variety of compounds on Figure 9, which gives plots of calculated mechanistic reactivities for experiments using the ethylene surrogate against those using the mini-surrogate for maximum reactivity, maximum ozone, and low NO_x conditions. The main difference is that reactivities tend to be lower (or more negative) under low NO_x conditions in experiments using the ethene surrogate than in those using the mini-surrogate or the ambient mixture. This is undoubtedly related to the fact that ethene has much weaker NO_x sinks in its mechanism than the other components of the mini-surrogate or the more realistic mixtures. Thus adding a compound with NO_x sinks to a NO_x-limited system with weak NO_x sinks has a greater effect than adding it to an otherwise comparable system with stronger NO_x sinks. This suggests that use of ethylene as the ROG surrogate in low NO_x reactivity experiments may provide a more sensitive test for this aspect of the mechanism than using more realistic surrogates which contain compounds which stronger NO_x sinks.

D. Comparison of Predicted Experimental Reactivities with the Maximum Reactivity and Maximum Ozone Reactivity Scales.

Figure 10 shows comparisons of mechanistic reactivities calculated for chamber conditions with those calculated for similar NO_x conditions in the

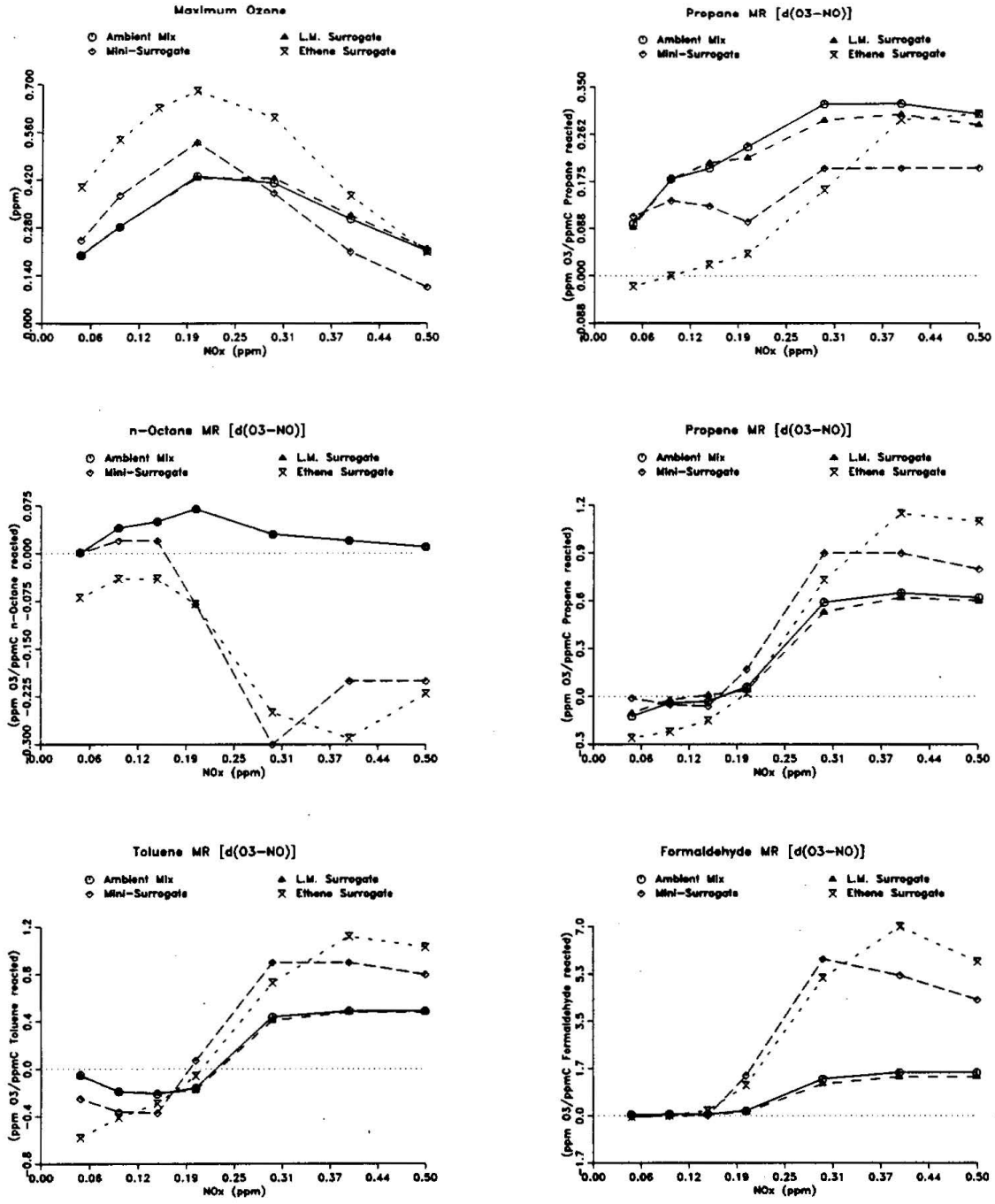

Figure 8. Plots of maximum ozone in base case experiments and of mechanistic reactivities for selected VOCs as a function of initial NO_x from model simulations of reactivity experiments employing the ambient ROG mixture and selected ROG surrogates.

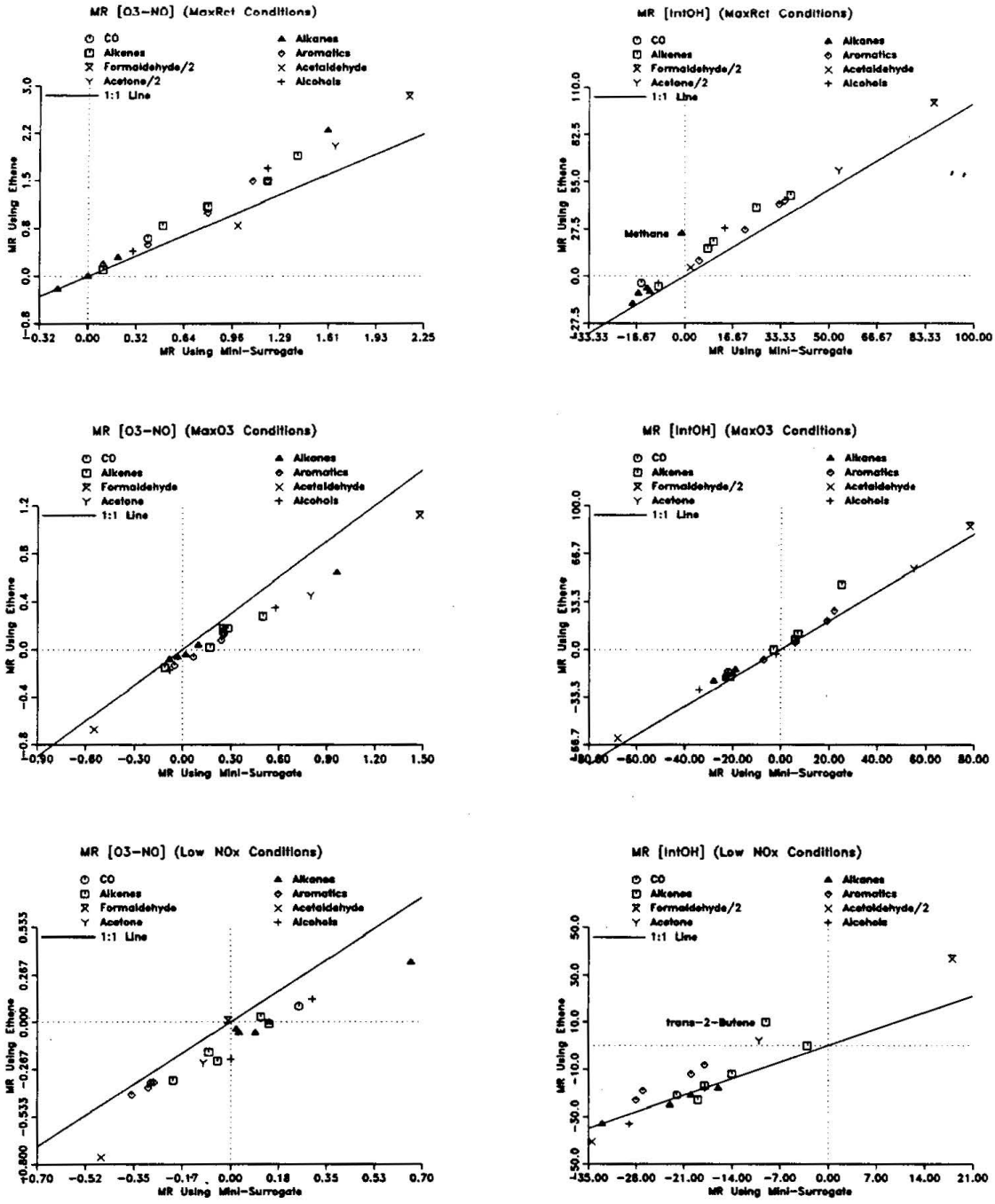

Figure 9. Plots of calculated mechanistic reactivities of selected species in chamber experiments using the ethene as the ROG surrogate against those for experiments using the mini-surrogate ROG mixture.

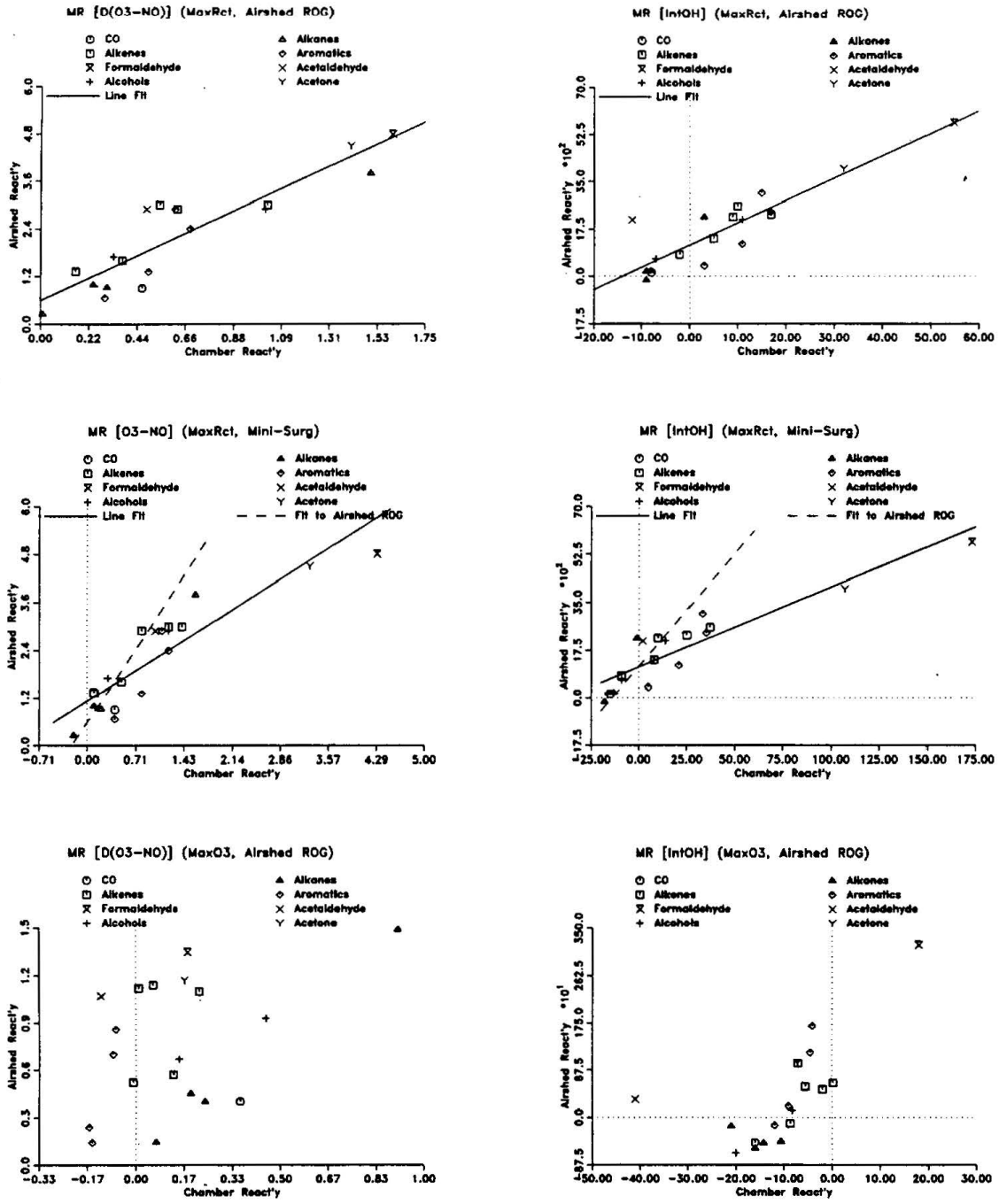

Figure 10. Plots of calculated mechanistic reactivities for chamber conditions, using either the airshed ROG or the 3-component mini-surrogate, against those calculated for airshed conditions.

atmosphere. The top four plots show mechanistic reactivities calculated for the "maximum reactivity" experiments, plotted against mechanistic reactivities in the MIR scale (Carter, 1994).

The bottom plots on Figure 10 compare mechanistic reactivities calculated for maximum ozone experiments with corresponding reactivities in the MOIR scale (Carter, 1994). The top two and bottom two plots are calculated with the same base ROG mixture in both the chamber experiments as used in the ambient air (MIR or MOR) calculations, and thus show the differences between chamber and atmospheric reactivities with the ROG mixture held constant. It can be seen that a fair correlation is obtained in the maximum reactivity case for both $d(O_3\text{-NO})$ and IntOH reactivities, but the slopes are less than one and the intercepts are significantly nonzero in both cases. The correlation is much worse under maximum ozone conditions, being essentially none in the case of $d(O_3\text{-NO})$ reactivities. This is probably because the maximum ozone reactivities are determined by a balance of several, often opposing, factors, whose relative importances apparently are different in the chamber than the atmosphere. Except for acetaldehyde, the correlation of IntOH reactivities is much better, presumably because it depends on only one aspect of the mechanism. The poor correlations for acetaldehyde must be due to different effects on the importance of PAN formation in the chamber vs the atmosphere.

The middle plots on Figure 10 compare chamber reactivities using the 3-component mini-surrogate with atmospheric MIR reactivities. The dotted lines on the plots are the best fit lines for the chamber reactivities using the ambient mixture, taken from the top two plots. Although the correlation with atmospheric reactivities is not as good as the case with the experiments using the ambient mixture, they are not significantly worse. The intercepts are approximately the same, but the slopes are different because the runs with the mini-surrogate tend to be more sensitive to the VOCs (yield higher mechanistic reactivities) than those with the ambient mixture.

The results of these calculations indicate that it is not possible to obtain exact correlations between chamber reactivities and atmospheric reactivities even if the exact same ROG mixture is employed. The correlation is almost non-existent in the case of $d(O_3\text{-NO})$ reactivities under maximum ozone or low-NO_x conditions, though it is better for IntOH reactivities. Nonzero intercepts of plots of chamber reactivities against atmospheric reactivities are consistently observed, i.e., based on the calculated correlations we would predict that if a VOC has a mechanistic reactivity of zero in the chamber it have a positive reactivity in the atmosphere. Using a more realistic ROG surrogate may improve the correlation for those cases where there is a correlation, but there would still be the nonzero intercept, and the improvement may not be that significant except for compounds which photolyze.

E. Summary

These calculations indicate that a 9-component "lumped" surrogate provides an excellent representation of the ambient ROG mixture for reactivity experiments, and that use of more complex mixtures would not yield experimentally distinguishable results. The effect of ignoring the "lost carbon" in the ROG surrogate was calculated to be negligible. The calculations also showed that the 9-component surrogate can be further simplified by using formaldehyde to represent both formaldehyde and acetaldehyde (on a molar basis) without yielding a measurable difference in reactivities, but that additional simplifications may have non-negligible effects. In particular, the 3-component "mini-surrogate" used in the previous study was calculated to yield measurable differences in reactivities for many species, and significantly higher reactivities for formaldehyde and acetone.

However, the calculations also showed that even if the exact same ROG mixture is used in the experiments as occurs in the atmosphere, reactivities in environmental chamber experiments would not necessarily be the same or even correlate with those in the atmosphere. The best correlations are obtained with reactivities under maximum reactivity conditions and with IntOH reactivities under various conditions. No correlation is obtained with ozone reactivities under maximum ozone or NO_x-limited conditions.

Using a realistic ROG surrogate may not necessarily be of greatest utility for mechanism testing. The calculations indicated that experiments with the simpler 3-component mini-surrogates are more sensitive to effects of differences among VOCs, and thus potentially more useful for mechanism evaluation. Since the use of this surrogate for mechanism evaluation was complicated by uncertainties in the m-xylene mechanism, calculations were conducted to determine whether use of an even simpler "surrogate" – ethylene alone – might provide equivalent information while minimizing problems due to base ROG mechanism uncertainties. It was found that the ethylene surrogate gives almost equivalent maximum reactivity results, but tends to be more sensitive to NO_x-sink species under NO_x-limited conditions. The latter may be an advantage from the point of view of evaluating this aspect of VOC mechanisms.

It is concluded that the 8-compound surrogate, the "lumped" surrogate with acetaldehyde removed, will provide an appropriate representation of the ambient ROG mixture in reactivity experiments where maximum correlation with atmospheric reactivities is desired. Calculations indicate that using more complex mixtures would complicate the experiment and analysis without yielding measurably different results. However, if the objective is mechanism evaluation, the mini-surrogate or even ethylene alone may be the superior ROG surrogate, since reactivity experiments using it are more sensitive to differences among VOCs, and (in the case of ethylene) possibilities for compensating errors are significantly fewer. The two types of experiments should be considered complementary and of equal importance to providing comprehensive data for reactivity analysis.

Based on these results, it was determined that incremental reactivity experiments using both the lumped surrogate, and ethylene alone as the surrogate, would, in conjunction with the mini-surrogate experiments already conducted, provide useful and complementary information concerning the effect of ROG surrogate on incremental reactivity. These experiments are discussed in the following sections.

III. EXPERIMENTAL FACILITY AND METHODS

A. Facility

1 New Indoor and Outdoor Chamber Laboratory Facility

The work plan for this program includes conducting both indoor and outdoor chamber experiments. (The outdoor chamber experiments are discussed elsewhere [Carter et al., 1995a].) When the program started, all the SAPRC indoor chambers were located in Fawcett Laboratory, where a number of research programs besides this one were being carried out. Because of acquisition of major new equipment for these programs, the space in Fawcett Laboratory became limited, and we were required to relocate the chamber used for into a room which lacked adequate temperature control – a problem which showed up in the data (Carter et al., 1993a). Furthermore, we felt it was important to construct a new type of indoor chamber more suitable for incremental reactivity studies (see discussion of the "DTC", below), but there was insufficient space in Fawcett for this purpose. There was also insufficient office space at Fawcett for the personnel on this program, who had to use offices in a trailer about a block away. Therefore, this program needed additional laboratory and office space.

A further problem with the existing facility was that the SAPRC outdoor chamber was located approximately one block away, and duplicate instrumentation was not available to allow conducting experiments in both facilities simultaneously. This meant that there would be significant down time while moving the equipment and setting them up for outdoor experiments, moving them back and setting them up again for indoor runs, and during periods of unfavorable weather when the laboratory was set up for outdoor runs. Much greater productivity and efficient use of the available resources could be obtained if the indoor chambers could be located in a laboratory adjacent to the outdoor chamber, so equipment can simultaneously used by both, and indoor runs can alternate with outdoor runs as weather or the demands of the program dictate.

To address both these problems, for this program (under funding from the SCAQMD) we obtained a new modular building at the site of the outdoor chamber laboratory which was large enough to house the indoor chambers needed for the program. A layout of this building, which also shows its location relative to the outdoor chamber, is shown on Figure 11. The building has a main laboratory area which houses the analytical instrumentation, and also has room for the ~3000-liter indoor Teflon chamber #2 ("ETC") used in the Phase I experiments, as well as a separate unit, ~3000-liter Teflon chamber which was used for calibrations and injection test experiments. A separate room was dedicated to the new Dividable Teflon Chamber (DTC) or the new Xenon Teflon Chamber (XTC) which was used for the indoor chamber experiments in this program and which are discussed below. (The DTC was constructed first, and it was replaced by the XTC later in the program.) The continuous monitoring instruments could be attached either to

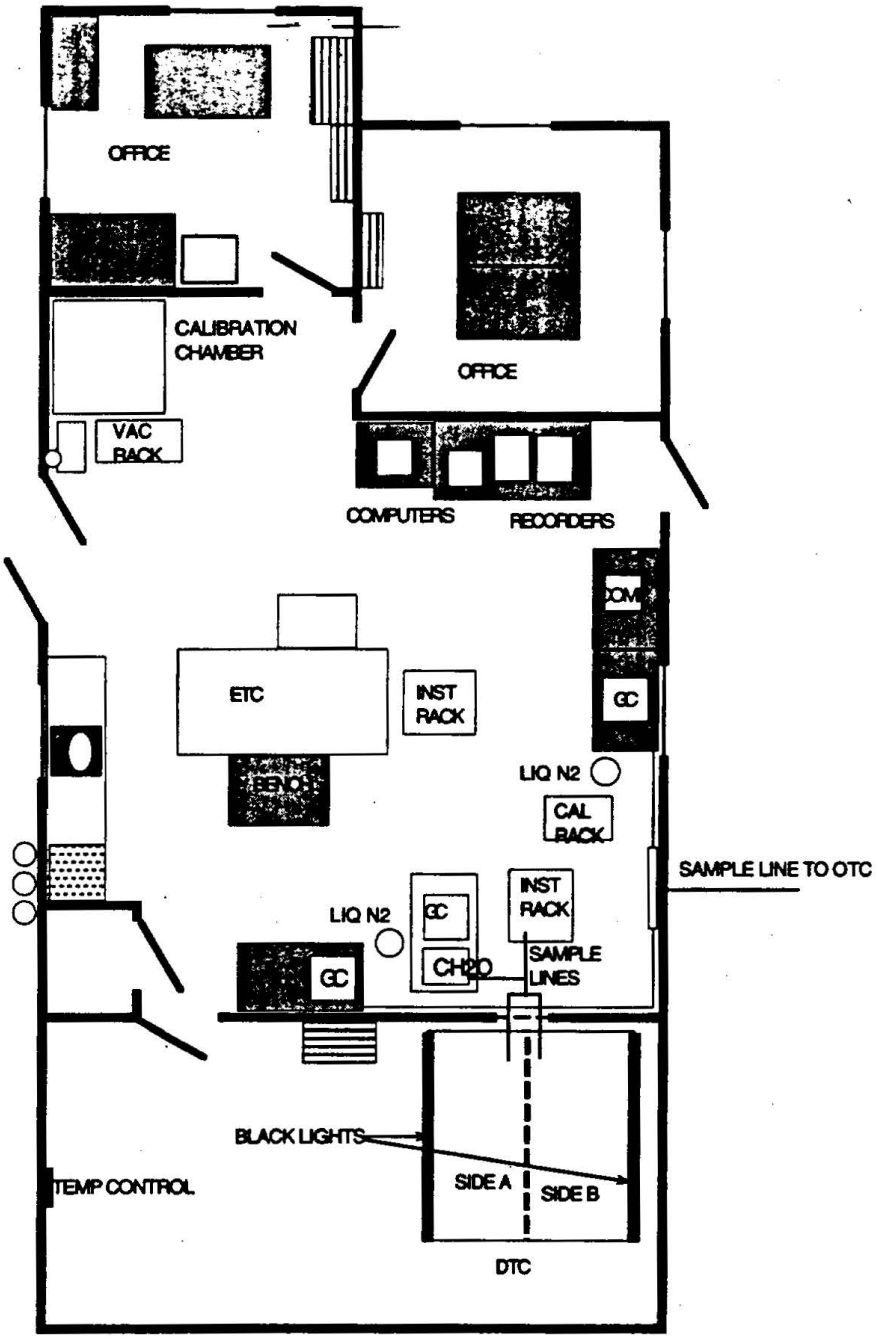

Figure 11. Diagram of SCAQMD-Funded SAPRC indoor and outdoor chamber laboratory for VOC reactivity studies.

one of the indoor chambers (ETC and XTC) or the sampling manifold for DTC and the outdoor chamber (OTC). The building also has offices which were used by the experimental personnel and for data processing. All the experiments discussed in this report were carried out using this facility and four chambers (ETC, DTC, XTC and OTC) were employed in this program..

The facility had an AADCO air purification system located nearby which provided dry pure air for all the chambers. Later in the program a second AADCO was added to provide a greater flow rate to allow more rapid flushing of more than one chamber at a time, and a drying system was added to improve the efficiency of the system and increase the useful lifetime of the air purification cartridges.

2. Indoor Teflon Chamber #2 (ETC)

The Indoor Teflon Chamber #2, which is called the "ETC". This chamber was described in our previous report (Carter et al., 1993a; see also Carter et al., 1995b). Briefly, it consisted of 1 2-mil thick FEP Teflon reaction bag fitted inside an aluminum frame of dimensions of 8 ft x 4 ft x 4 ft. The light source for the chamber consisted of two diametrically opposed banks of 30 Sylvania 40-W BL blacklights, one above and the other below the chamber.

3. Dividable Teflon Chamber (DTC)

The Dividable Teflon Chamber (DTC) was designed to allow irradiations of two separate mixtures at the same time and under the same reaction conditions. Such a chamber should be particularly useful for incremental reactivity experiments, which consist of repeated irradiations of the same mixture, with and without a test VOC added. In the ETC chamber, these experiments have to be carried out one at a time, with the "base case" experiment alternating with "test" experiments consisting of the same nominal reaction mixture, but with a test VOC added. Because of variability of reaction conditions (such as the variability in temperature) and slight differences in amounts of reactants injected from run-to-run, statistical regression analysis methods have to be used to correct for the differences between the runs when determining the effects of the added VOC (Carter et al., 1993a; see also below). This lead to some imprecisions in the reactivity analysis because not all the run-to-run variability could be accounted for in the regressions (Carter et al., 1993a). However, if the base case and the test experiments could be carried out simultaneously, with the same temperatures and concentrations of common reactants, then the precision of the reactivity determination could in principle be improved, and also the productivity of the program, in terms of compounds studies per run day, could be doubled.

The DTC, which is shown schematically in Figure 12, was constructed with these objectives in mind. It consists of two ~5000-liter reaction bags located adjacent to each other, and fitted inside an 8' cubic framework. The light source consisted of two diametrically opposed banks of 32 Sylvania 40-W BL

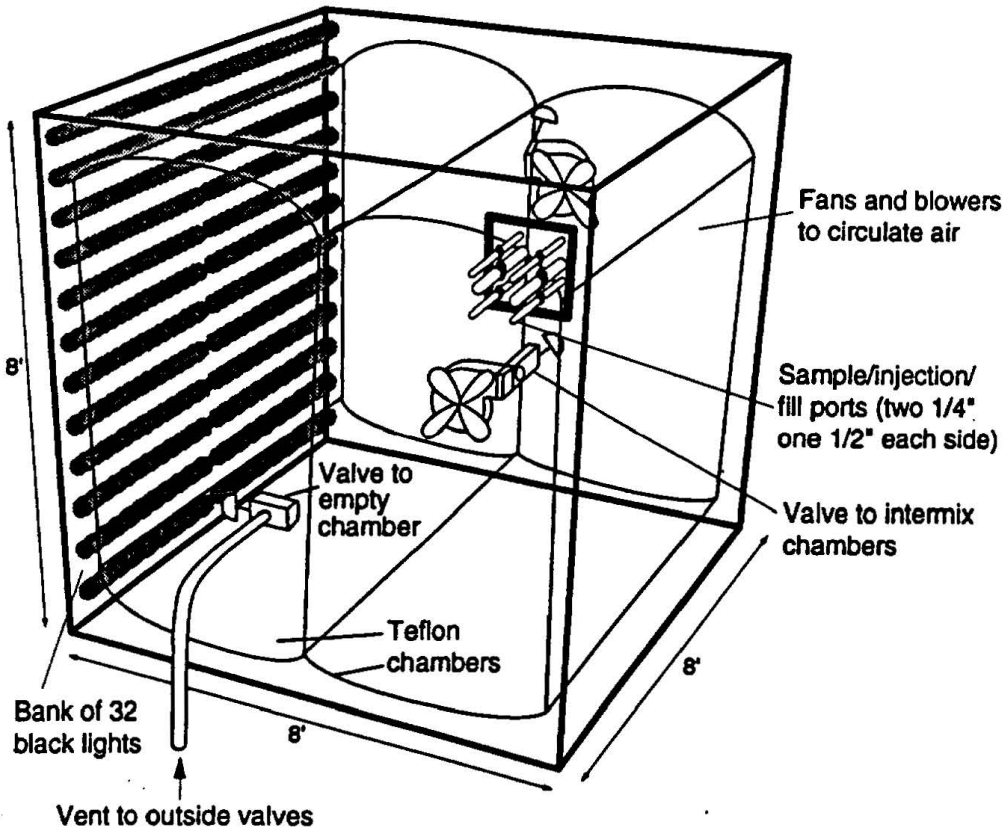

Figure 12. Diagram of SAPRC Dividable Teflon Chamber (DTC).

blacklights, whose intensity can be controlled by 16 switches, each of which operates 2 blacklights. The lights are backed by aluminum-coated plastic reflectors which are molded into the same shape as the Alzak reflectors in the SAPRC Indoor Teflon Chamber #1 (ITC) (Carter et al., 1995b). The roof, floor and the two end walls are covered with polished aluminum panels, except for a window in the middle of one of the end walls where the sampling, reactant injection, and air fill probes were located. (See also the diagram of the laboratory in Figure 11.) The light intensity in this system turned out to be so high that to achieve light intensities comparable to ambient conditions all the runs in the data base were carried out with 50% of the maximum light intensity.

A specially constructed system of two Teflon-coated fans and blowers was used to rapidly exchange and mix the contents of the two reaction bags. Each blower forces the air from one reaction bag into the other, and the fans mix the air in each bag. This results in equal concentrations of common reactants in both reaction bags, when desired. The valves connecting the two bags can be closed to isolate the two chambers after the injection of common reactants, and the fans can then be used to mix additional reactants in each of the sides separately.

Dry purified air was provided by the same AADCO air purification system discussed above. All runs were carried out under dry conditions RH ≤~5%, except for a few runs where water vapor was manually injected to yield ~50% RH.

The sampling to the continuous monitoring instruments were controlled by two computer-activated solenoid valves, which select the chamber side where air is withdrawn for analysis. One of these valves controls the sampling for the O_3 and NO_x analyzers, where the sides being sampled are usually alternated every 10 minutes. The other valve is used to control sampling for formaldehyde, which usually had a 15 minute sampling time for each reaction bag. The data acquisition system controlled the sampling valves and kept track of which reaction bag is being monitored when the data are being collected. In addition, a solenoid valve attached to vacuum pump, which was located under the modular building, was employed to withdraw air from one side at the same sampling flow rate as of the continuous analyzers when the other side was being drawn for the continuous analyzers. This was important to keep withdrawing air in both sampling lines so continuous analyzers could monitor each side promptly when the side was changed, especially for the outdoor Teflon Chamber because two longer sampling lines were used.

The two reaction bags are designated as sides "A" and "B". Because two separate mixtures are being irradiated simultaneously, each DTC run consists of two separate experiments. These are designated as runs DTCnnnA and DTCnnnB, where nnn is the run number.

B. Experimental Procedures

The chambers were flushed with dry purified air for 6-9 hours on the nights before the experiments. The continuous monitors were connected prior to reactant injection and the data system began logging data from the continuous monitoring systems. The reactants were injected as described previously (Carter et al, 1993a). For dual chamber (DTC) runs, the common reactants were injected in both sides simultaneously (using a "T" in the injection line) and were well mixed before the chamber was divided. In the case the DTC, the contents of side A were blown into side B and visa-versa using two separate blowers. Fans were used to mix the reactants in the indoor chambers during the injection period, but these were turned off prior to the irradiation. Dividing the DTC consisted of closing the ports which connected the two reaction sides. After the DTC was divided, the reactants for specific sides were injected and mixed. The irradiation began by turning on the lights (for the blacklight chambers), opening the cover (for the OTC), or sliding back the panels in front of the Xenon lights (which were turned on ~30 minutes previously). The irradiation proceeded for 6 hours. After the run, the contents of the chamber(s) were emptied (by allowing the bag to collapse) and flushed with purified air. A heater was turned on to preheat the ETC chamber to reach the experimental temperature desired and turned off when the irradiation began, as described in previous report (Carter et al, 1993a). Preheat for the DTC chamber was accomplished by turning on the temperature control system ~2 hours prior to the irradiation.

C. Analytical Methods

Ozone and nitrogen oxides were continuously monitored using commercially available continuous analyzers with PFA Teflon and borosilicate glass sample lines inserted directly into the chambers (ca 18 in.). For DTC and OTC chamber runs, the sampling lines from each half of the chamber were connected to solenoids which switched from side to side every 10 minutes, so the instruments alternately collected data from each side. Ozone was monitored using a Dasibi Model 1003AH UV photometric ozone analyzer and NO and total oxides of nitrogen (including HNO_3 and organic nitrates) were monitored using either a Columbia Model 1600 or a Teco Model 14B or 43 chemiluminescent NO/NO_x monitor. The output of these instruments, along with that from the temperature and (for OTC and XTC runs) light sensors were attached to a computer data acquisition system, which recorded the data at periodical intervals, using 30 second averaging times. For single mode (ETC or XTC) chamber runs, the O_3, NO_x, and other continuous data recorded every 15 minutes; for the divided chamber (DTC or OTC) runs, the data was collected every 10 minutes, yielding a sampling interval of 20 minutes for taking data from each side.

Organic reactants other than formaldehyde were measured by gas chromatography with FID detection as described elsewhere (Carter et al., 1993a). GC samples were taken for analysis at intervals from fifteen minutes to one hour using 100 ml gas-tight glass syringes. These samples were taken from ports directly connected to the chamber. The syringes were flushed with the chamber contents

several times before taking the sample for analysis. The various analysis systems, and their calibration data, are described in more detail elsewhere (Carter et al., 1995b).

Although we made numerous attempts to obtain a good analysis for PAN using the GC-ECD instrument acquired for this purpose (Carter et al., 1995b), during the period of this program we were not successful in obtaining reproducible data. Therefore, although PAN data are available for many of the experiments conducted for this program, we do not consider them to be sufficiently reliable for quantitative mechanism evaluation. The poorly-constructed sample injection system was subsequently rebuilt.

Formaldehyde was monitored using a diffusion scrubber system based on the design of Dasgupta and co-workers (Dasgupta et al, 1988, 1990; Dong and Dasgupta, 1987), as described elsewhere (Carter et al., 1993a). This system alternately collected data in sample (30 minutes), zero (15 minutes), and calibrate mode (15 minutes), for a one hour cycle time. The readings at the end of the time period for each mode, averaged for 30 seconds, were recorded on the computer data acquisition system, which subsequently processed the data to apply the calibration and zero corrections. A separate sampling line from the chamber was used for the formaldehyde analysis. For the DTC or OTC, a solenoid, which was separate from the one used for O_3 and NO_x sampling, was used to select the chamber side from which the formaldehyde sample was withdrawn, which alternated every 15 minutes. This yielded formaldehyde data as frequently as every 15 minutes for single chamber (e.g., ETC) runs, and every 30 minutes for each side for divided chamber (e.g. DTC) runs. The calibration data for this instrument are discussed elsewhere (Carter et al., 1995b).

D. Characterization Data

1. Light Source

NO_2 Actinometry. The absolute light intensity in the chambers was determined by conducting periodic NO_2 actinometry experiments using the quartz tube method as employed previously (Carter et al, 1993a), except that the "effective quantum yield" factor, Φ, was changed from 1.75 to 1.66 based on computer model simulations of a large number of such experiments as discussed in detail elsewhere (Carter et al., 1995b). The procedures for the actinometry runs in the ETC chamber were discussed previously (Carter et al., 1993a). Unless noted differently, in the actinometry runs for the DTC the quartz tube was located between the reaction bags and at about mid height, and parallel with the walls with the lights and the ceiling and the floor.

Spectral Measurements. The spectral measurements for the ETC and DTC chambers were taken periodically using a LiCor Li-1800 portable spectroradiometer. There was found to be no significant difference between the spectrum of this chamber and any other SAPRC blacklight chamber. As discussed

elsewhere (Carter et al., 1995b) a composite spectrum was developed, based on spectral measurements using several spectroradiometers, for use in modeling experiments in all SAPRC blacklight chambers. That spectrum, which gives a better representation of the sharp Hg lines than the lower resolution spectrum used previously (Carter et al., 1993a; Carter and Lurmann, 1991) was used in this work.

2. Temperature

Iron-Constantan thermocouple, interfaced directly to a temperature sensor board in the Keithly A-to-D converter, were used to monitor the temperature as a function of time in these experiments. The probes were calibrated as discussed elsewhere (Carter et al., 1995b). Some additional corrections are needed to the temperature data for the individual chambers. In the cases of the ETC and DTC, one temperature sensor was located in each of the reaction bags for the ETC and DTC chambers. No shielding was used for the probes because at the time it was believed that radiative heading by the blacklights was believed to be minor. However, subsequent comparison of temperatures monitored with this method with simultaneous readings using an aspirated temperature probe indicated that temperatures measured using this method need to be corrected by ~2°C (Carter et al., 1995b).

3. Dilution

Dilution due to sampling is expected to be small because the flexible reaction bags can collapse as sample is withdrawn for analysis. However, some dilution occasionally occurred because of small leaks, and several runs had larger than usual dilution due to a larger leak which was subsequently found and repaired. Information concerning dilution in an experiment can be obtained from relative rates of decay of added VOCs which react significantly only with OH radicals with differing rate constants (Carter et al., 1993a). All experiments had a more reactive compound (such as m-xylene or n-octane) present either as a reactant or added in trace amounts to monitor OH radical levels. Trace amounts (~0.1 ppm) of n-butane was added to experiments if needed to provide a less reactive compound for the purposes of monitoring dilution. In many experiments, dilution rates were zero within the uncertainties of the determinations.

4. Control Experiments

Several types of control experiments were conducted to characterize chamber conditions. Ozone decay rate measurements were conducted with new reactors, and the results were generally consistent with ozone decays observed in other Teflon bag reactors (Carter et. al. 1984, 1986). NO_x-air irradiations with trace amounts of propene or isobutene, or n-butane-NO_x-air experiments, were conducted to characterize the chamber radical source (Carter et al., 1982). The specific types of experiments are discussed where relevant in the section describing model calculation methods.

IV. EXPERIMENTAL ANALYSIS METHODS AND RESULTS

A chronological list of the experiments carried out in this phase of the program which are relevant to this report is given in Table 5, and Table 6 summarizes the types of incremental reactivity experiments which were carried out. The reactivity experiments include high NO_x (i.e., maximum reactivity) ethene surrogate experiments and high and low NO_x (maximum reactivity and NO_x-limited) lumped surrogate runs. The ethene surrogate experiments were carried out primarily in the ETC, while all the lumped surrogate experiments were carried out in the DTC. The methods used to analyze the data from these experiments, and the results obtained, are described in the following sections.

A. Reactivity Analysis Methods

With a few exceptions noted below, the methods used to analyze the results of the reactivity experiments were the same as discussed in our previous report (Carter et al., 1993a). The major features of this analysis, and the modifications to this analysis method made for this program, are summarized below. For a more detailed discussion and the derivations of some of the equations used, the reader is referred to the previous report (Carter et al., 1993a).

As indicated above, two types of reactivity experiments are carried out, the "base case" experiment designed to simulate (or be a simplified representation of) a particular type of chemical environment into which a VOC might be emitted, and a "test" experiment in which an appropriate amount of a VOC whose reactivity is being assessed is added to the base case experiment. The measured quantities in these experiments which are used in the reactivity analysis are as follows:

1. NO oxidized and Ozone Formed, [$d(O_3$-NO)]

The amount of O_3 formed and NO oxidized as a function of time, or $d(O_3\text{-NO})$, is defined as $([O_3]_t - [NO]_t) - ([O_3]_0 - [NO]_0)$, where $[O_3]_0$, $[NO]_0$, $[O_3]_t$ and $[NO]_t$ are the initial and final O_3 and NO concentrations, respectively. The change in $[O_3] - [NO]$ is a more useful quantity for reactivity assessment than the change in O_3 alone because, as discussed elsewhere (Johnson, 1983; Carter and Atkinson, 1987; Carter and Lurmann, 1990, 1991), it reflects the same chemical processes, and provides useful reactivity information even under conditions when O_3 is low and NO is high. These data are obtained from the simultaneous NO and O_3 measurements taken during the experiments, and the values after each hour of the experiments are used in the analysis. If O_3 and NO measurements are not available exactly on the hour for a particular run, the hourly values are obtained by interpolating the $d(O_3\text{-NO})$ data before and after the hour. Interpolation was necessary for the DTC runs because O_3 and NO measurements alternated from side to side every 10 minutes.

Table 5. Listing of all environmental chamber experiments relevant to this report. Gaps in run numbers are experiments for other purposes.

Run	Date	Description and Comments
ETC Experiments		
		Characterization Experiments
	4/22/92	New reaction bag installed.
370	4/23/92	Pure-air irradiation
371	4/23/92	Ozone decay (result in normal range)
374	5/12/92	Pure-air irradiation
375	5/18/92	Propene-NO_x
380	5/26/92	Tracer-NO_x
381	5/27/92	Ethene-NO_x
382	5/28/92	Acetaldehyde-air
448		NO_2 Actinometry
	10/30/92	Full (8-component, "lumped molecule") Surrogate test
455	11/2/92	Full Surrogate test
458	11/09/92	Pure air Irradiation
460	11/12/92	Full Surrogate test
461	11/13/92	NO_2 Actinometry
462	11/13/92	Tracer - NO_x
463	11/16/92	Full Surrogate test
		Ethylene Surrogate Incremental Reactivity Experiments (Unless noted otherwise, "Ethene" refers to 1.6 ppm Ethene, 0.5 ppm NO_x.)
464	11/20/92	Ethene
466	11/23/92	Ethene
467	11/25/92	Ethene
468	11/1/92	Ethene + Formaldehyde
469	12/2/92	Ethene
470	12/3/92	Ethene + Formaldehyde
472	12/7/92	Ethene + n-Octane
473	12/8/92	Ethene
474	12/9/92	Ethene + n-Octane
475	12/14/92	Propene - NO_x
476	12/15/92	Ethene
477	12/16/92	Ethene + m-Xylene
478	12/17/92	Ethene + m-Xylene
479	12/18/92	Ethene
480	12/21/92	Ethene + Acetone
482	1/5/93	Ethene
483	1/6/93	Ethene + CO
484	1/7/93	Ethene + n-Butane
485	1/8/93	Pure-air irradiation
486	1/11/93	Ethene
487	1/12/93	Ethene + CO
488	1/13/93	Ethene + n-Butane
489	1/14/93	Ethene + HCHO
490	1/15/93	Ethene + Acetone
496	1/27/93	Ethene + Propene
499	2/2/93	Ethene + m-Xylene
500	2/3/93	Ethene + Propene
501	2/4/93	Ethene + t-2-Butene
502	2/5/93	Ethene
506	2/17/93	Ethene + Ethane

Table 5 (continued)

Run	Date	Description and Comments
DTC Experiments		
		Characterization and Preliminary Experiments
	12/9/92	NO_2 Actinometry 100% lights
	12/10/92	NO_2 Actinometry with 50% lights Dual Teflon reactor bags installed. k_1 tube between bags
	1/4/93	NO_2 Actinometry. (50% lights for all subsequent runs unless noted)
	1/4/93	O_3 conditioning and decay determination: Initial $[O_3]$=0.63 ppm, in chamber for 15 hours. Decay rate in last 9 hours: 2.0 and 2.4%/hr in sides A, and B respectively.
	1/6/93	Test temperature system
001	1/21/93	Pure air photolysis.
002	1/22/93	O_3 decay. 1.63±0.08%/hr side A; 1.69±0.10%/hr, side B
003	1/27/93	Pure air photolysis
004	1/28/93	NO_2 Actinometry, variable positions
005	1/29/93	NO_2 Actinometry, variable positions
006	2/11/93	Ethene-NO_x, side equivalency. test.
007	2/18/93	Preliminary full surrogate - NO_x, side equivalency. test. (Unless indicated otherwise, "surrogate" means 8-component "lumped molecule" surrogate.)
008	2/24/93	Preliminary surrogate - NO_x (injection and analysis tests)
009	3/2/93	Preliminary surrogate - NO_x (injection and analysis tests)
010	3/4/93	Preliminary surrogate - NO_x (injection and analysis tests)
011	3/5/93	Preliminary surrogate - NO_x (injection and analysis tests)
012	3/10/93	Preliminary surrogate - NO_x (injection and analysis tests)
013	3/11/93	High NO_x surrogate, both sides. (Unless indicated otherwise, "High NO_x surrogate" is 0.5 ppm NO_x and 4 ppmC "lumped molecule" surrogate.)
		Lumped Molecule Surrogate Incremental Reactivity Experiments
014	3/12/23	High NO_x surrogate + CO (149 ppm added to side A)
015	3/16/23	High NO_x surrogate + CO (149 ppm, B)
016	3/17/93	High NO_x surrogate + CO (71.5 ppm, A)
017	3/18/93	High NO_x surrogate + Ethene (B)
018	3/22/93	High NO_x surrogate + Propene (A)
019	3/24/93	High NO_x surrogate + n-Butane (B)
020	3/25/93	High NO_x surrogate w/o formaldehyde + CO (96.7 ppm, B)
021	3/26/93	High NO_x surrogate + trans-2-Butene (B)
022	3/29/93	High NO_x surrogate + formaldehyde (B)
023	3/30/93	High NO_x surrogate + toluene (A)
024	3/31/93	High NO_x surrogate + n-Octane (B)
025	4/1/93	High NO_x surrogate + m-Xylene (A)
026	4/6/93	Propene-NO_x
027	4/7/93	Low NO_x surrogate side equivalency. test. (Unless indicated otherwise, "Low NO_x surrogate" is 0.17 ppm NO_x and 4 ppmC lumped molecule surrogate.)
028	4/8/93	High NO_x surrogate + Acetone (A)
029	4/9/93	Low NO_x surrogate + CO (A)
030	4/12/93	Low NO_x surrogate + Toluene (B)
031	4/13/93	Low NO_x surrogate + n-Butane (A)
032	4/15/93	Low NO_x surrogate + Propene (B)
033	4/16/93	Low NO_x surrogate + t-2-Butene (A)
034	4/19/93	Low NO_x surrogate + α-Pinene (B)
035	4/20/93	Low NO_x surrogate + m-Xylene (A)

Table 5 (continued)

Run	Date	Description and Comments
DTC		
036	4/21/93	Low NO_x surrogate + Formaldehyde (A)
037	4/21/93	Low NO_x surrogate + n-Octane (A)
038	4/26/93	Low NO_x surrogate + Ethene (B)
039	4/27/93	Low NO_x surrogate + Benzene (B)
040	4/30/93	surrogate w/o NO_x (control)
041	5/03/93	Low NO_x ethene surrogate + t-2-Butene (A)
042	5/05/93	Toluene + NO_x
043	5/06/93	High NO_x ethene surrogate + t-2-Butene (B)
049	5/17/93	Pure Air Irradiation (Temperature control test)
052	5/25/93	NO_x + propene (A); NO_z + Isobutene (B)
054	5/28/93	NO_x + propene (A); NO_x + Acetone (B)
055	6/01/93	NO_x + acetone (A); NO_x + Acetaldehyde (B)
064	7/15/93	High NO_x Surrogate + Acetone (B)
065	7/17/93	High NO_x surrogate + Acetaldehyde (A)
066	7/19/93	Low NO_x surrogate + Acetaldehyde (B)
067	7/20/93	Low NO_x surrogate + m-Xylene (B)
068	7/21/93	High NO_x surrogate + m-Xylene (B)
069	7/23/93	High NO_x Full-surrogate + t-2-butene (A)
070	7/26/93	High NO_x Full-Surrogate + n-C8 (A)
071	7/27/93	Low NO_x Full-Surrogate + n-C8 (B)
072	7/28/93	High NO_x Ethene Surrogate + n-C6 (A)

Table 6. Summary of reactivity experiments carried out for this program.

Test VOC	Number of Experiments		
	Ethene Surg. High NOx (ETC)	Lumped Molecule High NO_x (DTC)	Surrogate Low NO_x (DTC)
Carbon Monoxide	3	4	1
Ethane	1		
n-Butane	2	1	1
n-Hexane	1 [a]		
n-Octane	2	2	2
Ethene		1	1
Propene	2	1	1
trans-2-Butene	3	2	1
Benzene			1
Toluene		1	1
m-Xylene	3	2	2
Formaldehyde	3	1	1
Acetaldehyde		1	1

[a] DTC used

2. Integrated OH Radicals (IntOH)

The integrated OH radicals, or IntOH, is useful in providing information on the effect of the VOC on radical levels, which in turn provides information on the chemical basis for a VOC's reactivity (Carter et al, 1993a; see also below.) The IntOH can be derived from the measured concentrations of any compound present in the experiment which reacts only with OH radicals, provided (1) that its OH radical rate constant is well known and (2) that it reacts sufficiently rapidly that the amount consumed due to reaction can be determined as a function of time with a reasonable degree of precision. If $[Tracer]_0$ and $[Tracer]_t$ are the initial and time t concentration of the compound used as the "OH tracer", kOH^{tracer} is its OH rate constant, and D is the dilution rate of the experiment (derived as discussed below), then $IntOH_t$ is given by (Carter et al, 1993a):

$$IntOH_t = \int_0^t [OH]_t dt = \frac{\ln\left(\frac{[tracer]_0}{[tracer]_t}\right) - Dt}{kOH^{tracer}}. \qquad (I)$$

m-Xylene was used as the OH tracer in the experiments where this compound was present as a surrogate constituent. In the ethene surrogate runs, small amounts (75-100 ppb) of cyclohexane or methylcyclohexane were added as the OH radical tracer. (The specific tracer used in the ethene experiments is given in the tabulations of the results.) The rate constants used to derive the IntOH values in this work are: 3.46×10^4 ppm^{-1} min^{-1} for m-xylene, 1.11×10^4 ppm^{-1} min^{-1} for cyclohexane, and 1.51×10^4 ppm^{-1} min^{-1} for methylcyclohexane (Atkinson, 1989; Carter, 1990).

Hourly IntOH values were used in the data analysis. In our previous work, the ln([tracer]) data were fit by linear or quadratic function, and this function was then used for deriving the hourly IntOH values. This approach was useful in smoothing the data and also provided a means for using the scatter of the data to give uncertainty estimates. However, we subsequently found that this can sometimes introduce artifacts into the IntOH estimates for early time periods, particularly in runs with strong radical inhibitors. Therefore, this approach was not used in this work. Instead, the IntOH values were calculated for the times for which tracer data were available, and hourly values were determined by linear interpolation. The stated uncertainties in the IntOH values were derived by estimating a 2% minimum imprecision uncertainty in the tracer measurements. This is a minimum uncertainty estimate since it does not include uncertainties in the OH radical rate constant, nor does it take into account possible experiments where measurement scatter was greater than 2%.

3. Base Case $d(O_3\text{-}NO)$ and IntOH

For each "test" experiment where a test VOC is added, there is a corresponding "base case" experiment where the conditions are the same except that the test VOC is not present. In the DTC experiments, where two mixtures could be irradiated simultaneously and where the common NO_x and base ROG reactants can be added and mixed equally in both reactors prior to adding the test compound to one, the base case experiment was carried out simultaneously with each test experiment. In this case, the $d(O_3\text{-}NO)_t^{base}$ and $IntOH_t^{base}$ data corresponding to any test experiment are simply derived from the results of the simultaneous irradiation of the base case mixture.

In the ETC experiments, where only one mixture could be irradiated at a time, and where there is run-to-run variability in temperature and initial reactant concentrations, there is not necessarily a base case experiment which corresponds as closely to the conditions of any given test experiment as is possible in dual chamber runs. In this case, a linear regression analysis is used to derive the dependencies of the base case $d(O_3\text{-}NO)_t$ and $IntOH_t$ data on the variable run conditions, and the results of this analysis is used to derive the $d(O_3\text{-}NO)_t^{base}$ and $IntOH_t^{base}$ values corresponding to the condition of any given test experiment. This is the approach used in our previous incremental reactivity experiments in this chamber (Carter et al., 1993a). Note that when this approach is used, the analysis can also give uncertainty estimates for $d(O_3\text{-}NO)$ and IntOH due to variations in run conditions which are not accounted for by the regressions.

4. Amounts of Test VOC Added and Reacted

The amounts of test VOC added, $[VOC]_0$, was obtained from the measured test VOC concentration at or immediately prior to the start of the irradiation. The amount of VOC reacted at time=t, $[VOC\ reacted]_t$, was determined either from the experimental measurements of the VOC as a function of time during the experiment, corrected for dilution as shown below, or, for VOCs which react only with OH radicals, from the measured IntOH values and the VOC's OH radical rate constant. In the "direct" method, the amount reacted at time t is given by:

$$(VOC\ reacted)_t = [VOC]_0 - [VOC]_t - D\int_0^t [VOC]\ dt \qquad (II)$$

where D is the dilution and $[VOC]_t$ is the measured VOC concentration at time t. In the IntOH method the amount reacted is given by

$$(VOC\ reacted)_t = [VOC]_0 \frac{kOH^{VOC}\ IntOH_t}{kOH^{VOC}\ IntOH_t + Dt}\left(1 - e^{-kOH^{VOC}\ IntOH_t - Dt}\right) \qquad (III)$$

where kOH^{VOC} is the VOC's OH radical rate constant. (See Carter et al. [1993a] for the derivations of these equations.) As with the previous study (Carter et

al., 1993a), if the amount reacted could be estimated by either method, the method estimated to have the least uncertainty was used.

The uncertainties in the amounts reacted using the direct method (Equation II) were derived by assuming a minimum 2% imprecision uncertainty in the VOC measurements, together with the uncertainty in the dilution derived as discussed below. (The actual imprecision uncertainties for some VOCs were different from this, but this was not taken into account in this analysis.) The uncertainties in the amounts reacted derived from the IntOH method (Equation III) were derived from the uncertainties derived for IntOH and D, and also, for determining which estimation approach is least uncertain, by assuming a 20% uncertainty in kOH^{VOC}. The estimated uncertainty in kOH^{VOC} was used only in making the choice between Equation (II) or (III), and was not used in the minimum uncertainties in the amounts reacted given with the data tabulations (Carter et al., 1993a).

Amounts reacted could be estimated for all the test VOCs used in this study except for formaldehyde. Amounts of formaldehyde could not be estimated from Equation (III) because formaldehyde is consumed to a significant extent by photolysis, and could not be estimated from the measured formaldehyde concentrations because a significant amount of this compound is formed from the reactions of the base ROG surrogate. However, for VOCs which are strong radical inhibitors, the amounts of test VOC or OH tracer compound reacted are small relative to analytical imprecisions, and thus estimates of amounts reacted become uncertain.

5. Dilution

Note that the derivations of IntOH and VOC reacted require an estimate of the dilution rate, D, for each experiment. Although in principal experiments in flexible Teflon reaction chambers should not have dilution because the chamber can collapse as samples are withdrawn for analysis, in practice we find that some non-negligible dilution is occurring. The analysis of dilution in ETC experiments has been discussed in detail previously (Carter et al., 1993a), and an approximate dilution rate of 0.48 ± 0.25 %/hour was derived for experiments in this chamber. This value was used for the ETC experiments in this study as well.

For the DTC chamber, the dilution rate was derived from the rate of consumption of n-butane (a component of the full surrogate), corrected for its reaction with OH radicals by using its OH radical rate constant and the m-xylene data and its rate constant. The general method employed has been discussed previously (Carter et al., 1993a). If necessary data were missing or the data appeared to be too scattered for a reliable dilution estimate, the dilution rate was estimated based on results for other runs in the same side of the DTC carried out at approximately the same time. (In those cases, the dilutions were given uncertainty estimates of ~1 %/hour.) The dilution rates generally ranged from

highs of ~1-2 %/hr for the initial experiments to averages of ~0.3 %/hour in the later runs. Thus they were usually comparable to dilution rates in the ETC.

Uncertainties in dilution were taken into account in the estimates in the minimum uncertainties in the IntOH and amounts reacted data. Generally, the dilution corrections were not large contributors to the overall uncertainties in these quantities.

6. Total or d(O_3-NO) incremental reactivities

The term "total" incremental reactivity is used to refer to incremental reactivity relative to d(O_3-NO) because it reflects all aspects of a VOC's reaction mechanism which affects O_3. It is given by

$$IR_t^{total} = \frac{d(O_3\text{-}NO)_t^{test} - d(O_3\text{-}NO)_t^{base}}{[VOC]_0} \qquad (IV)$$

where $d(O_3\text{-}NO)_t^{test}$ and $d(O_3\text{-}NO)_t^{base}$ are the $d(O_3\text{-}NO)_t$ measured in the test experiment and either measured or derived for the corresponding base case experiment, respectively, for time t, and $[VOC]_0$ is the initial VOC concentration.

The minimum uncertainties in the overall incremental reactivities are estimated differently depending on whether the experiment is a divided chamber (DTC) or single mode (e.g., ETC) chamber run. If it is a single mode run, the regression analysis used to derive the $d(O_3\text{-}NO)^{base}$ data also yields an uncertainty estimate for these data. The $d(O_3\text{-}NO)^{test}$ are assumed to have the same uncertainty for the purpose of estimating uncertainties in IR. For divided chamber runs, there is no uncertainty estimate for $d(O_3\text{-}NO)^{base}$ or $d(O_3\text{-}NO)^{test}$. In this case, we assume they each have a ~3% uncertainty for the purpose of estimating a minimum uncertainty for IR. This is based on the approximate level of equivalence observed when the same mixture is irradiated on both sides of the chamber.

Unless otherwise indicated, the overall incremental reactivities in this work are given in units of moles of ozone per mole of VOC. Note that this is not the same as gram basis or carbon basis incremental reactivities, which are more often used in a regulatory context. However, molar units are preferred in this work because they have a more direct relationship to the chemical basis of reactivity.

7. IntOH Incremental Reactivities.

The IntOH incremental reactivity is a measure of the effect of the VOC on OH radical levels. It is given by:

$$IR_t^{IntOH} = \frac{IntOH_t^{test} - IntOH_t^{base}}{[VOC]_0} \qquad (V)$$

where $IntOH^{test}$ is the IntOH measured in the test experiment with the added VOC and $IntOH^{base}$ is the IntOH measured or derived for the corresponding base case run. The IntOH reactivity results are given in units of ppt-min OH per ppm VOC added. The minimum uncertainties in the IR^{IntOH} values are derived from the uncertainties in the $IntOH^{test}$ and $IntOH^{base}$ data derived from either assuming a 2% imprecision uncertainty in the tracer data (for all the $IntOH^{test}$ data and the DTC $IntOH^{base}$ data), or (for the ETC $IntOH^{base}$ data) from the uncertainty in the regression estimate.

8. Direct and Indirect Incremental Reactivities

As discussed previously (Carter et al., 1993a), the total $d(O_3\text{-}NO)$ incremental reactivity can be broken down into its "direct" and "indirect" components,

$$IR^{total} = IR^{direct} + IR^{indirect} \qquad \text{(VI)}$$

where the "Direct" incremental reactivity is defined as the amount of O_3 formation and NO oxidation caused directly by the reactions of the radicals formed from the reactions of the test VOC and its reactive products, and the "indirect" incremental reactivity is the change in O_3 formation and NO oxidation resulting from the effect of the test VOC on the reactions of the other VOCs present, in both cases relative to the amount of test VOC added. In an incremental reactivity experiment, the "other VOCs" are the components of the base ROG mixture used in the base case experiments. An estimate of how the reactions of the test VOC effect $d(O_3\text{-}NO)$ from the reactions of the base ROG can be obtained if it is assumed that the relationship between IntOH and the $d(O_3\text{-}NO)$ formed from the reactions of the base ROG mixture is the same in the test experiments as it is in the base case runs. This is a reasonable assumption in high NO_x experiments where the addition of the test VOC does not cause a large perturbation on the system, but is not valid under NO_x-limited conditions where the effect of the VOC on NO_x levels will also affect ozone formation from the base ROG surrogate. If this is assumed, then

$$IR^{indirect} \simeq IR^{IntOH} \frac{d(O_3\text{-}NO)_t^{base}}{IntOH^{base}} \qquad \text{(VII)}$$

and thus, from (VI)

$$IR^{direct} \simeq IR^{total} - IR^{IntOH} \frac{d(O_3\text{-}NO)_t^{base}}{IntOH_t^{base}} \qquad \text{(VIII)}$$

Because the assumptions behind these equations are not valid under NO_x-limited conditions, direct and indirect reactivities are only reported for high NO_x experiments, or portions of lower NO_x experiments where ozone formation is not NO_x-limited.

The $d(O3\text{-}NO)^{base}/IntOH^{base}$ ratios for the DTC experiments were taken directly from the results of the base case experiment conducted along with the test run. For the single chamber ETC runs, a linear regression analysis was used to determine how this ratio depended on reaction conditions, and this was used to derive the $d(O3\text{-}NO)^{base}/IntOH^{base}$ ratios for the conditions of each test experiment. The ratio tended to be less variable than $d(O_3\text{-}NO)^{base}$ or $IntOH^{base}$, so the ratio for a test run derived based on the regression analysis on the base case ratio tended to have less uncertainty than the ratio of the $d(O_3\text{-}NO)^{base}$ and $IntOH^{base}$ derived from the separate regressions on each.

9. Mechanistic Reactivities

Mechanistic reactivities are analogous to incremental reactivities except they are relative to the amount of test VOC reacted up to the time of the observation, rather than the amount added. Thus

$$MR_t^{total} = \frac{d(O_3\text{-}NO)_t^{test} - d(O_3\text{-}NO)_t^{base}}{(\text{VOC Reacted})_t} \qquad \text{(IX)}$$

$$MR_t^{IntOH} = \frac{IntOH_t^{test} - IntOH_t^{base}}{(\text{VOC reacted})_t} \qquad \text{(X)}$$

$$MR^{total} = MR^{direct} + MR^{indirect} \qquad \text{(XI)}$$

$$MR^{indirect} \simeq MR^{IntOH} \frac{d(O_3\text{-}NO)_t^{base}}{IntOH^{base}} \qquad \text{(XII)}$$

and

$$MR^{direct} \simeq MR^{total} - MR^{IntOH} \frac{d(O_3\text{-}NO)_t^{base}}{IntOH^{base}} \qquad \text{(XIII)}$$

Mechanistic reactivities are useful because, to a first approximation, they are independent on how rapidly the VOC reacts, and thus allow comparisons of reactivity characteristics of VOCs which react at different rates. However, measurements of mechanistic reactivities are useful only for VOCs where the amount reacted can be determined with a reasonable degree of precision. Thus, no mechanistic reactivity data could be obtained for formaldehyde, and determinations of mechanistic reactivities in some experiments with strong radical inhibition are probably insufficiently precise to be useful for mechanism evaluation.

B. Ethene Surrogate Reactivity Results

1. Base Case results

The conditions and selected results of the ethene surrogate reactivity experiments are summarized on Table 7. The base case experiments consisted of irradiations of 0.43±0.04 ppm NO_x and 1.66±0.10 ppm ethene, with ~100 ppb each of cyclohexane (or methylcyclohexane) and n-butane as dilution and radical tracers. Concentration-time plots for O_3, NO, NO_2 and ethene in a typical "ethene surrogate" base case experiment is shown in Figure 13. Results of model simulations of the experiment, discussed later in this report, are also shown. It can be seen that this can be considered a "high NO_x" experiment since NO_2 is still being consumed and O_3 is still forming when the run is ended at 6 hours. The continued formation of O_3 and the presence of reacting NO_2 means that O_3 is not NO_x-limited. Thus the base case for experiments can be considered to approximate "maximum reactivity" conditions, though, as discussed below, this is not true for many of the added test VOC runs.

Table 7 shows that except for run ETC467, which had higher than the usual NO levels, good reproducibility was observed in these ethene-NO_x base case experiments. Nevertheless, there was sufficient variability in the results that the uncertainties in the incremental reactivity derivations could be reduced by using linear regression analyses to take into account the dependencies of the results on the variable reaction conditions. The set of parameters used for the regressions depended on the base case result being predicted, being chosen to minimize the uncertainty in the predictions using the regressions. (Note that while using the maximum number of dependent parameters in the regression may give the best fits of the predictions to the base case data, it does not necessarily give the least uncertain estimates of the predicted values because increasing the number of degrees of parameters beyond the optimum number tends to increase uncertainties of the predictions). The set of parameters which gave the least uncertainties in the predictions were as follows:

Predicted Quantity	Parameters Used
hour 1 d(O_3-NO)	none (simple average used)
hour 2-6 d(O_3-NO)	average temperature, initial NO_2 and ethene
hour 1-5 IntOH	average temperature, initial NO and ethene
hour 6 IntOH	average temperature, initial NO, NO_2 and ethene
hour 1 d(O_3-NO)/IntOH	none
hour 2-3 d(O_3-NO)/IntOH	average temperature, initial NO_2 and ethene
hour 4-6 d(O_3-NO)/IntOH	average temperature, initial NO and NO_2.

Figure 14 shows plots of the predicted vs. observed 6-hour d(O_3-NO), IntOH and d(O_3-NO)/IntOH results of the base case experiments, with the error bars showing the uncertainties of the regression predictions.

It is interesting to note that although the range of average temperatures in these experiments was less than 2°C, the variation in temperature was found

Table 7. Summary of conditions and selected results of the ETC ethene surrogate reactivity experiments.

ETC Run No.	Test VOC Name	(ppm)	Avg. T (K)	Initial Reactants [a] NO	NO2	NOx	Ethene	Results (t=6 hrs) [b] d(O_3-NO)	IntOH	Ratio
464 [c]			301.7	279	96	375	1.48	1.162	41.1	28.3
466 [c]			301.0	308	105	413	1.48	1.080	35.0	30.9
467 [c,d]			301.0	400	125	525	1.46	0.732	20.5	35.8
469			301.4	341	114	455	1.77	1.136	32.6	34.8
471			302.3	342	110	452	1.77	1.268	42.1	30.1
473			301.4	344	116	460	1.86	1.233	38.3	32.2
476			301.1	300	131	431	1.68	1.043	32.8	31.8
479			301.3	312	106	418	1.75	1.150	37.5	30.7
482			301.2	315	95	410	1.57	1.139	33.7	33.8
486			301.4	339	101	440	1.56	1.076	32.1	33.5
497			301.9	319	135	454	1.74	1.184	38.4	30.9
505			301.0	283	115	398	1.61	1.080	38.4	28.1
487	CO	107	301.8	335	122	457	1.64	1.431	33.4	
483	CO	155	300.7	312	111	423	1.58	1.475	25.9	
506	ETHANE	50	300.6	290	122	412	1.54	1.209	20.0	
488	N-C4	10.3	300.5	311	108	419	1.56	1.323	16.9	
484	N-C4	15	300.7	338	118	456	1.67	1.400	14.2	
472	N-C8	1.6	301.4	314	107	421	1.78	0.966	13.6	
474	N-C8	2.3	301.4	318	138	456	1.76	0.920	11.6	
500	PROPENE	0.21	300.7	303	116	419	1.66	1.270	36.5	
496	PROPENE	0.30	301.5	280	96	376	1.59	1.226	45.0	
501	T-2-BUTE	0.066	300.9	303	120	423	1.70	1.274	48.6	
493	T-2-BUTE	0.14	301.4	314	110	424	1.79	1.247	55.0	
478	M-XYLENE	0.097	300.9	301	128	429	1.70	1.298	48.7	
499	M-XYLENE	0.16	301.2	317	112	429	1.73	1.274	39.5	
477	M-XYLENE	0.19	301.4	319	142	461	1.75	1.295	53.9	
468	FORMALD	0.11	301.2	324	104	428	1.67	1.280	40.7	
470	FORMALD	0.26	301.8	294	96	390	1.63	1.371	56.8	
489	FORMALD	0.29	302.0	314	105	419	1.63	1.377	56.1	
Average			301.3	313	114	430	1.66			
Std. Deviation			0.5	6%	11%	5%	5%			

[a] Initial NO, NO_2, and NO_x in ppb; initial ethene in ppm.
[b] d(O3-NO) in units of ppm; IntOH in units of ppt-min; Ratio is base case d(O3-NO)/IntOH in units of 10^3 min^{-1}
[c] Initial ethene appears to be anomalously low. Model more constent with entire set if these runs are assumed to have the same ethene as the other runs.
[d] Initial NO unusually high. Results not used for base case results regression.

to be a statistically significant factor in affecting the results, with both d(O_3-NO) and IntOH (though not their ratio) increasing with temperature. The temperature dependence indicated by the regression analysis for t=6 hour d(O_3-NO) corresponds to an apparent activation energy of 19 kcal/mole. As discussed elsewhere (Carter et al., 1995a), this is comparable to the temperature dependence observed in the phase I mini-surrogate runs (Carter et al., 1993a), and in both cases the temperature dependence is far grater than can be accounted for in the mechanism, even after considering possible temperature-dependent chamber effects.

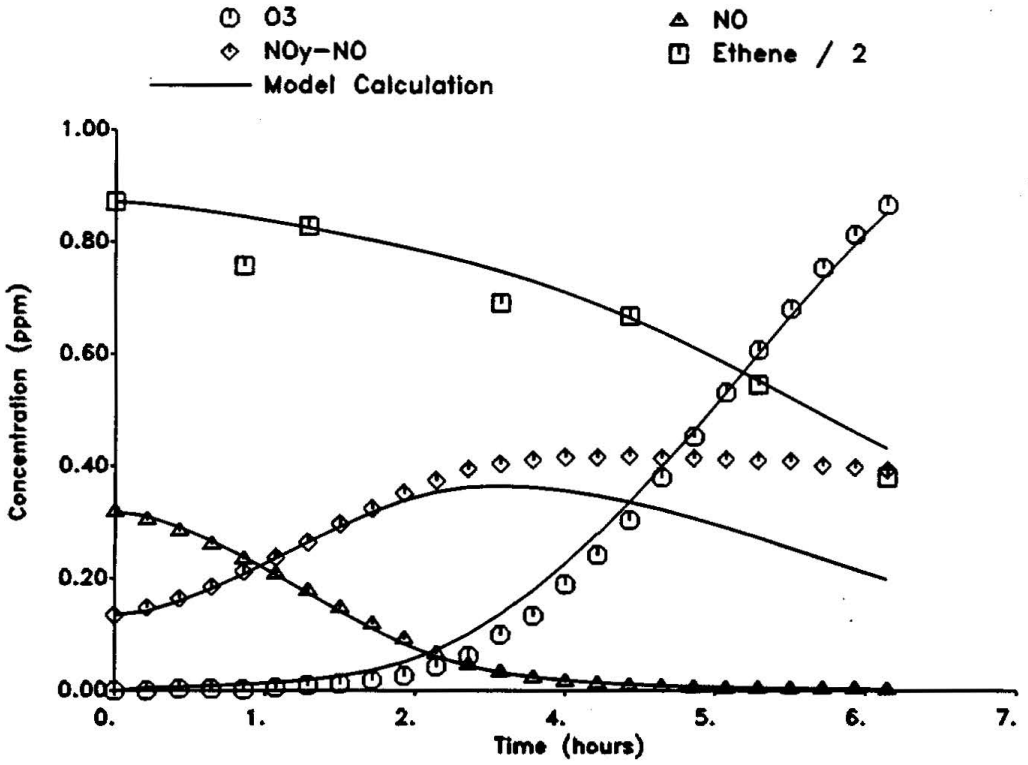

Figure 13. Concentration time plots of selected species in a representative "base case" ethene surrogate run. Results of model simulations are also shown.

2. Reactivity Results

As indicated in Table 6, ethene surrogate reactivity experiments were carried out for carbon monoxide, ethane, n-butane, n-octane, propene, trans-2-butene, m-xylene and formaldehyde, in most cases with two experiments for each VOC. The conditions and selected results of the added test VOC runs are included on Table 7, the detailed results of the ethene surrogate reactivity experiments are shown on Tables 8-10. These include, for each hour in the experiment, the estimated amount of test VOC reacted and its uncertainty, the method used to estimate the amount reacted, the $d(O_3\text{-NO})$ and IntOH observed in the added VOC run and their corresponding base case values derived from linear regressions of the base case experiments for the conditions of the added VOC runs, the corresponding $d(O_3\text{-NO})$ and IntOH incremental and mechanistic reactivities, the $d(O_3\text{-NO})^{base}/IntOH^{vase}$ ratio derived from the linear regression of this ratio in the base case runs, the amount of $d(O_3\text{-NO})$ formed from the reactions of the base ROG estimated using $d(O_3\text{-NO})^{base}/IntOH^{vase}$ and $IntOH^{test}$, and the corresponding estimated

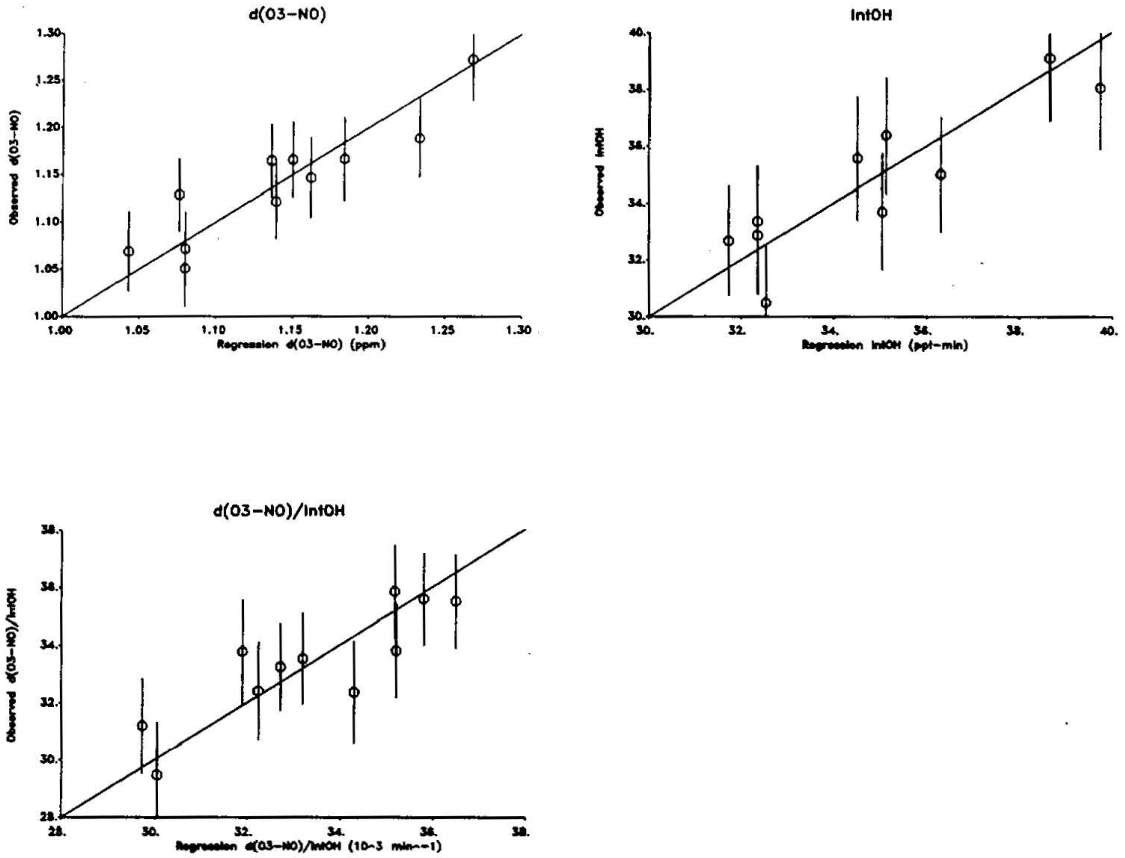

Figure 14. Plots of observed vs regression predicted 6-hour $d(O_3\text{-}NO)$, IntOH and $d(O_3\text{-}NO)/IntOH$ ratios for the base case ethene surrogate experiments.

direct incremental and mechanistic reactivities. Data whose estimated minimum uncertainties are too large to be meaningful are not shown.

Plots of representative results for the added VOC ethene surrogate experiments are shown on Figures 15-23. Results of model calculations, discussed later, are also shown. Except as noted, the figures include the following plots for each VOC:

(1) The concentration-time plots of $d(O_3\text{-}NO)$ for the added VOC runs and the hourly average base case $d(O_3\text{-}NO)$ results. The standard deviations of the averages for the base case are also shown.

Table 8. Derivation of hourly d(O_3-NO) reactivities from the results of the ethene surrogate experiments.

ETC Run No.	Added (ppm)	Time (hr)	Reacted [a] (ppm)	Deriv.	d(O3-NO) (ppm) Test	Base Fit	Change	Reactivity (mol/mol) Incremental	Mechanistic
Carbon Monoxide									
487	107.	1	[b]		0.168	0.088 ±0.015	0.080 ±0.022	0.0007 ± 28%	
	± 2.	2	[b]		0.412	0.216 ±0.019	0.196 ±0.027	0.0018 ± 14%	
		3	0.326 ±0.099	IntOH	0.752	0.379 ±0.028	0.373 ±0.039	0.0035 ± 11%	1.14 ± 32%
		4	0.547 ±0.102	IntOH	1.115	0.605 ±0.045	0.510 ±0.063	0.0048 ± 13%	0.93 ± 22%
		5	0.803 ±0.106	IntOH	1.352	0.894 ±0.059	0.458 ±0.083	0.0043 ± 18%	0.57 ± 23%
		6	1.121 ±0.113	IntOH	1.431	1.151 ±0.041	0.280 ±0.058	0.0026 ± 21%	0.25 ± 23%
483	155.	1	[b]		0.184	0.088 ±0.015	0.096 ±0.022	0.0006 ± 23%	
	± 3.	2	0.261 ±0.141	IntOH	0.446	0.210 ±0.020	0.236 ±0.028	0.0015 ± 12%	0.90 ± 55%
		3	0.461 ±0.143	IntOH	0.825	0.350 ±0.028	0.475 ±0.040	0.0031 ± 9%	1.03 ± 32%
		4	0.713 ±0.147	IntOH	1.198	0.528 ±0.046	0.670 ±0.065	0.0043 ± 10%	0.94 ± 23%
		5	0.979 ±0.153	IntOH	1.392	0.777 ±0.060	0.615 ±0.085	0.0040 ± 14%	0.63 ± 21%
		6	1.223 ±0.160	IntOH	1.475	1.038 ±0.042	0.437 ±0.059	0.0028 ± 14%	0.36 ± 19%
Ethane									
506	49.7	1	[b]		0.130	0.088 ±0.015	0.042 ±0.022	0.0008 ± 53%	
	±1.0	2	0.101 ±0.051	IntOH	0.317	0.197 ±0.022	0.120 ±0.030	0.0024 ± 25%	1.19 ± 57%
		3	0.181 ±0.052	IntOH	0.547	0.328 ±0.031	0.219 ±0.044	0.0044 ± 20%	1.21 ± 35%
		4	0.211 ±0.054	IntOH	0.827	0.494 ±0.050	0.333 ±0.070	0.0067 ± 21%	1.58 ± 33%
		5	0.241 ±0.056	IntOH	1.076	0.729 ±0.066	0.346 ±0.093	0.0070 ± 27%	1.44 ± 35%
		6	0.382 ±0.058	IntOH	1.209	0.991 ±0.046	0.218 ±0.065	0.0044 ± 30%	0.57 ± 34%
n-Butane									
488	10.31	1	[b]		0.130	0.088 ±0.015	0.042 ±0.022	0.0040 ± 53%	
	±0.21	2	[b]		0.320	0.209 ±0.021	0.111 ±0.030	0.0108 ± 27%	
		3	0.221 ±0.100	IntOH	0.594	0.344 ±0.030	0.250 ±0.042	0.024 ± 17%	1.13 ± 48%
		4	0.316 ±0.101	IntOH	0.945	0.514 ±0.049	0.431 ±0.069	0.042 ± 16%	1.37 ± 36%
		5	0.462 ±0.104	IntOH	1.209	0.753 ±0.064	0.456 ±0.090	0.044 ± 20%	0.99 ± 30%
		6	0.504 ±0.107	IntOH	1.323	1.015 ±0.045	0.308 ±0.063	0.030 ± 21%	0.61 ± 30%
484	15.2	1	[b]		0.183	0.088 ±0.015	0.095 ±0.022	0.0062 ± 23%	
	±0.3	2	[b]		0.451	0.210 ±0.020	0.241 ±0.028	0.0159 ± 12%	
		3	0.341 ±0.146	IntOH	0.828	0.353 ±0.029	0.475 ±0.041	0.031 ± 9%	1.39 ± 44%
		4	0.410 ±0.149	IntOH	1.206	0.532 ±0.047	0.674 ±0.066	0.044 ± 10%	1.64 ± 38%
		5	0.425 ±0.154	IntOH	1.374	0.786 ±0.061	0.587 ±0.087	0.039 ± 15%	1.38 ± 39%
		6	0.645 ±0.158	IntOH	1.400	1.051 ±0.043	0.349 ±0.061	0.023 ± 18%	0.54 ± 30%
n-Octane									
472	1.60	1	[b]		0.057	0.088 ±0.015	-0.031 ±0.022	-0.0196 ± 70%	
	±0.03	2	[b]		0.154	0.235 ±0.019	-0.081 ±0.027	-0.050 ± 33%	
		4	0.123 ±0.046	Direct	0.452	0.625 ±0.044	-0.173 ±0.062	-0.108 ± 36%	-1.40 ± 52%
		5	0.185 ±0.047	Direct	0.700	0.920 ±0.058	-0.220 ±0.081	-0.137 ± 37%	-1.19 ± 45%
		6	0.278 ±0.047	Direct	0.966	1.183 ±0.040	-0.217 ±0.057	-0.135 ± 26%	-0.78 ± 31%
474	2.27	1	[b]		0.053	0.088 ±0.015	-0.035 ±0.022	-0.0156 ± 62%	
	±0.05	2	[b]		0.147	0.206 ±0.020	-0.059 ±0.029	-0.026 ± 49%	
		3	[b]		0.273	0.361 ±0.029	-0.088 ±0.041	-0.039 ± 47%	
		4	0.128 ±0.066	Direct	0.429	0.566 ±0.047	-0.137 ±0.067	-0.060 ± 49%	-1.07 ± 71%
		5	0.172 ±0.068	Direct	0.656	0.847 ±0.062	-0.191 ±0.088	-0.084 ± 46%	-1.11 ± 61%
		6	0.286 ±0.068	Direct	0.920	1.111 ±0.044	-0.191 ±0.062	-0.084 ± 32%	-0.67 ± 40%
n-Hexane									
72A [c]	2.88	1	[b]		0.057	0.067 ±0.002	-0.010 ±0.003	-0.0035 ± 26%	
	±0.06	2	[b]		0.140	0.180 ±0.005	-0.040 ±0.007	-0.0139 ± 17%	
		3	[b]		0.256	0.326 ±0.010	-0.070 ±0.012	-0.024 ± 18%	
		4	[b]		0.405	0.492 ±0.015	-0.087 ±0.019	-0.030 ± 22%	
		5	[b]		0.608	0.718 ±0.022	-0.110 ±0.028	-0.038 ± 26%	
		6	0.166 ±0.121	IntOH	0.914	1.022 ±0.031	-0.108 ±0.041	-0.037 ± 38%	-0.65 ± 82%
Propene									
500	0.213	1	0.011 ±0.006	Direct	0.136	0.088 ±0.015	0.048 ±0.022	0.22 ± 46%	4.48 ± 72%
	±0.004	2	0.050 ±0.005	Direct	0.349	0.211 ±0.020	0.138 ±0.028	0.65 ± 21%	2.75 ± 23%
		3	0.121 ±0.005	Direct	0.681	0.354 ±0.029	0.327 ±0.041	1.53 ± 13%	2.71 ± 13%
		4	0.174 ±0.005	Direct	1.003	0.534 ±0.046	0.469 ±0.066	2.2 ± 14%	2.70 ± 14%
		5	0.201 ±0.005	Direct	1.192	0.788 ±0.061	0.404 ±0.086	1.89 ± 21%	2.01 ± 21%
		6	0.208 ±0.005	Direct	1.270	1.052 ±0.043	0.218 ±0.060	1.02 ± 28%	1.05 ± 28%
496	0.301	1	0.032 ±0.008	Direct	0.149	0.088 ±0.015	0.061 ±0.022	0.20 ± 36%	1.92 ± 44%
	±0.006	2	0.104 ±0.007	Direct	0.451	0.232 ±0.018	0.219 ±0.026	0.73 ± 12%	2.10 ± 14%
		3	0.222 ±0.006	Direct	0.873	0.396 ±0.026	0.477 ±0.037	1.58 ± 8%	2.15 ± 8%
		4	[b]		1.114	0.619 ±0.043	0.495 ±0.060	1.65 ± 12%	
		5	0.301 ±0.006	Direct	1.205	0.903 ±0.056	0.302 ±0.080	1.00 ± 26%	1.00 ± 26%
		6	0.301 ±0.006	Direct	1.226	1.158 ±0.039	0.068 ±0.056	0.23 ± 82%	0.23 ± 82%

Table 8 (continued)

ETC Run No.	Added (ppm)	Time (hr)	Reacted [a] (ppm)	Deriv.	d(O3-NO) (ppm) Test	Base Fit	Change	Reactivity (mol/mol) Incremental	Mechanistic
trans-2-Butene									
501	0.066 ±0.001	1	0.038 ±0.001	Direct	0.319	0.088 ±0.015	0.231 ±0.022	3.5 ± 10%	6.07 ± 10%
		2	0.066 ±0.001	Direct	0.638	0.212 ±0.019	0.426 ±0.027	6.5 ± 7%	6.47 ± 7%
		3	0.066 ±0.001	Direct	0.881	0.360 ±0.027	0.521 ±0.039	7.9 ± 8%	7.92 ± 8%
		4	0.066 ±0.001	Direct	1.096	0.549 ±0.044	0.547 ±0.063	8.3 ± 12%	8.32 ± 12%
		5	0.066 ±0.001	Direct	1.219	0.812 ±0.059	0.407 ±0.083	6.2 ± 20%	6.18 ± 20%
		6	0.066 ±0.001	Direct	1.274	1.076 ±0.041	0.198 ±0.058	3.0 ± 29%	3.01 ± 29%
43B [c]	0.097 ±0.002	1	0.066 ±0.002	Direct	0.350	0.063 ±0.002	0.287 ±0.011	3.0 ± 4%	4.36 ± 5%
		2	0.097 ±0.002	Direct	0.715	0.174 ±0.005	0.541 ±0.022	5.6 ± 5%	5.60 ± 5%
		3	0.097 ±0.002	Direct	0.979	0.318 ±0.010	0.661 ±0.031	6.8 ± 5%	6.84 ± 5%
		4	0.097 ±0.002	Direct	1.224	0.485 ±0.015	0.739 ±0.039	7.6 ± 6%	7.65 ± 6%
		5	0.097 ±0.002	Direct	1.363	0.712 ±0.021	0.651 ±0.046	6.7 ± 7%	6.74 ± 7%
		6	0.097 ±0.002	Direct	1.410	1.009 ±0.030	0.401 ±0.052	4.1 ± 13%	4.15 ± 13%
493	0.142 ±0.003	1	0.142 ±0.003	Direct	0.674	0.088 ±0.015	0.586 ±0.022	4.1 ± 4%	4.14 ± 4%
		2	0.142 ±0.003	Direct	0.932	0.233 ±0.019	0.699 ±0.026	4.9 ± 4%	4.94 ± 4%
		3	0.142 ±0.003	Direct	1.117	0.400 ±0.027	0.717 ±0.038	5.1 ± 6%	5.07 ± 6%
		4	0.142 ±0.003	Direct	1.218	0.621 ±0.043	0.597 ±0.061	4.2 ± 10%	4.22 ± 10%
		5	0.142 ±0.003	Direct	1.244	0.916 ±0.057	0.328 ±0.080	2.3 ± 25%	2.32 ± 25%
		6	0.142 ±0.003	Direct	1.247	1.179 ±0.040	0.068 ±0.056	0.48 ± 82%	0.48 ± 82%
m-Xylene									
478	0.095 ±0.002	1	0.013 ±0.003	Direct	0.125	0.088 ±0.015	0.037 ±0.022	0.39 ± 60%	2.72 ± 63%
		2	0.027 ±0.002	Direct	0.393	0.205 ±0.020	0.188 ±0.028	1.99 ± 15%	6.86 ± 17%
		3	0.045 ±0.002	Direct	0.736	0.349 ±0.029	0.387 ±0.040	4.1 ± 11%	8.66 ± 12%
		4	0.059 ±0.002	Direct	1.056	0.534 ±0.046	0.522 ±0.065	5.5 ± 13%	8.90 ± 13%
		5	0.070 ±0.002	Direct	1.232	0.794 ±0.061	0.438 ±0.086	4.6 ± 20%	6.28 ± 20%
		6	0.075 ±0.002	Direct	1.298	1.059 ±0.043	0.239 ±0.060	2.5 ± 25%	3.18 ± 25%
499	0.147 ±0.003	1	0.015 ±0.004	Direct	0.192	0.088 ±0.015	0.104 ±0.022	0.71 ± 21%	6.84 ± 34%
		2	0.046 ±0.004	Direct	0.544	0.225 ±0.018	0.320 ±0.026	2.2 ± 8%	7.01 ± 11%
		4	0.097 ±0.003	Direct	1.182	0.591 ±0.042	0.591 ±0.059	4.0 ± 10%	6.12 ± 11%
		5	0.108 ±0.003	Direct	1.261	0.872 ±0.055	0.390 ±0.078	2.7 ± 20%	3.61 ± 20%
		6	0.117 ±0.003	Direct	1.274	1.134 ±0.039	0.140 ±0.055	0.95 ± 39%	1.20 ± 39%
477	0.173 ±0.003	1	0.023 ±0.005	Direct	0.249	0.088 ±0.015	0.161 ±0.022	0.93 ± 14%	6.95 ± 24%
		2	0.062 ±0.004	Direct	0.690	0.202 ±0.022	0.488 ±0.030	2.8 ± 7%	7.85 ± 9%
		3	0.098 ±0.004	Direct	1.083	0.354 ±0.031	0.729 ±0.044	4.2 ± 6%	7.45 ± 7%
		4	0.118 ±0.004	Direct	1.259	0.558 ±0.050	0.701 ±0.070	4.1 ± 10%	5.93 ± 11%
		5	0.133 ±0.004	Direct	1.295	0.835 ±0.066	0.460 ±0.093	2.7 ± 20%	3.46 ± 20%
		6	0.139 ±0.004	Direct	1.295	1.099 ±0.046	0.196 ±0.065	1.13 ± 33%	1.41 ± 33%
Formaldehyde									
468	0.108 ±0.002	1	[b]		0.161	0.088 ±0.015	0.073 ±0.022	0.67 ± 30%	
		2	[b]		0.336	0.228 ±0.018	0.108 ±0.026	1.00 ± 24%	
		3	[b]		0.542	0.387 ±0.026	0.155 ±0.037	1.44 ± 24%	
		4	[b]		0.812	0.596 ±0.042	0.216 ±0.060	2.0 ± 28%	
		5	[b]		1.085	0.875 ±0.055	0.210 ±0.078	1.95 ± 37%	
		6	[b]		1.280	1.135 ±0.039	0.145 ±0.055	1.35 ± 38%	
470	0.260 ±0.005	1	[b]		0.262	0.088 ±0.015	0.174 ±0.022	0.67 ± 13%	
		2	[b]		0.563	0.239 ±0.019	0.324 ±0.027	1.25 ± 9%	
		3	[b]		0.916	0.412 ±0.027	0.505 ±0.039	1.94 ± 8%	
		4	[b]		1.193	0.650 ±0.044	0.543 ±0.063	2.1 ± 12%	
		5	[b]		1.320	0.950 ±0.058	0.371 ±0.083	1.42 ± 22%	
		6	[b]		1.371	1.204 ±0.041	0.167 ±0.058	0.64 ± 35%	
489	0.286 ±0.006	1	[b]		0.216	0.088 ±0.015	0.128 ±0.022	0.45 ± 17%	
		2	[b]		0.511	0.233 ±0.019	0.278 ±0.027	0.97 ± 10%	
		3	[b]		0.880	0.407 ±0.028	0.473 ±0.039	1.66 ± 9%	
		4	[b]		1.182	0.649 ±0.045	0.533 ±0.063	1.86 ± 12%	
		5	[b]		1.328	0.953 ±0.059	0.375 ±0.083	1.31 ± 22%	
		6	[b]		1.377	1.206 ±0.041	0.171 ±0.058	0.60 ± 34%	

[a] Derivation methods: "IntOH" = hourly amounts reacted computed from the experimentally measured IntOH and VOC's OH rate constant; "Direct" = hourly amounts reacted determined by interpolating experimental measurements of the VOC, with a correction for dilution.

[b] Amount reacted could not be determined for this VOC, or amount reacted could not be determined for this time with sufficient precision to be useful.

[c] This is a DTC run. "Base fit" data is from base case run carried out in the other side of the chamber.

Table 9. Derivation of hourly IntOH reactivities from the results of the ethene surrogate experiments.

ETC Run No	Added (ppm)	Time (hr)	Reacted (ppm)	IntOH (ppt-min) Test Run	Base Fit	Change	Reactivity (ppt-min/ppm) Incremental	Mechanistic
Carbon Monoxide								
487	107.	1	[a]	1.1 ±2.6	1.0 ±1.0	0.1 ±2.8	(0.0007 ±0.03)	
		2	[a]	2.8 ±2.6	3.7 ±1.5	-0.9 ±3.0	(-0.008 ±0.03)	
		3	0.326 ±0.099	8.7 ±2.6	7.6 ±1.6	1.1 ±3.1	(0.010 ±0.03)	(3. ± 10.)
		4	0.547 ±0.102	14.7 ±2.7	12.8 ±2.6	1.9 ±3.8	(0.02 ±0.04)	(3. ± 7.)
		5	0.803 ±0.106	21.6 ±2.8	22.0 ±2.2	-0.3 ±3.5	(-0.003 ±0.03)	(0. ± 4.)
		6	1.121 ±0.113	30.3 ±2.9	32.5 ±2.2	-2.2 ±3.6	(-0.02 ±0.03)	(-2. ± 3.)
483	155.	1	[a]	1.4 ±2.6	3.2 ±1.1	-1.8 ±2.8	(-0.012 ±0.02)	
		2	0.261 ±0.141	4.8 ±2.6	5.5 ±1.6	-0.7 ±3.0	(-0.004 ±0.02)	(-3. ± 12.)
		3	0.461 ±0.143	8.5 ±2.6	9.2 ±1.7	-0.7 ±3.1	(-0.005 ±0.02)	(-2. ± 7.)
		4	0.713 ±0.147	13.2 ±2.8	13.2 ±2.8	0.0 ±3.9	(0.0003 ±0.03)	(0. ± 5.)
		5	0.979 ±0.153	18.2 ±2.8	20.8 ±2.3	-2.6 ±3.6	(-0.02 ±0.02)	(-3. ± 4.)
		6	1.223 ±0.160	22.8 ±2.9	29.5 ±2.1	-6.7 ±3.6	-0.043 ± 53%	-5. ± 55%
Ethane								
506	49.7	1	[a]	1.2 ±2.6	4.0 ±1.1	-2.8 ±2.8	(-0.06 ±0.06)	
		2	0.101 ±0.051	5.1 ±2.6	6.0 ±1.6	-0.9 ±3.1	(-0.02 ±0.06)	(-9. ± 31.)
		3	0.181 ±0.052	9.2 ±2.6	10.4 ±1.7	-1.3 ±3.2	(-0.03 ±0.06)	(-7. ± 18.)
		4	0.211 ±0.054	10.7 ±2.8	14.7 ±2.8	-4.0 ±4.0	(-0.08 ±0.08)	(-19. ± 20.)
		5	0.241 ±0.056	12.3 ±2.8	22.6 ±2.3	-10.3 ±3.6	-0.21 ± 35%	-43. ± 42%
		6	0.382 ±0.058	19.5 ±2.9	29.9 ±2.3	-10.4 ±3.7	-0.21 ± 35%	-27. ± 38%
n-Butane								
488	10.31	1	[a]	1.6 ±2.6	3.4 ±1.1	-1.8 ±2.8	(-0.2 ± 0.3)	
		2	[a]	3.4 ±2.6	5.7 ±1.7	-2.3 ±3.1	(-0.2 ± 0.3)	
		3	0.221 ±0.100	5.8 ±2.6	9.3 ±1.8	-3.5 ±3.2	-0.34 ± 92%	(-16. ± 16.)
		4	0.316 ±0.101	8.4 ±3.0	12.8 ±3.0	-4.5 ±4.2	-0.43 ± 94%	-14. ± 99%
		5	0.462 ±0.104	12.3 ±2.8	20.0 ±2.5	-7.7 ±3.7	-0.74 ± 49%	-17. ± 53%
		6	0.504 ±0.107	13.5 ±2.9	28.4 ±2.3	-14.9 ±3.7	-1.44 ± 25%	-30. ± 32%
484	15.2	1	[a]	1.2 ±2.6	2.6 ±1.2	-1.4 ±2.8	(-0.09 ± 0.2)	
		2	[a]	2.9 ±2.6	5.0 ±1.7	-2.1 ±3.1	(-0.14 ± 0.2)	
		3	0.341 ±0.146	6.1 ±2.6	7.9 ±1.8	-1.9 ±3.2	(-0.12 ± 0.2)	(-5. ± 10.)
		4	0.410 ±0.149	7.4 ±3.0	11.6 ±3.0	-4.2 ±4.2	(-0.3 ± 0.3)	(-10. ± 11.)
		5	0.425 ±0.154	7.7 ±2.8	19.0 ±2.5	-11.4 ±3.7	-0.75 ± 33%	-27. ± 49%
		6	0.645 ±0.158	11.7 ±2.9	27.0 ±2.3	-15.3 ±3.7	-1.01 ± 24%	-24. ± 34%
n-Hexane								
72A [b]	2.88	3	[a]	3.7 ±3.2	3.9 ±2.4	-0.2 ±4.0	(-0.07 ± 1.4)	
		4	[a]	3.9 ±3.8	7.9 ±2.6	-4.0 ±4.7	(-1.4 ± 2.)	
		5	[a]	5.3 ±4.5	9.0 ±2.8	-3.7 ±5.3	(-1.3 ± 2.)	
		6	0.166 ±0.121	7.3 ±5.2	17.2 ±3.1	-10.0 ±6.1	-3.5 ± 61%	-60. ± 95%
n-Octane								
472	1.60	1	[a]	2.7 ±2.2	2.9 ±1.0	-0.2 ±2.4	(-0.14 ± 2.)	
		2	[a]	3.0 ±2.2	4.8 ±1.5	-1.9 ±2.7	(-1.2 ± 2.)	
		3	0.095 ±0.046	4.8 ±2.3	9.2 ±1.6	-4.5 ±2.8	-2.8 ± 62%	-47. ± 78%
		4	0.123 ±0.046	6.3 ±2.6	15.5 ±2.6	-9.2 ±3.6	-5.7 ± 39%	-75. ± 54%
		5	0.185 ±0.047	9.6 ±2.4	25.5 ±2.1	-15.9 ±3.2	-9.9 ± 20%	-86. ± 32%
		6	0.278 ±0.047	15.1 ±2.5	37.0 ±2.1	-22.0 ±3.2	-13.7 ± 15%	-79. ± 22%
474	2.27	1	[a]	1.0 ±2.2	2.7 ±1.0	-1.6 ±2.4	(-0.7 ± 1.1)	
		2	[a]	1.7 ±2.2	4.7 ±1.5	-3.1 ±2.7	-1.35 ± 87%	
		3	[a]	2.8 ±2.3	9.0 ±1.5	-6.2 ±2.7	-2.7 ± 44%	
		4	0.128 ±0.066	4.6 ±2.5	14.9 ±2.5	-10.4 ±3.5	-4.6 ± 34%	-81. ± 62%
		5	0.172 ±0.068	6.2 ±2.4	24.7 ±2.1	-18.5 ±3.2	-8.1 ± 17%	-107. ± 43%
		6	0.286 ±0.068	10.6 ±2.5	32.8 ±2.2	-22.2 ±3.3	-9.8 ± 15%	-78. ± 28%
Propene								
500	0.213	1	0.011 ±0.006	0.9 ±2.6	3.8 ±1.1	-2.9 ±2.8	-13.5 ± 96%	(-272. ±302.)
		2	0.050 ±0.005	2.1 ±2.6	5.8 ±1.6	-3.7 ±3.1	-17.2 ± 83%	-73. ± 84%
		3	0.121 ±0.005	10.2 ±2.6	9.9 ±1.7	0.3 ±3.1	(2. ± 15.)	(3. ± 26.)
		4	0.174 ±0.005	21.3 ±2.8	14.7 ±2.8	6.6 ±3.9	31. ± 59%	38. ± 59%
		5	0.201 ±0.005	30.9 ±2.8	23.1 ±2.3	7.8 ±3.6	37. ± 46%	39. ± 46%
		6	0.208 ±0.005	33.9 ±2.9	31.5 ±2.1	2.3 ±3.6	(11. ± 17.)	(11. ± 17.)
496	0.301	1	0.032 ±0.008	1.7 ±2.6	3.3 ±1.1	-1.5 ±2.8	(-5. ± 9.)	(-49. ± 89.)
		2	0.104 ±0.007	7.7 ±2.6	5.2 ±1.6	2.5 ±3.0	(8. ± 10.)	(24. ± 29.)
		3	0.222 ±0.006	18.2 ±2.6	10.7 ±1.7	7.4 ±3.1	25. ± 42%	33. ± 42%
		4	[a]	27.6 ±2.7	17.1 ±2.7	10.6 ±3.8	35. ± 36%	
		5	0.301 ±0.006	37.0 ±2.8	27.0 ±2.3	10.0 ±3.6	33. ± 36%	33. ± 36%
		6	0.301 ±0.006	42.5 ±2.9	39.8 ±2.3	2.7 ±3.7	(9. ± 12.)	(9. ± 12.)

Table 9 (continued)

ETC Run No	Added (ppm)	Time (hr)	Reacted (ppm)	IntOH (ppt-min) Test Run	IntOH (ppt-min) Base Fit	IntOH (ppt-min) Change	Reactivity (ppt-min/ppm) Incremental	Reactivity (ppt-min/ppm) Mechanistic
trans-2-Butene								
501	0.066	1	0.038 ±0.001	3.5 ±2.6	3.7 ±1.0	-0.1 ±2.8	(-2. ± 42.)	(-4. ± 73.)
		2	0.066 ±0.001	12.6 ±2.6	5.6 ±1.6	7.0 ±3.0	106. ± 43%	106. ± 43%
		3	0.066 ±0.001	19.0 ±2.6	9.9 ±1.6	9.1 ±3.1	138. ± 34%	138. ± 34%
		4	0.066 ±0.001	31.8 ±2.7	15.2 ±2.7	16.6 ±3.8	252. ± 23%	252. ± 23%
		5	0.066 ±0.001	38.8 ±2.8	24.2 ±2.2	14.6 ±3.6	222. ± 24%	222. ± 24%
		6	0.066 ±0.001	41.9 ±2.9	32.9 ±2.0	9.0 ±3.5	137. ± 39%	137. ± 39%
43B [b]	0.097	1	0.066 ±0.002	6.3 ±2.3	1.2 ±2.3	5.1 ±3.3	52. ± 65%	77. ± 65%
		2	0.097 ±0.002	15.9 ±2.7	3.9 ±2.7	12.0 ±3.8	124. ± 32%	124. ± 32%
		3	0.097 ±0.002	24.1 ±3.2	8.5 ±3.2	15.7 ±4.6	162. ± 29%	162. ± 29%
		4	0.097 ±0.002	32.3 ±3.8	13.6 ±3.8	18.7 ±5.4	193. ± 29%	194. ± 29%
		5	0.097 ±0.002	38.5 ±4.5	17.1 ±4.5	21.5 ±6.4	222. ± 30%	222. ± 30%
		6	0.097 ±0.002	41.8 ±5.2	24.4 ±5.2	17.5 ±7.4	180. ± 42%	181. ± 42%
493	0.142	1	0.142 ±0.003	7.1 ±2.6	2.9 ±1.0	4.2 ±2.7	30. ± 65%	30. ± 65%
		2	0.142 ±0.003	14.9 ±2.6	4.8 ±1.5	10.1 ±3.0	71. ± 30%	71. ± 30%
		3	0.142 ±0.003	22.9 ±2.6	9.2 ±1.6	13.7 ±3.1	97. ± 23%	97. ± 23%
		4	0.142 ±0.003	28.3 ±2.7	15.5 ±2.6	12.7 ±3.7	90. ± 29%	90. ± 29%
		5	0.142 ±0.003	34.0 ±2.8	25.6 ±2.1	8.4 ±3.5	59. ± 42%	59. ± 42%
		6	0.142 ±0.003	58.0 ±2.9	36.9 ±2.1	21.2 ±3.5	150. ± 17%	150. ± 17%
m-Xylene								
478	0.095	1	0.013 ±0.003	4.5 ±1.0	3.7 ±1.0	0.7 ±1.5	(8. ± 16.)	(53. ±110.)
		2	0.027 ±0.002	9.9 ±1.6	5.6 ±1.6	4.3 ±2.2	46. ± 52%	157. ± 52%
		3	0.045 ±0.002	18.7 ±1.6	10.0 ±1.6	8.7 ±2.3	92. ± 27%	195. ± 27%
		4	0.059 ±0.002	28.5 ±2.7	15.4 ±2.7	13.1 ±3.8	139. ± 29%	223. ± 29%
		5	0.070 ±0.002	39.7 ±2.2	24.4 ±2.2	15.3 ±3.2	162. ± 21%	219. ± 21%
		6	0.075 ±0.002	47.5 ±2.1	32.2 ±2.1	15.3 ±3.0	162. ± 20%	203. ± 20%
499	0.147	1	0.015 ±0.004	3.2 ±1.0	2.8 ±1.0	0.3 ±1.4	(2. ± 9.)	(21. ± 90.)
		2	0.046 ±0.004	10.8 ±1.5	4.9 ±1.5	5.9 ±2.1	40. ± 35%	129. ± 36%
		3	0.076 ±0.003	21.4 ±1.5	9.0 ±1.5	12.4 ±2.2	84. ± 18%	162. ± 18%
		4	0.097 ±0.003	31.5 ±2.5	14.5 ±2.5	17.0 ±3.5	116. ± 21%	176. ± 21%
		5	0.108 ±0.003	39.3 ±2.1	23.8 ±2.1	15.6 ±2.9	106. ± 19%	144. ± 19%
		6	0.117 ±0.003	47.1 ±1.9	34.1 ±1.9	13.1 ±2.7	89. ± 21%	112. ± 21%
477	0.173	1	0.023 ±0.005	4.2 ±1.0	2.6 ±1.0	1.6 ±1.4	9.2 ± 86%	69. ± 88%
		2	0.062 ±0.004	13.0 ±1.4	4.7 ±1.4	8.3 ±2.0	48. ± 25%	134. ± 25%
		3	0.098 ±0.004	24.5 ±1.5	8.9 ±1.5	15.6 ±2.1	90. ± 14%	159. ± 14%
		4	0.118 ±0.004	34.0 ±2.5	14.8 ±2.5	19.3 ±3.5	112. ± 18%	163. ± 18%
		5	0.133 ±0.004	43.5 ±2.1	24.4 ±2.1	19.1 ±2.9	111. ± 15%	144. ± 16%
		6	0.139 ±0.004	48.8 ±2.3	32.1 ±2.3	16.7 ±3.2	97. ± 20%	120. ± 20%
Formaldehyde								
468	0.108	1	[a]	3.0 ±2.6	2.4 ±1.0	0.6 ±2.7	(6. ± 25.)	
		2	[a]	6.1 ±2.6	4.7 ±1.4	1.4 ±3.0	(13. ± 28.)	
		3	[a]	12.2 ±2.6	8.5 ±1.5	3.7 ±3.0	34. ± 83%	
		4	[a]	18.3 ±2.7	13.4 ±2.5	4.8 ±3.7	45. ± 76%	
		5	[a]	29.3 ±2.8	22.1 ±2.1	7.1 ±3.5	66. ± 49%	
		6	[a]	37.8 ±2.9	33.1 ±1.9	4.7 ±3.5	43. ± 75%	
470	0.260	1	[a]	6.0 ±2.6	2.5 ±1.0	3.5 ±2.8	13.3 ± 80%	
		2	[a]	13.2 ±2.6	4.6 ±1.6	8.6 ±3.0	33. ± 35%	
		3	[a]	22.0 ±2.6	9.9 ±1.7	12.0 ±3.1	46. ± 26%	
		4	[a]	32.3 ±2.7	16.5 ±2.7	15.8 ±3.8	61. ± 24%	
		5	[a]	44.7 ±2.8	26.8 ±2.2	17.9 ±3.6	69. ± 20%	
		6	[a]	52.8 ±2.9	40.4 ±2.2	12.4 ±3.7	48. ± 30%	
489	0.286	1	[a]	2.1 ±2.6	1.5 ±1.0	0.6 ±2.8	(2. ± 10.)	
		2	[a]	8.0 ±2.6	3.9 ±1.6	4.1 ±3.0	14.2 ± 74%	
		3	[a]	16.5 ±2.6	8.7 ±1.6	7.7 ±3.1	27. ± 40%	
		4	[a]	29.4 ±2.7	14.9 ±2.7	14.4 ±3.8	51. ± 26%	
		5	[a]	39.0 ±2.8	24.9 ±2.2	14.1 ±3.6	49. ± 25%	

[a] Amount reacted could not be determined for this VOC, or amount reacted could not be determined for this time with sufficient precision to be useful.
[b] This is a DTC run. "Base fit" data is from base case run carried out in the other side of the chamber.

Table 10. Derivation of the hourly direct reactivities from the results of the ethene surrogate reactivity experiments. [a]

ETC Run No.	Added (ppm)	Time (hr)	Reacted (ppm)	IntOH (ppt-min)	d(O3-NO)/ IntOH (base) (10^3 min-1)	d(O3-NO) (ppm) Total	d(O3-NO) (ppm) From Base ROG	Direct d(O3-NO)/mol VOC) Incremental	Reactivity (mol d(O3-NO)/mol VOC) Mechanistic
Carbon Monoxide									
487	107. ± 2.	2	[b]	2.8±2.6	46.2±15.1	0.412	0.131±0.127	0.0026 ± 45%	
		3	0.326±30%	8.7±2.6	41.5± 8.8	0.752	0.361±0.133	0.0036 ± 34%	1.2 ±46%
		4	0.547±19%	14.7±2.7	44.4± 5.0	1.115	0.652±0.141	0.0043 ± 30%	0.8 ±36%
483	155. ± 3.	2	0.261±54%	4.8±2.6	38.3±15.4	0.446	0.184±0.124	0.0017 ± 47%	1.0 ±72%
		3	0.461±31%	8.5±2.6	37.0± 8.9	0.825	0.316±0.124	0.0033 ± 24%	1.1 ±39%
		4	0.713±21%	13.2±2.8	41.0± 5.4	1.198	0.542±0.134	0.0042 ± 20%	0.9 ±29%
Ethane									
506	49.7 ±1.0	2	0.101±51%	5.1±2.6	25.4±16.8	0.317	0.129±0.108	0.0038 ± 57%	1.9 ±77%
		3	0.181±29%	9.2±2.6	30.5± 9.7	0.547	0.279±0.120	0.0054 ± 45%	1.5 ±53%
		4	0.211±25%	10.7±2.8	34.8± 5.7	0.827	0.373±0.116	0.0091 ± 26%	2.1 ±36%
n-Butane									
488	10.31 ±0.21	2	[b]	3.4±2.6	36.5±16.4	0.320	0.123±0.109	0.0191 ± 56%	
		3	0.221±45%	5.8±2.6	35.9± 9.5	0.594	0.209±0.109	0.037 ± 28%	1.7 ±53%
		4	0.316±32%	8.4±3.0	41.1± 5.8	0.945	0.343±0.131	0.058 ± 22%	1.9 ±39%
484	15.2 ±0.3	2	[b]	2.9±2.6	40.1±15.7	0.451	0.117±0.113	0.022 ± 34%	
		3	0.341±43%	6.1±2.6	39.2± 9.1	0.828	0.238±0.117	0.039 ± 20%	1.7 ±47%
		4	0.410±36%	7.4±3.0	44.2± 5.9	1.206	0.326±0.139	0.058 ± 16%	2.1 ±40%
n-Hexane									
72A [c]	2.88	6	0.166±73%	7.3±5.2	59.4±10.6	0.914	0.431±0.320	0.168 ± 66%	(2.9 ±2.9)
n-Octane									
472	1.60 ±0.03	4	0.123±37%	6.3±2.6	43.1± 4.7	0.452	0.270±0.114	0.114 ± 63%	1.5 ±73%
		5	0.185±25%	9.6±2.4	38.2± 1.9	0.700	0.367±0.093	0.21 ± 28%	1.8 ±38%
		6	0.278±17%	15.1±2.5	33.2± 1.5	0.966	0.500±0.086	0.29 ± 18%	1.7 ±25%
474	2.27 ±0.05	3	[b]	2.8±2.3	39.8± 9.3	0.273	0.110±0.094	0.072 ± 58%	
		4	0.128±52%	4.6±2.5	37.8± 5.5	0.429	0.172±0.098	0.113 ± 38%	2.0 ±64%
		5	0.172±39%	6.2±2.4	33.7± 2.2	0.656	0.209±0.082	0.197 ± 18%	2.6 ±43%
		6	0.286±24%	10.6±2.5	33.3± 1.8	0.920	0.354±0.085	0.25 ± 15%	2.0 ±28%

[a] Data are not shown for times in runs where it appears that O_3 formation is becoming NO_x-limited, because the assumptions behind the derivation of direct reactivities are not valid for such conditions. Data are also not shown when the uncertainties of the direct reactivity estimates are too high to provide meaningful data.
[b] Amount reacted could not be determined for this time with sufficient precision to be useful.
[c] This is a DTC run. "Base fit" data is from base case run carried out in the other side of the chamber.

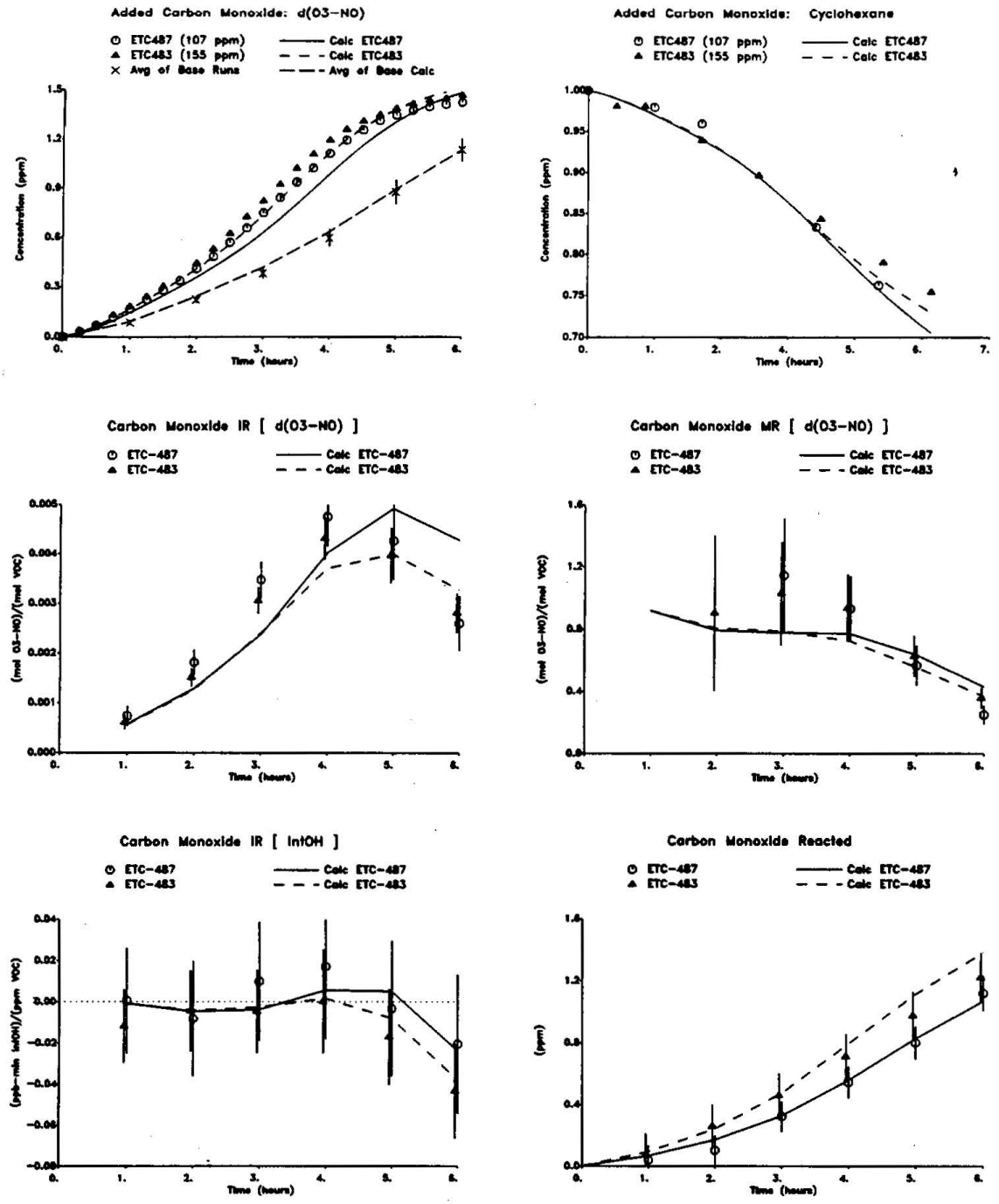

Figure 15. Plots of selected results of ethene surrogate reactivity experiments for **carbon monoxide**

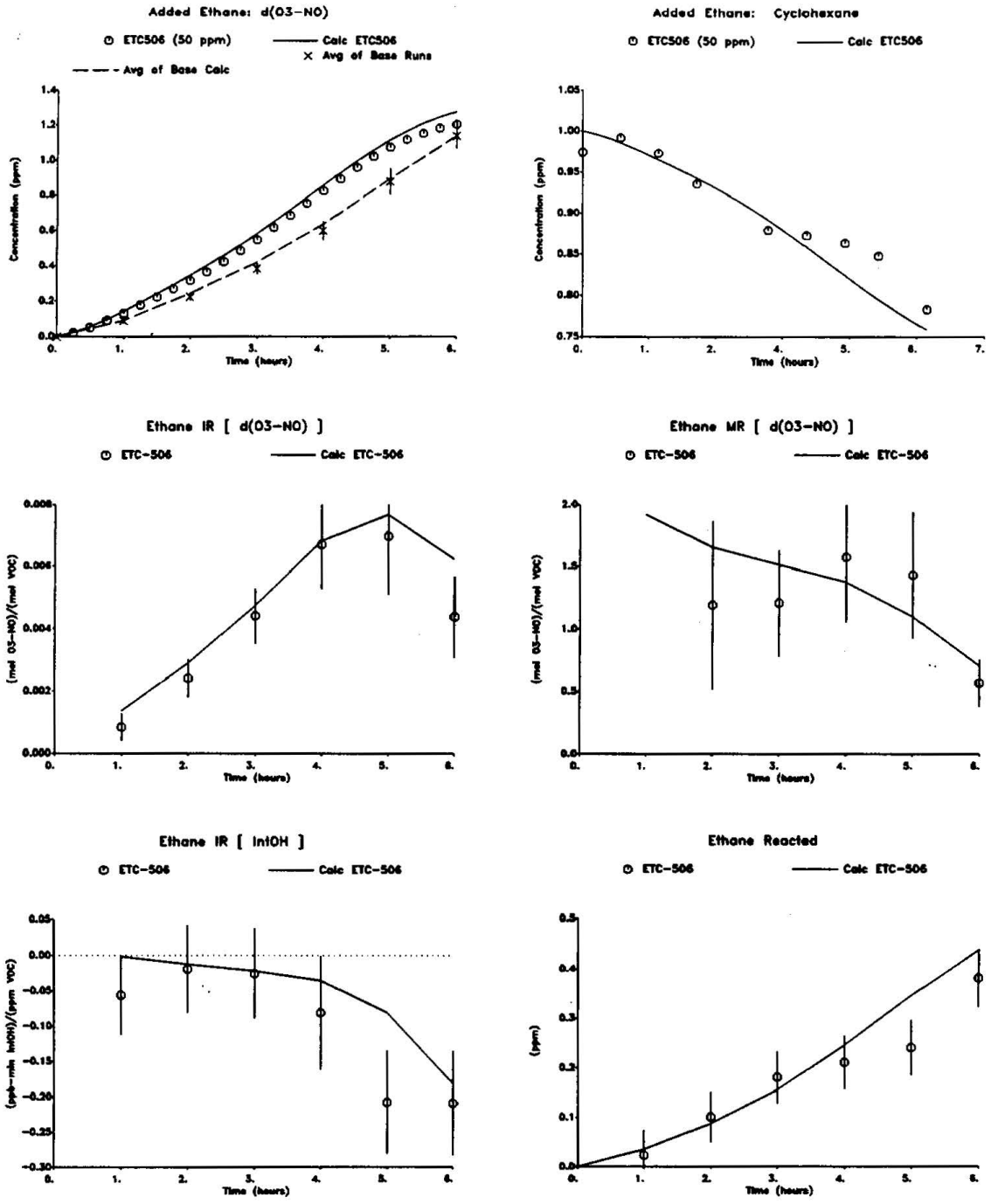

Figure 16. Plots of selected results of ethene surrogate reactivity experiments for **Ethane**.

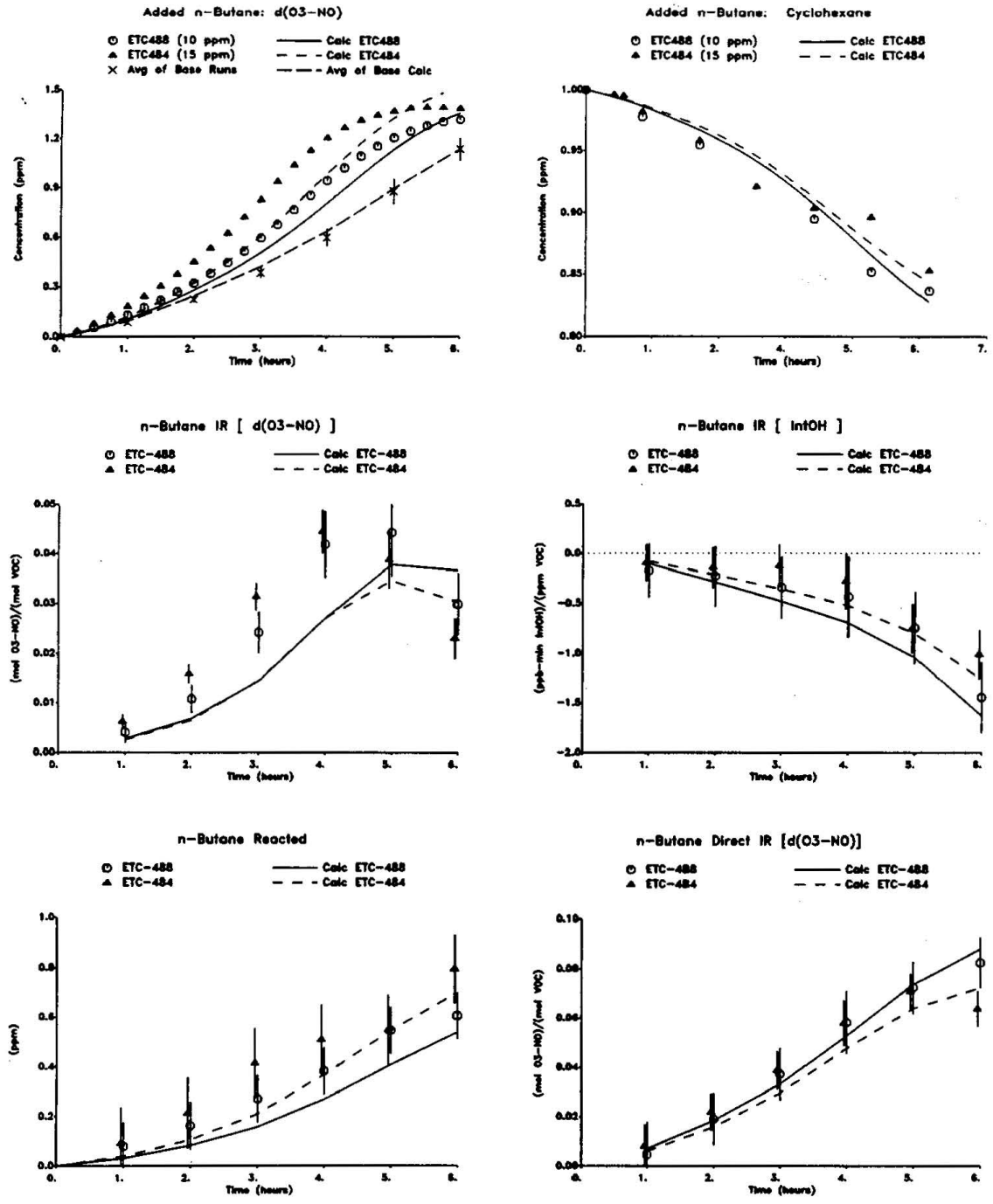

Figure 17. Plots of selected results of ethene surrogate reactivity experiments for **n-Butane**

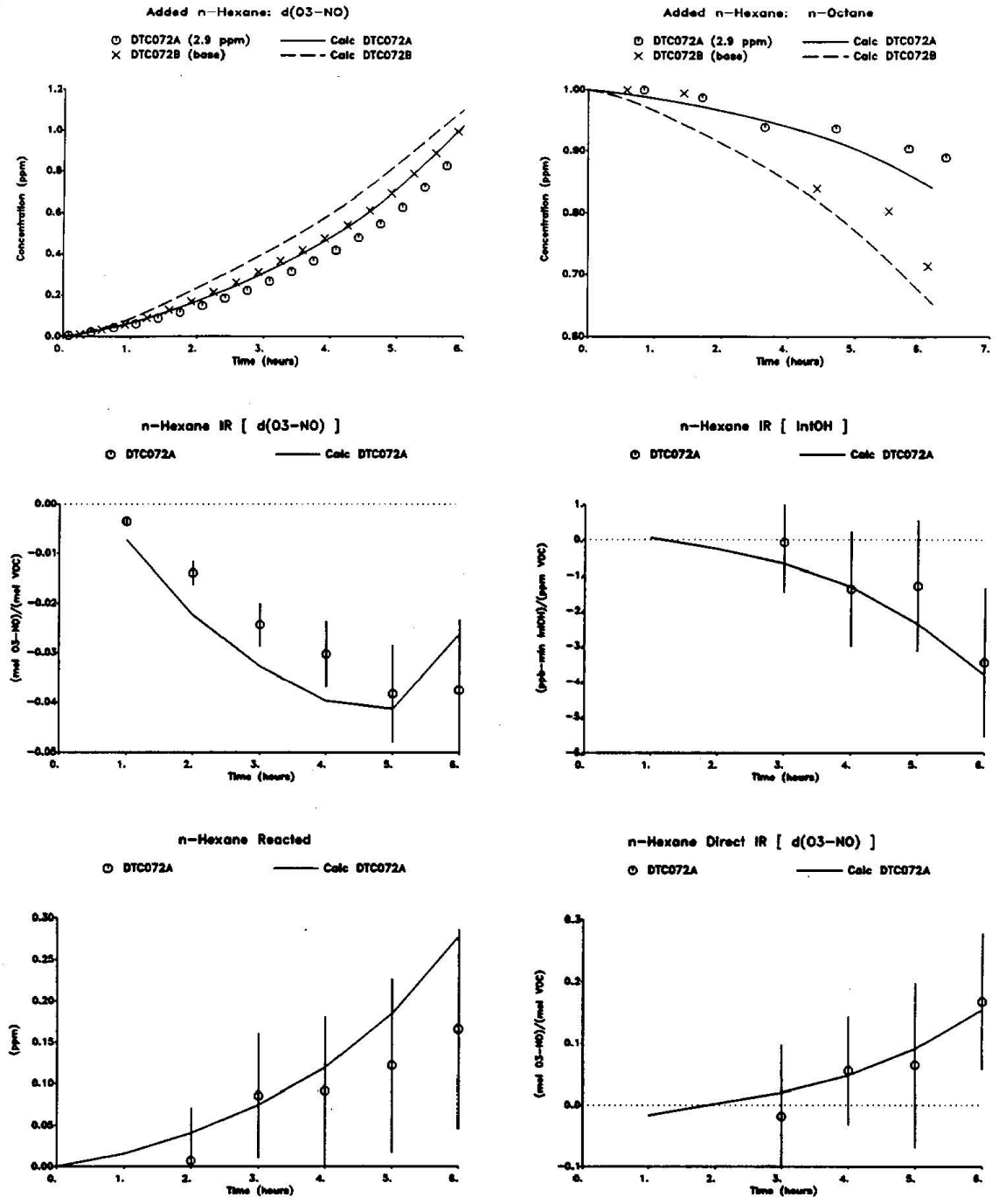

Figure 18. Plots of selected results of ethene surrogate reactivity experiments for **n-Hexane**

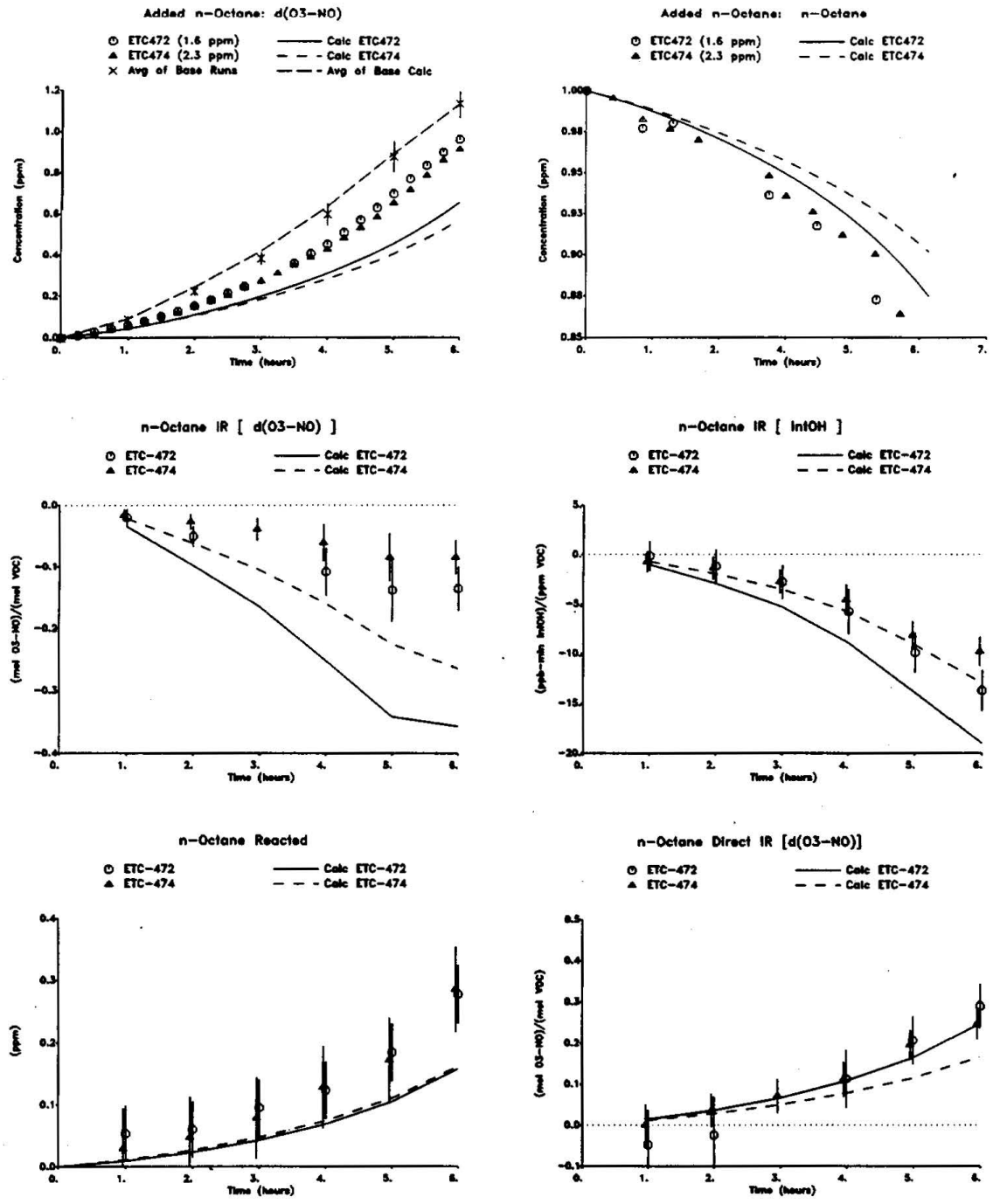

Figure 19. Plots of selected results of ethene surrogate reactivity experiments for n-Octane

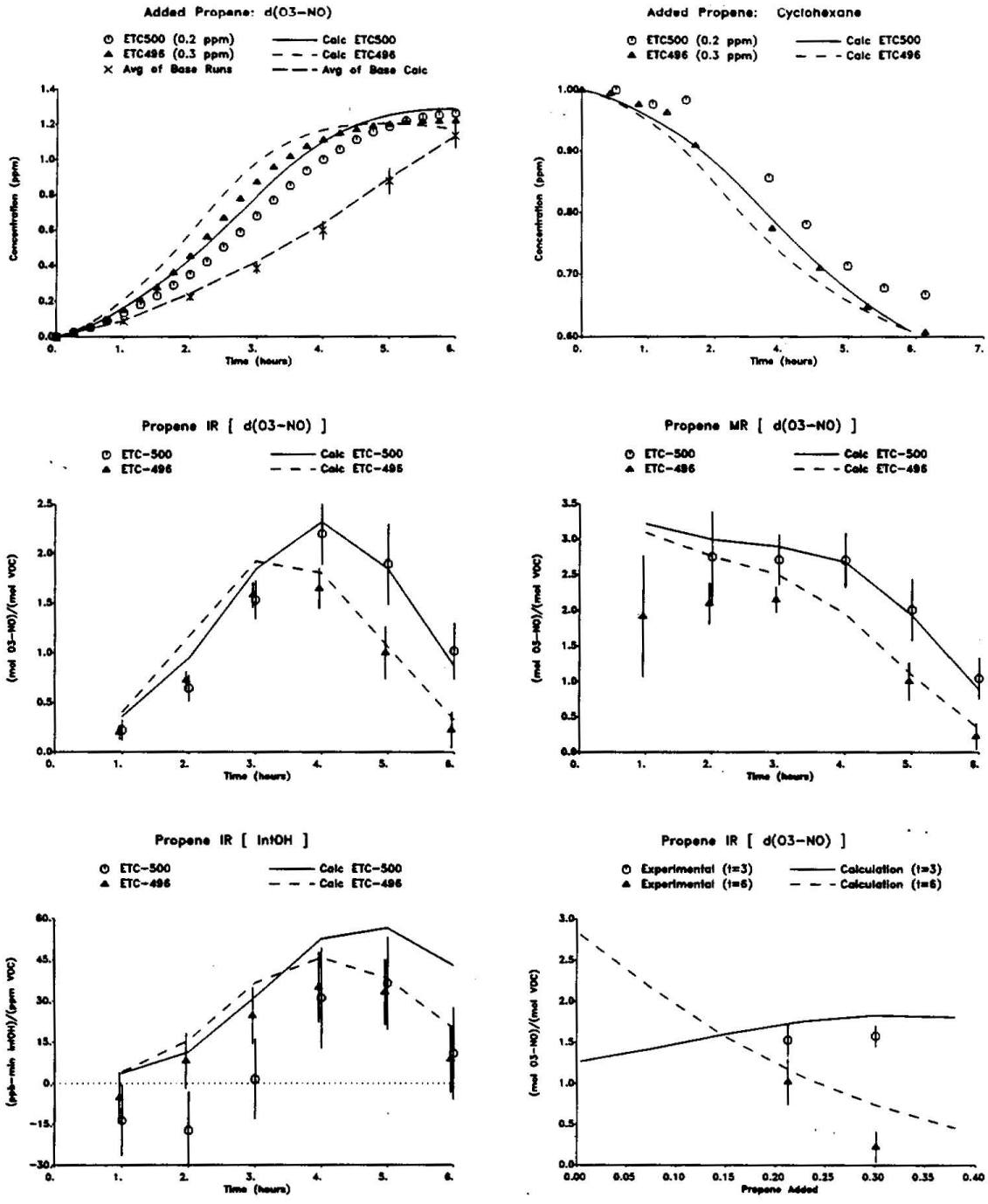

Figure 20. Plots of selected results of ethene surrogate reactivity experiments for **Propene**

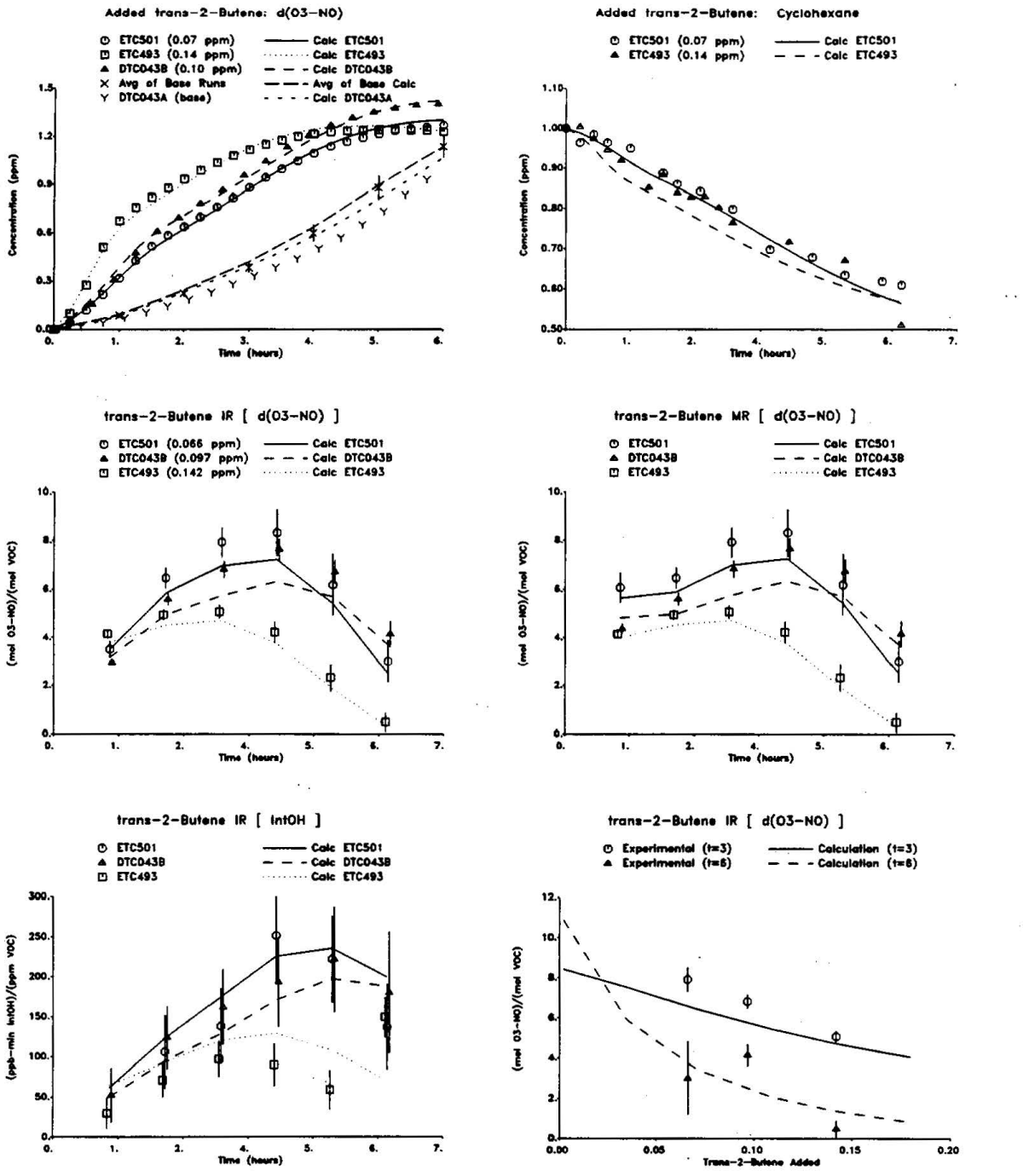

Figure 21. Plots of selected results of ethene surrogate reactivity experiments for <u>trans</u>-2-Butene

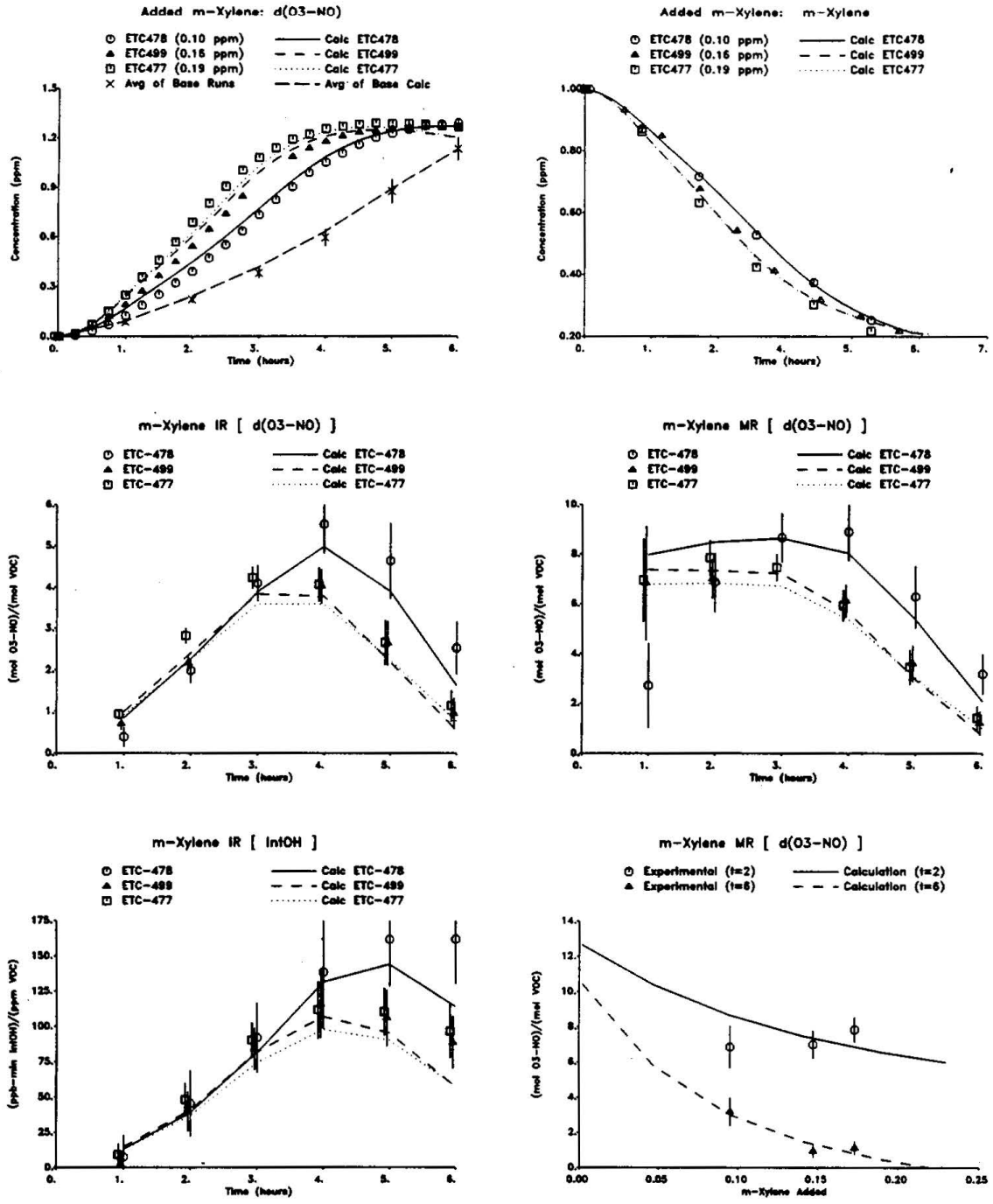

Figure 22. Plots of selected results of ethene surrogate reactivity experiments for **m-Xylene**

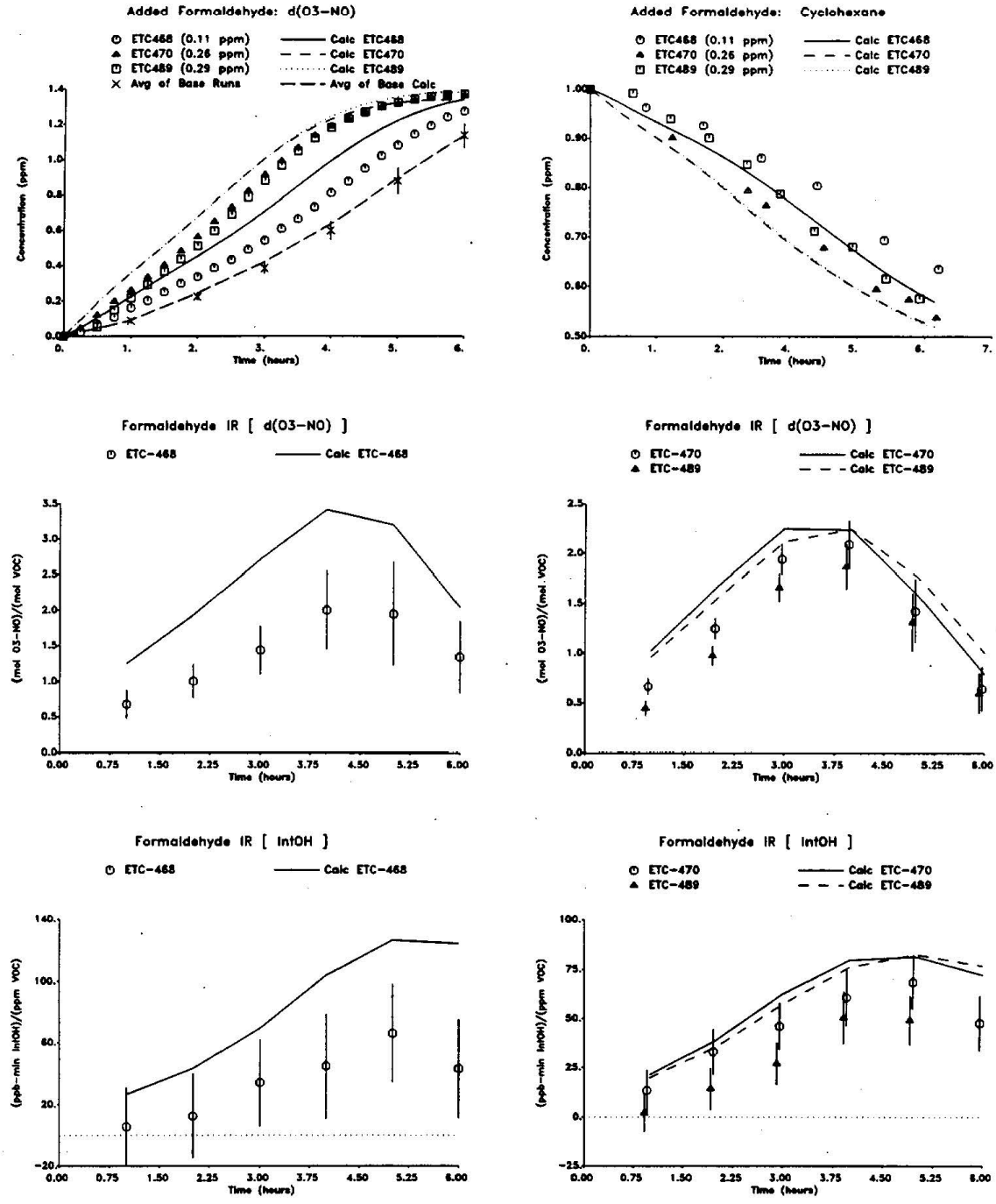

Figure 23. Plots of selected results of ethene surrogate reactivity experiments for **Formaldehyde**

(2) The concentration-time plots of the species (usually cyclohexane) used as the OH tracer for the derivation of IntOH in the added VOC experiments. (These plots are useful for showing how well the model could fit the IntOH data in the individual runs.)
(3) The $d(O_3\text{-}NO)$ and IntOH incremental reactivities for each experiment as a function of time.
(4) The $d(O_3\text{-}NO)$ mechanistic reactivities for each species as a function of time. This is not shown for n-hexane and n-octane because the amounts reacted could not be determined with sufficient precision, nor for formaldehyde, where the amount reacted could not be determined because it is formed as a product from the reactions of the base ROG components.
(5) The amount of VOC reacted as a function of time for the slower reacting VOCs. These data are not shown for propene, trans-2-butene and m-xylene, which react rapidly and whose amounts reacted are reasonably well predicted by the model, or for formaldehyde, where the amount reacted could not be determined.
(6) For n-hexane and n-octane, the estimates of the direct incremental reactivities are shown as a function of time.
(7) For propene, trans-2-butene, and m-xylene, whose incremental reactivities appeared to depend on the amount of VOC added, plots of the $d(O_3\text{-}NO)$ incremental reactivities for selected times against amount of added VOC are also shown.

All the VOCs studied but n-hexane and n-octane were found to have positive effects on $d(O_3\text{-}NO)$, with the negative reactivity of the higher alkanes being due to their large negative effect on OH radicals. (Note that because of scatter in the tracer data, combined with the larger amount of dilution uncertainty in the n-hexane reactivity experiment, IntOH and IR (IntOH) could not be determined very precisely in the n-hexane experiments.) Butane also tended to inhibit OH radical levels, though in this case the positive effect of its direct reactivity was more than enough to counteract this, giving it a positive net $d(O_3\text{-}NO)$ reactivity. The alkenes, m-xylene, and formaldehyde had positive effects on both IntOH and $d(O_3\text{-}NO)$, except perhaps for one of the propene runs at early reaction times, where there may be a problem with the data. CO and ethane did not have a significant effect on OH radicals until around the end of the experiments, when they tended to slightly inhibit radical levels.

Note that in many of the added VOC experiments, particularly the runs with the larger amounts of n-butane, propene, m-xylene and formaldehyde, and in both of the trans-2-butene runs, the rate of ozone formation slowed down significantly or stopped by the end of the experiment. This indicates that O_3 formation in those runs is becoming NO_x-limited by the end of the runs. Not only are the reactivities in those experiments far from the "incremental" limit, their final incremental reactivities no longer represent high NO_x "maximum reactivity" conditions. In such cases, the mechanistic reactivities tended to be relatively constant with time (causing incremental reactivities to increase with time

because of increasing amounts of VOC reacted) up to about t=4 hours, and then decreased. The decrease in reactivities after about t=4 is due to the effect of the system becoming NO_x-limited, which causes VOCs to be less efficient in forming ozone. The $d(O_3\text{-}NO)$ plots on Figures 15-23 suggest that the final reactivities may be reflecting either NO_x-limited or near NO_x-limited conditions for almost all of the experiments with positively reactive VOCs (i.e., for all VOCs except n-octane), but that all experiments are still in the excess NO_x regime for up to at least 3 hours. Therefore, reactivity data for up to t=3 hours can be considered to approximate maximum reactivity conditions, and thus can be compared with maximum reactivity data obtained by other methods. However, this is not the case for the t=6 hour reactivity data except for n-octane.

Note that the assumptions behind the derivation of the "direct reactivity" estimates are valid only for conditions where O_3 is not NO_x-limited. For that reason, Table 10 does not show direct reactivity derivations for the latter parts of experiments where O_3 appears to becoming NO_x-limited.

A comparison of these ethene surrogate reactivity results with results using other base ROG surrogates, and the results of model simulations, will be discussed later in this report.

C. Lumped Surrogate Reactivity Results

1. Base Case results

Table 11 gives a summary of the conditions of the reactivity experiments where the 8-component lumped molecule surrogate was used as the base ROG mixture. The initial base case ROG in these experiments averaged 4.0 ppmC (±4%), the initial NO_x levels averaged 0.48 and 0.17 ppm (±3%) in the high and low NO_x experiments, respectively. Concentration-time plots for selected species typical high and low NO_x base case experiments are shown in Figures 24 and 25. Results of model simulations of the experiments, discussed later in this report, are also shown. It can be seen that NO_2 is still being consumed and O_3 is still forming at the end of the high NO_x experiment, indicating that this approximates maximum reactivity conditions. On the other hand, ozone formation stops after about 3 hours in the low NO_x base case run, indicating that the final O_3 is NO_x-limited.

Table 11 shows that the temperature and initial base case reactant concentrations in these DTC surrogate runs were quite reproducible. The base case $d(O_3\text{-}NO)$, IntOH, and $d(O_3\text{-}NO)$/IntOH results for the high and low NO_x experiments are shown on Figures 26 and 27. The only variable input which had any apparent effect on the results was the initial base ROG; the temperature variation in the experiments was insufficient for any temperature effects to become apparent. The runs in Figures 26 and 27 are ordered by increasing initial ROG, to show the dependence of the results on this factor.

Table 11. Summary of average temperatures and initial reactant concentrations of the DTC surrogate reactivity experiments.

Run	Test VOC	T	NO	NO_2	NO_x	Surg C	N-C4	N-C8	ETHENE	PROPENE	T-2-BUTE	TOLUENE	M-XYLENE	FORMALD
low NOx Runs														
DTC029A	CO	301.0	0.144	0.030	0.175	4.20	0.390	0.092	0.078	0.058	0.057	0.085	0.081	0.101
DTC029B		301.0	0.144	0.031	0.174	4.27	0.396	0.094	0.079	0.059	0.059	0.087	0.082	0.101
DTC030A		300.4	0.141	0.026	0.167	4.00	0.365	0.088	0.073	0.054	0.054	0.087	0.076	0.096
DTC030B	TOLUENE	300.4	0.140	0.026	0.166		0.363	0.089	0.073	0.052	0.054	[a]	0.079	0.095
DTC031A	N-C4	300.7	0.142	0.030	0.171		[a]	0.095	0.075	0.059	[b]	0.087	0.082	0.100
DTC031B		300.7	0.141	0.031	0.171	4.27	0.394	0.095	0.076	0.059	0.059	0.087	0.083	0.100
DTC032A		300.4	0.142	0.033	0.174	4.21	0.386	0.093	0.077	0.058	0.058	0.086	0.084	0.100
DTC032B	PROPENE	300.4	0.142	0.033	0.175		0.381	0.092	0.073	[a]	0.056	0.084	0.080	0.097
DTC033A	T-2-BUTE	300.3	0.137	0.031	0.168		0.380	0.092	0.073	0.055	[a]	0.084	0.081	0.095
DTC033B		300.3	0.137	0.031	0.168	4.15	0.381	0.093	0.073	0.056	0.056	0.085	0.082	0.096
DTC034A		300.9	0.134	0.030	0.165	3.90	0.365	0.086	0.073	0.054	0.055	0.079	0.073	0.092
DTC034B	A-PINENE	300.9	0.134	0.031	0.165	3.95	0.368	0.087	0.072	0.055	0.054	0.080	0.076	0.090
DTC035A	M-XYLENE	300.6	0.134	0.032	0.166		0.368	0.090	0.074	0.054	0.055	0.082	[a]	0.098
DTC035B		300.6	0.134	0.033	0.167	3.98	0.372	0.089	0.074	0.052	0.055	0.081	0.074	0.096
DTC036A	FORMALD	300.2	0.147	0.035	0.182		0.409	0.098	0.081	0.060	0.060	0.089	0.083	[a]
DTC036B		300.2	0.146	0.035	0.181	4.35	0.408	0.097	0.081	0.059	0.060	0.088	0.080	0.105
DTC037A		300.6	0.143	0.032	0.174	4.25	0.389	0.101	0.076	0.054	0.058	0.084	0.081	0.106
DTC037B	N-C8	300.6	0.143	0.032	0.175		0.388	[a]	0.076	0.057	0.058	0.085	0.080	0.100
DTC038A	ETHENE	300.7	0.138	0.031	0.169		0.357	0.087	[a]	0.052	0.052	0.079	0.073	0.090
DTC038B		300.7	0.138	0.031	0.169	3.91	0.358	0.088	0.072	0.049	0.052	0.081	0.077	0.095
DTC039A		300.9	0.145	0.033	0.178		0.380	0.091	[b]	0.049	0.056	0.084	0.079	0.100
DTC039B	BENZENE	300.9	0.145	0.033	0.178		0.373	0.092	[b]	0.050	0.054	0.085	0.078	0.095
DTC066A		301.6	0.141	0.032	0.173	3.80	0.347	0.086	0.066	0.051	0.050	0.078	0.076	0.083
DTC066B	ACETALD	301.6	0.144	0.031	0.175	3.91	0.365	0.087	0.067	0.053	0.053	0.080	0.075	0.097
DTC067A		301.4	0.139	0.032	0.171	3.84	0.345	0.089	0.065	0.051	0.049	0.081	0.078	0.086
DTC067B	M-XYLENE	301.4	0.138	0.033	0.171		0.336	0.085	0.064	0.051	0.047	0.077	[a]	0.085
DTC071A		301.7	0.146	0.032	0.178	3.97	0.367	0.090	0.070	0.055	0.051	0.081	0.077	0.093
DTC071B	N-C8	301.7	0.146	0.031	0.177		0.354	[a]	0.068	0.054	0.045	0.078	0.076	0.096
Average		**300.8**	**0.141**	**0.032**	**0.172**	**4.06**	**0.373**	**0.091**	**0.073**	**0.054**	**0.054**	**0.083**	**0.079**	**0.096**
St.Dev		**0.5**	**3%**	**6%**	**3%**	**4%**	**5%**	**4%**	**6%**	**6%**	**7%**	**4%**	**4%**	**6%**
High NOx Runs														
DTC014A	CO	300.6	0.374	0.103	0.477	3.96	0.377	0.086	0.075	0.055	0.054	0.079	0.075	0.089
DTC014B		300.6	0.373	0.103	0.477	3.93	0.370	0.086	0.074	0.056	0.052	0.078	0.075	0.088
DTC015A		301.1	0.389	0.114	0.503	4.10	0.385	0.090	0.077	0.057	0.056	0.083	0.079	0.086
DTC015B	CO	301.1	0.390	0.115	0.505	4.11	0.384	0.090	0.078	0.056	0.054	0.083	0.080	0.087
DTC016A	CO	300.2	0.374	0.105	0.479	3.93	0.376	0.086	0.073	0.045	0.053	0.079	0.075	0.092
DTC016B		300.2	0.372	0.103	0.475	3.87	0.371	0.085	0.073	0.042	0.052	0.078	0.073	0.090
DTC017A	ETHENE	300.1	0.374	0.105	0.479		0.370	0.087	[a]	0.043	0.053	0.079	0.074	0.095
DTC017B		300.1	0.374	0.105	0.479	3.89	0.368	0.086	0.071	0.044	0.052	0.079	0.075	0.093
DTC018A	PROPENE	300.6	0.380	0.103	0.482		0.396	0.093	0.077	[a]	0.057	0.085	0.082	0.091
DTC018B		300.6	0.381	0.103	0.484	4.17	0.394	0.092	0.076	0.053	0.056	0.084	0.080	0.088
DTC019A		300.3	0.359	0.100	0.459	4.07	0.384	0.090	0.069	0.050	0.055	0.083	0.079	0.090
DTC019B	N-C4	300.3	0.360	0.100	0.460		[a]	0.089	0.069	0.050	[b]	0.081	0.077	0.091
DTC020A		300.4	0.386	0.115	0.501		0.380	0.093	0.073	0.052	0.057	0.086	0.083	[c]
DTC020B	CO	300.4	0.387	0.115	0.502		0.380	0.092	0.076	0.052	0.057	0.084	0.081	[c]
DTC021A		300.1	0.387	0.106	0.492	4.10	0.378	0.092	0.071	0.051	0.057	0.084	0.078	0.114
DTC021B	T-2-BUTE	300.1	0.386	0.106	0.492		0.374	0.092	0.070	0.052	[a]	0.085	0.080	0.111
DTC022A		300.3	0.399	0.105	0.503	3.95	0.366	0.089	0.070	0.050	0.054	0.081	0.076	0.103
DTC022B	FORMALD	300.3	0.401	0.105	0.505		0.367	0.091	0.070	0.050	0.055	0.083	0.080	[a]
DTC023A	TOLUENE	300.6	0.373	0.096	0.469		0.370	0.090	0.070	0.050	0.055	[a]	0.079	0.100
DTC023B		300.6	0.374	0.098	0.471	4.03	0.372	0.090	0.071	0.051	0.055	0.084	0.078	0.099
DTC024A		300.9	0.397	0.105	0.502	4.03	0.376	0.091	0.075	0.052	0.056	0.081	0.075	0.103
DTC024B	N-C8	300.9	0.397	0.105	0.503		0.377	[a]	0.074	0.053	0.056	0.081	0.076	0.104
DTC025A	M-XYLENE	301.7	0.368	0.099	0.467		0.381	0.093	0.071	0.058	0.057	0.085	[a]	0.099
DTC025B		301.7	0.369	0.097	0.466	4.14	0.382	0.093	0.072	0.057	0.057	0.084	0.080	0.097
DTC028A	ACETONE	300.9	0.381	0.102	0.483	4.09	0.373	0.092	0.076	0.056	0.055	0.084	0.080	0.095
DTC028B		300.9	0.383	0.102	0.485	4.11	0.377	0.092	0.075	0.058	0.056	0.084	0.081	0.096
DTC064A		301.5	0.385	0.101	0.486	3.97	0.365	0.089	0.072	0.054	0.054	0.081	0.077	0.095
DTC064B	ACETONE	301.5	0.385	0.102	0.487	3.80	0.354	0.084	0.069	0.052	0.051	0.077	0.073	0.092
DTC065A	ACETALD	301.3	0.355	0.100	0.455	3.89	0.358	0.088	0.066	0.050	0.052	0.080	0.077	0.096
DTC065B		301.3	0.378	0.099	0.477	3.95	0.357	0.090	0.068	0.053	0.053	0.082	0.079	0.097
DTC068A		301.1	0.384	0.100	0.484	3.80	0.349	0.086	0.065	0.051	0.050	0.079	0.074	0.097
DTC068B	M-XYLENE	301.1	0.383	0.100	0.484		0.339	0.085	0.064	0.051	0.048	0.078	[a]	0.097
TC069A	T-2-BUTE	301.5	0.381	0.097	0.478		0.339	0.086	0.065	0.051	[a]	0.079	0.076	0.094
DTC069B		301.5	0.381	0.097	0.478	3.65	0.328	0.083	0.063	0.049	0.047	0.076	0.073	0.097
DTC070A	N-C8	301.2	0.389	0.099	0.488		0.370	[a]	0.071	0.056	0.054	0.084	0.082	0.094
DTC070B		301.2	0.389	0.098	0.487	4.01	0.364	0.091	0.069	0.055	0.053	0.083	0.080	0.093
Average		**300.8**	**0.381**	**0.102**	**0.483**	**3.99**	**0.367**	**0.090**	**0.070**	**0.053**	**0.054**	**0.082**	**0.078**	**0.098**
St.Dev		**0.5**	**3%**	**5%**	**3%**	**4%**	**4%**	**3%**	**5%**	**5%**	**5%**	**3%**	**4%**	**6%**

[a] Concentration increased for reactivity determinatin
[b] No data or data unreliable.
[c] Not added

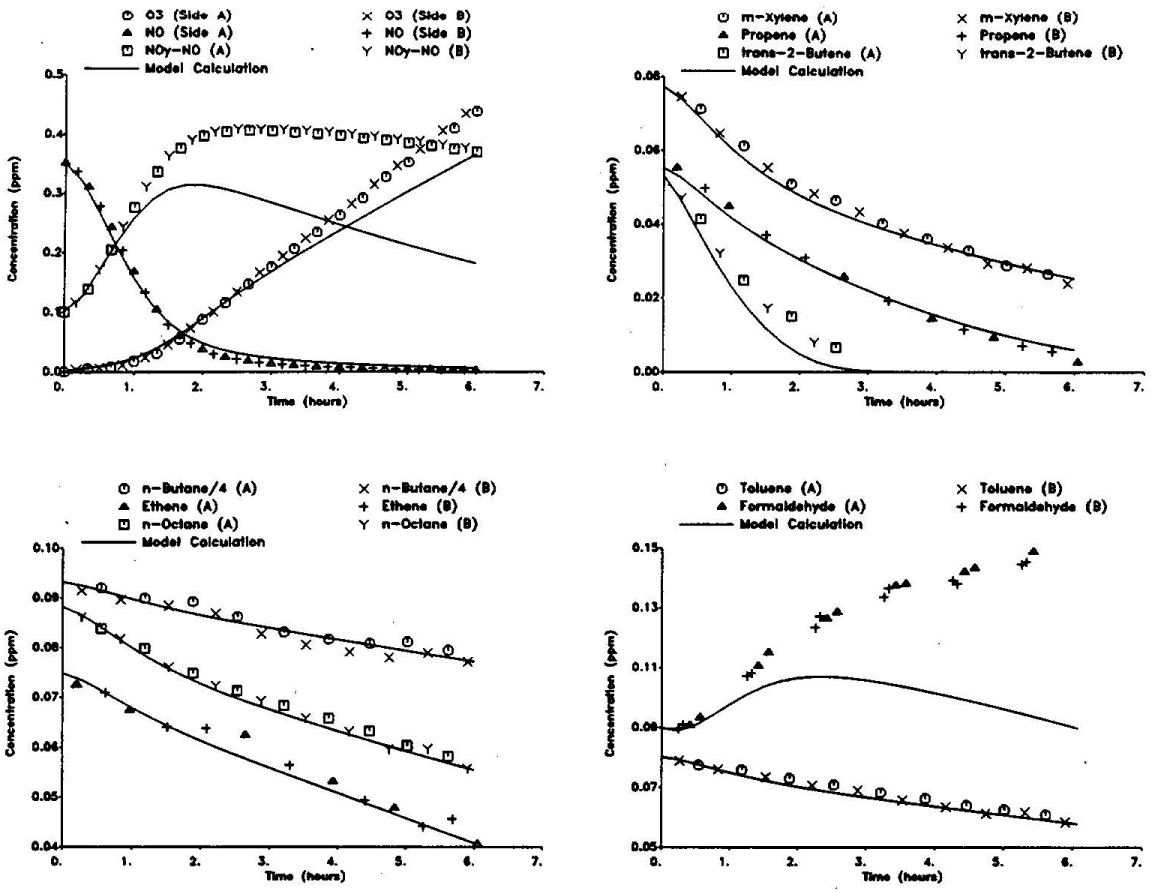

Figure 24. Concentration - time plots for selected species in the base case high NO_x lumped surrogate run DTC013. This run is a side equivalency test with the same mixture irriadiated on both sides. Results of model calculations are also shown.

It is interesting to note that the slight variation in the initial ROG affected $d(O_3\text{-}NO)$ primarily through affecting the $d(O_3\text{-}NO)$/IntOH ratio, rather than by affecting IntOH. In other words, slight increases in the initial ROG did not affect the overall radical levels as much as it affects the amount of NO oxidized and O_3 formed at a given radical level. The latter effect is presumably because increasing ROG means that there is more ROG reaction if radical levels are the same. In the low NO_x experiments, all of the initial ROG components were highly correlated to each other, so the relative importance of the components in affecting this variability could not be determined. In the high NO_x experiments, the $d(O_3\text{-}NO)$ correlated primarily with the variations in the gas-phase reactants (n-butane, ethene, trans-2-butene, and propene), and had a slightly negative and probably insignificant correlation (-25%) with the initial formaldehyde.

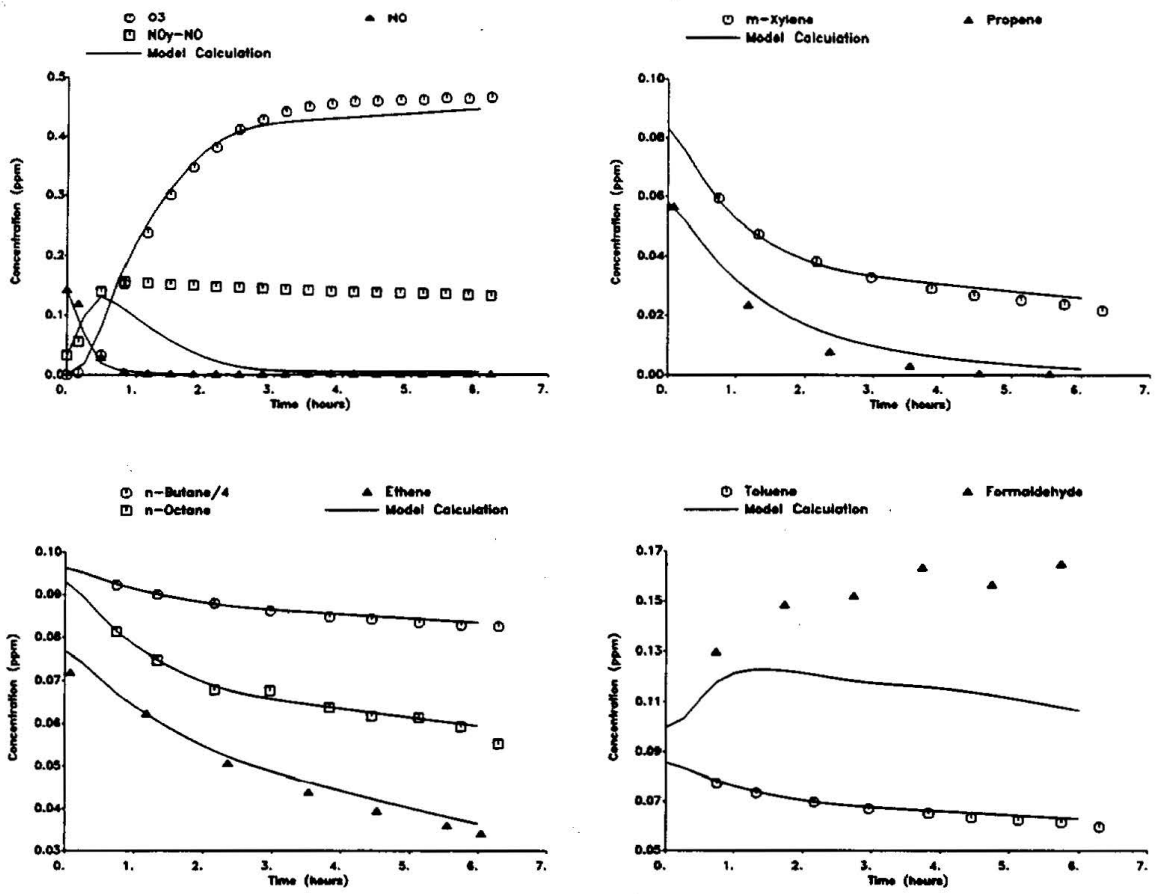

Figure 25. Concentration - time plots for selected species in the base case low NO_x lumped surrogate run DTC032A. Results of model calculations are also shown.

Note that all these runs were divided chamber runs where the base case and the added test VOC irradiations were carried out at the same time, with the base case reactants being mixed in both chamber "sides" before injecting the test compound. As discussed above, the simultaneous base case experiment is assumed to have the same conditions of the test run on the other side, so no regression to account for variability of conditions was carried out. The averages of the side-by-side discrepancies of initial concentrations of the base case reactants were less than 2% in all cases except for formaldehyde, where the average discrepancy was 4%. These differences are in the range of measurement variabilities and do not indicate real differences in initial reactant concentrations.

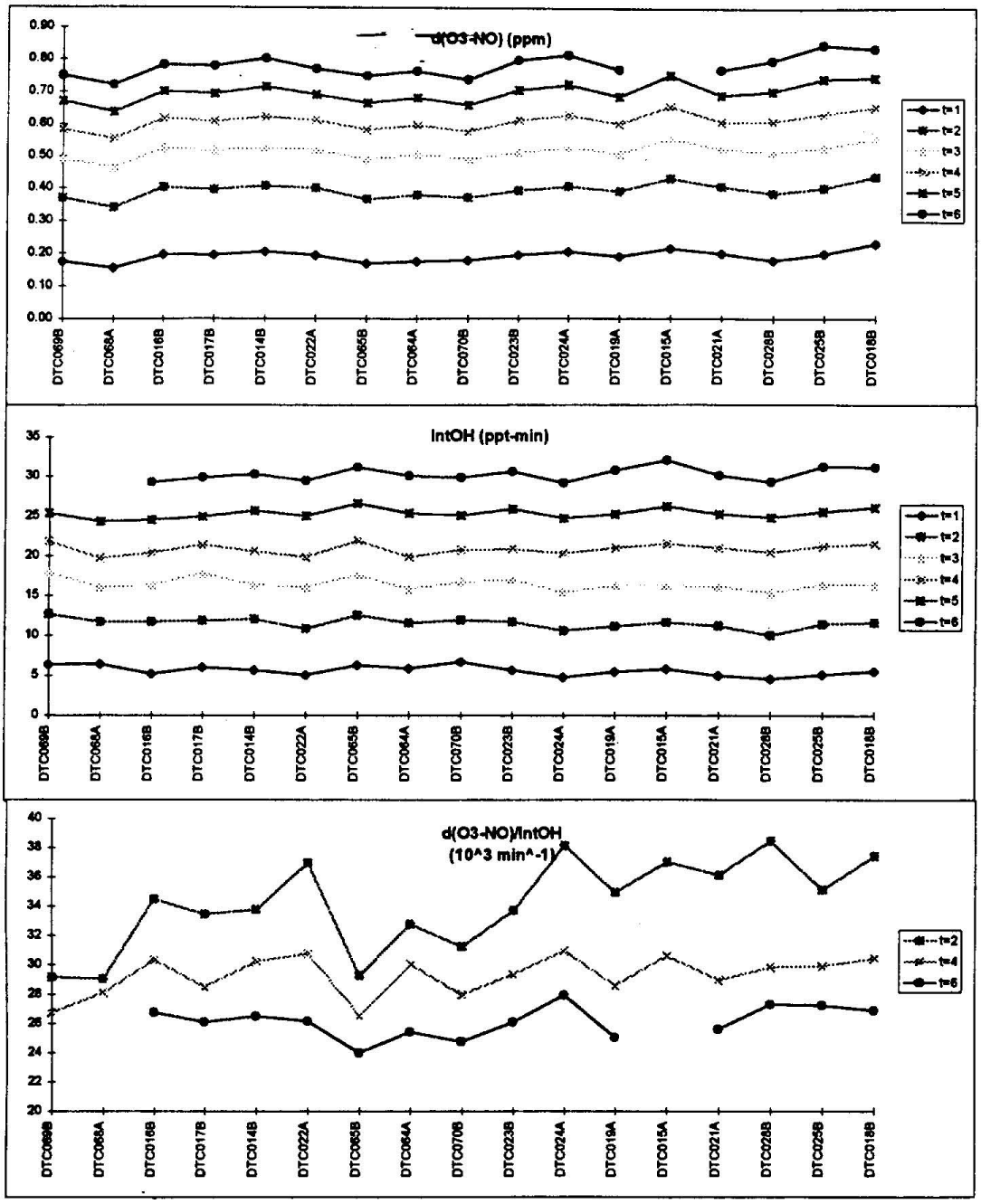

Figure 26. Base case $d(O_3\text{-NO})$, IntOH, and $d(O_3\text{-NO})$/IntOH results for the high NO_x lumped surrogate runs. Runs are given in order of increasing initial ROG carbon concentrations.

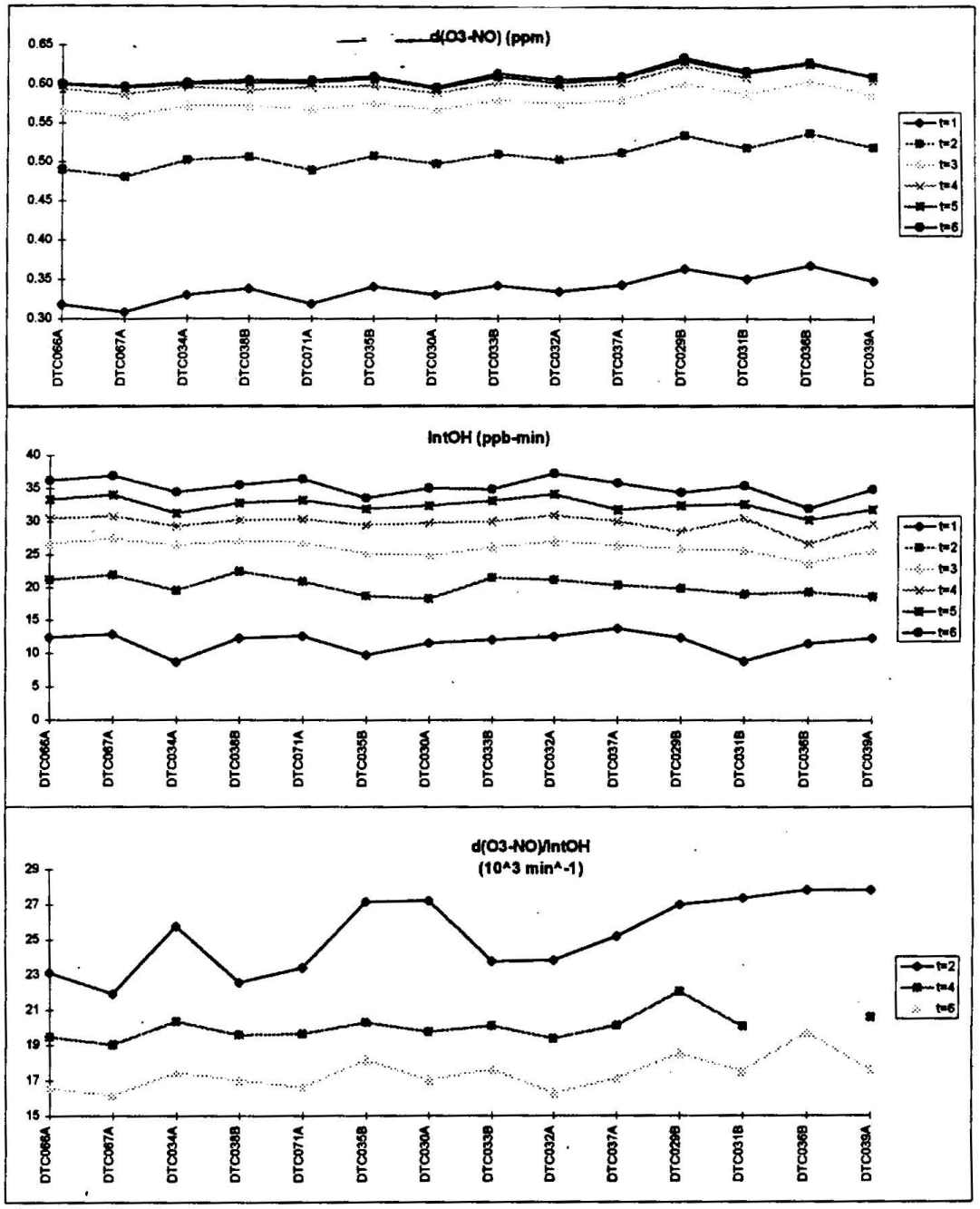

Figure 27. Base case $d(O_3\text{-NO})$, IntOH, and $d(O_3\text{-NO})/\text{IntOH}$ results for the low NO_x lumped surrogate runs. Runs are given in order of increasing initial ROG carbon concentrations.

Several experiments were carried out early in the program to test for equivalency of results of irradiations in the two sides of the chamber. The results of one such experiment are shown in Figure 24, above, where it can be seen that the differences between the sides are minor. Figure 28 shows plots of the side differences in $d(O_3\text{-NO})$ and IntOH as a function of time, where the "error bars" are derived in the same manner as used when estimating uncertainties of incremental reactivities. It can be seen that, except for the first hour $d(O_3\text{-NO})$, the inequivalency is well within the estimated minimum uncertainty ranges used in the reactivity derivation. Comparable side equivalency was also seen in replicate propene-NO_x irradiations, which were carried out at various times in this chamber throughout this program.

2. High NO_x Reactivity Results

As indicated in Table 6, high NO_x lumped surrogate reactivity experiments were carried out for each of the 8 surrogate components plus carbon monoxide and acetaldehyde. Three reactivity experiments were carried out for CO and two each were conducted for n-octane, trans-2-butene and m-xylene, and one experiment was carried out for the other VOCs. Because of the good precision and reproducibility in reactivity results (discussed below), it was not considered necessary to repeat reactivity experiments for all the VOCs. The detailed results and reactivity analysis of the DTC surrogate experiments are given in Tables 12-14, and plots of selected reactivity results for the high NO_x experiments are shown on Figures 29-38. Model calculations, discussed later, are also shown.

The format of the data in these tables and figures are similar to those discussed previously for the ethene reactivity experiments. However, the figures also include IntOH mechanistic reactivities and estimated $d(O_3\text{-NO})$ mechanistic reactivities for those VOCs where these could be derived with sufficient precision to be meaningful.

A notable feature of the reactivity results of these experiments, when compared to the ethene surrogate runs discussed above and the mini-surrogate experiments discussed in the Phase I report (Carter et al., 1993a) is the much lower level of estimated uncertainties of the incremental reactivity numbers which were derived. The appropriateness of these lower error estimates are supported by the level of reproducibility in reactivity results observed in the runs with CO, n-octane, and m-xylene, as shown on Figures 27, 31, and 36. (The differences between the two reactivity experiments with trans-2-butene, shown on Figure 34, are more likely due to differences in amount of butene added, rather than imprecisions in the reactivity derivations.) This greater apparent precision can be attributed to the use of the dual chamber system, where the corresponding base case run is conducted simultaneously for each added VOC run. Thus there is much less uncertainty due to the variability in temperature, initial reactant concentrations, and perhaps other conditions, when estimating the base case conditions for each run. The main uncertainty would be due to

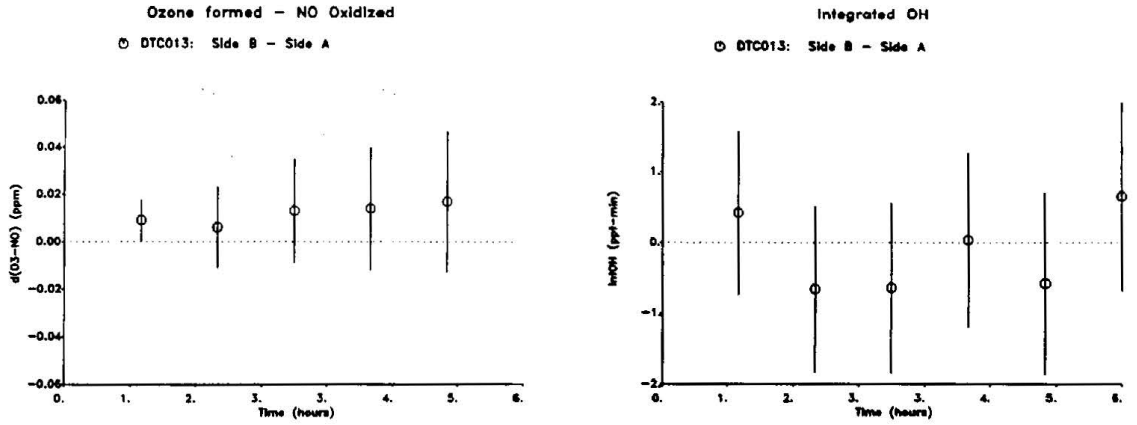

Figure 28. Differences in $d(O_3\text{-}NO)$ and IntOH in a DTC side equivalency test experiment. The "error bars" show the uncertainty ranges as used in the incremental reactivity derivations.

inequivalency in conditions in the different chamber sides, which, as shown in Figures 24, appear to be small. Figure 28 suggests that the uncertainty estimates derived with the reactivity data appropriately encompass the uncertainty due to possible side equivalency.

Unlike many of the ethene reactivity experiments, most of the high NO_x added VOC experiments remained out of the NO_x-limited regime throughout the run. The exceptions include the added propene run, the run with the higher amount of added trans-2-butene, and the added toluene run. For those runs, data for times less than 6 hours were used when the results are discussed in terms of maximum reactivity conditions. Note that the "direct reactivity" estimates shown for the latter periods of those runs do not necessarily indicate true direct reactivity. (However, the comparison with the model calculations are still a valid measure of model performance, since they are both derived in the same way.)

All the VOCs studied were found to have positive effects on $d(O_3\text{-}NO)$ in these experiments, including n-octane, which had a negative $d(O_3\text{-}NO)$ reactivity in the ethene surrogate and mini-surrogate runs. As with the ethene and/or mini-surrogate runs, n-butane, n-octane, and acetaldehyde inhibited OH radical levels, while the alkenes, the aromatics, and formaldehyde enhanced radicals. Because of the greater precision of the data, reasonably precise direct reactivity estimates could be obtained for most of the VOCs studied, except for the aromatics and formaldehyde. These results, and how they vary depending on the ROG surrogate employed, are discussed in more detail later.

Table 12. Derivation of hourly d(O_3-NO) reactivities from the results of the lumped molecule surrogate experiments.

ETC Run No.	Added (ppm)	Time (hr)	Reacted [a] (ppm)	Deriv.	d(O3-NO) (ppm) Test	Base min.Unc	Change	Reactivity (mol/mol) Incremental	Mechanistic
Carbon Monoxide (High NOx)									
14	155. ± 0.	1	0.363 ±0.045	A	0.548	0.205 ±0.006	0.343 ±0.018	0.0022 ± 5%	0.95 ± 13%
		2	0.635 ±0.045	A	0.907	0.409 ±0.012	0.498 ±0.030	0.0032 ± 6%	0.78 ± 9%
		3	0.870 ±0.047	A	1.135	0.528 ±0.016	0.607 ±0.038	0.0039 ± 6%	0.70 ± 8%
		4	0.978 ±0.049	A	1.301	0.623 ±0.019	0.678 ±0.043	0.0044 ± 6%	0.69 ± 8%
		5	1.107 ±0.052	A	1.405	0.716 ±0.021	0.689 ±0.047	0.0044 ± 7%	0.62 ± 8%
		6	1.209 ±0.056	A	1.463	0.803 ±0.024	0.660 ±0.050	0.0043 ± 8%	0.55 ± 9%
15	161. ± 0.	1	0.396 ±0.046	B	0.637	0.216 ±0.006	0.421 ±0.020	0.0026 ± 5%	1.06 ± 13%
		2	0.649 ±0.047	B	1.023	0.432 ±0.013	0.591 ±0.033	0.0037 ± 6%	0.91 ± 9%
		3	0.857 ±0.047	B	1.266	0.558 ±0.017	0.708 ±0.042	0.0044 ± 6%	0.83 ± 8%
		4	1.100 ±0.049	B	1.417	0.660 ±0.020	0.757 ±0.047	0.0047 ± 6%	0.69 ± 8%
		5	1.244 ±0.052	B	1.501	0.755 ±0.023	0.746 ±0.050	0.0046 ± 7%	0.60 ± 8%
		6	1.358 ±0.054	B	1.532		2.532 ±0.055		
16	74.2 ±0.0	1	0.155 ±0.021	A	0.354	0.197 ±0.006	0.157 ±0.012	0.0021 ± 8%	1.01 ± 16%
		2	0.297 ±0.021	A	0.654	0.404 ±0.012	0.250 ±0.023	0.0034 ± 9%	0.84 ± 12%
		3	0.400 ±0.022	A	0.835	0.524 ±0.016	0.311 ±0.030	0.0042 ± 10%	0.78 ± 11%
		4	0.496 ±0.023	A	0.992	0.618 ±0.019	0.374 ±0.035	0.0050 ± 9%	0.75 ± 10%
		5	0.606 ±0.024	A	1.121	0.702 ±0.021	0.419 ±0.040	0.0056 ± 9%	0.69 ± 10%
		6	0.684 ±0.025	A	1.223	0.783 ±0.023	0.440 ±0.044	0.0059 ± 10%	0.64 ± 11%
20	103. ± 0.	1	0.154 ±0.030	B	0.316	0.134 ±0.004	0.182 ±0.010	0.0018 ± 6%	1.18 ± 20%
		2	0.306 ±0.030	B	0.656	0.320 ±0.010	0.336 ±0.022	0.0033 ± 7%	1.10 ± 12%
		3	0.455 ±0.030	B	0.837	0.446 ±0.013	0.391 ±0.028	0.0038 ± 7%	0.86 ± 10%
		4	0.622 ±0.031	B	0.999	0.532 ±0.016	0.467 ±0.034	0.0045 ± 7%	0.75 ± 9%
		5	0.738 ±0.032	B	1.140	0.605 ±0.018	0.535 ±0.039	0.0052 ± 7%	0.73 ± 8%
		6	0.869 ±0.034	B	1.251	0.678 ±0.020	0.573 ±0.043	0.0055 ± 7%	0.66 ± 8%
Carbon Monoxide (Low NOx)									
29	85.8 ±0.2	1	0.282 ±0.025	A	0.557	0.364 ±0.011	0.193 ±0.020	0.0022 ± 10%	0.68 ± 14%
		2	0.437 ±0.025	A	0.735	0.537 ±0.016	0.198 ±0.027	0.0023 ± 14%	0.45 ± 15%
		3	0.497 ±0.025	A	0.809	0.605 ±0.018	0.204 ±0.030	0.0024 ± 15%	0.41 ± 16%
		4	0.586 ±0.026	A	0.840	0.628 ±0.019	0.212 ±0.031	0.0025 ± 15%	0.36 ± 15%
		5	0.626 ±0.027	A	0.845	0.634 ±0.019	0.211 ±0.032	0.0025 ± 15%	0.34 ± 16%
		6	0.659 ±0.028	A	0.845	0.638 ±0.019	0.207 ±0.032	0.0024 ± 15%	0.31 ± 16%
n-Butane (High NOx)									
19	6.48 ±0.13	1	0.098 ±0.020	B	0.372	0.190 ±0.006	0.182 ±0.013	0.028 ± 7%	1.86 ± 21%
		2	0.203 ±0.020	B	0.716	0.392 ±0.012	0.324 ±0.024	0.050 ± 8%	1.60 ± 12%
		3	0.273 ±0.020	B	0.907	0.509 ±0.015	0.398 ±0.031	0.061 ± 8%	1.46 ± 11%
		4	0.333 ±0.021	B	1.073	0.602 ±0.018	0.471 ±0.037	0.073 ± 8%	1.42 ± 10%
		5	0.395 ±0.022	B	1.207	0.688 ±0.021	0.519 ±0.042	0.080 ± 8%	1.32 ± 10%
		6	0.441 ±0.023	B	1.295	0.771 ±0.023	0.524 ±0.045	0.081 ± 9%	1.19 ± 10%
n-Butane (Low NOx)									
31	5.48 ±0.11	1	0.119 ±0.017	A	0.523	0.351 ±0.011	0.172 ±0.019	0.031 ± 11%	1.45 ± 18%
		2	0.185 ±0.017	A	0.701	0.520 ±0.016	0.181 ±0.026	0.033 ± 15%	0.98 ± 17%
		3	0.244 ±0.017	A	0.774	0.590 ±0.018	0.184 ±0.029	0.034 ± 16%	0.75 ± 17%
		4	0.270 ±0.018	A	0.801	0.612 ±0.018	0.189 ±0.030	0.034 ± 16%	0.70 ± 17%
		5	0.287 ±0.018	A	0.803	0.618 ±0.019	0.185 ±0.030	0.034 ± 17%	0.64 ± 18%
		6	0.281 ±0.019	A	0.803	0.621 ±0.019	0.182 ±0.030	0.033 ± 17%	0.65 ± 18%
n-Octane (High NOx)									
24	1.102 ±0.022	1	[b]		0.176	0.205 ±0.006	-0.029 ±0.008	-0.026 ± 28%	
		2	0.073 ±0.031	B	0.409	0.407 ±0.012	0.002 ±0.017	(0.002 ±0.02)	(0.0 ± 0.2)
		3	0.117 ±0.030	B	0.586	0.530 ±0.016	0.056 ±0.024	0.051 ± 42%	0.48 ± 50%
		4	0.154 ±0.030	B	0.720	0.629 ±0.019	0.091 ±0.029	0.083 ± 32%	0.59 ± 37%
		5	0.179 ±0.031	B	0.857	0.724 ±0.022	0.133 ±0.034	0.121 ± 25%	0.74 ± 31%
		6	0.216 ±0.031	B	0.995	0.816 ±0.024	0.179 ±0.039	0.162 ± 22%	0.83 ± 26%
70	0.746 ±0.015	1	0.039 ±0.021	A	0.160	0.179 ±0.005	-0.019 ±0.007	-0.025 ± 38%	-0.49 ± 66%
		2	0.080 ±0.020	A	0.382	0.374 ±0.011	0.008 ±0.016	(0.011 ±0.02)	(0.1 ± 0.2)
		3	0.110 ±0.020	A	0.543	0.494 ±0.015	0.049 ±0.022	0.066 ± 45%	0.44 ± 49%
		4	0.132 ±0.020	A	0.658	0.580 ±0.017	0.078 ±0.026	0.105 ± 34%	0.59 ± 37%
		5	0.157 ±0.020	A	0.765	0.661 ±0.020	0.104 ±0.030	0.139 ± 29%	0.66 ± 32%
		6	0.176 ±0.020	A	0.870	0.740 ±0.022	0.130 ±0.034	0.174 ± 26%	0.74 ± 29%

Table 12 (continued)

ETC Run No.	Added (ppm)	Time (hr)	Reacted [a] (ppm)	Deriv.	d(O3-NO) (ppm) Test	Base min.Unc	Change	Reactivity (mol/mol) Incremental	Mechanistic
n-Octane (Low NOx)									
37	1.126 ±0.023	1	0.065 ±0.031	B	0.326	0.343 ±0.010	-0.017 ±0.014	-0.0151 ± 84%	-0.26 ± 96%
		2	0.128 ±0.031	B	0.543	0.514 ±0.015	0.029 ±0.022	0.026 ± 77%	0.23 ± 81%
		3	0.168 ±0.031	B	0.630	0.583 ±0.017	0.047 ±0.026	0.042 ± 55%	0.28 ± 58%
		4	0.170 ±0.032	B	0.664	0.605 ±0.018	0.059 ±0.027	0.052 ± 46%	0.35 ± 49%
		5	0.180 ±0.033	B	0.672	0.611 ±0.018	0.061 ±0.027	0.054 ± 45%	0.34 ± 48%
		6	0.201 ±0.034	B	0.672	0.613 ±0.018	0.059 ±0.027	0.052 ± 46%	0.29 ± 49%
71	0.647 ±0.013	1	0.057 ±0.007	B	0.299	0.319 ±0.010	-0.020 ±0.013	-0.031 ± 66%	-0.35 ± 67%
		2	0.100 ±0.008	B	0.520	0.490 ±0.015	0.030 ±0.021	0.046 ± 71%	0.30 ± 72%
		3	0.113 ±0.010	B	0.607	0.568 ±0.017	0.039 ±0.025	0.060 ± 64%	0.35 ± 65%
		4	0.128 ±0.012	B	0.645	0.597 ±0.018	0.048 ±0.026	0.074 ± 55%	0.38 ± 56%
		5	0.135 ±0.014	B	0.653	0.603 ±0.018	0.050 ±0.027	0.077 ± 53%	0.37 ± 54%
		6	0.142 ±0.017	B	0.653	0.606 ±0.018	0.047 ±0.027	0.073 ± 57%	0.33 ± 58%
Ethene (High NOx)									
17	0.608 ±0.012	1	0.042 ±0.017	A	0.285	0.195 ±0.006	0.090 ±0.010	0.148 ± 12%	2.12 ± 41%
		2	0.095 ±0.016	A	0.563	0.398 ±0.012	0.165 ±0.021	0.27 ± 13%	1.73 ± 21%
		3	0.155 ±0.016	A	0.755	0.518 ±0.016	0.237 ±0.027	0.39 ± 12%	1.53 ± 15%
		4	0.215 ±0.015	A	0.938	0.610 ±0.018	0.328 ±0.034	0.54 ± 10%	1.52 ± 12%
		5	0.279 ±0.015	A	1.093	0.695 ±0.021	0.398 ±0.039	0.66 ± 10%	1.43 ± 11%
		6	0.340 ±0.015	A	1.188	0.779 ±0.023	0.409 ±0.043	0.67 ± 11%	1.20 ± 11%
Ethene (Low NOx)									
38	0.659 ±0.013	1	0.103 ±0.018	A	0.464	0.338 ±0.010	0.126 ±0.017	0.191 ± 14%	1.22 ± 23%
		2	0.183 ±0.020	A	0.628	0.507 ±0.015	0.121 ±0.024	0.184 ± 20%	0.66 ± 23%
		3	0.240 ±0.022	A	0.663	0.573 ±0.017	0.090 ±0.026	0.137 ± 29%	0.38 ± 31%
		4	0.289 ±0.025	A	0.663	0.593 ±0.018	0.070 ±0.027	0.106 ± 38%	0.24 ± 39%
		5	0.324 ±0.028	A	0.663	0.603 ±0.018	0.060 ±0.027	0.091 ± 45%	0.19 ± 46%
		6	[b]		0.663	0.606 ±0.018	0.057 ±0.027	0.086 ± 47%	
Propene (High NOx)									
18	0.350 ±0.007	1	0.096 ±0.009	A	0.402	0.230 ±0.007	0.172 ±0.014	0.49 ± 8%	1.80 ± 12%
		2	0.211 ±0.008	A	0.728	0.437 ±0.013	0.291 ±0.025	0.83 ± 9%	1.38 ± 9%
		3	0.291 ±0.007	A	0.960	0.557 ±0.017	0.403 ±0.033	1.15 ± 9%	1.38 ± 9%
		4	0.328 ±0.007	A	1.093	0.655 ±0.020	0.438 ±0.038	1.25 ± 9%	1.34 ± 9%
		5	0.347 ±0.007	A	1.157	0.747 ±0.022	0.410 ±0.041	1.17 ± 10%	1.18 ± 10%
		6	0.348 ±0.007	A	1.169	0.837 ±0.025	0.332 ±0.043	0.95 ± 13%	0.95 ± 13%
Propene (Low NOx)									
32	0.305 ±0.006	1	0.099 ±0.007	B	0.510	0.334 ±0.010	0.176 ±0.018	0.58 ± 11%	1.78 ± 13%
		2	0.216 ±0.006	B	0.610	0.505 ±0.015	0.105 ±0.024	0.34 ± 23%	0.49 ± 23%
		3	0.271 ±0.006	B	0.610	0.577 ±0.017	0.033 ±0.025	0.108 ± 76%	0.12 ± 76%
		4	0.289 ±0.006	B	0.610	0.599 ±0.018	0.011 ±0.026	(0.04 ±0.08)	(0.0 ± 0.1)
		5	0.298 ±0.006	B	0.610	0.604 ±0.018	0.006 ±0.026	(0.02 ±0.08)	(0.0 ± 0.1)
		6	0.303 ±0.006	B	0.610	0.608 ±0.018	0.002 ±0.026	(0.007 ±0.08)	(0.0 ± 0.1)
trans-2-Butene (High NOx)									
21	0.324 ±0.007	1	[b]		0.773	0.201 ±0.006	0.572 ±0.024	1.76 ± 5%	
		2	0.320 ±0.007	B	0.901	0.407 ±0.012	0.494 ±0.030	1.52 ± 6%	1.54 ± 6%
		3	0.320 ±0.007	B	0.998	0.524 ±0.016	0.474 ±0.034	1.46 ± 7%	1.48 ± 7%
		4	0.320 ±0.007	B	1.070	0.610 ±0.018	0.460 ±0.037	1.42 ± 8%	1.44 ± 8%
		5	0.320 ±0.007	B	1.110	0.693 ±0.021	0.417 ±0.039	1.29 ± 10%	1.30 ± 10%
		6	0.320 ±0.007	B	1.118	0.772 ±0.023	0.346 ±0.041	1.07 ± 12%	1.08 ± 12%
69	0.190 ±0.004	1	0.157 ±0.004	A	0.503	0.175 ±0.005	0.328 ±0.016	1.73 ± 5%	2.09 ± 5%
		2	0.190 ±0.004	A	0.694	0.370 ±0.011	0.324 ±0.024	1.71 ± 8%	1.71 ± 8%
		3	0.190 ±0.004	A	0.793	0.490 ±0.015	0.303 ±0.028	1.60 ± 9%	1.60 ± 9%
		4	0.190 ±0.004	A	0.894	0.583 ±0.017	0.311 ±0.032	1.64 ± 10%	1.64 ± 10%
		5	0.190 ±0.004	A	0.984	0.671 ±0.020	0.313 ±0.036	1.65 ± 12%	1.65 ± 12%
		6	0.190 ±0.004	A	1.060	0.750 ±0.023	0.310 ±0.039	1.63 ± 13%	1.63 ± 13%
trans-2-Butene (Low NOx)									
33	0.156 ±0.003	1	[b]		0.476	0.342 ±0.010	0.134 ±0.018	0.86 ± 13%	
		2	0.154 ±0.004	A	0.554	0.512 ±0.015	0.042 ±0.023	0.27 ± 54%	0.27 ± 54%
		3	0.154 ±0.004	A	0.572	0.582 ±0.017	-0.010 ±0.024	(-0.06 ± 0.2)	(-0.1 ± 0.2)
		4	0.154 ±0.004	A	0.580	0.604 ±0.018	-0.024 ±0.025	(-0.2 ± 0.2)	(-0.2 ± 0.2)
		5	0.154 ±0.004	A	0.587	0.612 ±0.018	-0.025 ±0.025	(-0.2 ± 0.2)	(-0.2 ± 0.2)
		6	0.154 ±0.004	A	0.594	0.616 ±0.018	-0.022 ±0.026	(-0.14 ± 0.2)	(-0.1 ± 0.2)

Table 12 (continued)

ETC Run No.	Added (ppm)	Time (hr)	Reacted [a] (ppm)	Deriv.	d(O3-NO) (ppm) Test	Base min.Unc	Change	Reactivity (mol/mol) Incremental	Mechanistic
Benzene (Low NOx)									
39	7.39 ±0.15	1	0.147 ±0.012	B	0.486	0.348 ±0.010	0.138 ±0.018	0.0187 ± 13%	0.94 ± 15%
		2	0.213 ±0.012	B	0.531	0.520 ±0.016	0.011 ±0.022	(0.001±0.003)	(0.1 ± 0.1)
		3	0.250 ±0.012	B	0.531	0.588 ±0.018	-0.057 ±0.024	-0.0077 ± 42%	-0.23 ± 42%
		4	0.261 ±0.013	B	0.531	0.607 ±0.018	-0.076 ±0.024	-0.0103 ± 32%	-0.29 ± 32%
		5	0.280 ±0.013	B	0.531	0.612 ±0.018	-0.081 ±0.024	-0.0110 ± 30%	-0.29 ± 30%
		6	0.296 ±0.014	B	0.531	0.612 ±0.018	-0.081 ±0.024	-0.0110 ± 30%	-0.27 ± 30%
Toluene (High NOx)									
23	0.573 ±0.012	1	0.035 ±0.016	A	0.301	0.196 ±0.006	0.105 ±0.011	0.183 ± 10%	2.99 ± 46%
		2	0.077 ±0.015	A	0.599	0.396 ±0.012	0.203 ±0.022	0.35 ± 11%	2.64 ± 23%
		3	0.108 ±0.015	A	0.822	0.513 ±0.015	0.309 ±0.029	0.54 ± 10%	2.85 ± 17%
		4	0.143 ±0.015	A	1.003	0.614 ±0.018	0.389 ±0.035	0.68 ± 9%	2.72 ± 14%
		5	0.167 ±0.015	A	1.080	0.708 ±0.021	0.372 ±0.039	0.65 ± 11%	2.23 ± 14%
		6	0.181 ±0.015	A	1.083	0.800 ±0.024	0.283 ±0.040	0.49 ± 14%	1.56 ± 17%
Toluene (Low NOx)									
30	1.134 ±0.023	1	0.096 ±0.031	B	0.471	0.330 ±0.010	0.141 ±0.017	0.124 ± 12%	1.47 ± 35%
		2	0.145 ±0.031	B	0.507	0.499 ±0.015	0.008 ±0.021	(0.007 ±0.02)	(0.1 ± 0.1)
		3	0.159 ±0.031	B	0.507	0.569 ±0.017	-0.062 ±0.023	-0.055 ± 37%	-0.39 ± 42%
		4	0.176 ±0.031	B	0.507	0.590 ±0.018	-0.083 ±0.023	-0.073 ± 28%	-0.47 ± 33%
		5	0.186 ±0.031	B	0.507	0.596 ±0.018	-0.089 ±0.023	-0.079 ± 26%	-0.48 ± 31%
		6	0.201 ±0.032	B	0.507	0.598 ±0.018	-0.091 ±0.024	-0.080 ± 26%	-0.45 ± 30%
m-Xylene (High NOx)									
25	0.085 ±0.004	1	0.018 ±0.002	A	0.289	0.198 ±0.006	0.091 ±0.011	1.07 ± 12%	5.10 ± 17%
		2	0.034 ±0.002	A	0.566	0.402 ±0.012	0.164 ±0.021	1.94 ± 13%	4.79 ± 14%
		3	0.045 ±0.002	A	0.735	0.528 ±0.016	0.207 ±0.027	2.4 ± 14%	4.61 ± 14%
		4	0.054 ±0.002	A	0.908	0.635 ±0.019	0.273 ±0.033	3.2 ± 13%	5.03 ± 13%
		5	0.060 ±0.002	A	1.051	0.743 ±0.022	0.308 ±0.039	3.6 ± 13%	5.10 ± 13%
		6	0.066 ±0.002	A	1.141	0.848 ±0.025	0.293 ±0.043	3.5 ± 15%	4.43 ± 15%
68	0.064 ±0.003	1	0.014 ±0.002	B	0.217	0.155 ±0.005	0.062 ±0.008	0.96 ± 14%	4.40 ± 17%
		2	0.026 ±0.002	B	0.467	0.340 ±0.010	0.127 ±0.017	1.97 ± 15%	4.87 ± 15%
		3	0.032 ±0.001	B	0.616	0.464 ±0.014	0.152 ±0.023	2.4 ± 16%	4.69 ± 16%
		4	0.038 ±0.001	B	0.749	0.555 ±0.017	0.194 ±0.028	3.0 ± 15%	5.09 ± 15%
		5	0.043 ±0.001	B	0.879	0.638 ±0.019	0.241 ±0.033	3.7 ± 14%	5.56 ± 14%
		6	0.047 ±0.001	B	0.997	0.722 ±0.022	0.275 ±0.037	4.3 ± 14%	5.81 ± 14%
m-Xylene (Low NOx)									
35	0.106 ±0.004	1	0.038 ±0.003	A	0.423	0.341 ±0.010	0.082 ±0.016	0.77 ± 20%	2.15 ± 21%
		2	0.052 ±0.002	A	0.543	0.509 ±0.015	0.034 ±0.022	0.32 ± 66%	0.65 ± 66%
		3	0.059 ±0.002	A	0.556	0.577 ±0.017	-0.021 ±0.024	(-0.2 ± 0.2)	(-0.4 ± 0.4)
		4	0.064 ±0.002	A	0.556	0.599 ±0.018	-0.043 ±0.025	-0.41 ± 57%	-0.67 ± 57%
		5	0.068 ±0.002	A	0.556	0.608 ±0.018	-0.052 ±0.025	-0.49 ± 48%	-0.77 ± 48%
		6	0.069 ±0.002	A	0.557	0.611 ±0.018	-0.054 ±0.025	-0.51 ± 46%	-0.78 ± 46%
67	0.173 ±0.005	1	0.068 ±0.004	B	0.458	0.308 ±0.009	0.150 ±0.017	0.87 ± 11%	2.21 ± 13%
		2	0.088 ±0.005	B	0.535	0.481 ±0.014	0.054 ±0.022	0.31 ± 40%	0.62 ± 40%
		3	0.094 ±0.005	B	0.537	0.558 ±0.017	-0.021 ±0.023	(-0.12 ±0.13)	(-0.2 ± 0.2)
		4	0.099 ±0.006	B	0.537	0.587 ±0.018	-0.050 ±0.024	-0.29 ± 48%	-0.51 ± 48%
		5	0.105 ±0.006	B	0.537	0.595 ±0.018	-0.058 ±0.024	-0.34 ± 42%	-0.55 ± 42%
		6	0.107 ±0.007	B	0.537	0.597 ±0.018	-0.060 ±0.024	-0.35 ± 40%	-0.56 ± 41%
Formaldehyde (High NOx)									
22	0.408 ±0.007	1	[b]		0.393	0.193 ±0.006	0.200 ±0.013	0.49 ± 7%	
		2	[b]		0.616	0.400 ±0.012	0.216 ±0.022	0.53 ± 10%	
		3	[b]		0.762	0.519 ±0.016	0.243 ±0.028	0.60 ± 11%	
		4	[b]		0.891	0.612 ±0.018	0.279 ±0.032	0.68 ± 12%	
		5	[b]		0.997	0.693 ±0.021	0.304 ±0.036	0.74 ± 12%	
		6	[b]		1.079	0.771 ±0.023	0.308 ±0.040	0.75 ± 13%	
Formaldehyde (Low NOx)									
36	0.247 ±0.004	1	[b]		0.452	0.368 ±0.011	0.084 ±0.017	0.34 ± 21%	
		2	[b]		0.598	0.539 ±0.016	0.059 ±0.024	0.24 ± 41%	
		3	[b]		0.638	0.607 ±0.018	0.031 ±0.026	0.125 ± 85%	
		4	[b]		0.643		1.643 ±0.036		
		5	[b]		0.643	0.629 ±0.019	0.014 ±0.027	(0.06 ±0.11)	
		6	[b]		0.643	0.631 ±0.019	0.012 ±0.027	(0.05 ±0.11)	

Table 12 (continued)

ETC Run No.	Added (ppm)	Time (hr)	Reacted [a] (ppm)	Deriv.	d(O3-NO) (ppm) Test	Base min.Unc	Change	Reactivity (mol/mol) Incremental	Mechanistic
Acetaldehyde (High NOx)									
65	1.53 ±0.03	1	[b]		0.353	0.169 ±0.005	0.184 ±0.012	0.120 ± 7%	
		2	0.108 ±0.052	A	0.543	0.368 ±0.011	0.175 ±0.020	0.114 ± 11%	1.63 ± 50%
		3	0.205 ±0.060	A	0.670	0.491 ±0.015	0.179 ±0.025	0.117 ± 14%	0.87 ± 32%
		4	0.242 ±0.070	A	0.786	0.582 ±0.017	0.204 ±0.029	0.133 ± 15%	0.84 ± 32%
		5	0.292 ±0.081	A	0.893	0.667 ±0.020	0.226 ±0.033	0.147 ± 15%	0.77 ± 31%
		6	0.377 ±0.091	A	0.977	0.749 ±0.022	0.228 ±0.037	0.148 ± 16%	0.60 ± 29%
Acetaldehyde (Low NOx)									
66	1.62 ±0.03	1	[b]		0.297	0.318 ±0.010	-0.021 ±0.013	-0.0130 ± 62%	
		2	0.092 ±0.055	B	0.429	0.490 ±0.015	-0.061 ±0.020	-0.038 ± 32%	-0.66 ± 68%
		3	0.131 ±0.065	B	0.481	0.567 ±0.017	-0.086 ±0.022	-0.053 ± 26%	-0.66 ± 56%
		4	0.168 ±0.076	B	0.507	0.594 ±0.018	-0.087 ±0.023	-0.054 ± 27%	-0.52 ± 52%
		5	0.206 ±0.088	B	0.527	0.599 ±0.018	-0.072 ±0.024	-0.044 ± 33%	-0.35 ± 54%
		6	0.247 ±0.100	B	0.545	0.601 ±0.018	-0.056 ±0.024	-0.035 ± 44%	-0.23 ± 59%

[a] Derivation methods: "IntOH" = hourly amounts reacted computed from the experimentally measured IntOH and VOC's OH rate constant; "Direct" = hourly amounts reacted determined by interpolating experimental measurements of the VOC, with a correction for dilution.

[b] Amount reacted could not be determined for this VOC, or amount reacted could not be determined for this time with sufficient precision to be useful.

Table 13. Derivation of hourly IntOH reactivities from the results of the lumped molecule surrogate experiments.

ETC Run No	Added (ppm)	Time (hr)	Reacted (ppm)	IntOH (ppt-min) Test Run	Base Run	Change	Reactivity (ppt-min/ppm) Incremental	Mechanistic
Carbon Monoxide (High NOx)								
14	155.	1	0.363 ±0.045	6.7 ±0.8	5.6 ±0.8	1.0 ±1.2	(0.007 ±0.007)	(3. ± 3.)
		2	0.635 ±0.045	11.8 ±0.8	12.1 ±0.8	-0.3 ±1.2	(-0.002 ±0.008)	(-1. ± 2.)
		3	0.870 ±0.047	16.2 ±0.9	16.4 ±0.8	-0.2 ±1.2	(-0.001 ±0.008)	(0. ± 1.)
		4	0.978 ±0.049	18.3 ±0.9	20.6 ±0.8	-2.3 ±1.2	-0.0148 ± 53%	-2. ± 53%
		5	1.107 ±0.052	20.8 ±0.9	25.8 ±0.9	-4.9 ±1.3	-0.032 ± 25%	-4. ± 26%
		6	1.209 ±0.056	22.8 ±1.0	30.3 ±0.9	-7.5 ±1.3	-0.048 ± 17%	-6. ± 18%
15	161.	1	0.396 ±0.046	7.0 ±0.8	5.8 ±0.8	1.2 ±1.2	0.0077 ± 94%	3. ± 94%
		2	0.649 ±0.047	11.6 ±0.8	11.7 ±0.8	0.0 ±1.2	(-.0003 ±0.007)	(0. ± 2.)
		3	0.857 ±0.047	15.5 ±0.8	16.3 ±0.8	-0.8 ±1.2	(-0.005 ±0.007)	(-1. ± 1.)
		4	1.100 ±0.049	20.0 ±0.9	21.5 ±0.9	-1.5 ±1.2	-0.0095 ± 80%	-1. ± 80%
		5	1.244 ±0.052	22.8 ±0.9	26.3 ±0.9	-3.5 ±1.2	-0.022 ± 36%	-3. ± 36%
		6	1.358 ±0.054	25.1 ±0.9	32.1 ±0.9	-7.0 ±1.3	-0.043 ± 18%	-5. ± 19%
16	74.2	1	0.155 ±0.021	6.0 ±0.8	5.2 ±0.8	0.8 ±1.2	(0.010 ±0.02)	(5. ± 7.)
		2	0.297 ±0.021	11.5 ±0.8	11.7 ±0.8	-0.2 ±1.2	(-0.003 ±0.02)	(-1. ± 4.)
		3	0.400 ±0.022	15.6 ±0.8	16.4 ±0.8	-0.8 ±1.2	(-0.011 ±0.02)	(-2. ± 3.)
		4	0.496 ±0.023	19.4 ±0.9	20.4 ±0.9	-1.0 ±1.2	(-0.013 ±0.02)	(-2. ± 2.)
		5	0.606 ±0.024	23.8 ±0.9	24.5 ±0.9	-0.7 ±1.2	(-0.010 ±0.02)	(-1. ± 2.)
		6	0.684 ±0.025	27.0 ±0.9	29.3 ±0.9	-2.2 ±1.3	-0.030 ± 57%	-3. ± 58%
20	103.	1	0.154 ±0.030	4.3 ±0.8	4.2 ±0.8	0.1 ±1.2	(0.0010 ±0.011)	(1. ± 8.)
		2	0.306 ±0.030	8.5 ±0.8	9.0 ±0.8	-0.6 ±1.2	(-0.005 ±0.011)	(-2. ± 4.)
		3	0.455 ±0.030	12.6 ±0.8	14.6 ±0.8	-1.9 ±1.2	-0.0187 ± 61%	-4. ± 62%
		4	0.622 ±0.031	17.3 ±0.8	18.2 ±0.9	-0.9 ±1.2	(-0.009 ±0.012)	(-1. ± 2.)
		5	0.738 ±0.032	20.5 ±0.9	22.9 ±0.9	-2.4 ±1.2	-0.023 ± 52%	-3. ± 52%
		6	0.869 ±0.034	24.3 ±0.9	25.7 ±0.9	-1.4 ±1.3	-0.0141 ± 87%	-2. ± 87%
Carbon Monoxide (Low NOx)								
29	85.8	1	0.282 ±0.025	9.4 ±0.8	12.4 ±0.8	-3.0 ±1.2	-0.035 ± 38%	-11. ± 39%
		2	0.437 ±0.025	14.5 ±0.8	19.9 ±0.8	-5.4 ±1.2	-0.062 ± 22%	-12. ± 23%
		3	0.497 ±0.025	16.5 ±0.8	25.9 ±0.8	-9.3 ±1.2	-0.109 ± 13%	-19. ± 14%
		4	0.586 ±0.026	19.5 ±0.8	28.5 ±0.8	-9.0 ±1.2	-0.104 ± 13%	-15. ± 14%
		5	0.626 ±0.027	20.9 ±0.9	32.4 ±0.9	-11.6 ±1.2	-0.135 ± 11%	-18. ± 11%
		6	0.659 ±0.028	22.0 ±0.9	34.4 ±0.9	-12.4 ±1.3	-0.145 ± 10%	-19. ± 11%

Table 13 (continued)

ETC Run No	Added (ppm)	Time (hr)	Reacted (ppm)	IntOH (ppt-min) Test Run	IntOH (ppt-min) Base Run	IntOH (ppt-min) Change	Reactivity (ppt-min/ppm) Incremental	Reactivity (ppt-min/ppm) Mechanistic
n-Butane (High NOx)								
19	6.48	1	0.098 ±0.020	4.0 ±0.8	5.5 ±0.8	-1.4 ±1.2	-0.22 ± 81%	-15. ± 83%
		2	0.203 ±0.020	8.5 ±0.8	11.2 ±0.8	-2.7 ±1.2	-0.42 ± 43%	-14. ± 44%
		3	0.273 ±0.020	11.4 ±0.8	16.3 ±0.8	-4.8 ±1.2	-0.75 ± 24%	-18. ± 26%
		4	0.333 ±0.021	14.0 ±0.8	21.0 ±0.8	-7.0 ±1.2	-1.08 ± 17%	-21. ± 18%
		5	0.395 ±0.022	16.8 ±0.9	25.3 ±0.9	-8.5 ±1.2	-1.31 ± 15%	-22. ± 15%
		6	0.441 ±0.023	18.8 ±0.9	30.7 ±0.9	-11.9 ±1.3	-1.84 ± 11%	-27. ± 12%
n-Butane (Low NOx)								
31	5.48	1	0.119 ±0.017	5.8 ±0.8	8.8 ±0.8	-3.0 ±1.2	-0.55 ± 39%	-25. ± 41%
		2	0.185 ±0.017	9.2 ±0.8	19.0 ±0.8	-9.8 ±1.2	-1.79 ± 12%	-53. ± 15%
		3	0.244 ±0.017	12.2 ±0.8	25.7 ±0.8	-13.5 ±1.2	-2.5 ± 9%	-55. ± 11%
		4	0.270 ±0.018	13.6 ±0.8	30.5 ±0.8	-16.9 ±1.2	-3.1 ± 7%	-63. ± 10%
		5	0.287 ±0.018	14.5 ±0.9	32.6 ±0.9	-18.1 ±1.2	-3.3 ± 7%	-63. ± 9%
		6	0.281 ±0.019	14.2 ±0.9	35.4 ±0.9	-21.2 ±1.3	-3.9 ± 6%	-75. ± 9%
n-Octane (High NOx)								
24	1.102	1	[b]	2.1 ±0.8	4.8 ±0.8	-2.6 ±1.2	-2.4 ± 44%	
		2	0.073 ±0.031	4.9 ±0.8	10.7 ±0.8	-5.8 ±1.2	-5.3 ± 20%	-79. ± 47%
		3	0.117 ±0.030	7.9 ±0.8	15.4 ±0.8	-7.5 ±1.2	-6.8 ± 16%	-64. ± 30%
		4	0.154 ±0.030	10.7 ±0.8	20.3 ±0.8	-9.6 ±1.2	-8.7 ± 13%	-62. ± 23%
		5	0.179 ±0.031	13.1 ±0.9	24.7 ±0.9	-11.6 ±1.2	-10.5 ± 11%	-65. ± 20%
		6	0.216 ±0.031	16.1 ±0.9	29.2 ±0.9	-13.1 ±1.3	-11.9 ± 10%	-61. ± 17%
70	0.746	1	0.039 ±0.021	4.2 ±0.8	6.7 ±0.8	-2.5 ±1.2	-3.4 ± 46%	-66. ± 71%
		2	0.080 ±0.020	8.1 ±0.8	12.0 ±0.8	-3.9 ±1.2	-5.2 ± 30%	-49. ± 40%
		3	0.110 ±0.020	11.5 ±0.8	16.7 ±0.8	-5.2 ±1.2	-7.0 ± 23%	-47. ± 29%
		4	0.132 ±0.020	14.0 ±0.8	20.7 ±0.9	-6.7 ±1.2	-9.0 ± 18%	-51. ± 24%
		5	0.157 ±0.020	17.3 ±0.9	25.1 ±0.9	-7.9 ±1.2	-10.5 ± 16%	-50. ± 20%
		6	0.176 ±0.020	19.7 ±0.9	29.9 ±0.9	-10.2 ±1.3	-13.6 ± 13%	-58. ± 17%
n-Octane (Low NOx)								
37	1.126	1	0.065 ±0.031	4.8 ±0.8	13.8 ±0.9	-9.0 ±1.2	-8.0 ± 13%	-138. ± 50%
		2	0.128 ±0.031	9.5 ±0.8	20.4 ±1.0	-10.9 ±1.3	-9.7 ± 12%	-85. ± 27%
		3	0.168 ±0.031	12.5 ±0.9	26.5 ±1.2	-14.0 ±1.5	-12.4 ± 11%	-83. ± 21%
		4	0.170 ±0.032	12.4 ±0.9	30.0 ±1.4	-17.7 ±1.7	-15.7 ± 10%	-104. ± 21%
		5	0.180 ±0.033	13.3 ±0.9	31.8 ±1.7	-18.5 ±1.9	-16.4 ± 11%	-103. ± 21%
		6	0.201 ±0.034	14.8 ±1.0	35.8 ±1.9	-21.0 ±2.2	-18.7 ± 11%	-105. ± 20%
71	0.647	1	0.057 ±0.007	7.1 ±0.9	12.6 ±0.9	-5.5 ±1.2	-8.5 ± 22%	-97. ± 25%
		2	0.100 ±0.008	13.0 ±1.0	21.0 ±1.0	-8.0 ±1.4	-12.3 ± 18%	-80. ± 20%
		3	0.113 ±0.010	15.0 ±1.2	26.9 ±1.2	-11.9 ±1.7	-18.4 ± 14%	-105. ± 17%
		4	0.128 ±0.012	17.2 ±1.4	30.4 ±1.4	-13.2 ±2.0	-20. ± 16%	-103. ± 18%
		5	0.135 ±0.014	18.4 ±1.7	33.2 ±1.7	-14.9 ±2.4	-23. ± 16%	-110. ± 19%
		6	0.142 ±0.017	19.4 ±1.9	36.4 ±1.9	-17.1 ±2.8	-26. ± 16%	-121. ± 20%
Ethene (High NOx)								
17	0.608	1	0.042 ±0.017	5.7 ±0.8	6.0 ±0.8	-0.4 ±1.2	(-0.6 ± 2.)	(-8. ± 28.)
		2	0.095 ±0.016	12.0 ±0.8	11.9 ±0.8	0.1 ±1.2	(0.2 ± 2.)	(1. ± 12.)
		3	0.155 ±0.016	19.4 ±0.8	17.8 ±0.8	1.6 ±1.2	2.6 ± 76%	10. ± 76%
		4	0.215 ±0.015	26.8 ±0.9	21.4 ±0.8	5.4 ±1.2	8.8 ± 23%	25. ± 24%
		5	0.279 ±0.015	34.0 ±0.9	24.9 ±0.9	9.1 ±1.2	14.9 ± 14%	33. ± 15%
		6	0.340 ±0.015	41.5 ±0.9	29.9 ±0.9	11.7 ±1.3	19.3 ± 11%	34. ± 12%
Ethene (Low NOx)								
38	0.659	1	0.103 ±0.018	12.6 ±0.9	12.3 ±0.9	0.2 ±1.2	(0.4 ± 2.)	(2. ± 12.)
		2	0.183 ±0.020	18.9 ±1.0	22.5 ±1.0	-3.5 ±1.4	-5.4 ± 40%	-19. ± 42%
		3	0.240 ±0.022	23.7 ±1.2	27.2 ±1.2	-3.5 ±1.7	-5.3 ± 49%	-14. ± 50%
		4	0.289 ±0.025	26.3 ±1.4	30.3 ±1.4	-4.0 ±2.0	-6.1 ± 51%	-14. ± 51%
		5	0.324 ±0.028	28.8 ±1.7	32.9 ±1.7	-4.1 ±2.4	-6.2 ± 58%	-13. ± 59%
		6	[b]	30.5 ±1.9	35.6 ±1.9	-5.1 ±2.8	-7.7 ± 54%	
Propene (High NOx)								
18	0.350	1	0.096 ±0.009	6.6 ±0.8	5.5 ±0.8	1.0 ±1.2	(3. ± 3.)	(11. ± 12.)
		2	0.211 ±0.008	15.6 ±0.8	11.7 ±0.8	3.9 ±1.2	11.2 ± 30%	19. ± 30%
		3	0.291 ±0.007	23.6 ±0.8	16.3 ±0.8	7.3 ±1.2	21. ± 16%	25. ± 16%
		4	0.328 ±0.007	31.4 ±0.9	21.5 ±0.8	9.9 ±1.2	28. ± 12%	30. ± 12%
		5	0.347 ±0.007	36.6 ±0.9	26.0 ±0.9	10.5 ±1.2	30. ± 12%	30. ± 12%
		6	0.348 ±0.007	41.0 ±0.9	31.1 ±0.9	9.9 ±1.3	28. ± 13%	28. ± 13%

Table 13 (continued)

ETC Run No	Added (ppm)	Time (hr)	Reacted (ppm)	IntOH (ppt-min) Test Run	Base Run	Change	Reactivity (ppt-min/ppm) Incremental	Mechanistic
Propene (Low NOx)								
32	0.305	1	0.099 ±0.007	10.5 ±0.8	12.6 ±0.8	-2.1 ±1.2	-6.8 ± 56%	-21. ± 57%
		2	0.216 ±0.006	18.0 ±0.8	21.2 ±0.8	-3.2 ±1.2	-10.4 ± 37%	-15. ± 37%
		3	0.271 ±0.006	20.9 ±0.8	27.0 ±0.8	-6.1 ±1.2	-20. ± 19%	-23. ± 19%
		4	0.289 ±0.006	23.2 ±0.8	30.9 ±0.8	-7.7 ±1.2	-25. ± 16%	-27. ± 16%
		5	0.298 ±0.006	25.8 ±0.9	34.2 ±0.9	-8.4 ±1.2	-27. ± 15%	-28. ± 15%
		6	0.303 ±0.006	27.5 ±0.9	37.3 ±0.9	-9.9 ±1.3	-32. ± 13%	-33. ± 13%
trans-2-Butene (High NOx)								
21	0.324	1	[b]	14.0 ±0.8	5.0 ±0.8	9.0 ±1.2	28. ± 13%	
		2	0.320 ±0.007	19.9 ±0.8	11.3 ±0.8	8.6 ±1.2	27. ± 14%	27. ± 14%
		3	0.320 ±0.007	23.6 ±0.8	16.2 ±0.8	7.4 ±1.2	23. ± 16%	23. ± 16%
		4	0.320 ±0.007	27.7 ±0.8	21.0 ±0.8	6.6 ±1.2	20. ± 18%	21. ± 18%
		5	0.320 ±0.007	31.6 ±0.9	25.3 ±0.9	6.3 ±1.2	19.5 ± 19%	20. ± 19%
		6	0.320 ±0.007	35.1 ±0.9	30.1 ±0.9	5.0 ±1.3	15.4 ± 25%	16. ± 25%
69	0.190	1	0.157 ±0.004	11.7 ±0.8	6.4 ±0.8	5.4 ±1.2	28. ± 22%	34. ± 22%
		2	0.190 ±0.004	19.6 ±0.8	12.7 ±0.8	7.0 ±1.2	37. ± 17%	37. ± 17%
		3	0.190 ±0.004	24.0 ±0.8	18.0 ±0.9	6.0 ±1.2	32. ± 20%	32. ± 20%
		4	0.190 ±0.004	29.3 ±0.9	21.8 ±0.9	7.4 ±1.2	39. ± 17%	39. ± 17%
		5	0.190 ±0.004	32.7 ±0.9	25.4 ±0.9	7.3 ±1.3	38. ± 18%	38. ± 18%
		6	0.190 ±0.004	37.0 ±0.9	-75.8 ±1.0	112.8 ±1.3	0.0 ± 0%	0. ± 0%
trans-2-Butene (Low NOx)								
33	0.156	1	[b]	15.5 ±0.8	12.1 ±0.8	3.4 ±1.2	22. ± 34%	
		2	0.154 ±0.004	20.7 ±0.8	21.5 ±0.8	-0.8 ±1.2	(-5. ± 8.)	(-5. ± 8.)
		3	0.154 ±0.004	22.7 ±0.8	26.1 ±0.8	-3.4 ±1.2	-22. ± 34%	-22. ± 34%
		4	0.154 ±0.004	25.7 ±0.8	30.0 ±0.8	-4.4 ±1.2	-28. ± 27%	-29. ± 27%
		5	0.154 ±0.004	27.5 ±0.9	33.2 ±0.9	-5.7 ±1.2	-37. ± 22%	-37. ± 22%
		6	0.154 ±0.004	29.6 ±0.9	34.9 ±0.9	-5.3 ±1.3	-34. ± 24%	-34. ± 24%
Benzene (Low NOx)								
39	7.39	1	0.147 ±0.012	10.7 ±0.8	12.4 ±0.8	-1.7 ±1.2	-0.24 ± 67%	-12. ± 67%
		2	0.213 ±0.012	15.5 ±0.8	18.7 ±0.8	-3.1 ±1.2	-0.42 ± 37%	-15. ± 38%
		3	0.250 ±0.012	18.3 ±0.8	25.5 ±0.8	-7.3 ±1.2	-0.98 ± 16%	-29. ± 17%
		4	0.261 ±0.013	19.1 ±0.8	29.5 ±0.8	-10.4 ±1.2	-1.41 ± 12%	-40. ± 13%
		5	0.280 ±0.013	20.5 ±0.9	31.8 ±0.9	-11.3 ±1.2	-1.52 ± 11%	-40. ± 12%
		6	0.296 ±0.014	21.8 ±0.9	34.8 ±0.9	-13.0 ±1.3	-1.76 ± 10%	-44. ± 11%
Toluene (High NOx)								
23	0.573	1	0.035 ±0.016	7.1 ±0.8	5.6 ±0.8	1.5 ±1.2	2.6 ± 78%	42. ± 90%
		2	0.077 ±0.015	16.4 ±0.8	11.8 ±0.8	4.6 ±1.2	8.1 ± 25%	60. ± 32%
		3	0.108 ±0.015	23.8 ±0.8	17.1 ±0.8	6.8 ±1.2	11.8 ± 18%	62. ± 22%
		4	0.143 ±0.015	33.0 ±0.8	20.9 ±0.8	12.2 ±1.2	21. ± 10%	85. ± 14%
		5	0.167 ±0.015	39.8 ±0.9	25.9 ±0.9	13.9 ±1.2	24. ± 9%	83. ± 13%
		6	0.181 ±0.015	44.3 ±0.9	30.6 ±0.9	13.6 ±1.3	24. ± 9%	75. ± 12%
Toluene (Low NOx)								
30	1.134	1	0.096 ±0.031	10.7 ±0.8	11.6 ±0.8	-0.9 ±1.2	(-0.8 ± 1.0)	(-9. ± 12.)
		2	0.145 ±0.031	16.4 ±0.8	18.3 ±0.8	-2.0 ±1.2	-1.73 ± 60%	-14. ± 63%
		3	0.159 ±0.031	18.5 ±0.8	24.9 ±0.8	-6.4 ±1.2	-5.7 ± 19%	-40. ± 27%
		4	0.176 ±0.031	20.5 ±0.8	29.8 ±0.8	-9.3 ±1.2	-8.2 ± 13%	-53. ± 22%
		5	0.186 ±0.031	21.7 ±0.9	32.4 ±0.9	-10.7 ±1.2	-9.4 ± 12%	-57. ± 20%
		6	0.201 ±0.032	23.3 ±0.9	35.1 ±0.9	-11.8 ±1.3	-10.4 ± 11%	-59. ± 19%
m-Xylene (High NOx)								
25	0.085	1	0.018 ±0.002	6.8 ±0.8	5.1 ±0.8	1.7 ±1.2	20. ± 67%	97. ± 68%
		2	0.034 ±0.002	15.0 ±0.8	11.4 ±0.8	3.6 ±1.2	42. ± 33%	105. ± 33%
		3	0.045 ±0.002	21.9 ±0.8	16.5 ±0.8	5.5 ±1.2	64. ± 22%	122. ± 22%
		4	0.054 ±0.002	29.8 ±0.8	21.2 ±0.8	8.6 ±1.2	102. ± 15%	158. ± 14%
		5	0.060 ±0.002	36.4 ±0.9	25.5 ±0.9	10.9 ±1.2	129. ± 12%	180. ± 12%
		6	0.066 ±0.002	44.4 ±0.9	31.1 ±0.9	13.2 ±1.3	156. ± 10%	200. ± 10%
68	0.064	1	0.014 ±0.002	7.2 ±0.8	6.4 ±0.8	0.8 ±1.2	(12. ± 18.)	(55. ± 82.)
		2	0.026 ±0.002	15.1 ±0.8	11.7 ±0.8	3.4 ±1.2	52. ± 35%	128. ± 35%
		3	0.032 ±0.001	20.3 ±0.8	16.0 ±0.8	4.3 ±1.2	67. ± 28%	134. ± 28%
		4	0.038 ±0.001	26.1 ±0.8	19.8 ±0.8	6.4 ±1.2	99. ± 20%	166. ± 19%
		5	0.043 ±0.001	32.6 ±0.9	24.4 ±0.9	8.2 ±1.2	128. ± 16%	190. ± 15%
		6	0.047 ±0.001	38.9 ±0.9	-75.9 ±0.9	114.8 ±1.3	0.0 ± 0%	0. ± 0%

Table 13 (continued)

ETC Run No	Added (ppm)	Time (hr)	Reacted (ppm)	IntOH (ppt-min) Test Run	Base Run	Change	Reactivity (ppt-min/ppm) Incremental	Mechanistic
m-Xylene (Low NOx)								
35	0.106	1	0.038 ±0.003	12.9 ±0.8	9.7 ±0.8	3.2 ±1.2	30. ± 37%	84. ± 37%
		2	0.052 ±0.002	19.6 ±0.8	18.7 ±0.8	0.9 ±1.2	(9. ± 11.)	(18. ± 22.)
		3	0.059 ±0.002	23.5 ±0.8	25.2 ±0.8	-1.7 ±1.2	-16.2 ± 69%	-29. ± 69%
		4	0.064 ±0.002	27.2 ±0.8	29.5 ±0.8	-2.3 ±1.2	-22. ± 53%	-35. ± 53%
		5	0.068 ±0.002	29.6 ±0.9	31.9 ±0.9	-2.3 ±1.2	-21. ± 54%	-34. ± 54%
		6	0.069 ±0.002	30.9 ±0.9	33.6 ±0.9	-2.7 ±1.3	-25. ± 47%	-39. ± 47%
67	0.173	1	0.068 ±0.004	14.4 ±0.9	12.9 ±0.9	1.5 ±1.2	8.7 ± 81%	22. ± 81%
		2	0.088 ±0.005	20.5 ±1.0	21.9 ±1.0	-1.5 ±1.4	-8.5 ± 96%	-17. ± 96%
		3	0.094 ±0.005	22.7 ±1.2	27.5 ±1.2	-4.7 ±1.7	-27. ± 36%	-50. ± 36%
		4	0.099 ±0.006	24.6 ±1.4	30.9 ±1.4	-6.3 ±2.0	-36. ± 33%	-63. ± 33%
		5	0.105 ±0.006	27.4 ±1.7	34.1 ±1.7	-6.7 ±2.4	-39. ± 36%	-64. ± 36%
		6	0.107 ±0.007	28.2 ±1.9	36.9 ±1.9	-8.7 ±2.8	-50. ± 32%	-81. ± 32%
Formaldehyde (High NOx)								
22	0.408	1	[b]	9.5 ±0.8	5.1 ±0.8	4.4 ±1.2	10.8 ± 26%	
		2	[b]	18.6 ±0.8	10.8 ±0.8	7.8 ±1.2	19.1 ± 15%	
		3	[b]	24.4 ±0.8	16.1 ±0.8	8.3 ±1.2	20. ± 14%	
		4	[b]	30.9 ±0.8	19.9 ±0.8	11.0 ±1.2	27. ± 11%	
		5	[b]	36.7 ±0.9	25.0 ±0.9	11.7 ±1.2	29. ± 11%	
		6	[b]	43.7 ±0.9	29.5 ±0.9	14.3 ±1.3	35. ± 9%	
Formaldehyde (Low NOx)								
36	0.247	1	[b]	13.6 ±0.8	11.6 ±0.8	2.1 ±1.2	8.4 ± 56%	
		2	[b]	22.0 ±0.8	19.3 ±0.8	2.6 ±1.2	10.7 ± 44%	
		3	[b]	26.3 ±0.8	23.7 ±0.8	2.6 ±1.2	10.7 ± 45%	
		4	[b]	28.6 ±0.8	26.6 ±0.8	1.9 ±1.2	7.9 ± 62%	
		5	[b]	32.0 ±0.9	30.2 ±0.9	1.8 ±1.2	7.4 ± 67%	
		6	[b]	33.5 ±0.9	32.0 ±0.9	1.6 ±1.3	6.3 ± 81%	
Acetaldehyde (High NOx)								
65	1.53	1	[b]	3.5 ±0.9	6.3 ±0.8	-2.8 ±1.2	-1.81 ± 43%	
		2	0.108 ±0.052	6.3 ±1.0	12.6 ±0.8	-6.2 ±1.3	-4.1 ± 21%	-58. ± 53%
		3	0.205 ±0.060	7.8 ±1.2	17.6 ±0.8	-9.8 ±1.5	-6.4 ± 15%	-48. ± 33%
		4	0.242 ±0.070	10.0 ±1.4	21.9 ±0.8	-11.9 ±1.7	-7.8 ± 14%	-49. ± 32%
		5	0.292 ±0.081	11.5 ±1.7	26.6 ±0.9	-15.1 ±1.9	-9.8 ± 13%	-52. ± 30%
		6	0.377 ±0.091	14.6 ±1.9	31.2 ±0.9	-16.6 ±2.1	-10.8 ± 13%	-44. ± 27%
Acetaldehyde (Low NOx)								
66	1.62	1	[b]	2.6 ±0.9	12.4 ±0.9	-9.8 ±1.2	-6.1 ± 13%	
		2	0.092 ±0.055	3.9 ±1.0	21.2 ±1.0	-17.3 ±1.4	-10.7 ± 8%	-188. ± 60%
		3	0.131 ±0.065	5.3 ±1.2	26.7 ±1.2	-21.4 ±1.7	-13.2 ± 8%	-164. ± 50%
		4	0.168 ±0.076	6.0 ±1.4	30.5 ±1.4	-24.5 ±2.0	-15.1 ± 9%	-146. ± 46%
		5	0.206 ±0.088	6.7 ±1.7	33.3 ±1.7	-26.6 ±2.4	-16.4 ± 9%	-129. ± 43%
		6	0.247 ±0.100	7.8 ±1.9	36.3 ±1.9	-28.5 ±2.8	-17.6 ± 10%	-115. ± 42%

[a] Amount reacted could not be determined for this VOC, or amount reacted could not be determined for this time with sufficient precision to be useful.

3. Low NO_x Reactivity Results

Low NO_x lumped surrogate reactivity experiments were carried out for each of the 8 surrogate components plus carbon monoxide, benzene, and acetaldehyde. Two reactivity experiments were carried out for n-octane and m-xylene, and one experiment was carried out for the other VOCs. The detailed results and reactivity analysis of the low NO_x surrogate experiments are given with the other DTC surrogate reactivity experiments in Tables 12-14, and plots of selected reactivity results for the low NO_x runs are shown on Figures 39-49. Model calculations, discussed later, are also shown.

Table 14. Derivation of the hourly direct reactivities from the results of the lumped molecule surrogate reactivity experiments. [a]

ETC Run No.	Added (ppm)	Time (hr)	Reacted (ppm)	IntOH (ppt-min)	d(O3-NO)/ IntOH (base) (10^3 min-1)	d(O3-NO) (ppm) Total	d(O3-NO) (ppm) From Base ROG	Direct d(O3-NO) Reactivity (mol d(O3-NO)/mol VOC) Incremental	Mechanistic
Carbon Monoxide (High NOx)									
14	155.	1	0.363+12%	6.7+0.8	36.3+ 5.3	0.548	0.242+0.046	0.0020 + 15%	0.8 +19%
		2	0.635+ 7%	11.8+0.8	33.8+ 2.3	0.907	0.398+0.039	0.0033 + 8%	0.8 +10%
		3	0.870+ 5%	16.2+0.9	32.2+ 1.6	1.135	0.521+0.038	0.0040 + 6%	0.7 + 8%
		4	0.978+ 5%	18.3+0.9	30.3+ 1.2	1.301	0.553+0.035	0.0048 + 5%	0.8 + 7%
		5	1.107+ 5%	20.8+0.9	27.8+ 0.9	1.405	0.579+0.032	0.0053 + 4%	0.7 + 6%
		6	1.209+ 5%	22.8+1.0	26.5+ 0.8	1.463	0.605+0.031	0.0055 + 4%	0.7 + 6%
15	161.	1	0.396+12%	7.0+0.8	37.2+ 5.3	0.637	0.262+0.048	0.0023 + 13%	0.9 +17%
		2	0.649+ 7%	11.6+0.8	37.0+ 2.6	1.023	0.431+0.043	0.0037 + 7%	0.9 +10%
		3	0.857+ 6%	15.5+0.8	34.2+ 1.8	1.266	0.529+0.040	0.0046 + 5%	0.9 + 8%
		4	1.100+ 4%	20.0+0.9	30.6+ 1.2	1.417	0.613+0.036	0.0050 + 4%	0.7 + 6%
		5	1.244+ 4%	22.8+0.9	28.7+ 1.0	1.501	0.655+0.034	0.0052 + 4%	0.7 + 6%
16	74.2	1	0.155+14%	6.0+0.8	37.8+ 6.0	0.354	0.226+0.047	0.0017 + 37%	0.8 +39%
		2	0.297+ 7%	11.5+0.8	34.5+ 2.4	0.654	0.397+0.040	0.0035 + 16%	0.9 +17%
		3	0.400+ 5%	15.6+0.8	32.0+ 1.6	0.835	0.498+0.037	0.0045 + 11%	0.8 +12%
		4	0.496+ 5%	19.4+0.9	30.3+ 1.3	0.992	0.589+0.036	0.0054 + 9%	0.8 +10%
		5	0.606+ 4%	23.8+0.9	28.6+ 1.0	1.121	0.681+0.035	0.0059 + 8%	0.7 + 9%
		6	0.684+ 4%	27.0+0.9	26.8+ 0.8	1.223	0.723+0.033	0.0067 + 7%	0.7 + 8%
20	103.	1	0.154+19%	4.3+0.8	32.3+ 6.4	0.316	0.137+0.038	0.0017 + 21%	1.2 +29%
		2	0.306+10%	8.5+0.8	35.5+ 3.3	0.656	0.300+0.040	0.0034 + 11%	1.2 +15%
		3	0.455+ 7%	12.6+0.8	30.7+ 1.8	0.837	0.387+0.034	0.0044 + 8%	1.0 +10%
		4	0.622+ 5%	17.3+0.8	29.2+ 1.4	0.999	0.505+0.034	0.0048 + 7%	0.8 + 9%
		5	0.738+ 4%	20.5+0.9	26.4+ 1.0	1.140	0.543+0.031	0.0058 + 5%	0.8 + 7%
		6	0.869+ 4%	24.3+0.9	26.3+ 0.9	1.251	0.640+0.032	0.0059 + 5%	0.7 + 7%
Carbon Monoxide (Low NOx)									
29	85.8	1	0.282+ 9%	9.4+0.8	29.4+ 1.9	0.557	0.275+0.030	0.0033 + 11%	1.0 +14%
		2	0.437+ 6%	14.5+0.8	27.0+ 1.1	0.735	0.392+0.028	0.0040 + 8%	0.8 +10%
n-Butane (High NOx)									
19	6.48	1	0.098+20%	4.0+0.8	34.7+ 5.2	0.372	0.140+0.035	0.036 + 15%	2.4 +25%
		2	0.203+10%	8.5+0.8	35.0+ 2.6	0.716	0.296+0.036	0.065 + 9%	2.1 +13%
		3	0.273+ 7%	11.4+0.8	31.3+ 1.6	0.907	0.358+0.032	0.085 + 6%	2.0 + 9%
		4	0.333+ 6%	14.0+0.8	28.6+ 1.2	1.073	0.402+0.029	0.104 + 5%	2.0 + 8%
		5	0.395+ 6%	16.8+0.9	27.2+ 0.9	1.207	0.456+0.028	0.116 + 4%	1.9 + 7%
		6	0.441+ 5%	18.8+0.9	25.1+ 0.7	1.295	0.472+0.026	0.127 + 4%	1.9 + 6%
n-Butane (Low NOx)									
31	5.48	1	0.119+14%	5.8+0.8	39.7+ 3.7	0.523	0.232+0.039	0.053 + 14%	2.5 +19%
		2	0.185+ 9%	9.2+0.8	27.4+ 1.2	0.701	0.251+0.025	0.082 + 6%	2.4 +11%
n-Octane (High NOx)									
24	1.102	1	[c]	2.1+0.8	43.1+ 7.4	0.176	0.091+0.039	0.077 + 46%	
		2	0.073+42%	4.9+0.8	38.1+ 3.0	0.409	0.186+0.035	0.20 + 16%	3.1 +45%
		3	0.117+26%	7.9+0.8	34.4+ 1.9	0.586	0.271+0.032	0.29 + 10%	2.7 +28%
		4	0.154+20%	10.7+0.8	31.0+ 1.3	0.720	0.331+0.030	0.35 + 8%	2.5 +21%
		5	0.179+17%	13.1+0.9	29.3+ 1.0	0.857	0.384+0.029	0.43 + 6%	2.6 +18%
		6	0.216+14%	16.1+0.9	27.9+ 0.8	0.995	0.450+0.028	0.49 + 6%	2.5 +15%
70	0.746	1	0.039+54%	4.2+0.8	26.7+ 3.3	0.160	0.111+0.026	0.066 + 53%	1.3 +75%
		2	0.080+26%	8.1+0.8	31.3+ 2.2	0.382	0.253+0.031	0.173 + 24%	1.6 +35%
		3	0.110+18%	11.5+0.8	29.6+ 1.5	0.543	0.340+0.030	0.27 + 15%	1.8 +24%
		4	0.132+15%	14.0+0.8	28.0+ 1.2	0.658	0.391+0.029	0.36 + 11%	2.0 +19%
		5	0.157+13%	17.3+0.9	26.3+ 0.9	0.765	0.454+0.028	0.42 + 9%	2.0 +16%
		6	0.176+12%	19.7+0.9	24.8+ 0.7	0.870	0.488+0.026	0.51 + 7%	2.2 +13%
n-Octane (Low NOx)									
37	1.126	1	0.065+48%	4.8+0.8	24.8+ 1.6	0.326	0.119+0.022	0.183 + 11%	3.2 +49%
		2	0.128+24%	9.5+0.8	25.2+ 1.2	0.543	0.239+0.024	0.27 + 8%	2.4 +25%
71	0.647	1	0.057+12%	7.1+0.9	25.2+ 1.7	0.299	0.180+0.025	0.184 + 21%	2.1 +24%
		2	0.100+ 8%	13.0+1.0	23.4+ 1.1	0.520	0.304+0.028	0.33 + 13%	2.2 +15%
Ethene (High NOx)									
17	0.608	1	0.042+40%	5.7+0.8	32.5+ 4.4	0.285	0.184+0.037	0.167 + 36%	2.4 +54%
		2	0.095+17%	12.0+0.8	33.5+ 2.3	0.563	0.401+0.039	0.27 + 24%	1.7 +30%
		3	0.155+10%	19.4+0.8	29.0+ 1.4	0.755	0.564+0.036	0.31 + 19%	1.2 +21%
		4	0.215+ 7%	26.8+0.9	28.5+ 1.1	0.938	0.763+0.039	0.29 + 22%	0.8 +23%
		5	0.279+ 5%	34.0+0.9	27.9+ 1.0	1.093	0.948+0.041	0.24 + 29%	0.5 +29%
		6	0.340+ 4%	41.5+0.9	26.1+ 0.8	1.188	1.084+0.040	0.171 + 39%	0.3 +39%

Table 14 (continued)

ETC Run No.	Added (ppm)	Time (hr)	Reacted (ppm)	IntOH (ppt-min)	d(O3-NO)/ IntOH (base) (10^3 min-1)	d(O3-NO) (ppm) Total	d(O3-NO) (ppm) From Base ROG	Direct d(O3-NO) Reactivity (mol d(O3-NO)/mol VOC) Incremental	Mechanistic
Ethene (Low NOx)									
38	0.659	1	0.103+18%	12.6+0.9	27.4+ 1.9	0.464	0.345+0.034	0.181 + 29%	1.2 +34%
Propene (High NOx)									
18	0.350	1	0.096+ 9%	6.6+0.8	41.5+ 6.1	0.402	0.272+0.053	0.37 + 41%	1.4 +42%
		2	0.211+ 4%	15.6+0.8	37.5+ 2.7	0.728	0.584+0.052	0.41 + 36%	0.7 +36%
		3	0.291+ 3%	23.6+0.8	34.2+ 1.8	0.960	0.807+0.051	0.44 + 33%	0.5 +33%
		4	0.328+ 2%	31.4+0.9	30.5+ 1.2	1.093	0.956+0.046	0.39 + 34%	0.4 +34%
		5	0.347+ 2%	36.6+0.9	28.7+ 1.0	1.157	1.050+0.043	0.31 + 40%	0.3 +40%
		6	0.348+ 2%	41.0+0.9	26.9+ 0.8	1.169	1.103+0.040	0.190 + 60%	0.2 +60%
Propene (Low NOx)									
32	0.305	1	0.099+ 8%	10.5+0.8	26.6+ 1.7	0.510	0.279+0.028	0.76 + 12%	2.3 +14%
trans-2-Butene (High NOx)									
21	0.324	1	[c]	14.0+0.8	40.4+ 6.7	0.773	0.566+0.099	0.64 + 48%	
	+0.007	2	0.320+ 2%	19.9+0.8	36.2+ 2.7	0.901	0.718+0.061	0.56 + 33%	0.6 +33%
		3	0.320+ 2%	23.6+0.8	32.3+ 1.7	0.998	0.763+0.048	0.72 + 20%	0.7 +20%
		4	0.320+ 2%	27.7+0.8	29.0+ 1.2	1.070	0.802+0.041	0.83 + 15%	0.8 +15%
		5	0.320+ 2%	31.6+0.9	27.4+ 0.9	1.110	0.867+0.038	0.75 + 16%	0.8 +16%
		6	0.320+ 2%	35.1+0.9	25.6+ 0.8	1.118	0.900+0.035	0.67 + 16%	0.7 +16%
69	0.190	1	0.157+ 2%	11.7+0.8	27.5+ 3.6	0.503	0.322+0.047	0.95 + 26%	1.1 +26%
		2	0.190+ 2%	19.6+0.8	29.2+ 1.9	0.694	0.573+0.045	0.64 + 37%	0.6 +37%
		3	0.190+ 2%	24.0+0.8	27.3+ 1.3	0.793	0.655+0.039	0.73 + 28%	0.7 +28%
		4	0.190+ 2%	29.3+0.9	26.7+ 1.1	0.894	0.781+0.039	0.59 + 35%	0.6 +35%
		5	0.190+ 2%	32.7+0.9	26.4+ 1.0	0.984	0.863+0.039	0.64 + 32%	0.6 +32%
trans-2-Butene (Low NOx)									
33	0.156	1	[c]	15.5+0.8	28.4+ 1.9	0.476	0.440+0.038	(0.2 + 0.2)	
Benzene (Low NOx)									
39	7.39	1	0.147+ 8%	10.7+0.8	28.0+ 1.9	0.486	0.299+0.030	0.025 + 16%	1.3 +18%
Toluene (High NOx)									
23	0.573	3	0.108+14%	23.8+0.8	30.0+ 1.5	0.822	0.716+0.043	0.185 + 41%	1.0 +43%
		4	0.143+10%	33.0+0.8	29.4+ 1.2	1.003	0.971+0.047	(0.06 +0.08)	(0.2 +0.3)
		5	0.167+ 9%	39.8+0.9	27.3+ 0.9	1.080	1.087+0.043	(-0.013 +0.08)	(0.0 +0.3)
		6	0.181+ 8%	44.3+0.9	26.1+ 0.8	1.083	1.156+0.041	-0.128 + 55%	-0.4 +56%
Toluene (Low NOx)									
30	1.134	1	0.096+32%	10.7+0.8	28.5+ 2.0	0.471	0.305+0.032	0.147 + 19%	1.7 +38%
Acetaldehyde (High NOx)									
65	1.53	1	[c]	3.5+0.9	26.9+ 3.5	0.353	0.094+0.026	0.169 + 10%	
		2	0.108+48%	6.3+1.0	29.3+ 1.9	0.543	0.185+0.032	0.23 + 9%	3.3 +49%
		3	0.205+29%	7.8+1.2	27.9+ 1.3	0.670	0.218+0.035	0.29 + 8%	2.2 +30%
		4	0.242+29%	10.0+1.4	26.6+ 1.0	0.786	0.265+0.039	0.34 + 8%	2.1 +30%
		5	0.292+28%	11.5+1.7	25.0+ 0.8	0.893	0.289+0.043	0.39 + 7%	2.1 +29%
		6	0.377+24%	14.6+1.9	24.0+ 0.7	0.977	0.351+0.048	0.41 + 8%	1.7 +25%
Acetaldehyde (Low NOx)									
66	1.62	1	[c]	2.6+0.9	25.6+ 1.8	0.297	0.066+0.023	0.143 + 10%	
	+0.03	2	0.092+60%	3.9+1.0	23.1+ 1.1	0.429	0.090+0.024	0.21 + 7%	3.7 +60%

[a] Data are not shown for times in runs where it appears that O_3 formation is becoming NO_x-limited, because the assumptions behind the derivation of direct reactivities are not valid for such conditions. Data are also not shown when the uncertainties of the direct reactivity estimates are too high to provide meaningful data.
[b] Amount reacted could not be determined for this time with sufficient precision to be useful.
[c] This is a DTC run. "Base fit" data is from base case run carried out in the other side of the chamber.

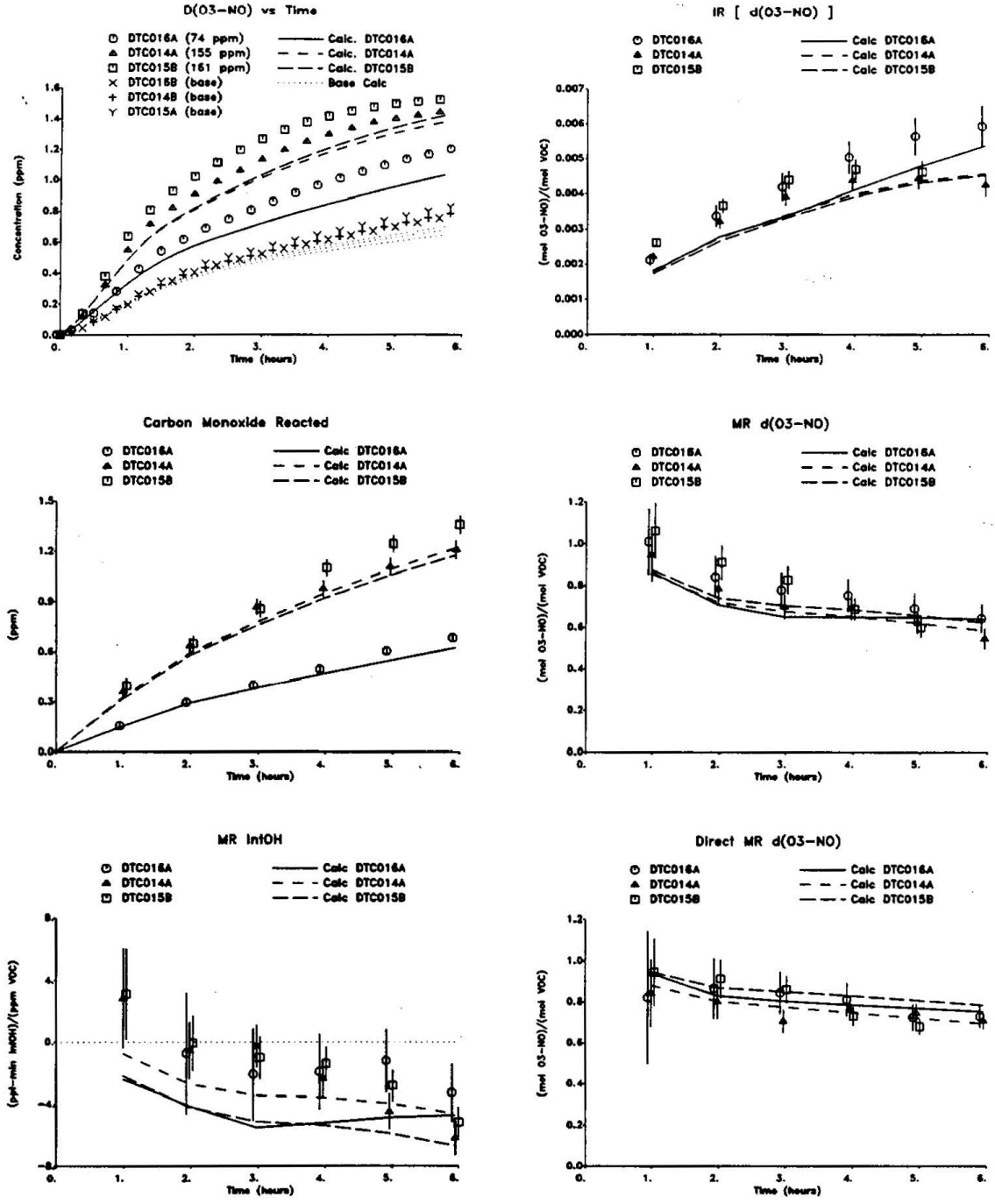

Figure 29. Plots of selected results of the high NO_x lumped molecule surrogate reactivity experiments for **carbon monoxide**

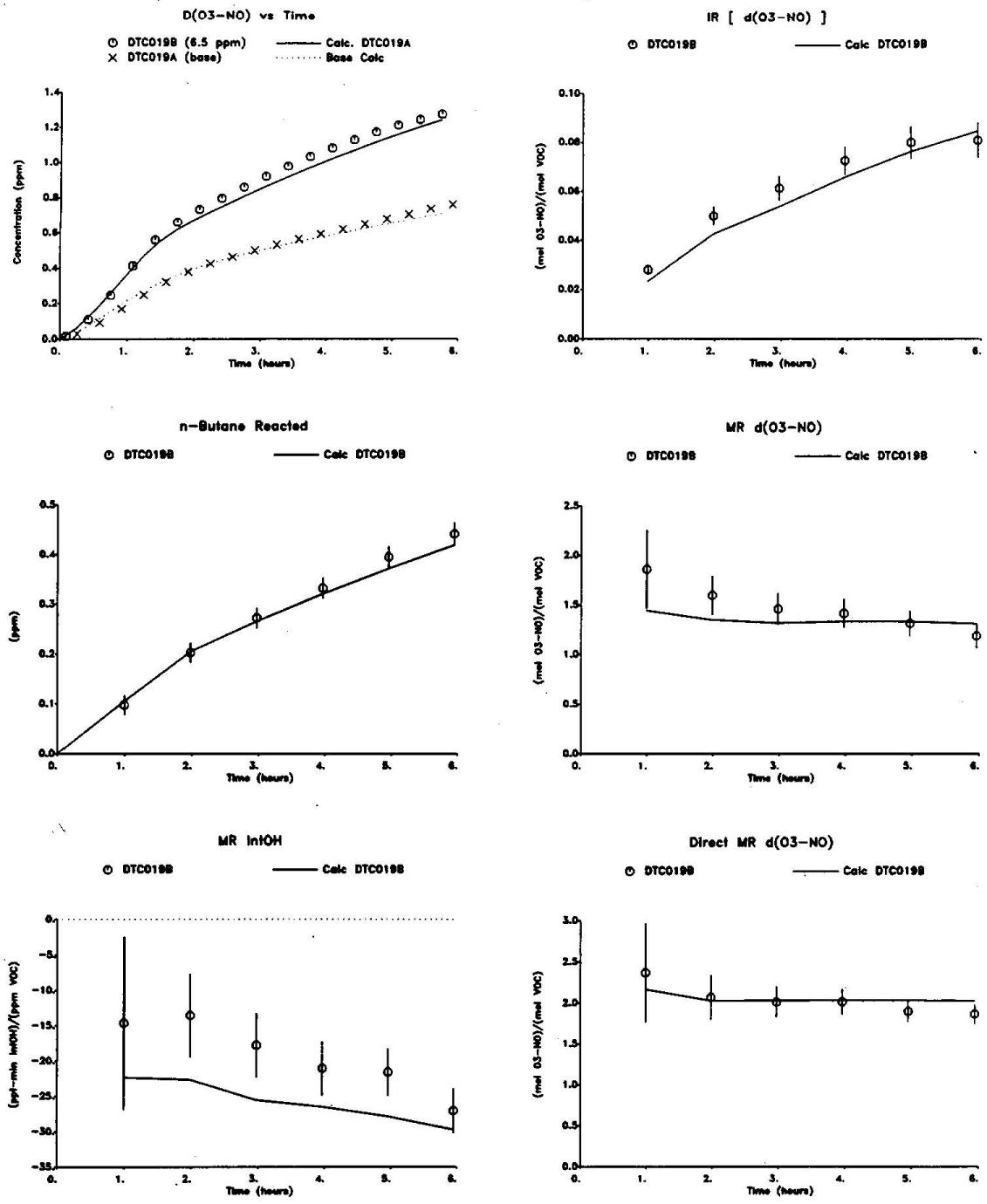

Figure 30. Plots of selected results of the high NO_x lumped molecule surrogate reactivity experiment for **n-butane**

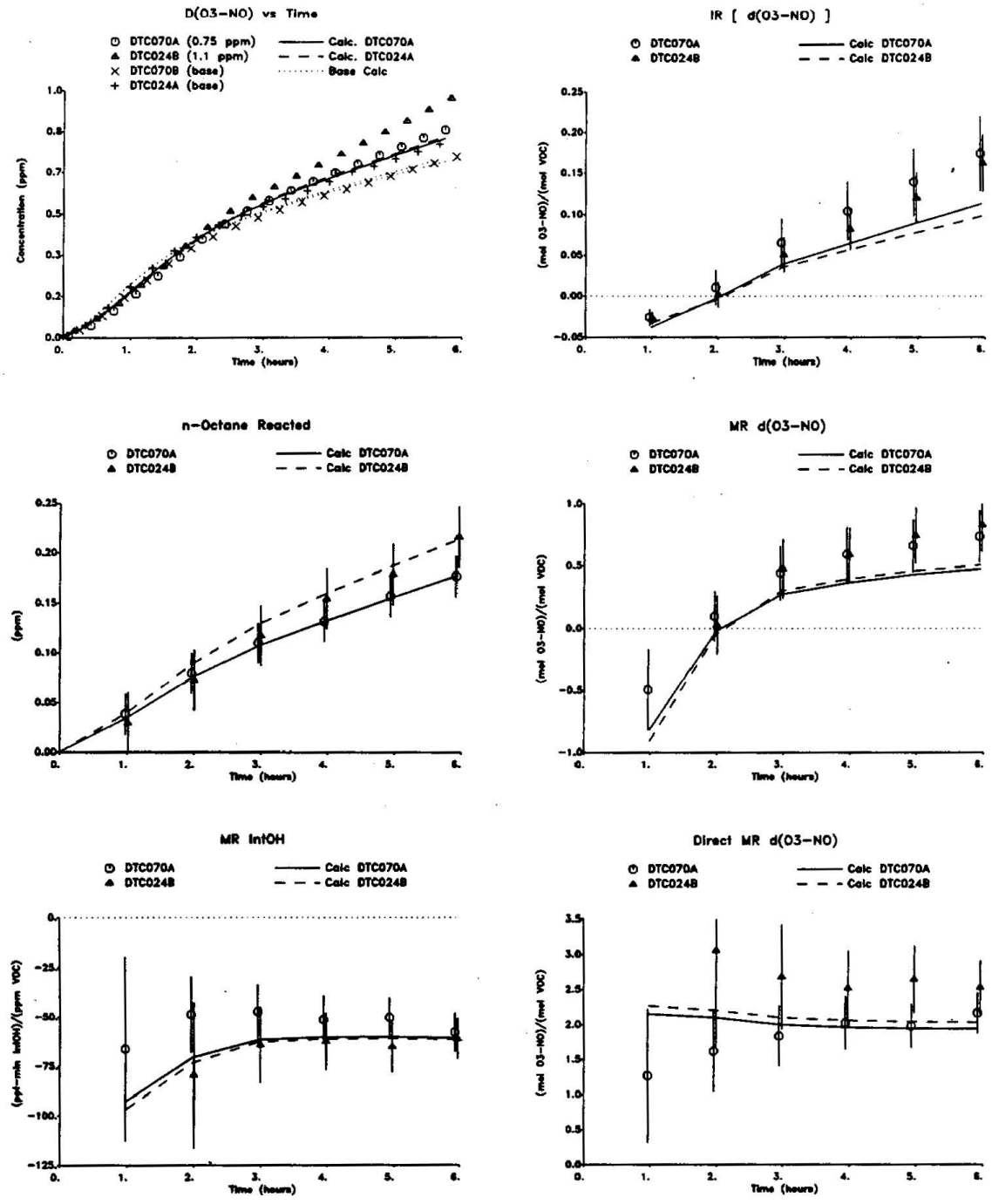

Figure 31. Plots of selected results of the high NO_x lumped molecule surrogate reactivity experiments for **n-octane**

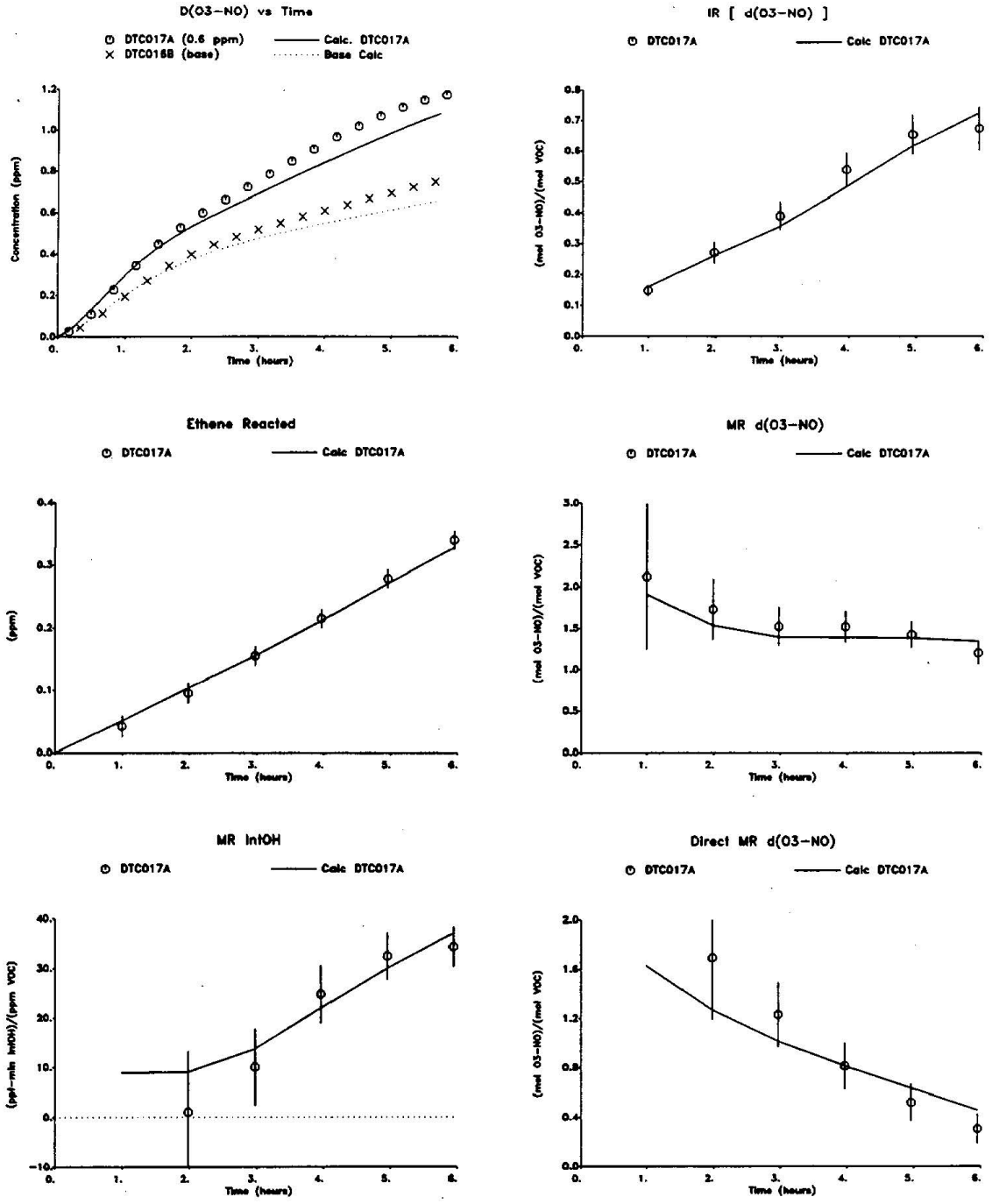

Figure 32. Plots of selected results of the high NO_x lumped molecule surrogate reactivity experiment for **ethene**

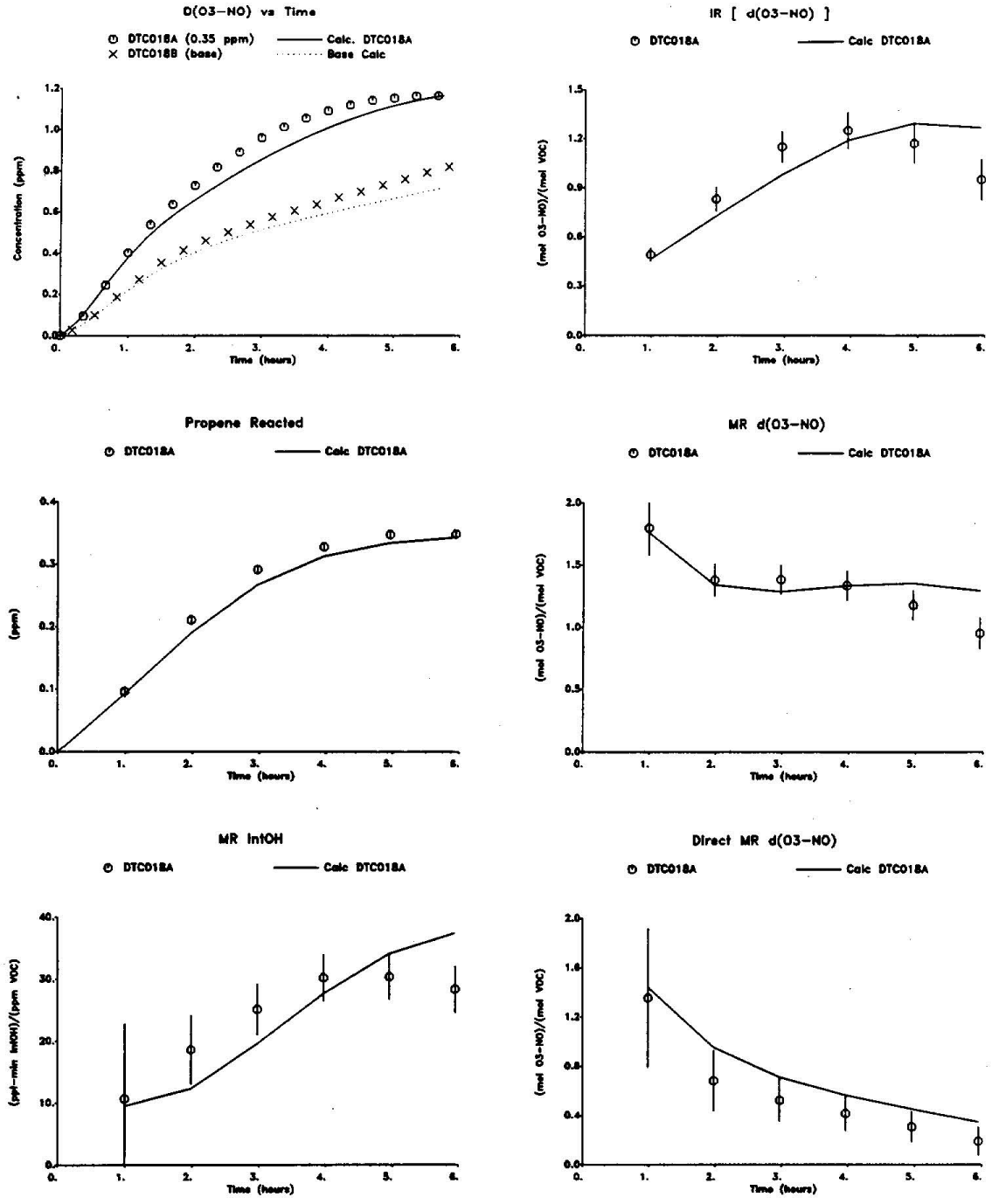

Figure 33. Plots of selected results of the high NO_x lumped molecule surrogate reactivity experiment for **propene**

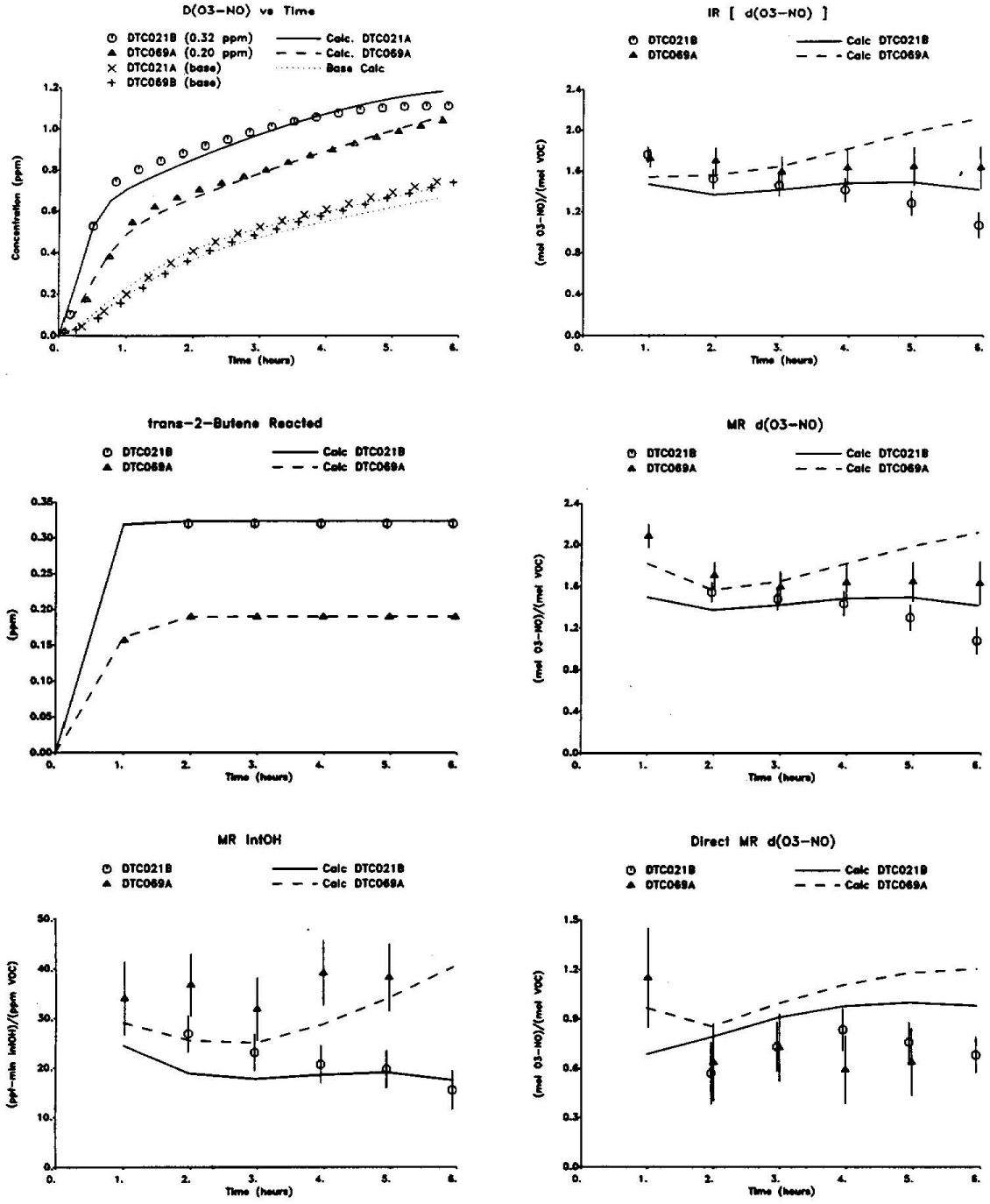

Figure 34. Plots of selected results of the high NO_x lumped molecule surrogate reactivity experiments for **trans-2-Butene**

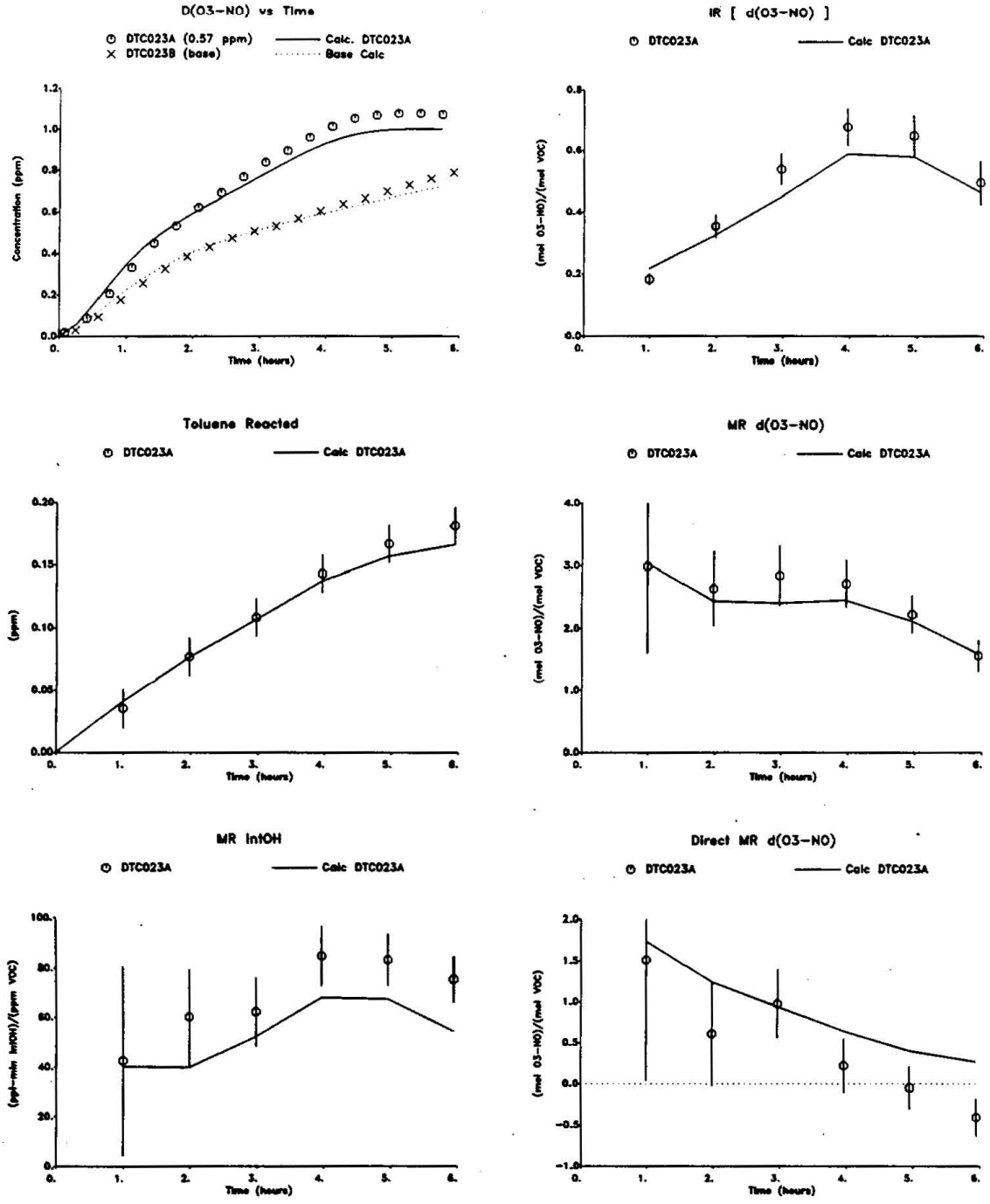

Figure 35. Plots of selected results of the high NO_x lumped molecule surrogate reactivity experiment for **toluene**

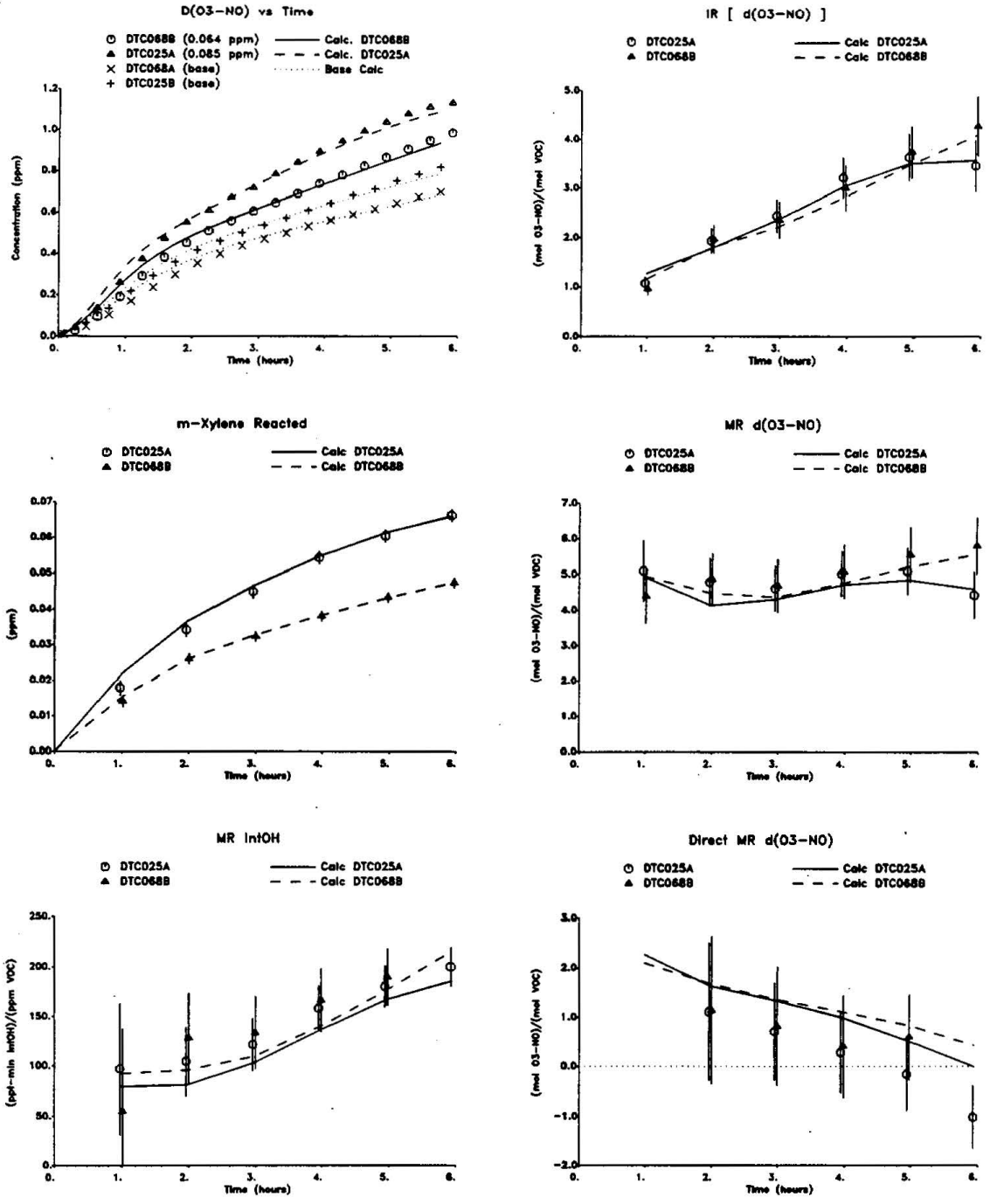

Figure 36. Plots of selected results of the high NO_x lumped molecule surrogate reactivity experiments for **m-xylene**

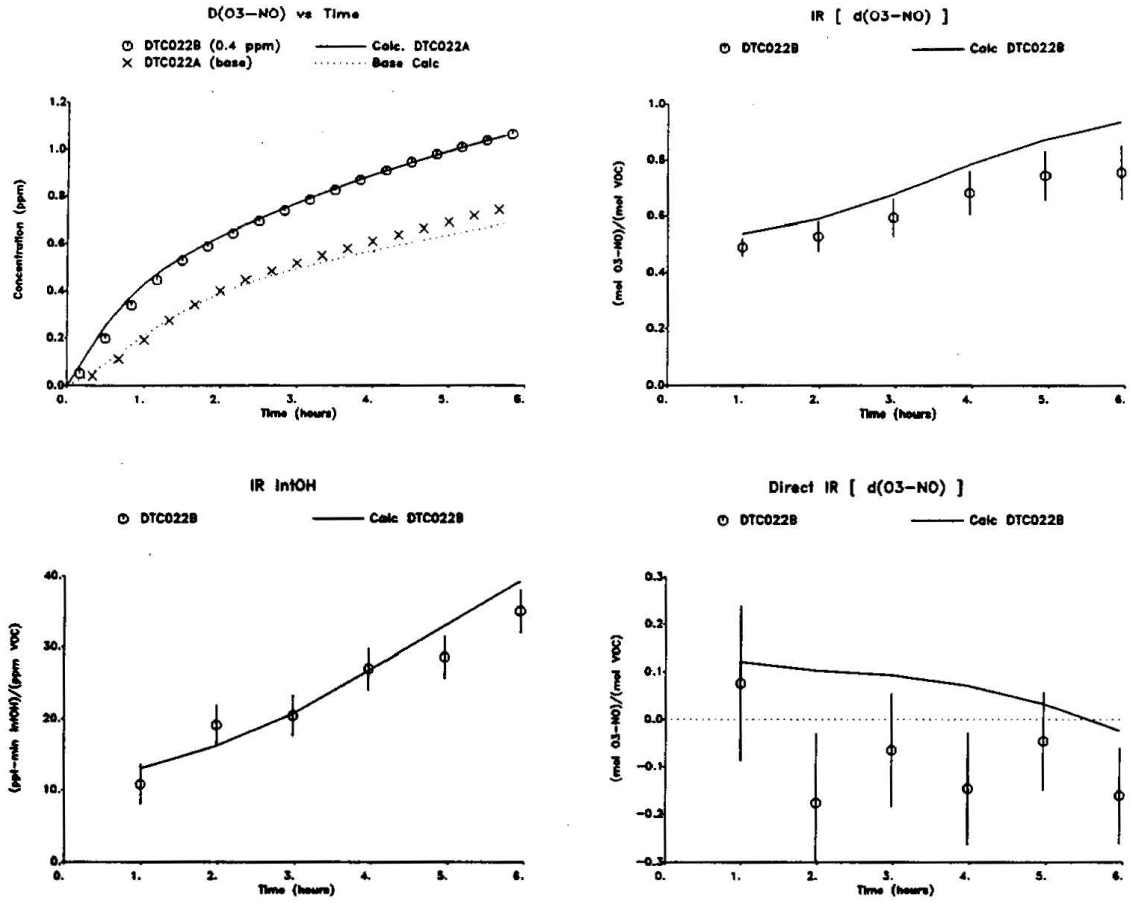

Figure 37. Plots of selected results of the high NO_x lumped molecule surrogate reactivity experiment for **formaldehyde**

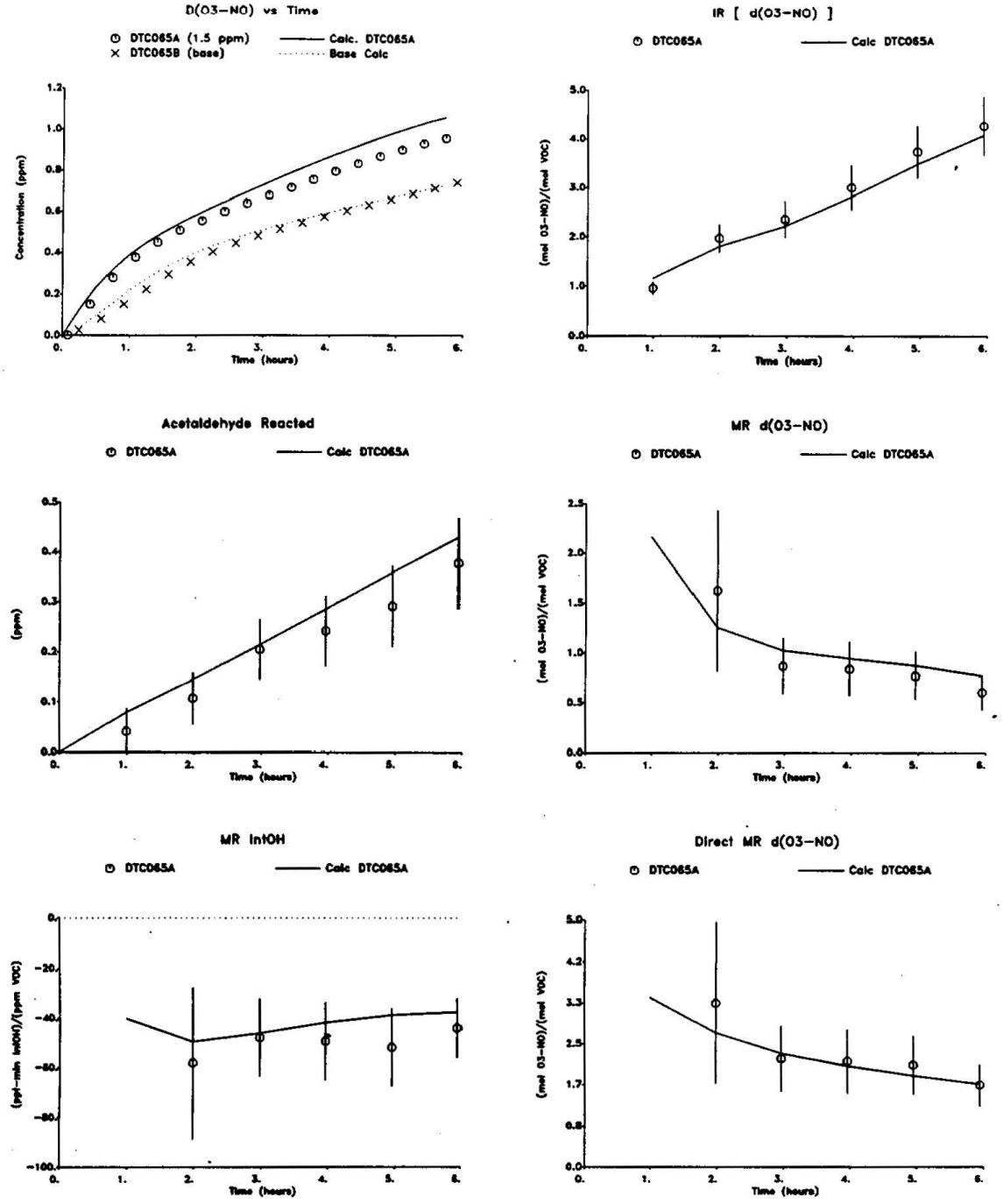

Figure 38. Plots of selected results of the high NO_x lumped molecule surrogate reactivity experiment for **acetaldehyde**

For most VOCs, the reactivities with respect to $d(O_3\text{-NO})$ tended to be more dependent on reaction time in the low NO_x experiments than was the case under thehigher NO_x conditions. This is presumably because the NO_x conditions change significantly with time in the run, with the experiment having sufficient NO_x to promote rapid O_3 formation in the first hour or so, but then becoming NO_x-limited

by the end of the run. Although both carbon monoxide and n-butane had positive incremental $d(O_3\text{-NO})$ reactivities which were essentially constant throughout the experiments their mechanistic reactivities decreased with time. This is because the amounts reacted increased with time. However, their mechanistic reactivities were still significantly positive at the NO_x-limited end of the experiment. Octane was unique in that its incremental and mechanistic $d(O_3\text{-NO})$ reactivities tended to increase with time, being slightly negative initially, and then becoming significantly positive by the end of the run. In the case of acetaldehyde, the $d(O_3\text{-NO})$ reactivities were initially slightly negative, became more negative until around the middle of the run, and then became slightly less negative. For all the other VOCS, the $d(O_3\text{-NO})$ reactivities (both mechanistic and incremental) tended to decrease with time, i.e., as the conditions became more NO_x-limited. In the case of the olefins and formaldehyde, the $d(O_3\text{-NO})$ reactivities were significantly positive at the beginning, but approached zero or (for trans-2-butene) became slightly negative by the end of the run. In the case of the aromatics, the $d(O_3\text{-NO})$ reactivities were significantly positive initially, but became significantly negative as conditions became NO_x-limited. This behavior for the aromatics is expected based on other experimental (e.g., Carter and Atkinson, 1987) and modeling (Carter and Atkinson, 1989) studies of these compounds.

All the VOCs studied were found to have much more negative effects on integrated OH radical levels under NO_x-limited conditions than was observed in the high NO_x experiments. For example, CO, which had almost no effect on IntOH in the high NO_x experiments, had definite negative IntOH reactivities in these low NO_x runs. Even alkenes and aromatics, which significantly positive effects on radicals under high NO_x conditions, tended to significantly inhibit OH radicals by the end of these experiments. However, trans-2-butene and the aromatics, the strongest radical initiators under high NO_x conditions, had significantly positive effects on radicals around the beginning of the experiments, when NO_x was still present. In terms of magnitude of IntOH inhibition on a per molecule reacted basis, the ordering was CO ≈ ethene < propene < trans-2-butene ≈ benzene ≈ toluene ≈ m-xylene < n-butane < acetaldehyde ≈ n-octane. This is quite different than their ordering of IntOH reactivities under high NO_x conditions. (On a per carbon reacted basis, the inhibition by acetaldehyde was much greater than all other VOCs studied.) Although the IntOH reactivity for formaldehyde was found to be always positive in these low NO_x experiments, the magnitude of the IntOH reactivity was far less than observed in the higher NO_x runs.

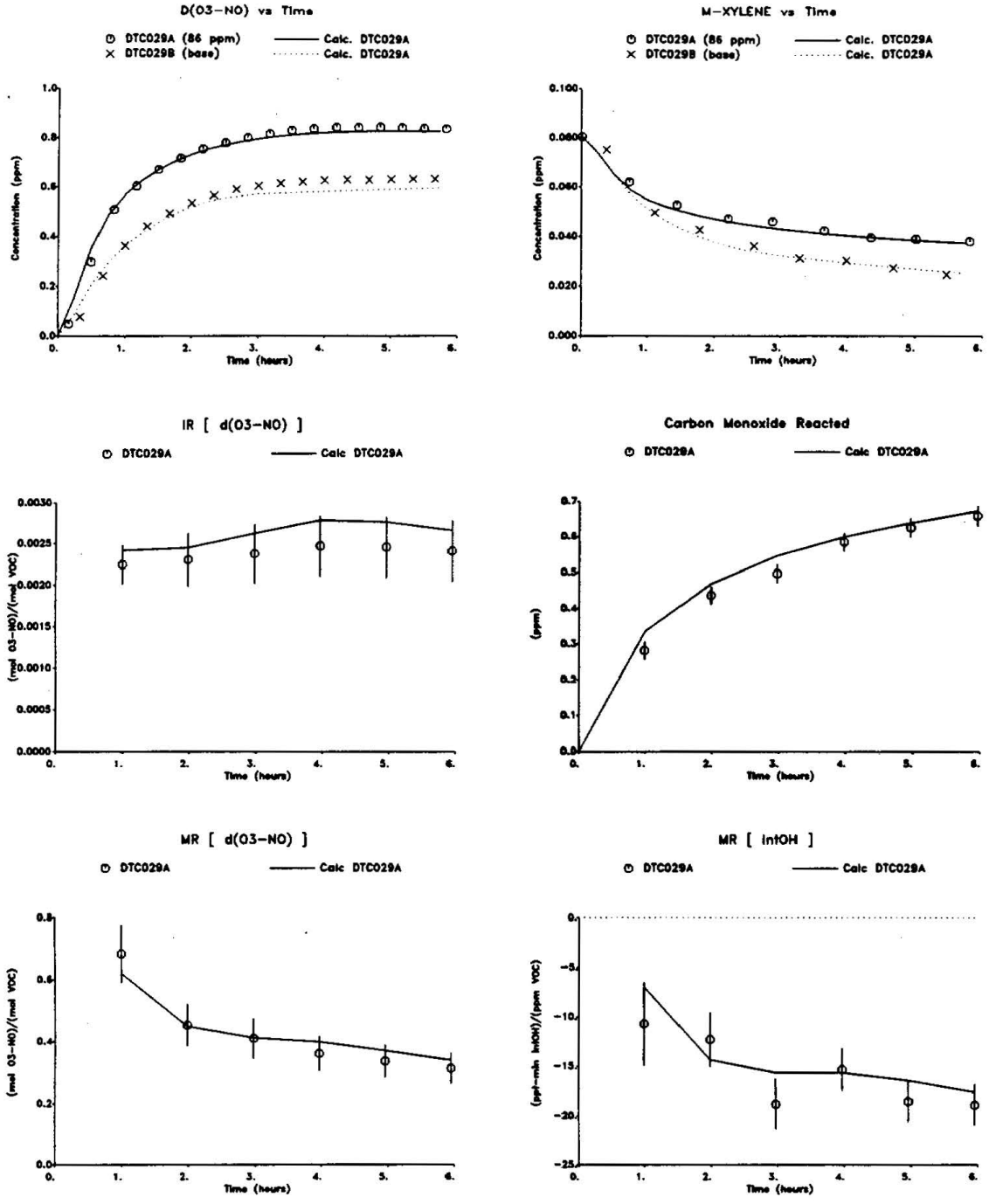

Figure 39. Plots of selected results of the low NO_x lumped molecule surrogate reactivity experiment for **carbon monoxide**

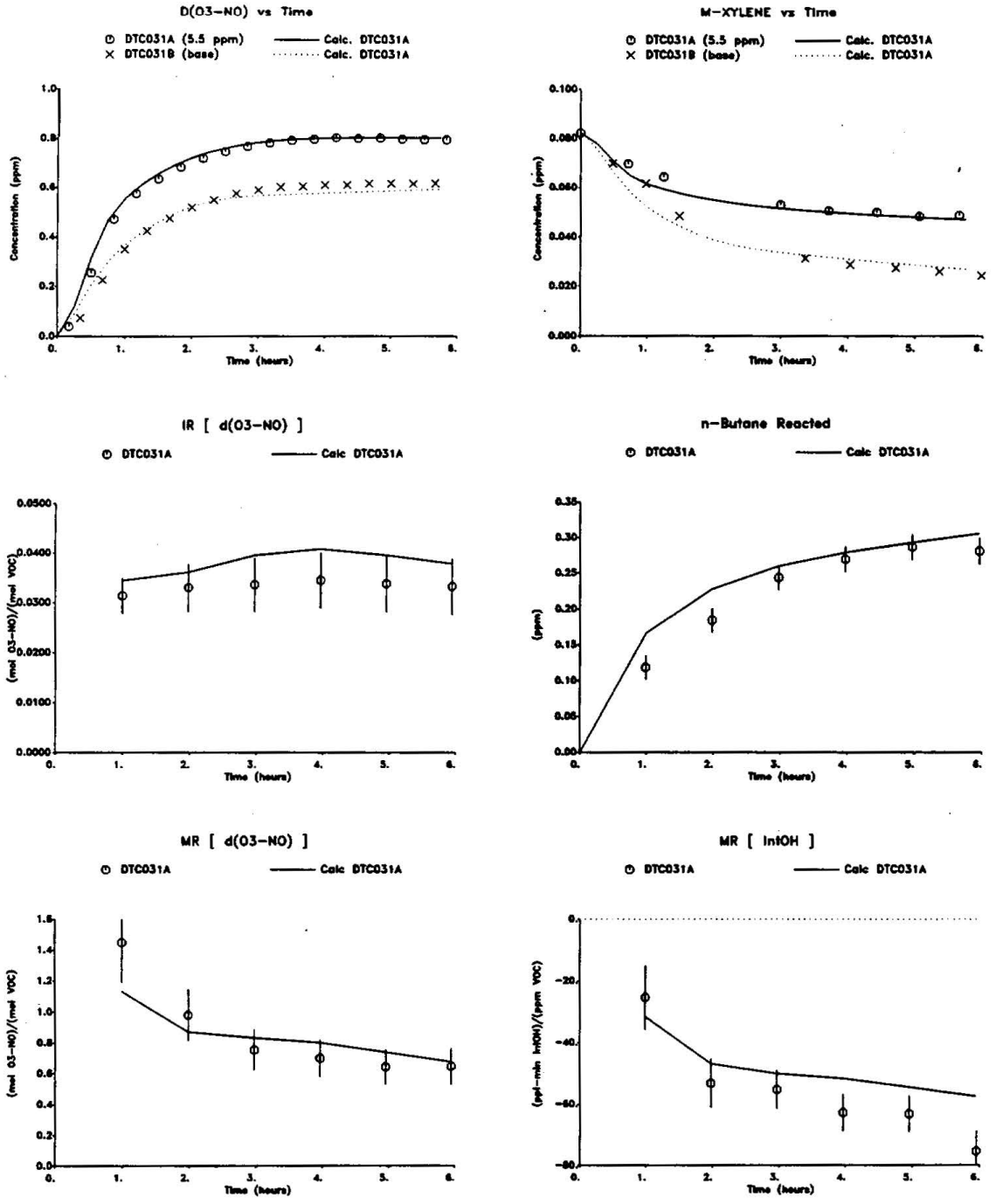

Figure 40. Plots of selected results of the low NO_x lumped molecule surrogate reactivity experiment for **n-butane**

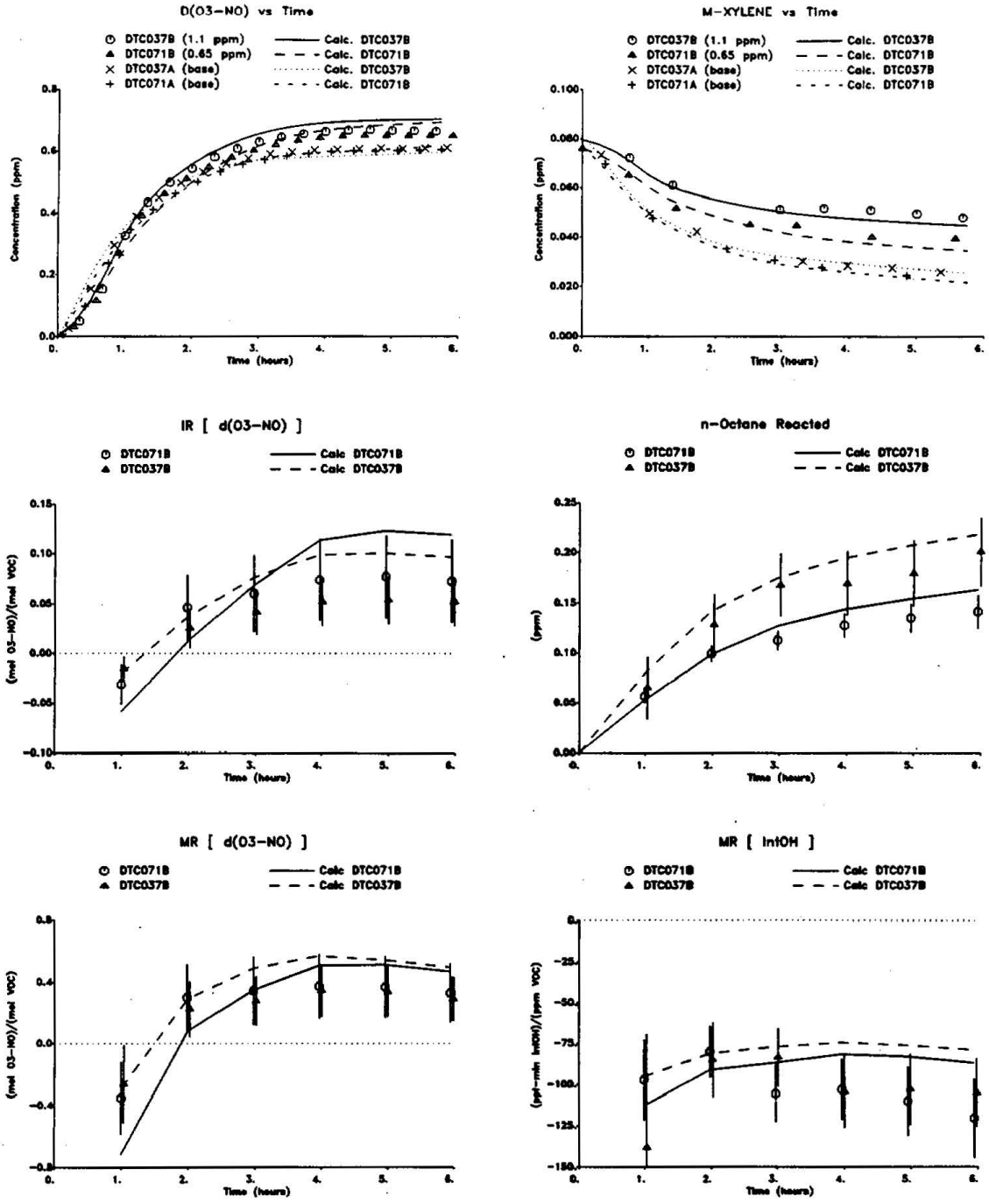

Figure 41. Plots of selected results of the low NO_x lumped molecule surrogate reactivity experiments for **n-octane**

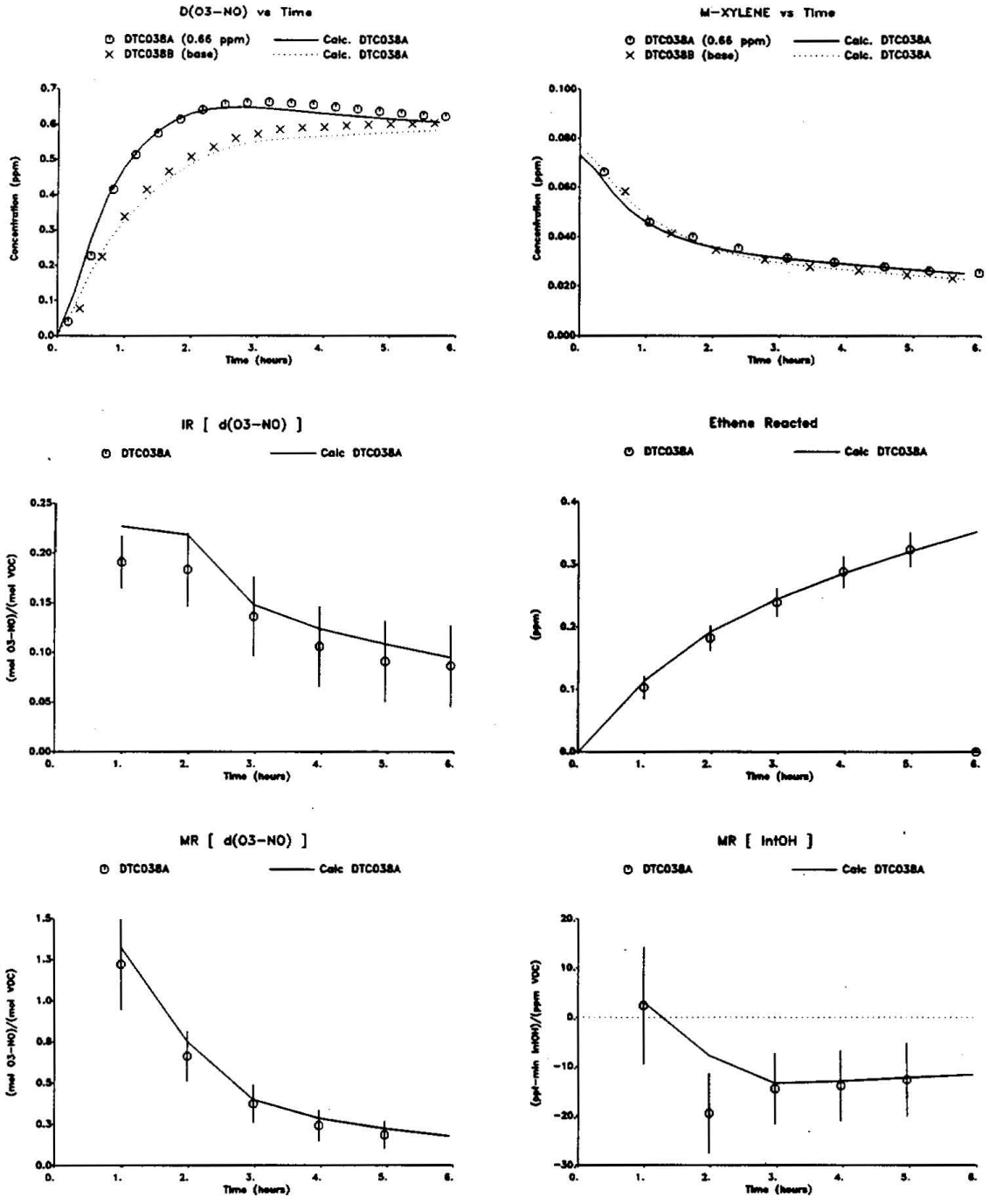

Figure 42. Plots of selected results of the low NO_x lumped molecule surrogate reactivity experiment for **ethene**

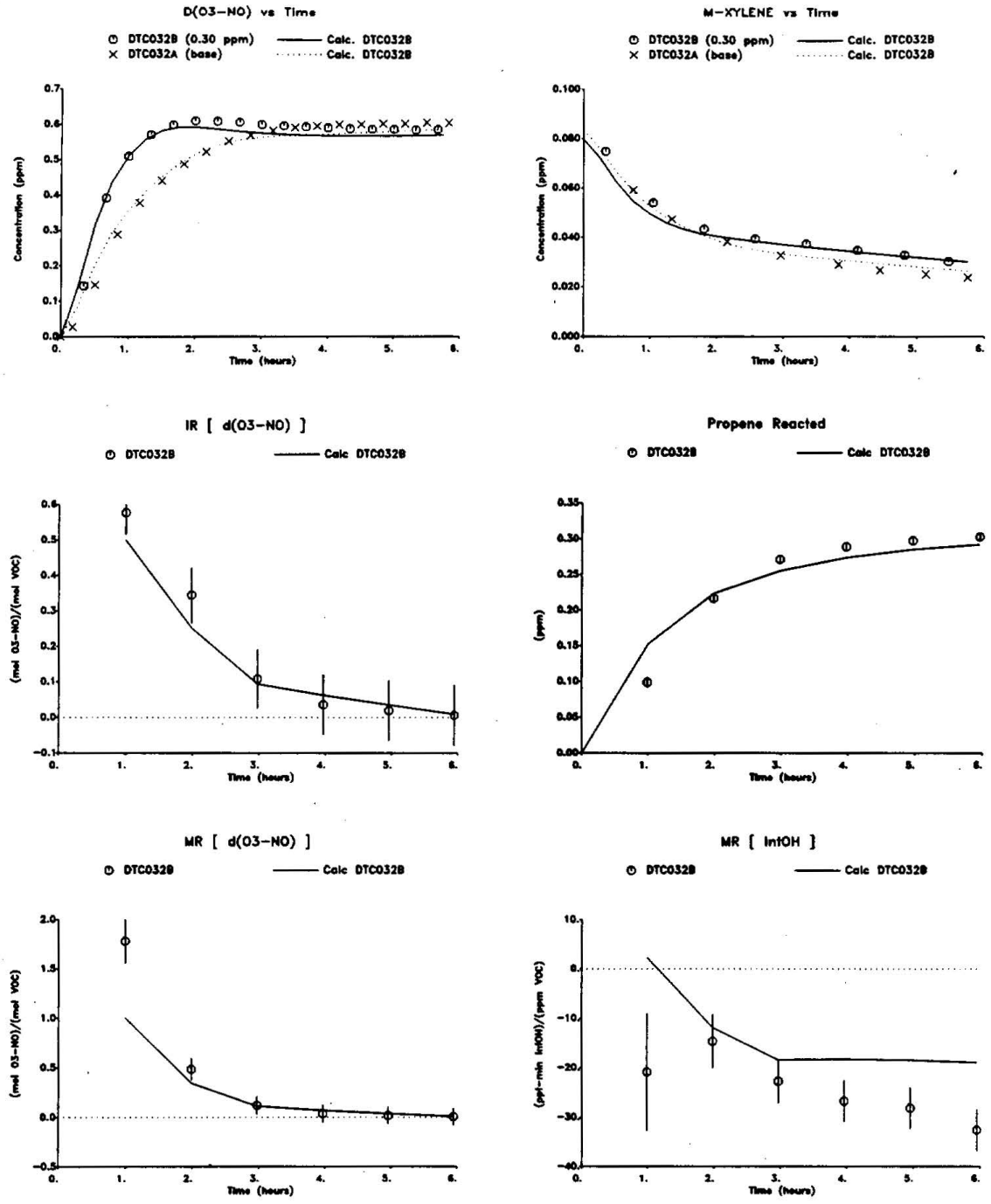

Figure 43. Plots of selected results of the low NO_x lumped molecule surrogate reactivity experiment for **propene**

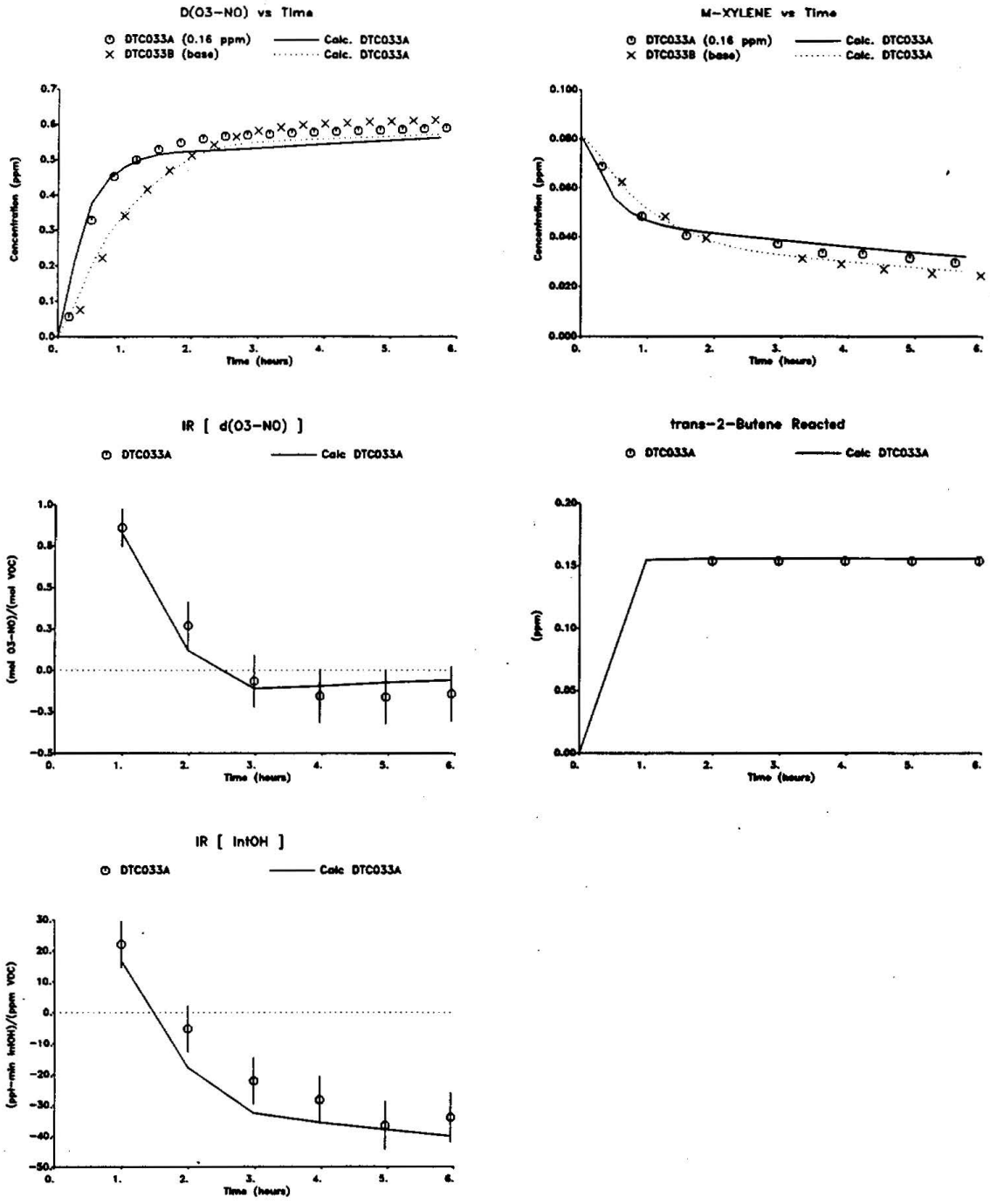

Figure 44. Plots of selected results of the low NO_x lumped molecule surrogate reactivity experiment for **trans-2-Butene**

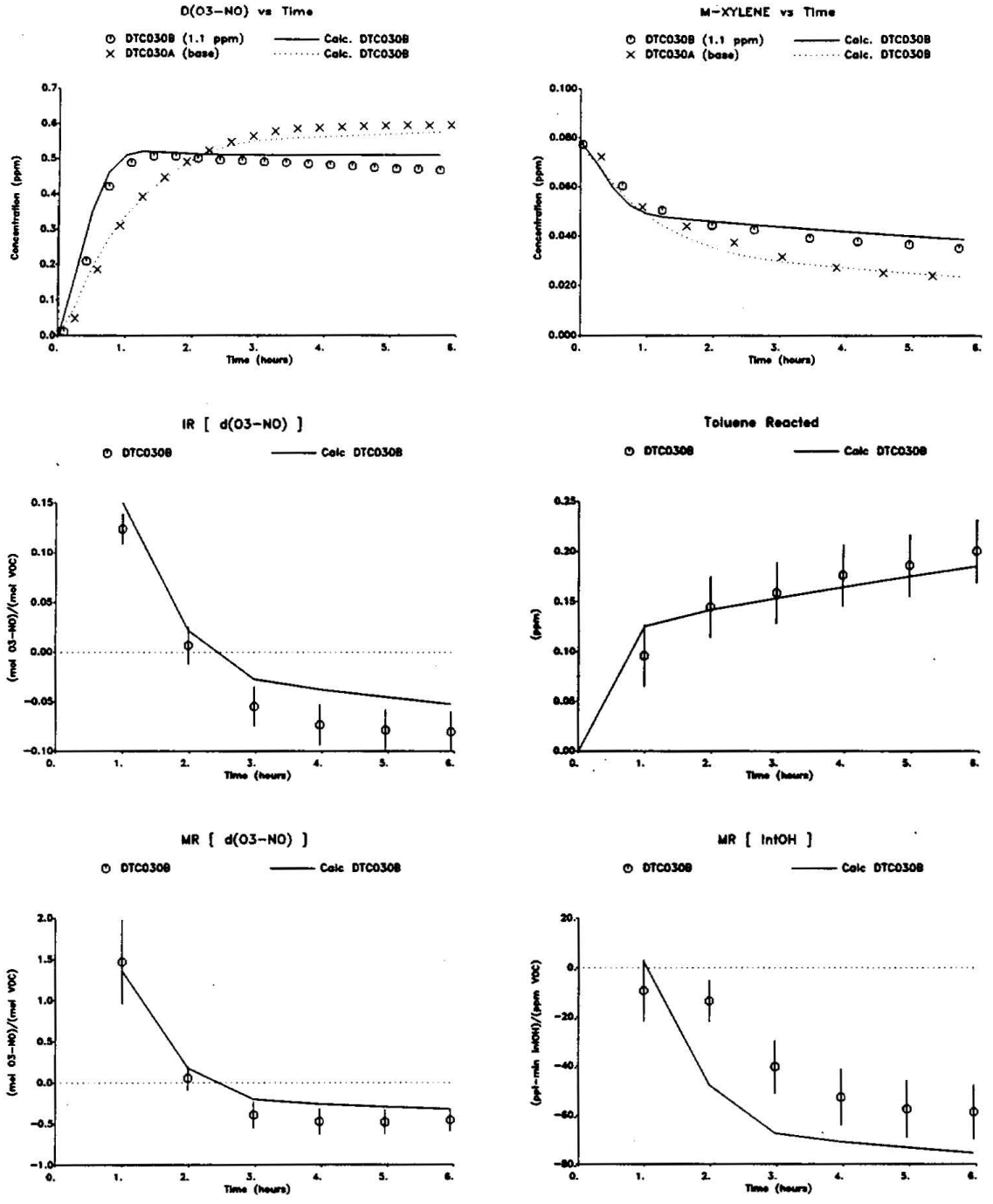

Figure 45. Plots of selected results of the low NO_x lumped molecule surrogate reactivity experiment for **toluene**

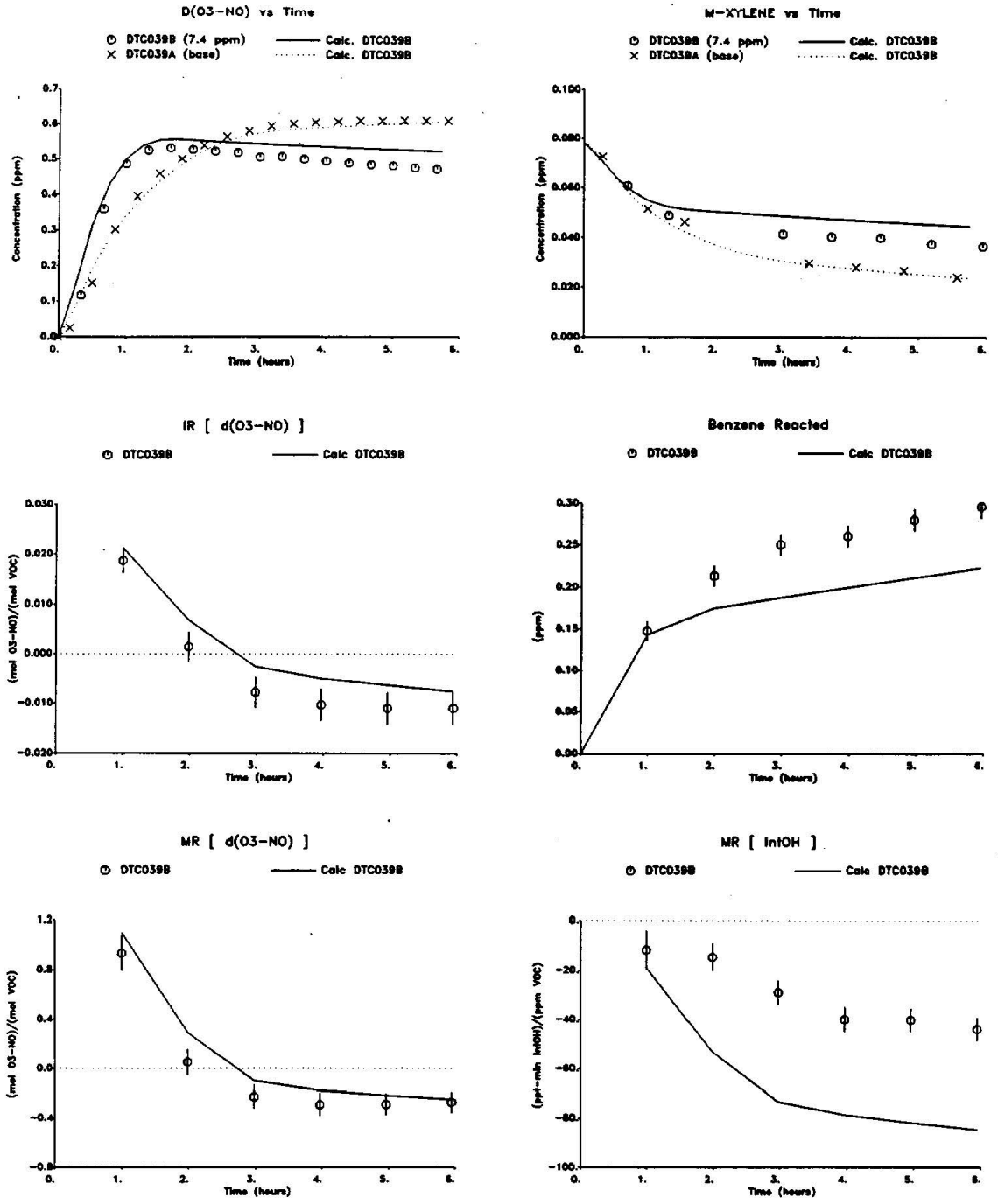

Figure 46. Plots of selected results of the low NO_x lumped molecule surrogate reactivity experiment for **benzene**

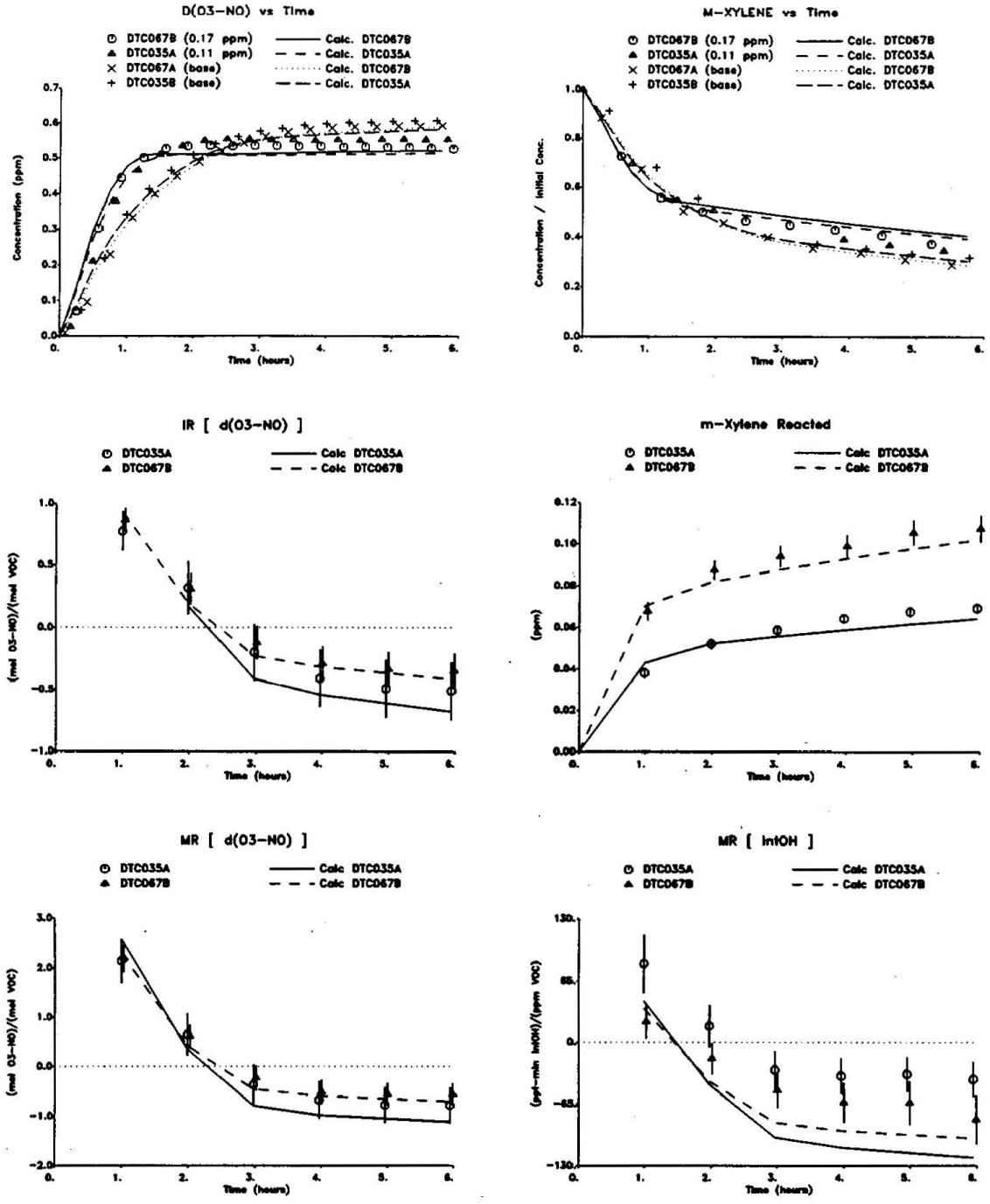

Figure 47. Plots of selected results of the low NO_x lumped molecule surrogate reactivity experiments for **m-xylene**

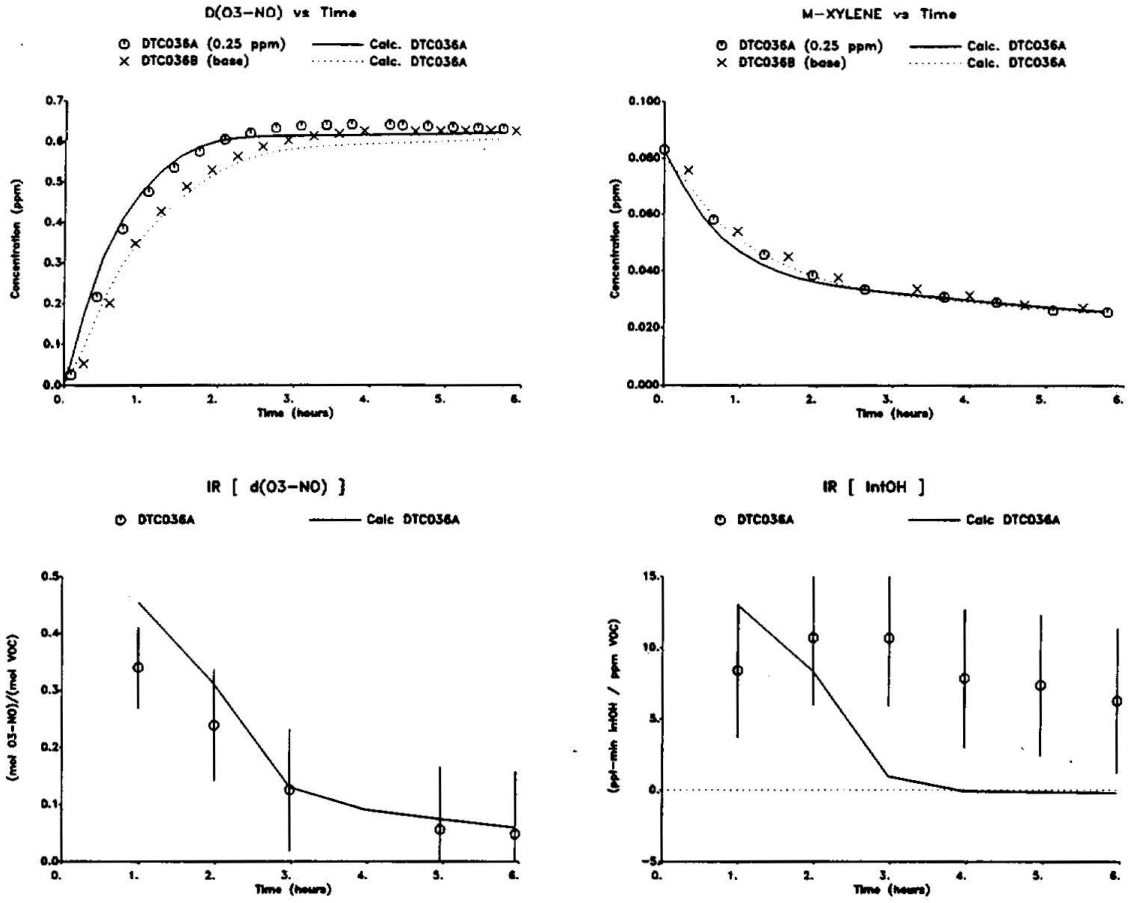

Figure 48. Plots of selected results of the low NO_x lumped molecule surrogate reactivity experiment for **formaldehyde**

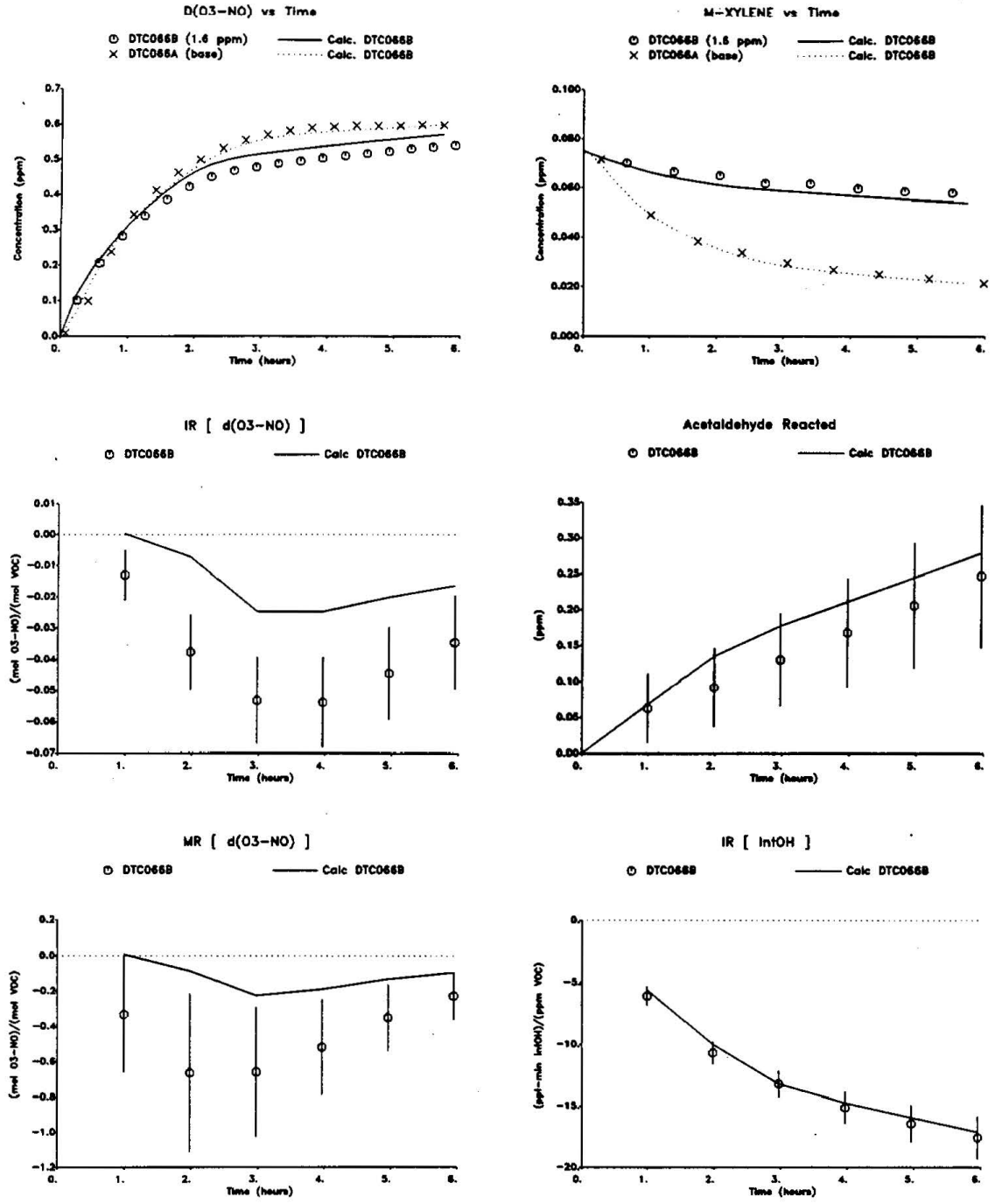

Figure 49. Plots of selected results of the low NO_x lumped molecule surrogate reactivity experiment for **acetaldehyde**

V. MODEL SIMULATIONS

A major objective of this study is to provide data to test the ability of chemical mechanisms used in airshed models to correctly predict VOC reactivities, and in particular how VOC reactivities vary with differing base ROG and NO_x. Although a complete mechanism evaluation and update using these data is beyond the scope of the present report, model calculations were carried out to determine the extent to which the predictions of an updated version of the detailed SAPRC mechanism (Carter, 1990, Carter et al. 1993a; Carter, 1993, Carter et. al., 1993b) are consistent with these new data. The mechanism and approach used to simulate the chamber experiments, and the results obtained, are summarized in this section. The implications of these results are discussed in the Discussion and Conclusions sections.

A. Chemical Mechanism

The chemical mechanism employed in the chamber model simulations given in this report has been documented in the report on our study of the reactivity of acetone (Carter et al., 1993b). The starting point for this mechanism was the "SAPRC-91" mechanism documented in the report on Phase I of this program (Carter et al., 1993b), which was further updated and modified as discussed below. The SAPRC-91 mechanism is an updated version of the "SAPRC-90" mechanism which was used to calculate the MIR reactivity scale used in the CARB regulation (Carter, 1993, 1994; 1991). The differences between the current mechanism, which will be referred to as the "SAPRC-93" mechanism in the subsequent discussion, and the earlier versions of the SAPRC detailed mechanisms are summarized below. Note that some of the changes are not relevant to the specific simulations in this report, but are included in the discussion below for completeness.

(1) The updates to the formaldehyde absorption cross-sections and the kinetics of PAN formation incorporated in the SAPRC-91 mechanism were also incorporated in this mechanism. The changes in PAN kinetics cause the model to predict somewhat higher ozone formation rates than the SAPRC-90 mechanism.

(2) The SAPRC mechanisms use model species whose photolysis rates are adjusted to fit aromatic-NO_x-air chamber experiments to represent the unknown photoreactive aromatic fragmentation products (Carter, 1990). In the SAPRC-91 and the current mechanisms, the action spectra (absorption coefficients x quantum yields) for these products were assumed to be proportional to the absorption cross section for acrolein (Gardner et al., 1987), rather than using the somewhat arbitrary action spectrum in the SAPRC-90 mechanism. The yields of these products were reoptimized based on the simulations of the available chamber data using the updated mechanism. In the SAPRC-91 mechanism, different optimizations were used for m-xylene, depending on which experiments were being simulated (Carter et al., 1993a). In this work, the same m-xylene was used in all simulations, with the parameters optimized to fit m-xylene - NO_x - air

experiments. This resulted in a mechanism which somewhat underpredicted the results of many of the "Set 3" Phase I mini-surrogate experiments, though it performed much better than did the "unadjusted SAPRC-91" mechanism used in the Phase I report, and it performed reasonably well in simulating the base case experiments in this study (see below). The NO_x data for all the relevant aromatic experiments were corrected as discussed by Carter et al. (1995b) prior to reoptimizing the aromatic product yield parameters.

(3) The mechanisms for the reactions of ozone with alkenes were modified to be consistent with the data of Atkinson and Aschmann (1993), who observed much higher yields of OH radicals than predicted by the SAPRC-90 and SAPRC-91 mechanisms. To account for these data, it was assumed that (1) the formation of OH radicals dominates over other radical-forming fragmentation processes, and (2) in the reactions of unsymmetrical alkenes, the more substituted Criegee biradical, which forms higher OH yields, are formed in relatively higher yields than the less substituted biradicals. The modified ozone reactions for the alkenes discussed in this paper are:

Ethene + O3 ⟶ HCHO + (HCHO2)
Propene + O3 ⟶ 0.6 HCHO + 0.4 CCHO + 0.4 (HCHO2) + 0.6 (CCHO2)
trans-2-Butene + O3 ⟶ CCHO + (CCHO2)
Isobutene + O3 ⟶ 0.82 HCHO + 0.18 ACET + 0.18 (HCHO2) + 0.82 (C(C)CO2)

where CCHO and ACET represent acetaldehyde and acetone, and (HCHO2), etc., represent the excited Criegee biradicals, which are represented as reacting as follows:

(HCHO2) $\xrightarrow{fast}$ 0.12 CO + 0.12 HO. + 0.12 HO2. + 0.88 (unreactive carbon)

(CCHO2) $\xrightarrow{fast}$ 0.3 HCHO + 0.3 CO + 0.6 HO. + 0.3 {CCO-O2.+ RCO3.} + 0.3 {RO2-R.+ RO2.} + 0.9 (unreactive carbon)

(C(C)CO2) $\xrightarrow{fast}$ HCHO + HO. + {R2O2.+ RO2.} + {CCO-O2.+ RCO3.}

[See Carter (1990) for a description of the model species and the methods used to represent peroxy radical reactions.] This is clearly an oversimplification of this complex system (e.g., see Atkinson, 1990, 1994), but is intended to account for the observed OH radical yields and represent the major features affecting these compounds' reactivities. Note that this new mechanism gives substantially higher radical yields in the ozone + alkene systems than the SAPRC-90 mechanism, particularly for internal alkenes.

(4) The reaction of NO with the peroxy radical formed in the reaction of OH radicals with isobutene was assumed to form the corresponding hydroxyalkyl nitrate 10% of the time. This assumption resulted in significant improvements

to the fit of model simulations to ozone and PAN yields in isobutene - NO_x - air chamber experiments. Without this assumption, the model with the OH yields indicated by the O_3 + isobutene data of Atkinson and Aschmann (1993) significantly overpredicts O_3 formation rates. If lower radical yields in the O_3 + isobutene reaction are assumed, the model significantly underpredicts PAN (unpublished results from this laboratory).

(5) The representation of iso-octane was modified to improve the model simulations of its reactivity (Carter et al., 1993a).

(6) Several changes were made to the mechanism for acetone. These are documented elsewhere (Carter et al., 1993b.) Note that the mechanism used in this work employed the acetone quantum yields based on the corrected data of Meyrahn et al. (1986), and not the values adjusted to fit our recent chamber experiments (Carter et al., 1993b). Although this is a potential source of uncertainty, it only affects predictions of acetone's reactivity, and has no substantial effect on any of the simulations discussed in this report.

A listing of the SAPRC-93 mechanism is given by Carter et al. (1993b). Further updates to this mechanism are planned, and the process of evaluating it against the full data base of chamber experiments (Carter and Lurmann, 1991; Carter et al., 1995b) is underway. However, it was evaluated in model simulations of the results of the extensive set of Phase I reactivity experiments (Carter et al, 1993c), and was found to perform somewhat better than the SAPRC-90 and SAPRC-91 mechanisms in simulating these data.

B. Chamber Modeling Procedures

The testing of a chemical mechanism against environmental chamber results requires including in the model appropriate representations for the characteristics of the light source, run conditions and chamber-dependent effects such as wall reactions and chamber radical sources. The methods used to represent them in this study are based on those discussed in detail by Carter and Lurmann (1991), modified as discussed by Carter et al. (1995b), and adapted for these specific sets of experiments as indicated below. Where possible, the parameters were derived based on analysis of results of characterization experiments carried out in conjunction with these runs. The specific chamber-dependent parameters used in chamber model simulations for this study, and their derivations are as follows:

1. Photolysis Rates

The photolysis rates when simulating indoor chamber experiments are calculated given the NO_2 photolysis rate and the relative spectral distribution assigned for the run. The NO_2 photolysis rate used in modeling the ETC runs in this study was 0.351 min^{-1}. This was derived using the fits to the ETC actinometry data discussed by Carter et al., 1993a, with the fits recalculated to incorporate the newer experiments carried out in conjunction with the runs for

this program, and using NO_2 photolysis rates derived using slightly modified effective quantum yield parameter as discussed elsewhere (Carter et al., 1995b). The results of the newer ETC experiments were entirely within the range predicted based on the earlier runs. The NO_2 photolysis rate used when modeling the DTC runs was based on the average of the results of all the actinometry experiments carried out in this chamber after the reaction bag was installed, which was 0.388 ± 0.011 min^{-1}. (No decay of NO_2 photolysis rate with time was observed for this chamber, presumably because the blacklights were turned on and "burned in" for several weeks before being used.) The detailed data base and derivation of the NO_2 photolysis rates of experiments in these and other chambers is given in a separate document (Carter et al., 1995b).

The quantum yields used when simulating the DTC and ETC experiments were based on the composite spectrum which we now recommend using when modeling SAPRC blacklight chamber runs (Carter et al. 1995b). It is somewhat different than that we employed previously in our simulations of chamber experiments (Carter and Lurmann, 1991; Carter et al., 1993a-c), being significantly better in representing the many mercury emission lines. This change was found to have a non-negligible effect on the calculation of certain photolysis rates, though the effect of this change has not yet been systematically evaluated.

2. Run Conditions

Temperature: The average temperatures for these experiments are given on Tables 7 and 11. The temperature used when modeling the experiments was based on fitting the temperature data to a series of line segments (usually two – one to represent the relatively rapid increase in temperature during the first ~15 minutes of the run, the other to represent any small trend in temperature later), as recommended when modeling SAPRC chamber runs (Carter et al., 1995b). The temperature in the model simulation changed linearly between the times defining the end points of these segments. Note that this differs slightly from our previous procedure of using a constant temperature (based on the average during the run) when modeling indoor chamber runs.

Humidity: Unhumidified air was used in these experiments because it minimizes chamber effects and improves reproducibility. Measurements made previously indicate the unhumidified output of the SAPRC pure air system typically has humidities of approximately 5%. This corresponds to approximately 5000 ppm of H_2O, which was used in the model simulations.

Dilution: The dilution rates used in simulating these experiments were the same as those used when analyzing the reactivity data, which were derived as discussed above. For non-reactivity experiments, the dilution rates were derived in an analogous manner. The values used for the individual experiments is given with documentation for the SAPRC chamber data base (Carter et al., 1995b).

3. Chamber Effects Parameters

Initial Nitrous Acid: Nitrous acid (HONO) can sometimes be introduced into the chamber during NO_x injection (Carter and Lurmann, 1990, 1991), and if present can affect rates of NO oxidation at the beginning of the run because of its rapid photolysis to form OH radicals. There was evidence for HONO contamination during our initial Phase I experiments, but this was apparently eliminated by injecting NO_x using vacuum techniques (Carter et al., 1993a). Since these vacuum methods were used for the NO_x injections in all the runs in this study, we assume that initial HONO is negligible in the simulations of these runs. Results of comparisons of model simulations with data from control and characterization runs are consistent with this assumption.

Continuous Chamber Radical Source: As discussed previously (Carter et al., 1982; Carter and Lurmann, 1990, 1991) there is a continuous chamber-dependent radical source which must be accounted for in model simulations of environmental chamber experiments. The magnitude of this radical source is extremely important in affecting simulations of alkane-NO_x-air experiments and other low reactivity runs, though it is less important – though not negligible – when simulating surrogate-NO_x-air runs such as these reactivity experiments (Carter and Lurmann, 1991). This can be determined by model simulations of radical tracer-NO_x-air experiments (Carter et al., 1982), or alkane-NO_x-air experiments. The radical input rate used in the model simulations of the ETC runs for this program was 0.04 ppb x k_1, based on model simulations of the tracer-NOx-air experiments ETC-380 and 472. This is slightly higher than the radical input rates used to simulate the Phase I ETC experiments, though is not inconsistent with results of the tracer-NO_x and n-butane-NO_x runs carried out in conjunction with those runs. The radical input used when modeling the DTC runs was 0.05 ppb x k_1, based on simulations of tracer-NO_x-air run DTC058 and n-butane-NO_x-air run DTC059. Note that this is not significantly different than that used when modeling the ETC runs.

NO_x Offgasing Rate A light-dependent offgasing of NO_x also occurs in environmental chamber experiments. This can affect predictions of maximum O_3 yields in low NO_x experiments. The rate of this offgasing can be derived by model simulations of O_3 formation in pure air irradiations and on O_3 and PAN formation in acetaldehyde-air irradiations. The NO_x offgasing rates used in the simulations of the ETC and DTC runs for this program were k_1 x 0.4 ppb and k_1 x 0.3 ppb, respectively. These are based on based on simulations of ozone formation in the acetaldehyde-air run ETC382 and in the pure air runs ETC458, ETC485 and DTC049. A slightly lower NO_x offgasing rate might be expected in the DTC than the ETC because of the larger chamber volume, though the difference is probably well within the uncertainty of the determination. Lower NO_x offgasing rates were assumed in the simulations of the Phase I experiments, but this was based on modeling a pure air irradiation in a relatively new chamber.

NO Conversion Due to Background VOCs. The effect of background organics is represented by a conversion of HO to HO_2 at a rate adjusted to fit pure air experiments (Carter and Lurmann, 1990, 1991). These simulations used the same rate as derived for the SAPRC ITC, or 250 min^{-1}. This fits model simulations of the ETC and DTC pure air runs reasonably well. The simulations of reactivity experiments are insensitive to this parameter.

Ozone Decay Rate: The O_3 dark decay rates measured in the ETC reaction bag used in this program were 2.7 x 10^{-4} min^{-1} when the bag was relatively new (ETC374) and was 1.21 and 1.23 x 10^{-4} min^{-1} in two experiments in the well conditioned bag. The average of the latter two values was used when modeling the ETC runs. The O_3 dark decay was measured in the DTC only when the reaction bags were new, and the result was 2.5 x 10^{-4} min^{-1} for both sides, making it very similar to the O_3 decay in the ETC with the new reaction bag. Based on the results with the ETC, one would expect lower O_3 decays when the bags were more conditioned. For modeling the DTC runs, where O_3 decay measurements were only made when the chamber was new, we assumed an O_3 decay rate of 1.5 x 10^{-4} min^{-1}, which is similar to the value used for the ETC and is the recommended default for modeling SAPRC ITC runs (Carter et al., 1995b).

N_2O_5 Hydrolysis: The rate of the heterogeneous hydrolysis of N_2O_5 used when modeling these experiments was as recommended by Carter et al. (1995b) for modeling SAPRC teflon chamber runs, and is as follows:

$$\text{Rate } (N_2O_5+H_2O) = 2.8 \times 10^{-3} + (1.5\times10^{-6}-k_g)\ [H_2O\ (ppm)]\ ppm\ min^{-1},$$

where k_g is the rate constant used in the gas-phase mechanism for the $N_2O_5+H_2O$ reaction. This is based on the N_2O_5 decay rate measurements in the ETC reported by Tuazon et al. (1983). Although we previously estimated there rate constants were lower in the larger Teflon bag chambers (Carter and Lurmann, 1990, 1991), we now consider it more reasonable to use the same rate constants for all such This parameter affects predictions of O_3 yields in runs which are NO_x-limited.

4. Modeling Experimental Incremental Reactivities

DTC Experiments. The model simulations of incremental reactivities measured in the DTC experiments consisted simply of conducting simulations of the added VOC (test) experiment and the simultaneous base case experiment, and then incremental and mechanistic reactivities from the calculated data in the same way as derived from the experimental data. Thus, each model simulation of incremental reactivity in the DTC took into account the particular conditions of each divided chamber experiment, and did not require any assumptions concerning consistency of conditions from experiment to experiment. This is applicable to the simulations of all the lumped surrogate experiments and the ethene surrogate experiment with n-hexane.

ETC Experiments. The approach used when modeling the reactivities in the ETC runs was to conduct simulations for the conditions of each test compound experiment, and then repeat the simulations with the same conditions, but with the test compound removed. The latter simulation was then used to represent the base case. Note that this is somewhat different than the approach used when modeling the Phase I ETC reactivity experiments (Carter et al., 1993a). In that study, the base case simulation for all experiments consisted of simulating an "averaged conditions" base case experiment, and then simulating individual reactivity experiments by simulating the averaged conditions base case with the appropriate amount of test compound added. The approach used in this work has the advantage that the specific conditions of each individual experiment are taken into account. However, the "averaged conditions" approach was used when preparing the calculated data on the plots of incremental reactivity as a function of VOC added.

C. Model Simulation Results

1. Base Case Experiments

Phase I Mini-Surrogate Runs. Before discussing the simulations of the mini-surrogate experiments in this work, it is useful to discuss the current status of the model in simulating the standard mini-surrogate run used in the Phase I reactivity study (Carter et al., 1993a). In the report on that program, we were unable to simulate all the three sets of base case experiments using the same version of the mechanism, and had to adjust the m-xylene mechanism to get acceptable fits to the "Set 3" mini-surrogate runs. To see if this is still the case, we used the current version of the mechanism to simulate the representative Phase I base case experiments which were used to illustrate model performance in the Phase I report (figures 7-9 in Carter et al., 1993a). The results are shown on Figure 50, which shows experimental and calculated concentration-time profiles for ozone, NO, NO2 (or NO_y-NO) and m-xylene. Figure 50 also gives a plot of the relative errors in the model calculation[4] against the average temperature in the Set 3 runs. It can be seen that the model now performs somewhat better in simulating these experiments. Although it still underpredicts the rate of O_3 formation in the many of the Set 3 run, the discrepancy is much less than was the case previously. The discrepancy for the Set 3 runs can also be seen to be dependent on the average temperature, with good fits being obtained for runs carried out at ~300°K. (The temperature effects on model performance are discussed in more detail elsewhere [Carter et al., 1995a].)

The reason for the improved performance of the mechanism in simulating the Phase I can be attributed in part to corrections to the SAPRC chamber data base carried out under EPA and CARB funding (Carter et al., 1995b), in part to a re-evaluation of chamber effects parameters for this chamber (Carter et al., 1995a), and in part to the updates to the chemical mechanism. However, none of these runs were used in optimizing the parameters of the current version of the

[4](model - experiment) / (average of model and experiment)

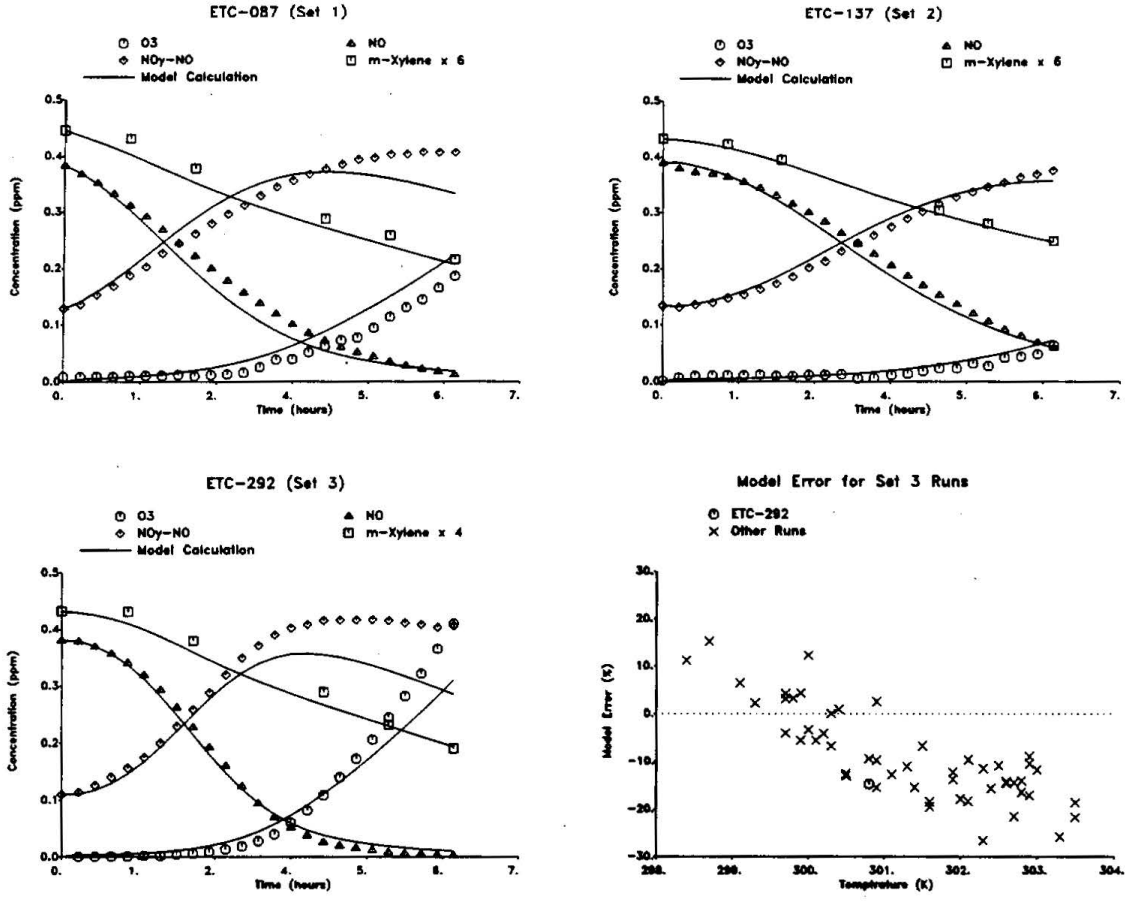

Figure 50. Experimental and calculated concentration-time profiles for selected species in selected Phase I base-case mini-surrogate experiments, and plots of relative errors in model calculations of the Set 3 runs against average temperature.

m-xylene mechanism, nor was there a change in the formulation of the m-xylene mechanism or the way it is parameterized. Non-negligible corrections were made to some of the NO_x data in several of the runs used to derive the aromatic mechanistic parameters, and the spectral distribution used to calculate photolysis rates when modeling runs with blacklight light sources was refined. The modifications to the chamber effects parameters used when simulating the ETC runs included increasing the magnitude of the chamber radical source parameter for the ETC for the period of time when most of the Set 3 runs were conducted. This latter change, which was based on modeling n-butane-NO_x and tracer-NO_x-air runs, is probably the major contributor to the improvement.

Ethene Surrogate Runs. Examples of results of model simulations of the base case ethene surrogate runs are shown on Figure 15, above, and Figure 51

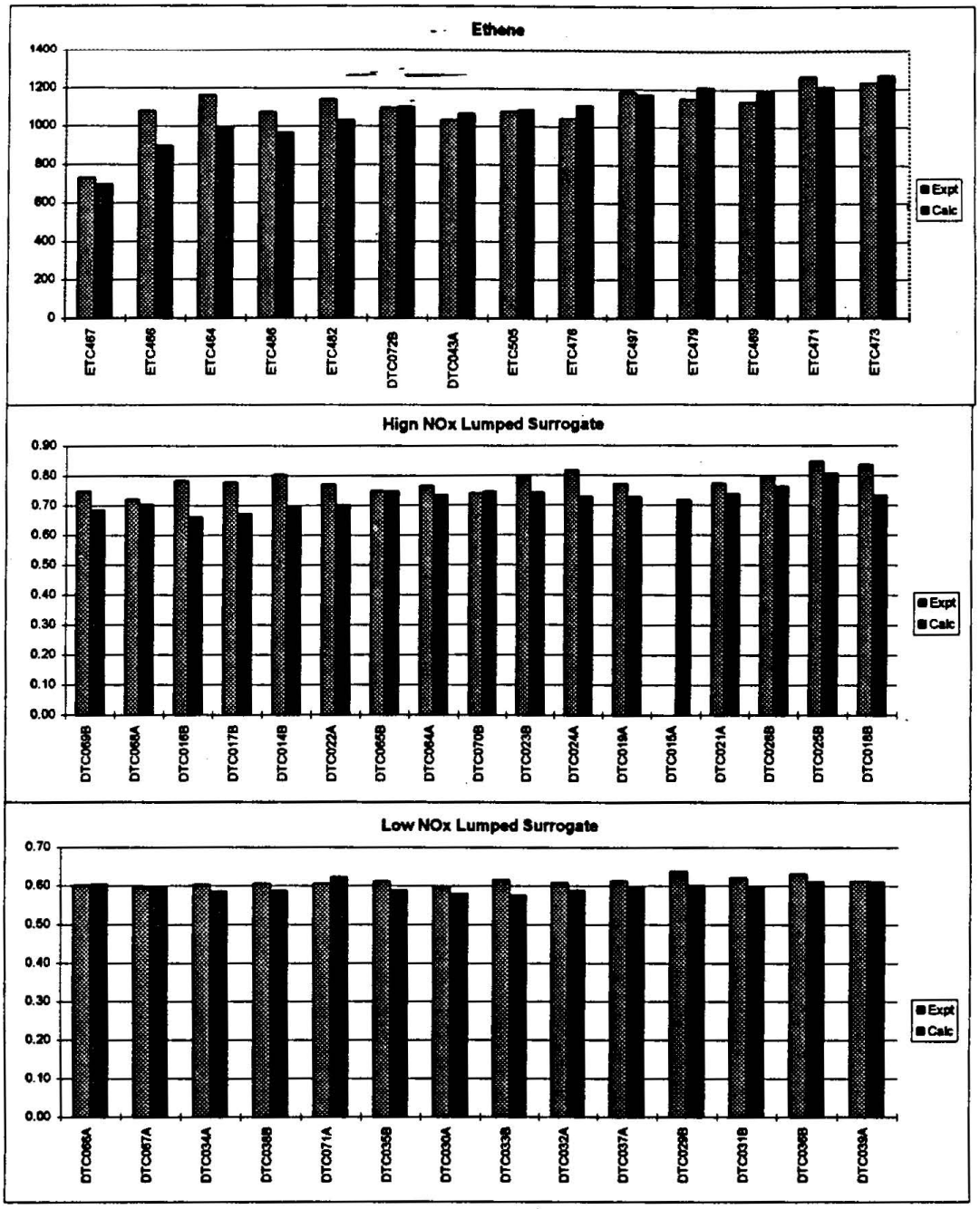

Figure 51. Comparisons of experimental and calculated 6-hour $d(O_3\text{-}NO)$ for the base case experiments.

shows a comparison of the experimental and calculated final $d(O_3\text{-}NO)$ for all the base case runs. The runs on Figure 51 are sorted by ascending initial base ROG concentration. It can be seen that reasonably good fits are obtained, but that there is some scatter in the fits to the ethene runs.

The scatter in model fits to the ethene runs appears to be due more to variation in the calculated $d(O_3\text{-}NO)$ than in the experimental data. A possible explanation for this may be errors in the measured values of ethene, which are used to determine the initial concentrations of the simulations. In particular, the runs with the underprediction of greater than 10% all have initial ethene concentrations which are less than the average, and much better fits of model simulations to the results of these experiments are used if initial ethene levels more typical of the other runs are used. However, there are no apparent problems with the ethene calibrations or data with those runs.

The regression analysis of the experimental ethene data suggest a slight temperature dependence in the ethene data. As discussed elsewhere (Carter et al., 1995a), this is not predicted by the model, even after taking into account possible temperature-dependent chamber effects. However, the effect of other variations in run conditions, particularly initial ethene, appears to be more important in affecting the fits than variations in temperature, since there is no clear correlation between average run temperature and model prediction error.

Lumped Surrogate Runs. Examples of model simulations of the high and low NO_x base case lumped surrogate runs are shown on Figures 24 and 25, above, and Figure 51 shows a comparison of the experimental and calculated final $d(O_3\text{-}NO)$ for all these runs. It can be seen that, with the exception of the formaldehyde data, the model performs reasonably well in simulating these runs. The model slightly underpredicts the O_3 formation rate in the high NO_x lumped surrogate runs, in a manner similar to the underprediction of O_3 formation in most of the Phase I mini-surrogate runs (see Figure 50). The discrepancy is not sufficient to warrant adjusting the mechanisms for the purpose of simulating incremental reactivity.

We have no explanation for the poor performance of the model in simulating the formaldehyde profiles in these runs. The mechanisms for some of the base ROG surrogate components may not be including sufficient formaldehyde sources. However, another explanation is that there is an interference in the formaldehyde analysis with some other product(s) formed in this system. This will be investigated in the subsequent program. This is not considered to be a major concern for this program, where the focus is effects of VOCs on ozone and OH radicals. We believe the initial formaldehyde measurements are correct, because they are consistent with the amounts of formaldehyde injected, which are measured with some accuracy using vacuum methods with capacitance manometers and bulbs of known volume.

2. Ethene Surrogate Reactivity Experiments

Figures 15-23, above, show the results of the model simulations of the d(O_3-NO) data and the various measures of reactivity in the ethene reactivity experiments with the various test VOCs. Figures 52-54 show plots of the calculated vs. experimental 6-hour d(O_3-NO), IntOH, and estimated direct mechanistic reactivities for the various experiments, where the performance of the model for the ethene surrogate experiments can be compared with that for the other surrogates. (Note that the reactivity data on Figures 52-54 are given on a per carbon basis, while all such data given on previous figures and tables are on a per molecule basis.) In general, the performance of the model in simulating reactivities in the ethene surrogate runs was variable. Good fits for essentially all reactivity measures were obtained with CO, ethane and m-xylene. Fair fits, which can probably be considered to be within experimental and/or model characterization variability, were obtained for n-hexane, propene, and trans-2-butene. Poor fits were obtained for n-octane, formaldehyde, and, to a lesser extent, n-butane.

The model was found to significantly overpredict the incremental reactivity of formaldehyde in the run with the lowest amount of added formaldehyde, and during the initial periods of all the runs. This is consistent with the underprediction of formaldehyde reactivity observed when modeling the Phase I mini-surrogate runs (Carter et al. 1993a). The model was also found to significantly underpredict, by approximately a factor of two, of the inhibition of d(O_3-NO) caused by n-octane. A similar result, though to a much lesser extent, is seen in the model simulations of the added n-butane and n-hexane runs. The quality of the IntOH data in the added alkane ethene surrogate runs is not sufficient to clearly indicate whether the source of the discrepancy is the model simulation of the effect of these alkanes on radical levels, or their direct reactivities. These cases of poor model performance will be discussed further below.

3. High NO_x Lumped Surrogate Reactivity Experiments

Figures 29-38, above, show the results of the model simulations of the data from the high NO_x lumped surrogate reactivity runs. In general, remarkably good performance in the model simulations of the reactivity data was observed, considerably better in general than the simulations of the reactivities in the ethene surrogate runs. Even the reactivities of n-octane and formaldehyde, which were poorly simulated by the model in the ethene surrogate, were well fit with the more complex lumped surrogate runs. This is despite the greater experimental precision observed in these runs, and the higher quality IntOH data, which gave a more precise test of the mechanism.

The only discrepancies between model and experiment which might be outside the range of experimental or run characterization uncertainty are as follows.

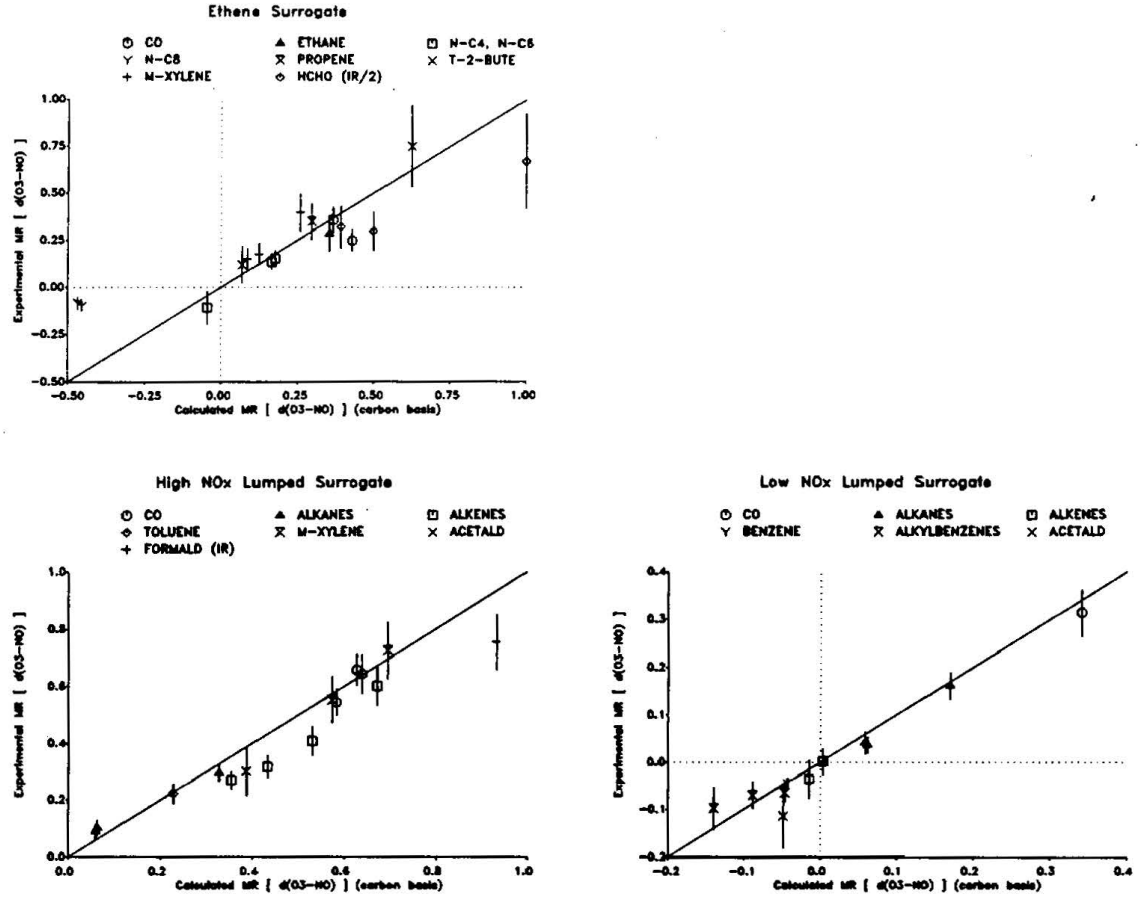

Figure 52. Plots of experimental vs calculated 6-hour $d(O_3\text{-}NO)$ mechanistic reactivities for the various types of reactivity runs. Note that the reactivities are given on a per-carbon basis.

The $d(O_3\text{-}NO)$ and IntOH reactivities of CO, n-butane (for the initial part of the experiment) and toluene are slightly underpredicted. (2) The IntOH reactivity of n-butane is slightly underpredicted. The model somewhat overpredicts the rates of O_3 formation at the end of the added propene and trans-2-butene runs, causing an overprediction of $d(O_3\text{-}NO)$ reactivities at the end of the runs. However, in all cases, the discrepancies are small and may not necessarily indicate problems with the mechanism.

4. Low NO_x Lumped Surrogate Reactivity Experiments

Figures 39-49, above, show the results of the model simulations of the low NO_x lumped surrogate reactivity runs. In general, the performance of the model was almost as good in simulating these runs as in simulating the high NO_x lumped surrogate runs, though there were some cases where perhaps more

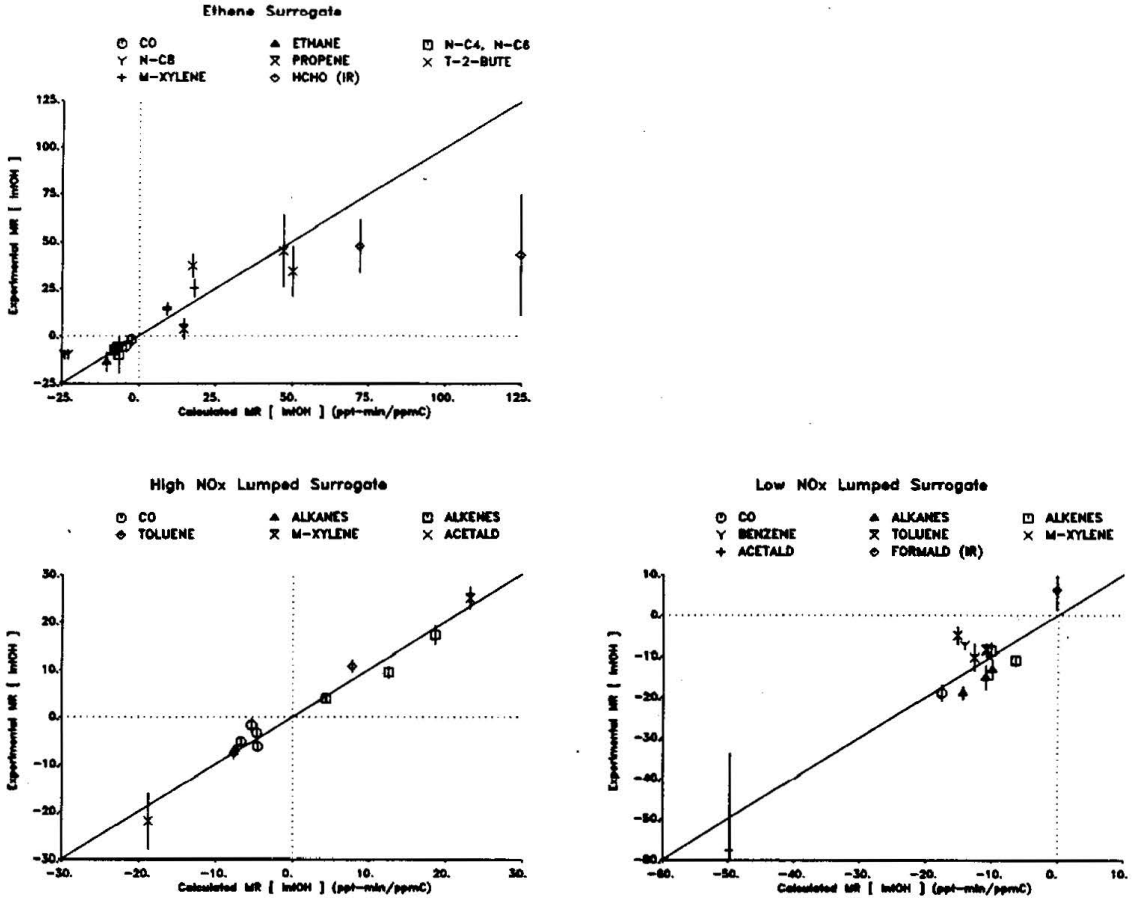

Figure 53. Plots of experimental vs calculated 6-hour IntOH mechanistic reactivities for the various types of reactivity experiments. Note that the reactivities are given on a per-carbon basis.

significant discrepancies were observed. As discussed above, one low NO_x reactivity characteristic observed for most VOCs is an inhibition of IntOH by the end of the run. The model gave good predictions of this low NO_x IntOH inhibition in the cases of CO, ethene, trans-2-butene, and acetaldehyde, but slightly underpredicted the IntOH inhibition for n-butane, n-octane and propene, slightly overpredicted it for toluene and one of the m-xylene experiments, and significantly overpredicted it for benzene and the other m-xylene run. The $d(O_3\text{-NO})$ incremental and mechanistic reactivities were reasonably well predicted in most cases except perhaps for the t=1 hour points for propene (which may be due to problems with the t=1 propene data), and a slight underprediction of the small $d(O_3\text{-NO})$ inhibition caused by acetaldehyde. The only discrepancy which is clearly outside the uncertainty of the data is the significant overprediction of the IntOH inhibition observed in the benzene experiment.

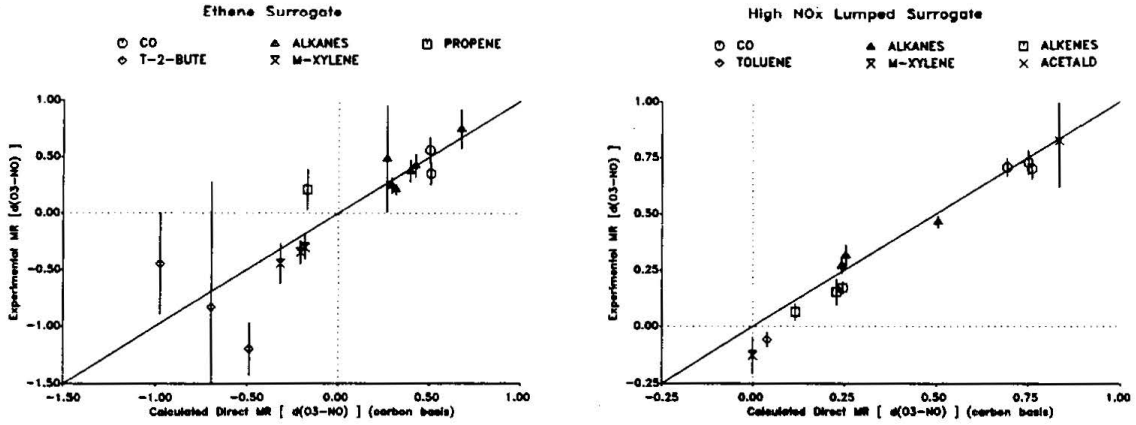

Figure 54. Plots of experimental vs calculated 6-hour direct $d(O_3\text{-}NO)$ mechanistic reactivities for the various types of high NO_x reactivity experiments. Note that the reactivities are given on a per-carbon basis.

The mechanistic implications of the results of the modeling of these and the other reactivity experiments are discussed in the following section.

VI. DISCUSSION

A. Effect of ROG Surrogate on Reactivity

A summary of the major experimental results using different ROG surrogates obtained from this and our previous work (Carter et al., 1993a) is given in Table 15. The results are given in terms of mechanistic reactivities for several reasons. First, it allows mechanistic effects for VOCs with different reaction rates to be directly compared. Otherwise, the significant differences in the VOCs in terms of their reaction rates will dominate the results. In addition, it allows mechanistic effects of a given VOC to be compared for experiments with differing radical levels. All else being equal, the incremental reactivity of a VOC will increase if the radical levels in the experiment increases, because more of the VOC will react during the experiment. Use of mechanistic reactivities allows this purely kinetic effect to be factored out when assessing the effect of the ROG on reactivity. Although the effects of differing VOC reaction rates and environmental radical levels are obviously important, they can be adequately predicted for VOCs whose reaction rates are known if the model for base case conditions adequately simulates the environment's radical levels. Factoring out kinetic effects by examining mechanistic reactivities provides information on whether other, perhaps less obvious, mechanistic effects are also important.

The high NO_x mechanistic reactivities can be further broken down into direct and indirect mechanistic reactivities. The former provides an estimate of the number of molecules of NO oxidized and O_3 formed caused directly by the reactions of the VOC its oxidation products, per molecule of VOC reacting. The latter refers to the effect of the test VOC's reactions on the amount of NO oxidized and O_3 formed from the reactions of the other VOCs' present, i.e., from the reactions of the components of the base ROG mixture. Under high NO_x conditions, the indirect reactivity is due entirely to the effect of the VOC on radical levels, which in turn affects how much of the components of the base ROG are reacting to oxidize NO or form ozone. The estimates of direct and indirect mechanistic reactivities in the various experiments are included in Table 15, and a comparison of the averages of these data for the various VOCs and ROG surrogates in the high NO_x experiments are shown on Figure 55.

Table 15 and Figure 55 show that, at least for high NO_x conditions and for those compounds where sufficient useful direct reactivity data could be obtained, the nature of the base ROG surrogate has no significant effect on direct reactivity. This is as expected, since the radicals formed in a VOC's oxidations which cause NO oxidation generally react primarily with NO_x, and not with radicals from other VOCs, at least under conditions when ozone formation is occurring. On the other hand, Table 15 and Figure 55 show that, for some VOCs at least, the indirect reactivity can depend significantly on the base ROG surrogate. In general, the indirect reactivities tend to have higher magnitudes,

Table 15. Summary of selected results for reactivity experiments using different ROG surrogates and NO_x levels.

Experiment [a]				Added (ppm)	Reacted (ppm)	Incr. React'y (mol O3-NO/ mol added)	Mech. React'y (mol O3-NO/mol reacted)		
NOx	Surg	Run	Hr.				Overall	Indirect	Direct
Carbon Monoxide									
Hi	Mini	E418	6	110.	0.662 ± 6%	0.0039 ±16%	0.6 ± 0.1	-0.2 ± 0.1	0.8 ± 0.1
Hi	Mini	E418	6	110.	0.662 ± 6%	0.0039 ±16%	0.6 ± 0.1	-0.2 ± 0.1	0.8 ± 0.1
Hi	Mini	E416	6	130.	0.726 ± 6%	0.0048 ±11%	0.9 ± 0.1	-0.1 ± 0.1	0.9 ± 0.1
Hi	Ethe	E487	3	107.	0.326 ±30%	0.0035 ±11%	1.1 ± 0.4	0.1 ± 0.4	1.2 ± 0.5
Hi	Ethe	E487	3	107.	0.326 ±30%	0.0035 ±11%	1.1 ± 0.4	0.1 ± 0.4	1.2 ± 0.5
Hi	Ethe	E483	3	155.	0.461 ±31%	0.0031 ± 9%	1.0 ± 0.3	-0.1 ± 0.3	1.1 ± 0.4
Hi	Surg	D014	6	155.	1.209 ± 5%	0.0043 ± 8%	0.5 ± 0.0	-0.2 ± 0.0	0.7 ± 0.0
Hi	Surg	D015	4	161.	1.100 ± 4%	0.0047 ± 6%	0.7 ± 0.1	0.0 ± 0.0	0.7 ± 0.0
Hi	Surg	D016	6	74.2	0.684 ± 4%	0.0059 ±10%	0.6 ± 0.1	-0.1 ± 0.1	0.7 ± 0.1
Hi	Surg	D020	6	103.	0.869 ± 4%	0.0055 ± 7%	0.7 ± 0.1	0.0 ± 0.0	0.7 ± 0.0
Lo	Surg	D029	6	85.8	0.659 ± 4%	0.0024 ±15%	0.3 ± 0.1	[b]	[b]
Ethane									
Hi	Mini	E235	6	43.7	0.306 ± 6%	0.0058 ±26%	0.8 ± 0.2	-0.6 ± 0.3	1.4 ± 0.3
Hi	Ethe	E506	3	49.7	0.181 ±29%	0.0044 ±20%	1.2 ± 0.4	-0.2 ± 0.5	1.5 ± 0.8
n-Butane									
Hi	Mini	E224	6	9.76	0.309 ±17%	0.0269 ±26%	0.8 ± 0.3	-1.4 ± 0.4	2.2 ± 0.4
Hi	Ethe	E488	3	10.31	0.221 ±45%	0.0242 ±17%	1.1 ± 0.5	-0.6 ± 0.6	1.7 ± 0.9
Hi	Ethe	E484	3	15.2	0.341 ±43%	0.0314 ± 9%	1.4 ± 0.6	-0.2 ± 0.4	1.7 ± 0.8
Hi	Surg	D019	6	6.48	0.441 ± 5%	0.0808 ± 9%	1.2 ± 0.1	-0.7 ± 0.1	1.9 ± 0.1
Lo	Surg	D031	6	5.48	0.281 ± 7%	0.0332 ±17%	0.6 ± 0.1	[b]	[b]
n-Hexane									
Hi	Ethe	D072	6	2.88	0.166 ±73%	-0.0375 ±38%	-0.6 ± 0.5	-3.6 ± 3.4	2.9 ± 2.9
n-Octane									
Hi	Mini	E239	6	1.55	0.064 ±28%	-0.243 ±18%	-5.9 ± 2.0	-9.7 ± 3.2	3.5 ± 1.4
Hi	Mini	E237	6	1.66	0.098 ±19%	-0.235 ±17%	-4.0 ± 1.0	-5.9 ± 1.5	1.9 ± 0.8
Hi	Ethe	E472	6	1.60	0.278 ±17%	-0.135 ±26%	-0.8 ± 0.2	-2.6 ± 0.6	1.7 ± 0.4
Hi	Ethe	E474	6	2.27	0.286 ±24%	-0.0839 ±32%	-0.7 ± 0.3	-2.6 ± 0.7	2.0 ± 0.6
Hi	Surg	D024	6	1.10	0.216 ±14%	0.162 ±22%	0.8 ± 0.2	-1.7 ± 0.3	2.5 ± 0.4
Hi	Surg	D070	6	0.74	0.176 ±12%	0.174 ±26%	0.7 ± 0.2	-1.4 ± 0.2	2.2 ± 0.3
Lo	Surg	D037	6	1.12	0.201 ±17%	0.0524 ±46%	0.3 ± 0.1	[b]	[b]
Lo	Surg	D071	6	0.647	0.142 ±12%	0.0727 ±57%	0.3 ± 0.2	[b]	[b]
Ethene									
Hi	Mini	E203	6	0.21	0.086 ±29%	0.912 ±35%	2.3 ± 1.0	2.0 ± 1.2	[c]
Hi	Mini	E199	6	0.38	0.172 ±20%	1.14 ±17%	2.5 ± 0.6	1.9 ± 0.8	[c]
Hi	Surg	D017	6	0.60	0.340 ± 4%	0.673 ±11%	1.2 ± 0.1	0.9 ± 0.1	0.3 ± 0.1
Lo	Surg	D038	6	0.65	[d]	0.0864 ±47%		[b]	[b]
Propene									
Hi	Surg	E106	6	0.081	0.057 ± 7%	2.61 ±13%	3.7 ± 0.5	2.1 ± 0.6	1.6 ± 0.6
Hi	Surg	E108	9	0.085	0.057 ± 5%	1.98 ±16%	3.0 ± 0.5	1.5 ± 0.6	1.6 ± 0.6
Hi	Surg	E118	6	0.148	0.108 ± 6%	1.63 ±12%	2.2 ± 0.3	1.3 ± 0.5	1.0 ± 0.5
Hi	Ethe	E500	3	0.21	0.121 ± 4%	1.53 ±13%	2.7 ± 0.4	0.1 ± 1.0	2.3 ± 1.2
Hi	Ethe	E496	3	0.30	0.222 ± 3%	1.58 ± 8%	2.2 ± 0.2	1.6 ± 0.7	0.1 ± 0.9
Hi	Surg	D018	6	0.35	0.348 ± 2%	0.950 ±13%	1.0 ± 0.1	0.8 ± 0.1	0.2 ± 0.1
Lo	Surg	D032	6	0.30	0.303 ± 2%	0.007 ±0.08	0.0 ± 0.1	[b]	[b]

Table 15 (continued)

Experiment [a]				Added (ppm)	Reacted (ppm)	Incr. React'y (mol O3-NO/ mol added)		Mech. React'y (mol O3-NO/mol reacted)		
NOx	Surg	Run	Hr.					Overall	Indirect	Direct
trans-2-Butene										
Hi	Mini	E309	6	0.06	0.068 ±11%	5.47	±21%	5.5 ± 1.2	4.2 ± 1.5	[c]
Hi	Mini	E307	6	0.08	0.086 ±35%	5.09	±38%	5.1 ± 1.9	4.5 ± 2.0	[c]
Hi	Ethe	E501	3	0.06	0.066 ± 2%	7.92	± 8%	7.9 ± 0.6	5.6 ± 2.3	[c]
Hi	Ethe	D043	3	0.09	0.097 ± 2%	6.82	± 5%	6.8 ± 0.4	6.1 ± 2.9	[c]
Hi	Ethe	E493	3	0.14	0.142 ± 2%	5.07	± 6%	5.1 ± 0.3	5.0 ± 1.4	[c]
Hi	Surg	D021	4	0.32	0.320 ± 2%	1.42	± 8%	1.4 ± 0.1	0.6 ± 0.1	0.8 ± 0.1
Hi	Surg	D069	5	0.19	0.190 ± 2%	1.65	±12%	1.6 ± 0.2	1.0 ± 0.2	0.6 ± 0.2
Lo	Surg	D033	6	0.15	0.154 ± 2%	-0.14	±0.2	-0.1 ± 0.2	[b]	[b]
Benzene										
Hi	Mini	E265	6	5.78	0.357 ±14%	0.0479	±24%	0.8 ± 0.2	[b]	[b]
Hi	Mini	E263	6	6.86	0.447 ±11%	0.0224	±44%	0.3 ± 0.2	[b]	[b]
Lo	Surg	D039	6	7.39	0.296 ± 5%	-0.0110	±30%	-0.3 ± 0.1	[b]	[b]
Toluene										
Hi	Mini	E101	6	0.170	0.030 ±16%	1.22	±13%	6.9 ± 1.4	5.9 ± 1.5	0.8 ± 1.2
Hi	Mini	E103	6	0.174	0.034 ±15%	1.34	±11%	7.0 ± 1.3	5.3 ± 1.4	1.6 ± 1.3
Hi	Surg	D023	3	0.57	0.108 ±14%	0.539	±10%	2.8 ± 0.5	1.9 ± 0.4	1.0 ± 0.4
Lo	Surg	D030	6	1.13	0.201 ±16%	-0.0803	±26%	-0.5 ± 0.1	[b]	[b]
m-Xylene										
Hi	Mini	E301	6	0.05	0.033 ±20%	6.16	±23%	9.9 ± 2.8	7.7 ± 3.2	[c]
Hi	Mini	E196	6	0.05	0.034 ±11%	3.41	±36%	5.7 ± 2.1	5.4 ± 2.8	[c]
Hi	Mini	E344	6	0.08	0.049 ±33%	5.70	±23%	9.3 ± 3.3	[e]	[e]
Hi	Ethe	E478	3	0.09	0.045 ± 5%	4.09	±11%	8.7 ± 1.0	7.4 ± 2.7	[c]
Hi	Ethe	E499	2	0.14	0.046 ± 8%	2.17	± 8%	7.0 ± 0.8	7.0 ± 3.1	[c]
Hi	Ethe	E477	3	0.17	0.098 ± 4%	4.22	± 6%	7.5 ± 0.5	6.0 ± 1.8	[c]
Hi	Surg	D025	6	0.08	0.066 ± 3%	3.46	±15%	4.4 ± 0.7	5.4 ± 0.6	-1.0 ± 0.6
Hi	Surg	D068	5	0.06	0.043 ± 3%	3.74	±14%	5.6 ± 0.8	5.0 ± 0.8	0.6 ± 0.9
Lo	Surg	D035	6	0.10	0.069 ± 3%	-0.510	±46%	-0.8 ± 0.4	[b]	[b]
Lo	Surg	D067	6	0.17	0.107 ± 6%	-0.347	±40%	-0.6 ± 0.2	[b]	[b]
Formaldehyde										
Hi	Mini	E352	6	0.10	[d]	2.37	±27%			
Hi	Mini	E357	6	0.26	[d]	1.35	±19%			
Hi	Ethe	E468	3	0.10	[d]	1.44	±24%			
Hi	Ethe	E470	3	0.26	[d]	1.94	± 8%			
Hi	Ethe	E489	3	0.28	[d]	1.66	± 9%			
Hi	Surg	D022	6	0.40	[d]	0.754	±13%			
Lo	Surg	D036	6	0.24	[d]	0.05	±0.11			
Acetaldehyde										
Hi	Mini	E335	6	0.69	0.261 ± 7%	0.226	±43%	0.6 ± 0.3	-0.9 ± 0.4	1.6 ± 0.3
Hi	Mini	E338	6	1.31	0.444 ± 8%	0.113	±46%	0.3 ± 0.2	-0.9 ± 0.2	1.3 ± 0.2
Hi	Surg	D065	6	1.53	0.377 ±24%	0.148	±16%	0.6 ± 0.2	-1.1 ± 0.3	1.7 ± 0.4
Lo	Surg	D066	6	1.62	0.247 ±40%	-0.0345	±44%	-0.2 ± 0.1	[b]	[b]

[a] Codes for NO_x conditions: "Hi" = maximum reactivity; "Lo" = NO_x-limited O_3. Codes for base ROG surrogates: "Mini" = Mini-surrogate (from Carter et al., [1993a]), "Ethe" = ethene surrogate; "Surg" = 8-component "lumped molecule" surrogate. ETC runs codes have "E" prefix; DTC runs have "D" prefix. Hr is hour in run where data given. Data given for t<6 hours in maximum reactivity experiments where the final O_3 appears to be nearly NO_x-limited, or if t=6 data missing.

[b] Methods used to estimate direct and indirect reactivities are not valid for NOx-limited conditions.

[c] Estimated minimum uncertainty to great to yield meaningful data.

[d] Amounts reacted could not be determined, or uncertainties too high for meaningful data.

[e] Indirect and direct reactivity results for this run appear to be anomalous

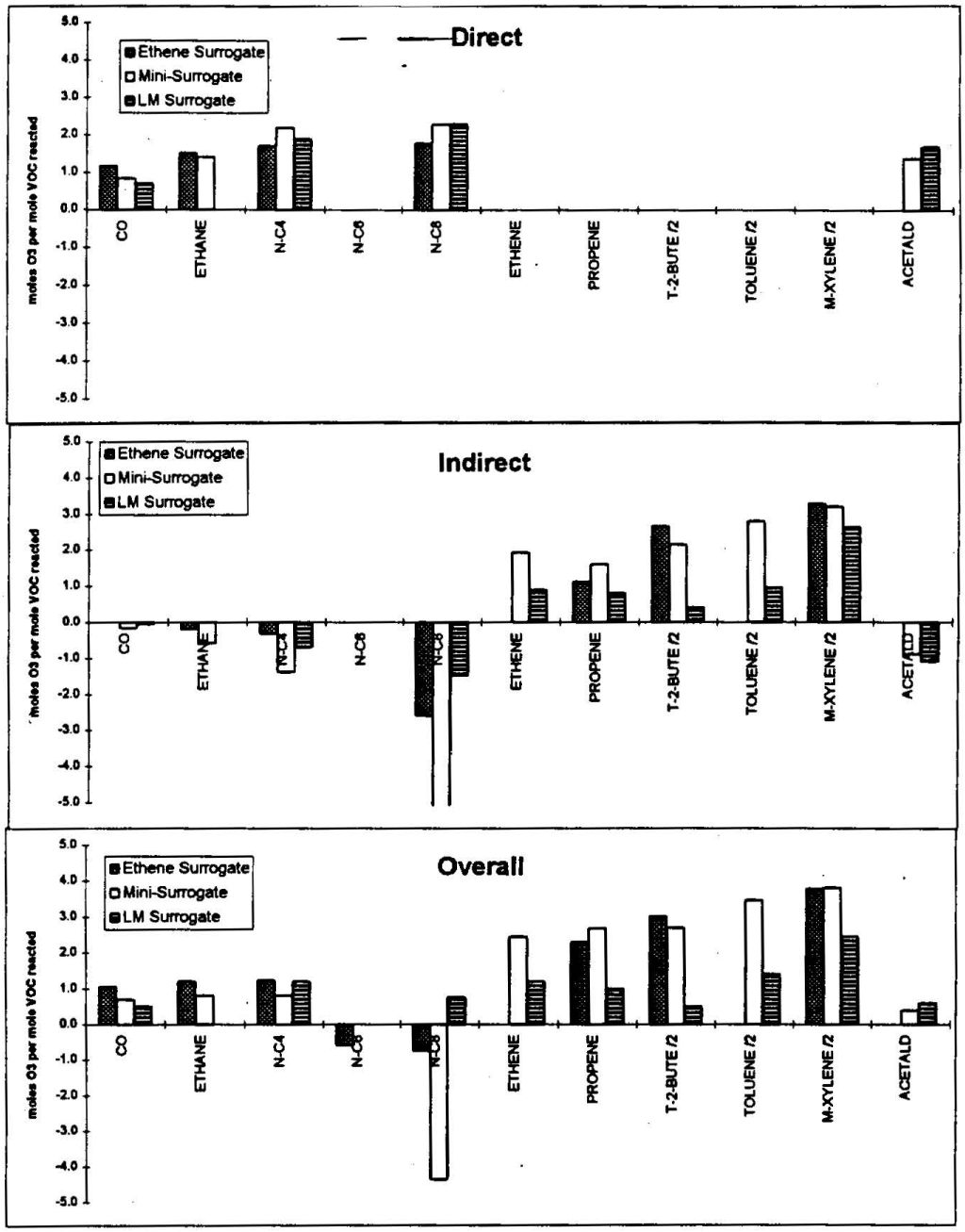

Figure 55 Comparisons of weighed averages of the direct, indirect, and overall mechanistic reactivities for high NO_x conditions for the three base ROG surrogates. The averages are of the data on Table 15. The units of the data are moles $d(O_3\text{-}NO)$ per mole VOC reacting.

both positive and negative, in the experiments using the ethene or the mini-surrogates than is the case when the full, lumped molecule, surrogate is used. For example, the radical inhibition by n-octane is much greater with the mini-surrogate, and somewhat greater with the ethene surrogate, than it is with the full surrogate. A similar effect is seen, though to a lesser extent, with n-butane and ethane, though in the case of n-butane the indirect reactivities for the ethene and the full surrogates are the essentially the same. Similarly; the positive indirect reactivities for trans-2-butene and toluene are much greater with the simpler surrogates than it is with the full surrogate, and similar results, though to a lesser extent, are seen with ethene, propene, and m-xylene. Acetaldehyde is somewhat unusual in that its indirect reactivity is essentially the same with the mini- and full surrogates.

Thus the effect of the base ROG on the VOC's indirect incremental reactivity is the primary factor affecting a how the base ROG affects the VOC's overall incremental reactivity under high NO_x conditions. Under such conditions, the indirect reactivity of a VOC depends on two factors: its IntOH reactivity and the $d(O_3\text{-NO})/\text{IntOH}$ ratio for the base ROG. The latter averaged 3.3, 3.2, and 2.6 x 10^4 min^{-1} for the ethene, mini-, and full surrogate base case runs, respectively. Thus the base ROG $d(O_3\text{-NO})/\text{IntOH}$ ratio is roughly equal for the two simpler surrogates, and is approximately 20% lower for the full surrogate. The difference for the full surrogate is not sufficient to explain the indirect reactivity differences for most of the VOCs. Therefore, the effect of the base ROG on the VOC's IntOH reactivity, i.e., on how the VOC affects OH radical levels, appears to be the primary factor determining the effect on overall reactivity.

In general, the use of the simpler surrogate tends to result in greater magnitudes of IntOH reactivities, whether positive or negative, than use of the more realistic lumped surrogate. In other words, the addition of VOCs cause greater changes in OH radical levels in runs with the simpler surrogates than in their addition in runs with more complex surrogates. This is probably due to species in the complex surrogate providing radicals earlier in the run than those in the simpler surrogates. In particular, the lumped surrogate contains formaldehyde and trans-2-butene, whose reactions cause relatively large radical inputs early in the experiment. The m-xylene and/or ethylene in the simpler surrogates also provide radical inputs, but generally not as much as early in the run as is the case for formaldehyde and trans-2-butene. The earlier radicals apparently make the system less sensitive to the radical input or radical inhibition caused by the addition of the test VOCs than would be the case if these early radical sources are missing.

The effects of the ROG surrogate on reactivity observed in this study are entirely consistent with the predictions of the model calculations discussed in Section II. Those calculations predicted that in general the use of the simpler ROG surrogates (i.e., ethene and the mini-surrogate) would give results which are

more sensitive to differences among VOCs than use of more realistic surrogates, and this is indeed what was observed. The model is also able to successfully simulate the results of most of the reactivity experiments, particularly for the experiments using the more complex ROG surrogate. The performance of the current mechanisms in simulating these data is discussed in more detail later.

B. Effect of NO_x on Reactivity

As expected based on modeling studies (e.g., Carter and Atkinson, 1989), NO_x conditions were found to significantly affect VOC reactivities, both in an absolute and a relative sense. Reducing NO_x levels reduced incremental reactivities for all VOCs studied, but the amount of reduction varied greatly among the VOCs. A number of VOCs whose mechanistic reactivities were both positive and high under high NO_x conditions were found to become negative in the low NO_x experiments. This was true not only of the aromatics, but also for trans-2-butene and acetaldehyde. In the case of propene, another relatively reactive compound under high NO_x conditions, the reactivity became essentially zero in the low NO_x experiments. The incremental reactivity of formaldehyde, while still positive, was a factor of ~15 times lower than under high NO_x conditions. On the other hand, the mechanistic reactivities for ethene only reduced by a factor of five, and those for CO and the alkanes reduced by only a factor of two.

The trends observed are consistent with the expectation that low NO_x reactivities are strongly influenced by NO_x sinks in the VOCs' mechanisms. The species whose reactivities changed the most as NO_x changed were all species believed to have the most important NO_x removal processes. In the case of the aromatics, the NO_x sinks are believed to include the formation of species such as nitrophenols from the aromatic ring-retaining products, and the formation of PAN from the dicarbonyls and other fragmentation products. In the case of acetaldehyde, it is the formation of PAN. In the case of propene and trans-2-butene, it is the formation of acetaldehyde, which in turn reacts to form PAN. Ethene, CO and n-butane have relatively small NO_x sinks, and thus reducing NO_x does not cause as great a change in reactivity for those compounds. However, reactivity is still reduced because of the lower efficiency for O_3 formation under lower NO_x conditions.

The effects of VOCs on radicals would still be expected to have some effect on reactivity under low NO_x conditions, though it is clearly does not have the overriding importance it does under high NO_x conditions. For the VOCs studied here, there is no correlation between IntOH and $d(O_3\text{-}NO)$ reactivities under low NO_x conditions – the correlation coefficient for the mechanistic reactivities (incremental for formaldehyde) is -0.17. (By contrast, the correlation coefficient for the high NO_x experiments with the same ROG surrogate is 0.99.) The reduced importance of radicals under low NO_x conditions is indicated by the relatively large reduction in the formaldehyde incremental reactivity, despite the fact that it does not have significant NO_x sinks in its mechanism. This is probably also one reason the change in incremental reactivity of n-octane is not

as large as might be expected given the formation of alkyl nitrates in its reactions. In this case, the large radical sinks in the n-octane mechanism, which is the major factor giving it a low reactivity under high NO_x conditions, is less important in suppressing its reactivity when NO_x is lower, and this tends to counteract the relative reduction of reactivity due to n-octane's NO_x sinks.

It is interesting to note that under low NO_x conditions all the VOCs studied except for formaldehyde suppressed radical levels. The high radical suppression by acetaldehyde can be attributed to the fact that most of its reaction with OH radicals involves formation of PAN, which is a radical sink process. In the case of VOCs with NO_x sinks, such as aromatics, radical suppression would be expected because termination by radical-radical reactions become more important when NO_x runs out. However, in the case of the other VOCs, the suppression is apparently simply due to the fact that the VOC is promoting ozone. Otherwise, it would be difficult to understand why CO, which has neither radical nor NO_x sinks in its mechanism, is suppressing IntOH such a large extent. This general suppression might be due to the higher O_3 levels caused by the test VOC causing lower steady state NO levels, which means that radical propagation reactions of peroxy radicals with NO are less competitive with termination by radical + radical reactions.

C. Mechanism Evaluation Results

With a few exceptions, discussed below, the current detailed mechanism performs remarkably well in simulating the reactivity results in this study. The most concise indication of the ability of the mechanism to simulate the various measured components of reactivity is obtained from Figures 52-54, above. The major effects on reactivity of changing the ROG surrogate and the NO_x levels, discussed above, are all successfully simulated by the model.

There were, however, a few cases of poor model performance suggesting possible problems in the mechanism. The poor model performance in simulating the low NO_x IntOH reactivity of benzene and to a lesser extent the other aromatics suggest problems in some fundamental aspect of the aromatics mechanisms. A similar problem was seen in the model simulation of the IntOH reactivity under high NO_x conditions with the Phase I mini-surrogate (Carter et al., 1993a), where a compensating error in the prediction of the direct reactivity caused a fairly good prediction of overall reactivity. However, the model is successful in simulating the $d(O_3\text{-NO})$ reactivities of toluene and m-xylene under all conditions studied, and in simulating their IntOH reactivities reasonably well under high NO_x conditions.

In general, the model performed better in simulating the reactivities in the experiments with the complex surrogate than it did in the ethene surrogate runs. This is despite the uncertainties in the mechanism for some of the components of the complex surrogate, and despite the fact that the model tended to underpredict the rate of ozone formation in the base case high NO_x surrogate

experiments. One part of the reason for this is that the system with the more complex surrogate appears to be less affected by radical initiation and inhibition effects of the added VOCs than is the case with ethene or the mini-surrogate. Thus, the more complex surrogate is less sensitive to mechanism differences among VOCs, so errors in these mechanisms will have less of an effect on the results. In addition, errors in the base case mechanisms of the components of the more complex surrogate may have less of an effect than errors in the base mechanisms for simpler surrogates, because with a complex mixture no single compound in the mixture tends to dominate the results.

The most serious discrepancies observed in the ethylene surrogate experiments were the predictions of the reactivities of n-octane and formaldehyde. In particular, the model overpredicted the initiation caused by adding n-octane, and overprotected the initiation caused by adding formaldehyde. There may be slight overpredictions in the high NO_x lumped surrogate runs with these compounds, but in these cases the model predictions are close to the experimental uncertainty ranges.

The problem with n-octane is difficult to rationalize, especially since the model successfully simulated the reactivity of n-octane in the mini-surrogate experiments (Carter et al., 1993a). There is an indication of a similar problem in the case of the predictions of the n-butane and n-hexane reactivities in the ethene surrogate runs, though the discrepancy for n-hexane is less than that for n-butane, which is not the trend one would expect. Unfortunately, the IntOH data in the ethene surrogate experiments are not sufficiently precise to clearly indicate whether the problem is due to problems in predicting direct or indirect reactivities. The model predictions are not inconsistent with the direct mechanistic reactivity data, but the uncertainty of the latter, due to the combined uncertainties in the IntOH data and the amounts of n-octane reacting, are such that this is not particularly meaningful.

However, the problem is most likely with the amount of radical inhibition caused by n-octane, i.e., with the indirect reactivity. Adjusting the n-octane mechanism by reducing the alkyl nitrate yield from ~33% to ~25% causes the model to give good fits to all the reactivity data in the ethene surrogate experiments. However, this adjusted n-octane model overpredicts the $d(O_3\text{-NO})$ reactivity of n-octane in the high NO_x lumped surrogate run, and somewhat underpredicts its $d(O_3\text{-NO})$ inhibition in the mini-surrogate runs. This adjusted mechanism is also inconsistent with the experimentally observed ~33±3% octyl nitrate yields reported by Atkinson et al. (1982), which is used as the basis for the current mechanism. This needs further investigation, including an independent confirmation of the octyl nitrate yields reported by Atkinson et al. (1982).

The overprediction by the model of the incremental reactivity of formaldehyde in both the ethene and the mini-surrogate experiments is disturbing because the atmospheric chemistry of formaldehyde has been considered to be

reasonably well established. The discrepancy appears to be the greatest in the run with the smallest amount of added formaldehyde, and (for both ethene and the mini-surrogate) is relatively greater earlier in the runs than it is later. In view of the consistent results with the quite different base ROG surrogates, it is unlikely to be due to a problem in the base ROG mechanism, a possibility considered in the Phase I report (Carter et al., 1993a). A slight overprediction of the $d(O_3-NO)$ formation rate and formaldehyde consumption rates are observed in model simulations of formaldehyde - NO_x experiments carried out for this program, though the extent of the model discrepancy is not as great as indicated by the incremental reactivity results. This is discussed in more detail elsewhere (Carter et al., 1995a).

D. Correlations Between Experimental and Atmospheric Reactivities

It is of interest to see how well experimental incremental reactivities can correlate with those calculated for the atmosphere. In Section II, we used model simulations to predict how well mechanistic reactivities measured in environmental chamber experiments would correlate with those in the atmosphere. A fair correlation was obtained for high NO_x maximum reactivity conditions, but no correlation was obtained for NO_x-limited conditions. However, better correlations might be expected for incremental reactivities, because of the large differences in VOC's reaction rates, which are not taken into account in correlations of mechanistic reactivities, would similarly affect incremental reactivities under both conditions. The best correlation would be expected for experiments with the most realistic base ROG mixtures, and as discussed in Section II the lumped surrogate appears to be sufficiently realistic for this purpose. Furthermore, since the model gives good simulations of the reactivities of the VOCs studied using this surrogate, one might expect the atmospheric model simulations to be reasonably accurate in terms of the aspects of the chemical mechanism which affect predictions of reactivity.

Figure 56 shows plots of the experimental per-carbon incremental reactivities of the VOCs studied against those calculated for the atmosphere for similar NO_x conditions. The experimental data is from the runs using the lumped surrogate. The high NO_x experimental reactivities are compared with those in the Maximum Incremental Reactivity (MIR) scale, since the MIR scale is based on atmospheric reactivities under high NO_x conditions (Carter, 1994). The low NO_x experimental reactivities are compared with those in the Equal Benefit Incremental Reactivity (EBIR) scale, which is a scale based on atmospheric reactivities under NO_x-limited conditions. (The EBIR scale was chosen rather than the MOIR scale – which represents intermediate NO_x conditions which are optimum for O_3 formation – because it corresponds more closely to the conditions of the low NO_x experiments. However, except for toluene, which has a relatively low EBIR reactivity, EBIR and MOIR reactivities are highly correlated [Carter, 1994].)

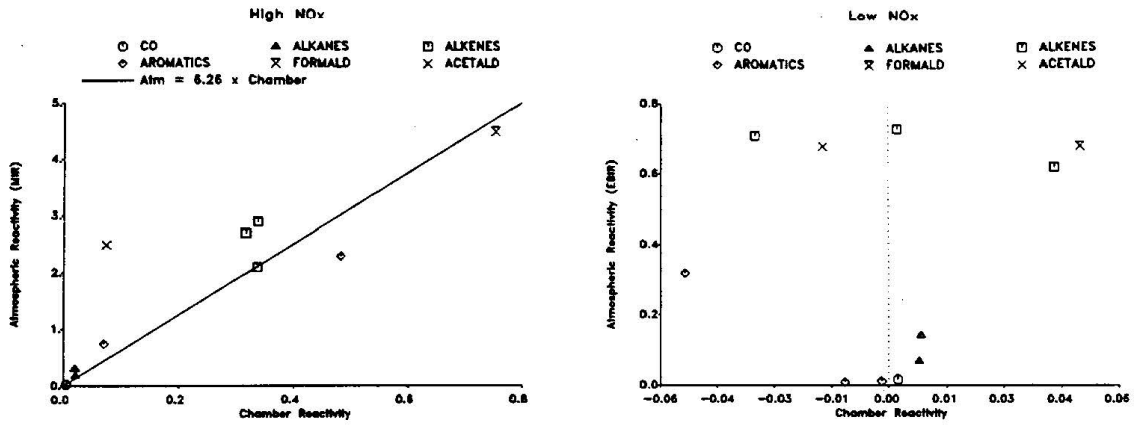

Figure 56. Plots of atmospheric incremental reactivities (carbon basis) against incremental reactivities in the environmental chamber experiments using the lumped surrogate. High NO_x chamber reactivities are plotted against atmospheric reactivities in the MIR scale, and low NO_x chamber reactivities are plotted against atmospheric reactivities in the low NO_x "Equal Benefit Incremental Reactivity" scale.

Figure 56 shows that there is a fair correlation between the high NO_x experimental and atmospheric MIR reactivities of all the VOCs studied except for acetaldehyde. Note, however, that the incremental reactivities in the chamber have much lower magnitudes than those in the atmosphere, the best fit line shown on the figure indicates that they are lower by over a factor of ~6. Although the correlation coefficient excluding acetaldehyde is 96% (it is 88% with acetaldehyde), using the best fit line only predicts the incremental reactivities to within ±50% in some cases. Therefore, although chamber experiments can indeed give an indication of atmospheric reactivity under high NO_x conditions without having to rely on modeling, the estimates cannot be considered to be highly precise.

The poor correlation in the case of acetaldehyde cannot be attributed to problems with the model because it is reasonably successful in simulating acetaldehyde reactivity experiments. Part of the problem may be the light source; the photolysis rate of acetaldehyde relative to that of NO_2 is calculated to be almost 3 times slower in the chamber experiment than in the atmosphere. However, a reasonably good correlation was obtained for formaldehyde, which photolyzes ~2 times slower relative to NO_2. Another probable factor is the fact that (unlike the model simulations of the chamber experiments in Section II) the experiments do not represent true incremental reactivities, since finite amounts of test compounds had to be added to yield measurable results.

Figure 56 also shows that there is essentially no correlation between low NO_x reactivities in the chamber and those in the atmosphere. This is despite the fact that the model gave quite good predictions of the low NO_x reactivities in the chamber. This is consistent with the model predictions given in Section II. As indicated there, this is attributed to the fact that low NO_x O_3 reactivities are determined by the interactions of several different factors, whose relative importance are apparently quite different in the chamber than in the atmosphere. It may be possible to design a chamber experiment where somewhat better low NO_x reactivity correlations could be obtained, though it unclear whether it would be worth the probably considerable effort and expense required to do this. Model simulations would probably be the only practical way to estimate low NO_x reactivities for the foreseeable future.

VII. CONCLUSIONS

This study, in conjunction with our Phase I work, has provided a large experimental data base on VOC reactivity. The Phase I work has provided information concerning reactivities of a wide variety of compounds under a single set of conditions, and this work has provided information concerning a smaller number of species under more varied conditions. These new data are useful for assessing how the presence of other pollutants in the atmosphere affect a VOC's reactivity, and for evaluating how well current photochemical models can predict these effects. This work has also provided useful information on the relative utility of various types of experimental data in reactivity assessment and mechanism evaluation.

Both model simulations and experimental data have shown that the presence of other VOC pollutants, referred to as the "base ROG", can significantly affect a VOC's ozone reactivity. For example, the model predicted, and the experimental data confirmed, that the incremental reactivity of n-octane could change sign, and the absolute reactivities of species such as alkenes, aromatics, and formaldehyde could change significantly, depending on the mixture used to represent the base ROG. VOCs were found to have much smaller differences in mechanistic reactivities (reactivities with effects of the VOC's reaction rates factored out) when reacting in the presence of a more complex mixture designed to represent ambient ROG pollutants than when reacting in the presence of the 3-component "mini-surrogate" used in our Phase I study, or when reacting in the presence of ethylene alone. This is attributed to species in the more complex mixture, such as formaldehyde and (perhaps to a lesser extent) internal alkenes, which provide radical sources early in the irradiations, and tend to make the system less sensitive to the radical input or termination processes caused by the test VOC.

On the other hand, model simulations showed that it is probably not necessary to use a highly complex mixture to adequately represent the effects of other ROG pollutants in experimental studies of incremental reactivity. Use of a simple 8-component mixture, containing approximately the level of chemical detail as incorporated in condensed "lumped molecule" mechanisms in airshed models, was calculated to provide indistinguishable reactivity results in chamber experiments as use of a ambient ROG mixture containing the full set of compounds measured in the atmosphere. But simplifying this 8-component mixture further was found to begin to have non-negligible effects on reactivity. The mixture was derived based on the amounts and types of reactive molecules present; representation of all the carbon present was found not to be important. It can be argued that this result may be an artifact due to the chemical mechanism having a comparable degree of condensation as the 8-component mixture. However, the chemical mechanism used in this assessment had sufficient detail to represent many, though not all, of the chemical complexities in the ambient mixture. In

any case, if there are any differences in reactivity in experiments using a more complex ROG surrogate than the 8-component mixture, they clearly cannot be accounted for by the present generation of detailed mechanisms.

Using a realistic ROG surrogate is obviously necessary if experimental reactivity data are to correspond to reactivities in the atmosphere. However, it is not sufficient. Model calculations showed that even if the ambient mixture itself is used as the ROG surrogate, the mechanistic reactivities in chamber studies would not necessarily correspond to those in the atmosphere. This was confirmed by the experimental data. The extent to which chamber reactivities correlate with those in the atmosphere depended significantly on NO_x conditions. Under high NO_x conditions, experimental incremental reactivities correlate moderately well with atmospheric reactivities in the MIR scale, though the correlation was poor for acetaldehyde, and the correlation with the chamber data could only predict the atmosphere reactivities for the other VOCs to within ±50%. Under low NO_x conditions, there was no correlation at all between atmospheric reactivity and reactivity in the chamber experiments. This was true whether using real chamber data or chamber data simulated by the model. Reactivities under low NO_x conditions are influenced by differing and often opposing factors, and apparently balances among these factors are quite different in the chamber experiments than in the atmosphere.

It may be possible someday to design an experimental system which gives better correlations between experimental and atmospheric reactivities, but we suspect it would be extremely difficult and expensive, and may yield data with large experimental uncertainties. In the meantime, we must rely on model simulations to predict reactivities in the atmosphere. The role of the chamber data is thus not to directly measure atmospheric reactivity, but rather to evaluate and if necessary calibrate the models which must be used for this purpose.

Experiments with both realistic and simplified ROG surrogates are necessary for an adequate evaluation of the ability of models to predict reactivity. Use of realistic surrogates are obviously necessary to test the ability of the mechanism to simulate reactivities in chemically realistic conditions. However, experiments with simpler surrogates are more sensitive to differences among VOCs, particularly in terms of their effects on radical levels. This means that model simulations of those experiments would be more sensitive to errors in the mechanisms of the VOCs. This is consistent with the results of this study, where in general the mechanism performed better in simulating reactivity in the experiments using the more complex surrogate than it did in the experiments using the mini-surrogate or ethylene alone.

The experimental data in this study confirmed the model predictions concerning the importance of NO_x in affecting a VOC's incremental reactivity. As expected, the incremental and mechanistic reactivities of all VOCs were

reduced under low NO_x conditions. As also expected, this reduction was the greatest for VOCs, such as aromatics, acetaldehyde, and the higher alkenes, which are believed to have significant NO_x sinks in their mechanisms. All these NO_x sink species were found to have negative reactivities in our low NO_x experiments. This includes species, such as alkenes and acetaldehyde, which are calculated to have positive reactivities under low NO_x conditions in the atmosphere (Carter, 1993, 1994). Thus, low NO_x chamber reactivity experiments appear to be highly sensitive to effects of NO_x sinks in VOC's mechanisms – much more so than is apparently the case in the atmosphere. This high sensitivity may be the cause of the poor correlation between low NO_x chamber data and atmospheric reactivities. However, this also means that the chamber data should provide a highly sensitive test to this aspect of the mechanism.

The current detailed chemical mechanism was found to perform remarkably well in simulating the reactivities of the VOCs with the realistic 8-component surrogate, both under high and low NO_x conditions. An exception was that the model did not correctly predict the effects of aromatics on radical levels under low NO_x conditions. The model performance was more variable in simulating the experiments with the highly simplified (ethylene only) surrogate, though the observed reactivity trends were correctly predicted. The greater variability is attributable in part to the greater sensitivity of the simpler systems to mechanism differences, as indicated above. However, it can also be attributable to the greater sensitivity of simulations of the ethene reactivity experiments to uncertainties in reaction conditions and the ethene mechanism. With more base ROG components present, errors in the mechanisms and amounts of each individual component becomes relatively less important in affecting the result.

In our previous study, we found that we could not simulate all the base mini-surrogate experiments with a single version of the m-xylene mechanism. That problem has now apparently been resolved in the process of correcting our chamber data base and revising our chamber effects models. It was also found that the ability of the model to simulate these experiments was dependent on the temperature in these runs, which was variable. The inability of the model to simulate temperature effects is considered in more detail elsewhere (Carter et al., 1995a).

Predictions of formaldehyde reactivity continues to be a problem with the model. The model was found previously to overpredict formaldehyde's reactivity in the mini-surrogate. Similar results were obtained using the ethylene surrogate. Thus, the discrepancy is unlikely to be due to a problem with the base ROG mechanism, unless it is a problem with ethylene. On the other hand, the model discrepancy was not large in simulating formaldehyde's reactivity in the presence of the more complex surrogate. Thus, the practical effect of this discrepancy in simulation of realistic mixtures may not be large. However, in view of the fundamental importance of formaldehyde, it clearly needs to be resolved.

The model significantly overpredicted the ozone inhibition caused by adding n-octane to the ethene surrogate runs, suggesting a potential problem with the higher alkane mechanism which was not indicated by previous data. Better fits to the ethene data are obtained if it is assumed the octyl nitrate yields are lower than indicated by data from a single laboratory study, though the fits to the more complex surrogate data are made somewhat worse. This needs further study, including confirmation of the nitrate yields from the C_{8+} alkanes, which are highly sensitive parameters affecting predictions of alkane reactivity.

While problems and uncertainties with the aromatics mechanisms remain, and the continuing discrepancies with formaldehyde and the new one with n-octane are a concern, the results of this study generally give a fairly optimistic picture of the ability of the model to simulate reactivities under atmospheric conditions. This optimism is in part due to the fact that systems with realistic mixtures tend to be less sensitive to errors in the mechanisms than systems that are perhaps most useful for mechanism evaluation. However, one would clearly have more confidence in the fundamental validity of reactivity predictions if the model could satisfactorily predict reactivities in simple as well as complex chemical systems. The data obtained thus far indicate that if the model can simulate reactivity with simple ROG surrogates, it should be able to do so in the more realistic chemical system.

Although this study, in conjunction with our Phase I work, has provided a large experimental data base on VOC reactivity, it is not comprehensive. For example, only 9 or 10 different VOCs have been studied using the realistic surrogate. The mini-surrogate data indicated problems with the model in simulating reactivities of branched alkanes and of aromatic isomers not studied in this work, and information is needed concerning how these problems affect predictions of reactivities in atmospheric systems. We believe the experiments with the simplified surrogates provide the most useful information for mechanism testing. Therefore, it is important that the data base of such experiments be comprehensive and of high quality. While the number of VOCs studied in Phase I study was fairly extensive, because of experimental problems the data for some was of low precision or quality. In addition, only one branched alkane was studied, and the model performed poorly in simulating its reactivity and had to be adjusted. The dividable chamber constructed under SCAQMD funding for this program was found to yield significantly more precise reactivity data than has been obtained previously, and could significantly improve the quality as well as the completeness of this data base. No information has been obtained concerning the effect of temperature on reactivity, and there is only limited information concerning the effects of using artificial light sources. The issues of temperature and light source effects, and other fundamental data needs for mechanism evaluation, are discussed in more detail in a separate report (Carter et al., 1995a).

VIII. REFERENCES

Atkinson, R. (1989): "Kinetics and Mechanisms of the Gas-Phase Reactions of the Hydroxyl Radical with Organic Compounds," J. Phys. Chem. Ref. Data, Monograph no 1.

Atkinson, R. (1990): "Gas-Phase Tropospheric Chemistry of Organic Compounds: A Review," Atmos. Environ., 24A, 1-24.

Atkinson, R. (1994): "Gas-Phase Tropospheric Chemistry of Organic Compounds," J. Phys. Chem. Ref. Data, Monograph No. 2.

Atkinson, R., S. M. Aschmann, W. P. L. Carter, A. M. Winer, and J. N. Pitts, Jr., (1982): "Alkyl Nitrate Formation from the NO_x-air Photooxidations of C_2-C_8 n-alkanes," J. Phys. Chem., 86, 4563-4569.

Atkinson, R. and S. M. Aschmann (1993): "OH Radical Production from the Gas-Phase Reactions of O_3 with a Series of Alkenes under Atmospheric Conditions," Environ. Sci. Technol, 27, 1357-1363.

CARB (1991): "Proposed Reactivity Adjustment Factors for Transitional Low-Emissions Vehicles – Staff Report and Technical Support Document," California Air Resources Board, Sacramento, CA, September 27.

Carter, W. P. L. (1990): "A Detailed Mechanism for the Gas-Phase Atmospheric Reactions of Organic Compounds," Atm. Environ., 24A, 481-518.

Carter, W. P. L. (1991): "Development of Ozone Reactivity Scales for Volatile Organic Compounds", EPA-600/3-91/050, August.

Carter, W. P. L. (1993): "Development and Application of an Up-To-Date Photochemical Mechanism for Airshed Modeling and Reactivity Assessment," Draft final report for California Air Resources Board Contract No. A934-094, April 26.

Carter, W. P. L. (1994): "Development of Ozone Reactivity Scales for Volatile Organic Compounds," J. Air and Waste Manage. Assoc., 44, 881-899.

Carter, W. P. L., R. Atkinson, A. M. Winer, and J. N. Pitts, Jr. (1982): "Experimental Investigation of Chamber-Dependent Radical Sources," Int. J. Chem. Kinet., 14, 1071.

Carter, W. P. L., Dodd, M. C., Long, W. D. and Atkinson, R. (1984): Outdoor Chamber Study to Test Multi-Day Effects. Volume I: Results and Discussion. Final report, EPA-600/3-84-115.

Carter, W. P. L., W. D. Long, L. N. Parker, and M. C. Dodd (1986): "Effects of Methanol Fuel Substitution on Multi-Day Air Pollution Episodes," Final Report on California Air Resources Board Contract No. A3-125-32, April.

Carter, W. P. L. and R. Atkinson (1987): "An Experimental Study of Incremental Hydrocarbon Reactivity," Environ. Sci. Technol., 21, 670-679

Carter, W. P. L. and R. Atkinson (1989): "A Computer Modeling Study of Incremental Hydrocarbon Reactivity", Environ. Sci. and Technol., 23, 864.

Carter, W. P. L., and F. W. Lurmann (1990): "Evaluation of the RADM Gas-Phase Chemical Mechanism," Final Report, EPA-600/3-90-001.

Carter, W. P. L., and F. W. Lurmann (1990): "Evaluation of the RADM Gas-Phase Chemical Mechanism," Final Report, EPA-600/3-90-001.

Carter, W. P. L. and F. W. Lurmann (1991): "Evaluation of a Detailed Gas-Phase Atmospheric Reaction Mechanism using Environmental Chamber Data," Atm. Environ. 25A, 2771-2806.

Carter, W. P. L., J. A. Pierce, I. L. Malkina, D. Luo and W. D. Long (1993a): "Environmental Chamber Studies of Maximum Incremental Reactivities of Volatile Organic Compounds," Report to Coordinating Research Council, Project No. ME-9, California Air Resources Board Contract No. A032-0692; South Coast Air Quality Management District Contract No. C91323, United States Environmental Protection Agency Cooperative Agreement No. CR-814396-01-0, University Corporation for Atmospheric Research Contract No. 59166, and Dow Corning Corporation. April 1.

Carter, W. P. L, D. Luo, I. L. Malkina, and J. A. Pierce (1993b): "An Experimental and Modeling Study of the Photochemical Ozone Reactivity of Acetone," Final Report to Chemical Manufacturers Association Contract No. KET-ACE-CRC-2.0. December 10.

Carter, W. P. L., J. A. Pierce, D. Luo and I. L. Malkina (1993c): "Environmental Chamber Studies of Maximum Incremental Reactivities of Volatile Organic Compounds," Submitted to Atmospheric Environment, November 23.

Carter, W. P. L., D. Luo, I. L. Malkina, J. A. Pierce, W. D. Long, and D. Fitz (1995a): "Environmental Chamber Studies of Atmospheric Reactivities of Volatile Organic Compounds. Effects of Varying Chamber and Light Source", March 26.

Carter, W. P. L., D. Luo, I. L. Malkina, and D. Fitz (1995b): "The University of California, Riverside Environmental Chamber Data Base for Evaluating Oxidant Mechanism. Indoor Chamber Experiments through 1993," Report submitted to the U. S. Environmental Protection Agency, EPA/AREAL, Research Triangle Park, NC., March 20..

Chang, T. Y. and S. J. Rudy (1990): "Ozone-Forming Potential of Organic Emissions from Alternative-Fueled Vehicles," Atmos. Environ., 24A, 2421-2430.

Croes, B. E. et al. (1993): "Southern California Air Quality Study Data Archive," Research Division, California Air Resources Board.

Dasgupta, P. K, Dong, S. and Hwang, H. (1988): "Continuous Liquid Phase Fluorometry Coupled to a Diffusion Scrubber for the Determination of Atmospheric Formaldehyde, Hydrogen Peroxide, and Sulfur Dioxide," Atmos. Environ. 22, 949-963.

Dasgupta, P.K, Dong, S. and Hwang, H. (1990): Aerosol Science and Technology 12, 98-104

Dong, S. and Dasgupta, P. K. (1987): "Fast Fluorometric Flow Analysis of Formaldehyde," Environ. Sci. and Technol. 21, 581-588.

Gardner, E. P., P. D. Sperry, and J. G. Calvert (1987): "Photodecomposition of Acrolein in O_2-N_2 Mixtures," J. Phys. Chem. 91, 1922.

Jeffries H. E., K. G. Sexton, J. R. Arnold, and T. L. Kale (1989): "Validation Testing of New Mechanisms with Outdoor Chamber Data. Volume 2: Analysis of

VOC Data for the CB4 and CAL Photochemical Mechanisms," Final Report, EPA-600/3-89-010b.

Jeffries, H. E. and K. G. Sexton (1992): "The Relative Ozone Forming Potential of Methanol-Fueled Vehicle Emissions and Gasoline-Fueled Vehicle Emissions in Outdoor Smog Chambers," Annual Report for the Coordinating Research Council Project No. ME-1, August 30.

Johnson, G. M. (1983): "Factors Affecting Oxidant Formation in Sydney Air," in "The Urban Atmosphere -- Sydney, a Case Study." Eds. J. N. Carras and G. M. Johnson (CSIRO, Melbourne), pp. 393-408.

Lurmann, F. W., H. H. Main, K. T. Knapp, L. Stockburrger, R. A. Rasmussen and K. Fung (1992): "Analysis of Ambient VOC Data Collected in the Southern California Air Quality Study," Final Report to California Air Resources Board Contract No. A382-130; Research Division, Sacramento, CA, February.

Lurmann, F. W., M. Gery, and W. P. L. Carter (1991): "Implementation of the 1990 SAPRC Chemical Mechanism in the Urban Airshed Model," Final Report to the California South Coast Air Quality Management District, Sonoma Technology, Inc. Report STI-99290-1164-FR, Santa Rosa, CA.

Meyrahn, H., J. Pauly, W. Schneider, and P. Warneck (1986): "Quantum Yields for the Photodissociation of Acetone in Air and an Estimate for the Life Time of Acetone in the Lower Troposphere," J. Atmos. Chem. 4, 277-291.

Russell, A. G. (1990): "Air Quality Modeling of Alternative Fuel Use in Los Angeles, CA: Sensitivity of Pollutant Formation to Individual Pollutant Compounds," the AWMA 83rd Annual Meeting, June 24-29.

Tuazon, E. C., R. Atkinson, C. N. Plum, A. M. Winer, and J. N. Pitts, Jr. (1983): "The Reaction of Gas-Phase N_2O_5 with Water Vapor," Geophys. Res. Lett. 10, 953-956.